

**Thermal performance of naturally ventilated
office buildings with double skin façade
under Brazilian climate conditions**

Sabrina Andrade Barbosa

A thesis submitted in partial fulfilment of the
requirements of the University of Brighton
for the degree of Doctor of Philosophy

November 2015

University of Brighton

ABSTRACT

Double skin façades (DSFs) are gaining recognition as a technology that, while giving a modern transparent appearance to buildings, have the capability to moderate the indoor thermal conditions and the potential to reduce energy demands.. A typical DSF consists of an additional fully glazed external skin installed over the conventional building façade forming an air cavity in which sunshade devices are often installed to prevent overheating in the internal rooms. The majority of the existing studies on DSF are based on air-conditioned models under temperate climate conditions, where most DSFs are implemented. However, developments in warmer climate countries such as Brazil are also considering the application of this technology as a solution to improve thermal performance in buildings. Therefore, investigations to understand the DSF thermal and airflow processes and implication of its use in naturally ventilated buildings under such climates are needed.

The aim of this study is to determine the thermal performance of office buildings with DSF under Brazilian climate conditions. Firstly, the key parameters affecting the thermal performance of buildings with DSF are identified through critical literature reviews. Using an office building as a reference model, computational thermal dynamic simulations are performed to demonstrate the influence of each individual key parameter on the building's thermal behaviour. From the findings of the parametric analysis, optimized models that utilise a combination of solutions to maximize the building thermal performance are developed and analysed. Finally, acceptable thermal comfort levels of the optimized model in different Brazilian climatic regions and periods of the year are determined.

This study evaluated the key parameters affecting the thermal performance of buildings with DSF, including: the significance of material selections in design solutions to maximize airflow through the building; the prevention of unintentional reverse flow on the upper floors and maintenance of balanced airflow rates across all floors; the impact of solar incidence and wind conditions on the DSF's thermal performance.

Results from the simulations of the optimized model under different bioclimatic zones of Brazil indicated that in most parts of the country the thermal comfort acceptance levels are as low as 60%, especially in the hotter areas of centre west regions, coastal areas and north of the country.

The outcomes of this research provide insight and understanding on the functioning of the DSF in naturally ventilated buildings in warm and hot climates. DSFs in naturally ventilated buildings under Brazilian climates generally presented lower thermal acceptability when compared to single skin models due to the high outside temperatures and the airflow resistance caused by the application of the second skin. Their application will therefore not have direct benefit to the thermal performance.

ABSTRACT.....	i
CONTENTS.....	ii
LIST OF TABLES.....	v
LIST OF FIGURES.....	vi
LIST OF APPENDICES.....	xi
ACRONYMS.....	xiv
ACKNOWLEDGEMENTS.....	xv
DECLARATION.....	xvi
CHAPTER 1. INTRODUCTION.....	1
1.1 Background.....	2
1.1.1 Introduction.....	2
1.1.2 Double skin façade evolution.....	3
1.1.3 Application of double skin façade in warm climates.....	3
1.1.4 The Brazilian context.....	5
1.2 Rationale.....	7
1.3 Scope of the research.....	8
1.4 Research aim and objectives.....	9
1.5 Thesis structure.....	9
CHAPTER 2. DOUBLE SKIN FAÇADE AND KEY PARAMETERS.....	11
2.1 Overview of studies on double skin façades.....	12
2.2 Double skin façade working principle.....	13
2.3 Façade design parameters.....	17
2.3.1 Height of the cavity/number of floors.....	17
2.3.2 Structure.....	19
2.3.3 Cavity depth.....	21
2.3.4 Cavity openings.....	22
2.3.5 Outer skin glazing properties.....	23
2.3.6 Shading device.....	26
2.4 Building parameters.....	29
2.4.1 Inner skin materials.....	29
2.4.2 Window to wall opening ratio.....	31
2.5 Site parameters.....	33
2.5.1 Solar irradiance and orientation.....	33
2.5.2 Wind speed and direction.....	36
2.5.3 Outdoor air temperature and humidity.....	37
2.6 Chapter summary.....	38
CHAPTER 3. CLIMATIC CONTEXT AND PERFORMANCE EVALUATION.....	42
3.1 The climatic context.....	43
3.1.1 The Brazilian climates.....	43
3.1.2 Climate characteristics of representative cities.....	45
Zone 1 - Curitiba city.....	47
Zone 2 - Piracicaba city.....	48
Zone 3 - Florianopolis city.....	49
Zone 4 – Brasilia city.....	50
Zone 5 – Niteroi city.....	51
Zone 6 – Campo Grande city.....	52
Zone 7 – Picos city.....	53
Zone 8 – Rio de Janeiro city.....	54
3.1.3 Climatic potential for natural ventilation.....	55
3.2 Building thermal performance evaluation.....	56
3.2.1 Thermal comfort.....	57

3.2.2	Computational simulation	60
	Computational fluid dynamic (CFD) simulation software	61
	Building dynamic thermal simulation software	63
	IESVE and FloVENT simulation tools: the model verification	64
3.3	Chapter summary.....	66
CHAPTER 4. RESEARCH METHODOLOGY		68
4.1	Research methodology outline	69
4.2	Development of base case model.....	71
4.2.1	Building characterization	72
4.2.2	Double skin façade characterization	74
4.3	Simulations and analyses procedures	75
4.3.1	Modelling processes	76
	Modelling on IESVE	76
	IESVE initial analysis and modelling modifications	77
	Modelling on FloVENT (CFD)	78
	Modelling simplifications	80
4.3.2	Simulations procedures.....	82
4.3.3	Presentation of results	83
4.4	Findings from base case model.....	84
4.4.1	Results of base case model.....	84
4.4.2	Verification of base case model results	88
4.5	Design parameters definitions	90
4.6	Site parameters definitions	95
CHAPTER 5. PARAMETRIC ANALYSIS: RESULTS AND DISCUSSIONS.....		97
5.1	Introduction	98
5.2	Design parameters.....	99
5.2.1	Group A: maximization of airflow	100
	Cavity width.....	100
	Cavity bottom opening	100
	Windows opening position	101
5.2.2	Group B: shading device and skins materials.....	102
	Shading device.....	102
	Inner skin material.....	103
5.2.3	Group C: reverse flows on top floors.....	104
	Cavity extension above roof.....	104
	Upper windows closed	104
5.2.4	Group D: balanced flows on all floors	105
	Tapered skin	105
	Windows size	105
5.2.5	Thermal comfort acceptance.....	107
5.3	Results of CFD verification.....	109
5.4	Optimized cases.....	111
5.5	Building dimension parameters.....	113
5.5.1	Group E: building shape.....	114
5.6	Site parameters.....	115
5.6.1	Group F: Level of solar irradiance and angle.....	116
5.6.2	Group G: Wind conditions	120
5.7	Chapter summary.....	123
CHAPTER 6. THERMAL ACCEPTANCE UNDER BRAZILIAN CLIMATES: RESULTS AND DISCUSSIONS		126
6.1	Introduction	127
6.2	Bioclimatic zone 1 – Curitiba.....	128
6.3	Bioclimatic zone 2 – Piracicaba	130

6.4	Bioclimatic zone 3 – Florianopolis.....	132
6.5	Bioclimatic zone 4 – Brasilia	134
6.6	Bioclimatic zone 5 – Niteroi.....	136
6.7	Bioclimatic zone 6 – Campo Grande	138
6.8	Bioclimatic zone 7 – Picos	140
6.9	Bioclimatic zone 8 – Rio de Janeiro.....	142
6.10	Chapter summary and remarks	143
CHAPTER 7. CONCLUSIONS.....		147
7.1	Introduction	148
7.2	Reviewing the objectives.....	148
7.3	Research contributions and impacts.....	150
7.4	Limitations of the research.....	152
7.5	Directions for future research.....	153
REFERENCES.....		156
APPENDIX A - Mean monthly airflow across the cavity and floors of the building		163
APPENDIX B - Calculation of window areas		180
ANNEX.....		181

LIST OF TABLES

Table 2.1 – Summary of research on ‘cavity height’ and key findings	19
Table 2.2 – Summary of research on ‘structure’ and key findings	21
Table 2.3 – Summary of research on ‘cavity depth’ and key findings	22
Table 2.4 – Summary of research on ‘cavity openings’ and key findings	23
Table 2.5 – Summary of research on ‘outer skin glazing properties’ and key findings	26
Table 2.6 – Summary of research on ‘shading device’ and key findings.....	28
Table 2.7 – Summary of research on ‘Inner skin materials’ and key findings	31
Table 2.8 – Summary of research on ‘WWR of openings’ and key findings.....	32
Table 2.9 – Summary of research on ‘orientation and solar irradiance’ and key findings	35
Table 2.10 – Summary of research on ‘wind speed and direction’ and key findings.....	37
Table 2.11 – Summary of research on ‘outdoor air temperature and humidity’ and key findings	38
Table 3.1 - Passive strategies recommendations for the 8 bioclimatic zones in Brazil	45
Table 3.2 – Monthly percentages of time in which natural ventilation is recommended according to psychometric analysis	55
Table 3.3 – Increase in acceptable operative temperature limits in the adaptive comfort approach resulting from increasing air speed above 0.3m/s.	59
Table 4.1 – Building model characterisation	73
Table 4.2 – Profile of internal heat gains	74
Table 4.3 – Specifications of the solar radiation defined for the FloVENT model	79
Table 4.4 – Maximum cell size defined for each region.....	79
Table 4.5 – Issues and strategies identified from the simulation of the base case model	91
Table 4.6 - Properties of the materials applied to the shading device	92
Table 4.7 - Parameters and variables defined for simulations.....	94
Table 4.8 - Parameters and variables defined for simulations of group E	95
Table 4.9 - Parameters and variables defined for simulations.....	96
Table 5.1 - Parameters and variables tested (Groups A to D – Design parameters).....	99
Table 5.2 – Effect of design parameters to annual thermal comfort.....	108
Table 5.3 - Parameters and variables tested (group E – Building dimension parameters)	114
Table 5.4 - Parameters and variables tested (Groups F and G – Site parameters)	115
Table 6.1 – Summary of thermal acceptance conditions of cases under bioclimatic zone 1 ...	130
Table 6.2 – Summary of thermal acceptance conditions of cases under bioclimatic zone 2 ...	132
Table 6.3 – Summary of thermal acceptance conditions of cases under bioclimatic zone 3 ...	134
Table 6.4 – Summary of thermal acceptance conditions of cases under bioclimatic zone 4 ...	136
Table 6.5 – Summary of thermal acceptance conditions of cases under bioclimatic zone 5 ...	138
Table 6.6 – Summary of thermal acceptance conditions of cases under bioclimatic zone 6 ...	140
Table 6.7 – Summary of thermal acceptance conditions of cases under bioclimatic zone 7 ...	142
Table 6.8 – Summary of thermal acceptance conditions of cases under bioclimatic zone 8 ...	143
Table 6.9 – Summary of thermal acceptance conditions of all cases under all bioclimatic zones	144

LIST OF FIGURES

Figure 1.1 - Annual mean daily solar irradiation in the Brazilian territory and comparison with other countries. Source: Martins and Pereira (2011).	7
Figure 2.1 - Heat transfer and airflow mechanisms occurring in the DSF and the adjacent office floor	14
Figure 2.2 – Schematic representation of pressure gradients inside the cavity and outside the building. Source: adapted from CIBSE (2005).	15
Figure 2.3 – DSF with thermal storage space above the cavity proposed by Ding et al. (2005).	18
Figure 2.4 – Classification of DSF structure: (a) box window, (b) shaft-box, (c) corridor and (d) multi-storey	20
Figure 2.5 – DSF performance according to the glazing characteristics by Pérez-Grande et al. (2005)	24
Figure 2.6 – Performance of a building with DSF under variations of the glazing properties resulting from study by Chan et al. (2009)	25
Figure 2.7- Variations of the shading device (a) position proposed by Gratia and De Herde (2007b) and (b) angle evaluate by Ji et al. (2007).	27
Figure 2.8 – Models using thermal mass (concrete) proposed by Fallahi et al. (2010)	30
Figure 2.9 – Percentage of reflection, absorption and transmission in relation to solar angle reaching the façade by Mulyadi (2012)	34
Figure 3.1 - Brazilian map with the incidence of eight bioclimatic zones	44
Figure 3.2 - Brazilian map with population distribution in 2010	44
Figure 3.3 – Givoni’s psychometric chart used by Analysis Bio software	46
Figure 3.4 - Monthly average temperature and global radiation of Curitiba (zone 1)	47
Figure 3.5 - Wind rose of Curitiba (zone 1)	47
Figure 3.6 – Dry-bulb temperatures during January and July for Curitiba (zone 1)	47
Figure 3.7 - Monthly average temperature and global radiation of Piracicaba (zone 2)	48
Figure 3.8 - Wind rose of Piracicaba (zone 2)	48
Figure 3.9 – Dry-bulb temperatures during January and July for Piracicaba (zone 2)	48
Figure 3.10 - Monthly average temperature and global radiation of Florianopolis (zone 3)	49
Figure 3.11 – Wind rose of Florianopolis (zone 3)	49
Figure 3.12 – Dry-bulb temperatures during January and July for Florianopolis (zone 3)	49
Figure 3.13 - Monthly average temperature and global radiation of Brasilia (zone 4)	50
Figure 3.14 – Wind rose of Brasilia (zone 4)	50
Figure 3.15 – Dry-bulb temperatures during January and July for Brasilia (zone 4)	50
Figure 3.16 - Monthly average temperature and global radiation of Niteroi (zone 5)	51
Figure 3.17 – Wind rose of Niteroi (zone 5)	51
Figure 3.18 – Dry-bulb temperatures during January and July for Niteroi (zone 5)	51
Figure 3.19 - Monthly average temperature and global radiation of Campo Grande (zone 6) ...	52
Figure 3.20 – Wind rose of Campo Grande (zone 6)	52
Figure 3.21 – Dry-bulb temperatures during January and July for Campo Grande (zone 6)	52
Figure 3.22 - Monthly average temperature and global radiation of Picos (zone 7)	53
Figure 3.23 – Wind rose of Picos (zone 7)	53
Figure 3.24 – Dry-bulb temperatures during January and July for Picos (zone 7)	53

Figure 3.25 - Monthly average temperature and global radiation of Rio de Janeiro (zone 8)	54
Figure 3.26 – Wind rose of Rio de Janeiro (zone 8)	54
Figure 3.27 – Dry-bulb temperatures during January and July for Rio de Janeiro (zone 8).....	54
Figure 3.28 - Acceptable operative temperature ranges for naturally ventilated spaces from ASHRAE 55 (2013)	59
Figure 4.1 - Methodology scheme	69
Figure 4.2 – Building model	75
Figure 4.3 - Airflow network node diagram	76
Figure 4.4 – Operative temperatures resulted for office room on the 1 st floor, when 6 thermal zones are applied.....	77
Figure 4.5 - Operative temperatures resulted for office room on the 1 st floor, when 2 thermal zones are applied.....	78
Figure 4.6 – CFD base case model in perspective	80
Figure 4.7 – CFD base case model with grid definition	80
Figure 4.8 - Annual mean outside and cavity temperature distributions and direct radiation on the north façade	85
Figure 4.9 – Graphical representation of descriptive statics for the airflow through the cavity in each month.....	85
Figure 4.10 – Annual mean airflows in and out of each floor for the base case.....	86
Figure 4.11 – Annual mean net airflow for each floor for the base case	86
Figure 4.12 – Annual operative temperatures of the base case (1 st and 10 th floors).....	87
Figure 4.13 - Annual distribution of thermal comfort (%) on each floor of the base case model	87
Figure 4.14 – CFD image of vectors of air speed with detail of the 1st, 2nd and 3rd floors.....	89
Figure 4.15 – Results of base case model simulated on FloVENT	90
Figure 4.16 - Pictorial diagrams of the design parameters simulation scenarios of groups A to D	94
Figure 4.17 - Pictorial diagrams of the building shape parameters simulation scenarios	95
Figure 4.18 - Pictorial diagrams of the site parameters simulation scenarios	96
Figure 5.1 - Annual mean of the net airflow for each floor for parameter 'cavity width'	100
Figure 5.2 - Annual mean of the net airflow for each floor for parameter 'cavity bottom opening'	101
Figure 5.3 - Annual mean of the net airflow for each floor for parameter 'windows position' ..	101
Figure 5.4 - Cavity temperature for the alternatives of case scenario B.1 'shading device'	102
Figure 5.5 - Annual mean of the net airflow for each floor for parameter 'shading device'	103
Figure 5.6 - Annual mean of the net airflow for each floor for parameter 'inner skin material' .	103
Figure 5.7 - Annual mean of the net airflow for each floor for parameter 'cavity extension above roof'	104
Figure 5.8 - Annual mean of the net airflow for each floor for parameter 'upper windows closed'	105
Figure 5.9 - Annual mean of the net airflow for each floor for parameter 'tapered skin'.....	105
Figure 5.10 - Annual mean of the net airflow for each floor for parameter 'windows size'	106
Figure 5.11 – Net airflow for each floor for parameter 'cavity depth' simulated on CFD	109
Figure 5.12 – Net airflow for each floor for parameter 'cavity bottom opening' simulated on CFD	109

Figure 5.13 – Net airflow for each floor for parameter ‘windows position’ simulated on CFD ..	110
Figure 5.14 – Net airflow for each floor for parameter ‘cavity extension above the building roof’ simulated on CFD	110
Figure 5.15 – Net airflow for each floor for parameter ‘tapered skin’ simulated on CFD	111
Figure 5.16 – Annual mean of the net airflow for each floor of ‘Optimized model 1’	112
Figure 5.17 - Annual operative temperatures of ‘Optimized model 1’ (5 th floor).....	112
Figure 5.18 – Annual mean of the net airflow for each floor of ‘Optimized model 2’	113
Figure 5.19 - Annual operative temperatures of ‘Optimized model 2’ (5 th floor)	113
Figure 5.20 - Annual mean of the net airflow for each floor for parameter ‘number of floors’ ..	115
Figure 5.21 - Annual mean of the net airflow for each floor for parameter ‘building depth’	115
Figure 5.22- Difference of temperature between the cavity and the outside air in relation to the solar incidence on the DSF	117
Figure 5.23 - Airflow on the 5 th floor of the model as a result of the solar incidence on the DSF	117
Figure 5.24 - Average of solar incidence on the façade surface for solar angles 15 - 20°, 45 - 50° and 85 - 90°	117
Figure 5.25 - Annual mean net airflow of the 5 th floor in three orientations	118
Figure 5.26 - Airflow occurring on the 5 th floor according to the time of the day during the occupancy hours	119
Figure 5.27 - Difference in airflow rates for the cavity and the rooms in a cloudy (07-Sep) and a sunny days (17-Sep) during the occupancy hours	120
Figure 5.28 - Diagram of static pressures created at different sides of the building according to wind direction	120
Figure 5.29 – Difference in airflow for winds speed varying from 2 to 6 m/s, for DSF facing the wind	121
Figure 5.30 – Difference in airflow for winds speed varying from 2 to 6 m/s, for DSF protected from wind	121
Figure 5.31 – Difference in airflow for winds speed varying from 1 to 4m/s, for DSF parallel to the wind	122
Figure 5.32 – Difference in airflow for winds speed varying from 2 to 6 m/s, for wind blowing at 45°	122
Figure 5.33 – Difference in airflow for winds speed varying from 2 to 6 m/s, for wind blowing at 135°	122
Figure 6.1 - Airflow mechanisms when south windows are open or closed	127
Figure 6.2 - Annual operative temperatures of optimized model under bioclimatic zone 1 plotted on the ASHRAE (2013) thermal comfort matrix	129
Figure 6.3 - Hourly thermal acceptance in the optimized building model with DSF in bioclimatic zone 1	129
Figure 6.4 - Annual operative temperatures of single skin model under bioclimatic zone 1 plotted on the ASHRAE (2013) thermal comfort matrix	129
Figure 6.5 - Hourly thermal acceptance in the single skin façade building model in bioclimatic zone 1	129
Figure 6.6 - Annual operative temperatures of optimized model under bioclimatic zone 2 plotted on the ASHRAE (2013) thermal comfort matrix	131
Figure 6.7 - Hourly thermal acceptance in the optimized building model with DSF in bioclimatic zone 2	131

Figure 6.8 - Annual operative temperatures of single skin model under bioclimatic zone 2 plotted on the ASHRAE (2013) thermal comfort matrix	131
Figure 6.9 - Hourly thermal acceptance in the single skin façade building model in bioclimatic zone 2.....	131
Figure 6.10 - Annual operative temperatures of optimized model under bioclimatic zone 3 plotted on the ASHRAE (2013) thermal comfort matrix	133
Figure 6.11 - Hourly thermal acceptance in the optimized building model with DSF in bioclimatic zone 3.....	133
Figure 6.12 - Annual operative temperatures of single skin model under Bioclimatic zone 3 plotted on the ASHRAE (2013) thermal comfort matrix	133
Figure 6.13 - Hourly thermal acceptance in the single skin façade building model in bioclimatic zone 3.....	133
Figure 6.14 – Annual operative temperatures of optimized model under ‘Bioclimatic zone 4’ plotted on the ASHRAE (2013) thermal comfort matrix	135
Figure 6.15 - Hourly thermal acceptance in the optimized building model with DSF in bioclimatic zone 4.....	135
Figure 6.16 – Annual operative temperatures of single skin model under Bioclimatic zone 4 plotted on the ASHRAE (2013) thermal comfort matrix	136
Figure 6.17 – Hourly thermal acceptance in the single skin façade building model in bioclimatic zone 4.....	136
Figure 6.18 – Annual operative temperatures of optimized model under ‘Bioclimatic zone 5’ plotted on the ASHRAE (2013) thermal comfort matrix	137
Figure 6.19 - Hourly thermal acceptance in the optimized building model with DSF in bioclimatic zone 5.....	137
Figure 6.20 – Annual operative temperatures of single skin model under Bioclimatic zone 5 plotted on the ASHRAE (2013) thermal comfort matrix	138
Figure 6.21 – Hourly thermal acceptance in the single skin façade building model in bioclimatic zone 5.....	138
Figure 6.22 – Annual operative temperatures of optimized model under ‘Bioclimatic zone 6’ plotted on the ASHRAE (2013) thermal comfort matrix	139
Figure 6.23 – Hourly thermal acceptance in the optimized building model with DSF in bioclimatic zone 6.....	139
Figure 6.24 – Annual operative temperatures of single skin model under Bioclimatic zone 6 plotted on the ASHRAE (2013) thermal comfort matrix	140
Figure 6.25 – Hourly thermal acceptance in the single skin façade building model in bioclimatic zone 6.....	140
Figure 6.26 – Annual operative temperatures of optimized model under bioclimatic zone 7 plotted on the ASHRAE (2013) thermal comfort matrix	141
Figure 6.27 – Hourly thermal acceptance in the optimized building model with DSF in bioclimatic zone 7.....	141
Figure 6.28 – Annual operative temperatures of single skin model under bioclimatic zone 7 plotted on the ASHRAE (2013) thermal comfort matrix	141
Figure 6.29 – Hourly thermal acceptance in the single façade skin building model in bioclimatic zone 7.....	141
Figure 6.30 - Annual operative temperatures of optimized model under ‘Bioclimatic zone 8’ plotted on the ASHRAE (2013) thermal comfort matrix	142
Figure 6.31 - Hourly thermal acceptance in the optimized building model with DSF in bioclimatic zone 8.....	142

Figure 6.32 - Annual operative temperatures of single skin model under bioclimatic zone 8 plotted on the ASHRAE (2013) thermal comfort matrix	143
Figure 6.33 - Hourly thermal acceptance in the single skin building model in bioclimatic zone 8	143
Figure 6.34 – Brazilian bioclimatic zones with indication of level of thermal acceptability	145

LIST OF APPENDICES

APPENDIX A

Appendix A. 1 - Monthly mean of difference of temperature between the cavity and the outside air – Base case	164
Appendix A. 2 - Monthly mean of airflow on the top of the cavity – Base case	164
Appendix A. 3 - Monthly mean of the net airflow for each floor – Base case	164
Appendix A. 4 - Monthly mean of difference of temperature between the cavity and the outside air - Case Cavity depth – 25cm.....	165
Appendix A. 5 - Monthly mean of airflow on the top of the cavity – Case Cavity depth – 25cm	165
Appendix A. 6 - Monthly mean of the net airflow for each floor – Case Cavity depth – 25cm	165
Appendix A. 7 - Monthly mean of difference of temperature between the cavity and the outside air– Case Cavity depth – 100cm.....	166
Appendix A. 8 - Monthly mean of airflow on the top of the cavity – Case Cavity depth – 100cm	166
Appendix A. 9 - Monthly mean of the net airflow for each floor – Case Cavity depth – 100cm	166
Appendix A. 10 - Monthly mean of difference of temperature between the cavity and the outside air – Case Cavity bottom opening – Bottom closed	167
Appendix A. 11 - Monthly mean of airflow on the top of the cavity – Case Cavity bottom opening – Bottom closed.....	167
Appendix A. 12 - Monthly mean of the net airflow for each floor – Case Cavity bottom opening – Bottom closed	167
Appendix A. 13 - Monthly mean of difference of temperature between the cavity and the outside air – Case Windows position – South windows on the bottom, north windows on the top of the wall	168
Appendix A. 14 - Monthly mean of airflow on the top of the cavity – Case Windows position – South windows on the bottom, north windows on the top of the wall	168
Appendix A. 15 - Monthly mean of the net airflow for each floor – Case Windows position – South windows on the bottom, north windows on the top of the wall	168
Appendix A. 16 - Monthly mean of difference of temperature between the cavity and the outside air – Case Shading devices - Concrete.....	169
Appendix A. 17 - Monthly mean of airflow on the top of the cavity – Case Shading devices - Concrete.....	169
Appendix A. 18 - Monthly mean of the net airflow for each floor – Case Shading devices - Concrete.....	169
Appendix A. 19 - Monthly mean of difference of temperature between the cavity and the outside air – Case Shading devices - Metal.....	170
Appendix A. 20 - Monthly mean of airflow on the top of the cavity – Case Shading devices - Metal.....	170
Appendix A. 21 - Monthly mean of the net airflow for each floor – Case Shading devices - Metal.....	170
Appendix A. 22 - Monthly mean of difference of temperature between the cavity and the outside air – Case Inner skin material – Insulation applied to the inner surface and black painting on the outer surface.....	171
Appendix A. 23 - Monthly mean of airflow on the top of the cavity – Case Inner skin material – Insulation applied to the inner surface and black painting on the outer surface.....	171

Appendix A. 24 - Monthly mean of the net airflow for each floor – Case Inner skin material – Insulation applied to the inner surface and black painting on the outer surface.....	171
Appendix A. 25 - Monthly mean of difference of temperature between the cavity and the outside air – Case Cavity extension above roof - 1.75m above roof.....	172
Appendix A. 26 - Monthly mean of airflow on the top of the cavity – Case Cavity extension above roof - 1.75m above roof.....	172
Appendix A. 27 - Monthly mean of the net airflow for each floor – Case Cavity extension above roof - 1.75m above roof.....	172
Appendix A. 28 - Monthly mean of difference of temperature between the cavity and the outside air – Case Cavity extension above roof – 3.50m above roof.....	173
Appendix A. 29 - Monthly mean of airflow on the top of the cavity – Case Cavity extension above roof – 3.50m above roof.....	173
Appendix A. 30 - Monthly mean of the net airflow for each floor – Case Cavity extension above roof – 3.50m above roof.....	173
Appendix A. 31 - Monthly mean of difference of temperature between the cavity and the outside air – Case Cavity extension above roof – 5.25m above roof.....	174
Appendix A. 32 - Monthly mean of airflow on the top of the cavity – Case Cavity extension above roof – 5.25m above roof.....	174
Appendix A. 33 - Monthly mean of the net airflow for each floor – Case Cavity extension above roof – 5.25m above roof.....	174
Appendix A. 34 - Monthly mean of difference of temperature between the cavity and the outside air – Case Upper windows closed – Window of 10th floor closed.....	175
Appendix A. 35 - Monthly mean of airflow on the top of the cavity – Case Upper windows closed – Window of 10th floor closed.....	175
Appendix A. 36 - Monthly mean of the net airflow for each floor – Case Upper windows closed – Window of 10th floor closed.....	175
Appendix A. 37 - Monthly mean of difference of temperature between the cavity and the outside air – Case Upper windows closed – Windows of 9th and 10th floor closed.....	176
Appendix A. 38 - Monthly mean of airflow on the top of the cavity – Case Upper windows closed – Windows of 9th and 10th floor closed.....	176
Appendix A. 39 - Monthly mean of the net airflow for each floor – Case Upper windows closed – Window of 9th and 10th floor closed.....	176
Appendix A. 40 - Monthly mean of difference of temperature between the cavity and the outside air – Case Tapered cavity – Inclined outer skin.....	177
Appendix A. 41 - Monthly mean of airflow on the top of the cavity – Case Tapered cavity – Inclined outer skin.....	177
Appendix A. 42 - Monthly mean of the net airflow for each floor – Case Tapered cavity – Inclined outer skin.....	177
Appendix A. 43 - Monthly mean of difference of temperature between the cavity and the outside air – Case Tapered cavity – Inclined inner skin.....	178
Appendix A. 44 - Monthly mean of airflow on the top of the cavity – Case Tapered cavity – Inclined inner skin.....	178
Appendix A. 45 - Monthly mean of the net airflow for each floor – Case Tapered cavity – Inclined inner skin.....	178
Appendix A. 46 - Monthly mean of difference of temperature between the cavity and the outside air – Case Windows size – Calculated windows size.....	179
Appendix A. 47 - Monthly mean of airflow on the top of the cavity – Case Windows size – Calculated windows size.....	179

Appendix A. 48 - Monthly mean of the net airflow for each floor – Case Windows size –
Calculated windows size 179

APPENDIX B

Appendix B. 1 – Windows size calculation - Optimized case 180
Appendix B. 2 – Windows size calculation – 5 floors case 180
Appendix B. 3 – Windows size calculation – 15 floors case 180
Appendix B. 4 – Windows size calculation – 20 floors case 180

ACRONYMS

DSF	Double skin façade
NPL	Neutral pressure line
SC	Shading device
CFD	Computational fluid dynamics
BES	Building energy simulation
WWR	Window to wall ratio
ETTV	Thermal transfer component value
ACH	Air changes per hour
TRY	Test reference year
PMV/PPD	Predicted mean vote/percentage of people dissatisfied
SSF	Single skin façade

ACKNOWLEDGEMENTS

First of all, my gratitude goes to my principal supervisor, Dr. Kenneth Ip, who believed in my idea and encouraged me to achieve this goal. His kind support and advice are greatly appreciated. Thank you for the valuable guidance during these years. I have been amazingly fortunate to have you as my supervisor. I owe you a lot for this.

My sincere thanks also go to my second supervisor Dr. Ryan Southall, for his assistance, many insightful discussions and suggestions. Your simulation and research expertise contributed a lot to my work.

My appreciation also goes to Dr. Poorang Piroozfar who gave his valuable time and effort at the beginning of this journey.

Many thanks to staff members of the Doctoral College and School of Environment and Technology of the University of Brighton for their cooperation throughout this process. I also would like to thank CNPq for the financial support and scholarship.

My time in Brighton was enjoyable in a big part due to the many friends that became part of my life. Thank you Francesco Pomponi, Matt Turley, Adeni Abigo, Janet Yakubu, Laura D'amico, Abdullah Alkharmany, Yahya Ibraheem, Nagham Al Qaysi, Dr. Magda Grove, and you guys of EPHReG. Thank you all for all the great moments that we have shared.

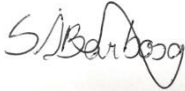
Thank you Brighton for being an open, fun and 'warm' city.

Finally, special thanks go to my husband and my family overseas, who never failed to show moral support and encouragement.

I dedicate this thesis to my country, to have a rising and bright future, so we can live and work in comfortable buildings, where the user and the sustainable design are priorities.

DECLARATION

I declare that the research contained in this thesis, unless otherwise formally indicated within the text, is the original work of the author. The thesis has not been previously submitted to this or any other university for a degree, and does not incorporate any material already submitted for a degree.

Signed:  _____

Dated: 14/01/2016

Chapter One

Introduction

This Chapter provides an overview of the background for double skin façades, its application in warm regions and the relevance of the study to Brazil. It also sets out the research rationale, scope, aim, objectives and structure of the thesis.

1.1 Background

1.1.1 Introduction

The incident solar radiation on the building surfaces, the high outside air temperatures entering the building through the openings and the heat transmission through the building fabric are some of the reasons to the increasing building indoor temperature to a level that causes discomfort in warm and hot climates. Fundamentally, when there is a gradual accumulation of heat inside the building that is not being removed or reduced it is said that the building is overheating. In hot and tropical climates, the overheating risk can occur during the whole year and it is often addressed by installing mechanical cooling, which leads to additional running costs and energy use, and increasing in carbon emissions (CIBSE, 2010).

The use of air conditioning was being extensively applied to buildings in hot and tropical climates as a strategy to mitigate the uncomfortable environment until 1970s and 1980s when the energy shortages triggered global awareness about energy efficiency and sustainable design in buildings. From that, professional designers started to raise interest in the application of passive architectural design solutions with the aim to improve the buildings' indoor thermal conditions to reduce or mitigate the energy demands. In a 'passive building' the indoor environment is regulated by its architectural design and components, making use of the resources available in the immediate surrounding environment in order to avoid the need of mechanical heating and cooling systems (Nayak and Prajapati, 2006; Nicol et al., 2012).

Nicol et al. (2012) identified the 'disconnection' of the building interior from its surrounding environment by unsuitable envelopes as one of the main reasons for the poor quality of the indoor conditions which results in user discomfort (Sadineni et al., 2011; Ochoa and Capeluto, 2009; IEA, 2013a; b). The envelope not only forms the primary thermal barrier between the interior and the exterior, playing an important role in determining levels of comfort and ventilation in the building, but it is also an important aspect of its aesthetics and image (Sadineni et al., 2011).

Within this context, the double skin façades (DSFs) are gaining recognition as a passive strategy technology that while giving a modern transparent appearance to office buildings, has been claimed to be able to moderate the indoor thermal conditions either for cold and hot areas and therefore reducing energy demands. It consists of an additional fully glazed external skin installed over the conventional building façade, forming an air cavity in which sunshade devices are often installed to protect the

internal rooms from overheating caused by excessive solar heat gains (Oesterle et al., 2001).

1.1.2 Double skin façade evolution

The DSF was firstly described by the director of the Industrial Museum of Brussels in 1849, Jean-Baptist Jobard, as an architectural solution that should allow warm air circulation within the cavity in winter. Examples of non-ventilated DSFs were adopted in the vernacular architecture of temperate climates, in which the cavity was used as a buffer zone. At beginning of 1900s an operable cavity opening was applied to the Steiff Machine Hall building in Germany, which can be regarded as an early example of a naturally ventilated DSF. In 1929, Le Corbusier designed DSF for the La Cité de Refuge claiming that the ventilated cavity would prevent heat transmission through the building façade and therefore improve the building thermal comfort conditions (Saelens, 2002).

The energy crises of the 1970's and 1980's motivated improvements on the solution and mechanically ventilated façades were increasingly implemented in European buildings (Saelens, 2002). From then on, the increasing environmental concerns and the positive corporate image of 'green buildings' strongly influenced the proliferation of DSFs. The UCB centre, built in Brussels in 1980's was one of the first DSFs to be reported with the application of shading devices within the south facing cavity as an attempt to mitigate the heat gains during the summer without conflicting the transparency design philosophy (Kragh, 2001).

Over the years, the DSF design has been progressively evolved as a solution that takes into account the aspiration for transparent aesthetic façades combined with environmental functionalities. Nowadays over 50% of DSFs are located in continental and northern European countries, of which 20% are in Germany, one of the first countries that started to develop and apply this concept. Japan also accounts for a large percentage, about 13% and the rest of the buildings with DSF are in Canada, USA, Australia and other parts of the world (Anđelković et al., 2015).

1.1.3 Application of double skin façade in warm climates

Low energy buildings with DSF in European and other moderate climates have adopted specific features such as use of highly insulated building skins, high quality low U-value glazing and heat recovery ventilation in winter, to deliver effective performance during cold months and to enable reduction of heating loads. However, a number of cases have presented poor performance during warmer months caused by

overheating, which consequently increases the cooling loads (Darkwa et al., 2014). In such cases, greater air-conditioning system capacities are needed, and their energy consumptions often exceed the winter heating energy savings. Therefore, the design solution could result in a step backward regarding energy efficiency and the beneficial use of passive solar energy (Streicher et al., 2007; Marques da Silva et al., 2015). This shortcoming has instigated the development of additional features such as sun protection devices, modification of façade geometry and ventilation schemes in order to achieve more effective performance during the summer periods (Gratia and De Herde, 2004b; Eicker et al., 2008). From that, different modes of DSF operations for both winter and summer conditions have been considered (Mingotti et al., 2011; Gratia and De Herde, 2007a).

The potential to reduce cooling loads during the summer in highly glazed buildings has motivated the adoption of the DSF technology in modern cities in warm and even hot climates as an iconic successful corporate image associated with sustainability. With these impetuses, a number of experimental and numerical studies about the viability of implementation of DSF have been performed considering the possibilities of using the technology in countries with warmer climates such as in China (Zhang et al., 2010), Spain (Torres et al., 2007), Singapore (Chou et al., 2009), United Arab Emirates (Radhi et al., 2013), India (Singh et al., 2011) and Malaysia (Rahmani et al., 2012).

Although most of the studies on DSF in warm and hot climates are based on air conditioned models, recently there is a growing interest in the application of the solution as a potential driver of ventilation to the building's user spaces. The re adoption of natural ventilation in buildings is obvious by their advantages over mechanical ventilation systems in terms of energy and environmental benefits, improved indoor air quality, reduced implementation and operational costs, and increased occupant satisfaction (Day and Gunderson, 2015; Aflaki et al., 2015; Wood and Salib, 2013).

In naturally ventilated buildings, the flow of air within the DSF cavity is driven by the thermal buoyancy force as a function of the temperature difference between the warmer cavity air and the surrounding cooler air. The hotter cavity air functions as a thermal chimney that induce the suction of cooler air from the outside driving a continuous convective air stream through the building. Thus, the higher the increase of cavity temperatures in relation to the outside air, the higher the air movement created within the building, which would increase occupant satisfaction in warm and hot areas. However, due to the complex interactions between the façade and the building, the application of natural ventilation for cooling proposes in hot climates may require

special features in the building design and operation, such as solar control devices to prevent excessive heat gains, appropriate form and shape of architectural building plan combined with adequate orientation according to sun and wind exposures (CIBSE, 2005).

Although being seen as potential a sustainable design solution to office buildings in warm and hot climates, the current inefficient design of the technology often add significant heat gains in such buildings. Extreme increasing of the temperature inside the cavity has been identified as a critical matter in DSF buildings placed in warm climates. This can be attributed to the limited cooling potential by the prevailing climate and by occupant expectations of thermal comfort (CIBSE, 2005). Although the greenhouse effect within the cavity can be moderately advantageous to the façade functioning by inducing ventilation through thermal buoyancy within the vertical cavity, the faulty operation of the façade openings are the most critical causes that contribute to uncomfortable temperatures in the buildings (Hamza, 2004; Gratia and De Herde, 2007a). Although some experiences has shown uncomfortable temperatures occurring during the hottest moments of the year in some climate conditions, no available research applying specific features to reduce the overheating risk in such buildings has been conducted.

Therefore, the DSF has been proposed as a passive strategy that if adequately designed may be able to improve the thermal performance of naturally ventilated buildings in hot climates (CIBSE, 2005; Nasrollahi and Salehi, 2015). Although the technology has recently been a subject of intense investigations, the understanding of its functioning on naturally ventilated buildings can be considered still at its infancy. Moreover, acquiring fundamental principles for the DSF design and operation across a wide range of climatic conditions is still needed (Mingotti et al., 2011; Darkwa et al., 2014).

1.1.4 The Brazilian context

The application of DSF is not common in Brazil despite the increasing demand for improved design and performance of buildings. This can be attributed to the lack of legal standards from governmental bodies, the under-developed building industry and the lack of knowledge pertaining to the technology's design and performance among the majority of the construction companies, designers, façades developers and suppliers (Marcondes, 2010). However, recent regulations (ABNT, 2010; 2013) have encouraged energy efficiency and more efficient design solutions of building systems. The expectations regarding the country's growing economic capability also create a

favourable impetus for the implementation of environmentally attractive design solutions such as DSF, especially in large corporate buildings.

In Brazil, one of the first buildings with DSF was completed in 2008 in Rio de Janeiro city. The same ventilated 60cm-cavity DSF was implemented on all external façades of the building without considering the orientations. The windows are sealed and air conditioned system is used all the year round (Marcondes, 2010). Beyond Rio de Janeiro, the applicability of DSF in office buildings in the federal and other eight capital of states in Brazil was evaluated by Leão et al. (2009) who demonstrated the potential energy savings based on air-conditioned building models.

Brazil presents a wide range of climate conditions that vary from the cold south region, where some similarities with European continental climates are found, to the typical tropical climates in the coastal areas, as a result of its large extension, variations in altitude and precipitation levels. With this great variability of climates, the potential of applicability of the DSF in naturally ventilated buildings is not obviously clear.

The amount of solar incidence is another determinant for the climate characteristics and plays an important role on the level of thermal buoyancy force and the consequent potential of ventilation in the DSF (Kim et al., 2009). As the Brazilian territory is mostly included in the inter-tropical region, it has a great potential to capture solar energy over the entire year. The daily horizontal global solar irradiation is fairly uniform in the territory and greater than those observed in Japan and some European countries, as shown in Figure 1.1. The greatest values for annual mean global solar irradiation are registered in the semi-arid area of Northeast region followed by Midwest and Southern regions. On the other hand, due to the high precipitation levels and low latitude localization, the lowest solar incidences are found for north and south regions, respectively (Martins et al., 2012). The abundance of solar energy resources, which is an essential mean to drive airflow through the DSF, indicates the country has the potential to exploit the DSF technology.

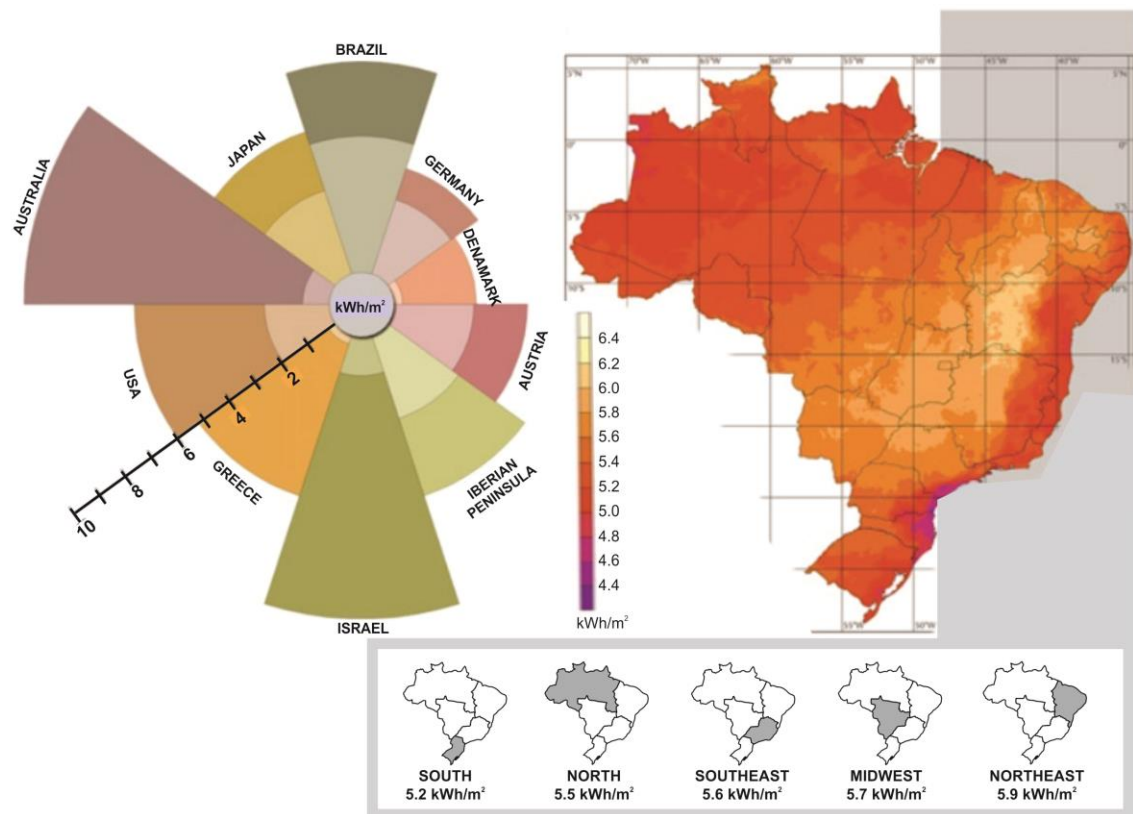


Figure 1.1 - Annual mean daily solar irradiation in the Brazilian territory and comparison with other countries. Source: Martins and Pereira (2011).

1.2 Rationale

The DSF is a complex design solution which, while providing transparent aesthetic of modern office buildings, has the potential to improve a building's thermal performance if appropriate design strategies are applied. However, the complexity of the thermal processes involved in the DSF operation and the numerous aspects to be considered such as the building geometry and materials selections, demand comprehensive and holistic studies, especially when applied to naturally ventilated buildings under warm and tropical climates. Moreover, the majority of the existing studies have been confined to the thermal performance of air conditioned models and focused on temperate climate conditions, where most DSFs are implemented.

In this study, thermal performance is expressed in terms of the occupancy periods during which defined thermal comfort conditions are acceptable or unacceptable. The determination of thermally comfortable or uncomfortable hours provides a means to evaluate whether or not the DSF is a viable solution. Establishing profile of likelihood of thermal comfort will enable understanding of the building's response to the changing outdoor climatic conditions and regulation of indoors conditions.

Currently, there is a lack of studies that investigate the individual or combined influences of architectural configurations together with the effects of surrounding site conditions on the building's thermal behaviour. Many of the current studies have focused on the DSF cavity as an 'isolated' structure, which is often treated as a local feature without taking into account its thermal influence on the user space. Although the occurrence of overheating during the warm and hot seasons has been recognized as a key issue, there is still a lack of understanding and validated design solutions.

The lack of knowledge, guidelines and validated methodology on design and performance prediction has been identified as barriers for the implementation of the DSF. Such issues are hardly addressed in warm climate countries (Shameri et al., 2011; Høseggen et al., 2008) such as in Brazil, especially when applied to naturally ventilated buildings. Therefore, with the purpose of contributing to a holistic view about the viability of implementation of DSF as a passive design solution for a naturally ventilated building with DSF in Brazil, this study aims to answer the following key questions:

What are the influences of architectural configurations and external climates on the thermal performance of naturally ventilated office buildings with DSF?

To what extent will naturally ventilated office buildings with DSF meet the thermal comfort requirements in different climate regions of Brazil?

Although studies have already identified that buildings with DSF under warm and hot climates presented risk of overheating specially during the warmer months, the ventilation promoted by the cavity thermal buoyancy can be able to provide occupant satisfaction due to the increase of air movement through the building. Thus, based on the possibility of applying different DSF design strategies to increase the building thermal performance by enhancing the natural ventilation to avoid overheating within the building, this thesis has the following hypothesis:

Enhancing the natural ventilation through the suitably applied double skin façade can improve the thermal performance of office buildings under Brazilian climates.

1.3 Scope of the research

Apart from thermal issues, there are a number of other considerations in the process of designing a DSF such as acoustic characteristics (Oesterle et al., 2001), night time ventilation (Gratia and De Herde, 2004b), maintenance of shading devices, increased

weight of the building structure, fire regulations and reduction of available floor space (Torres et al., 2007). Furthermore, the costs associated with the design, construction and maintenance, which are considerably higher than a traditional single façade (Oesterle et al., 2001; Poirazis, 2006), is one of the main considerations about the viability of implementation of DSF.

Although these aspects must be addressed when deciding about the implementation of the DSF technology, they are not part of this investigation, which focuses solely on the thermal performance. However, some of these aspects are touched upon in the discussions underpinning the final conclusions.

1.4 Research aim and objectives

The aim of this study is to determine the thermal performance of office buildings with DSF under Brazilian climate conditions.

In order to achieve this aim, the following objectives are developed with reference to office buildings with DSF in Brazil:

- I. To differentiate the characteristics of the Brazilian climates and to identify the corresponding thermal comfort requirements in naturally ventilated office buildings.
- II. To develop a reference model of a naturally ventilated office building appropriate for the DSF application.
- III. To identify and evaluate key parameters governing the building thermal performance.
- IV. To develop optimized naturally ventilated building models with DSF to operate under Brazilian climatic conditions.
- V. To establish the annual thermal comfort acceptability of optimized models under different Brazilian climates.

1.5 Thesis structure

Chapter one provided an overview of the evolution of the DSF and discussed its application in warm regions, indicating Brazil as a country with potential to exploit the DSF technology. It also demonstrated the research rationale, scope, aim and objectives of the thesis.

Chapter two reviews the current body of literature on studies of thermal performance of DSF and it explains the physical working principle of the technology when applied to naturally ventilated buildings. The main findings of the studies are analysed and ordered in three groups of identified parameters affecting the thermal performance of buildings with DSF. The chapter concludes with a set of guidelines for the design of naturally ventilated buildings with DSF in warm climates.

The **third chapter** describes the climatic conditions of the different bioclimatic zones of Brazil evaluating the climatic potential for natural ventilation. It also includes a discussion about the existing comfort criteria and establishes an indicator to evaluate the thermal performance of naturally ventilated buildings models.

Based on the knowledge gained from the literature review, **chapter four** defines the proposed methodology of this study. It describes the process of model development; the key design and site parameters selected to evaluate, the modelling and simulation processes and the procedures used to demonstrate the influence of each individual key parameter on the building's thermal performance.

Chapter five presents the results of the parametric analysis, demonstrating the influence of each individual key parameter on the building's thermal behaviour. It also includes the development and analysis of the optimized models, which utilise a combination of solutions to maximize the building's thermal performance.

Results from simulations of the optimized model of naturally ventilated office building with DSF for the Brazilian bioclimatic zones are presented in **Chapter six**. It establishes the thermal comfort levels of the model under different Brazilian climate conditions at different periods of the year.

Chapter seven summarises and concludes the study based on reflections upon the findings. It also includes the limitations of the research and proposes further studies that may follow from this study.

Chapter Two

Double skin façade and key parameters

This chapter presents an overview of current studies on DSF and introduces the heat exchanges and airflow processes that occur in the cavity. It also critically reviews the state of the art of current body of literature about the thermal and energy performance of the DSF. The studies analysed were divided into three groups to provide a clear and structured understanding of the individual parameters affecting the building thermal performance. The chapter concludes with the main findings from the studies reviewed, informing the development of a base case model and the identification of the key parameters affecting the building thermal performance.

This chapter begins with an overview of studies on general aspects of DSFs followed by a discussion on the fundamentals heat exchange and airflow mechanisms occurring in a building with a DSF. The fundamental thermodynamic principles and terminology applied to buildings were mostly derived from technical standards (ASHRAE, 2009; CIBSE, 2005) which address concepts, examples and calculations applied to generic thermal chimneys found in buildings.

It follows by the main body of computational simulations and experimental studies on DSF reviewed. They are grouped according to their contributions in relation to the parameters influencing the thermal and energy performance of buildings with DSF. Although a number of the studies reviewed used air conditioning models, which reflect the historical use of this type of system, their developed methodologies and findings are significantly relevant in informing the current and future advances of DSF applications in naturally ventilated buildings. Their inclusion is therefore, considered essential to this review. Some of the studies investigated several parameters and were therefore placed in more than one category. For each parameter, the main findings of the related studies that directly or indirectly contribute to the understanding and implementation of such technology are summarized in a table. Among many DSF aspects described in the literature, the parameters found to have the most prominent effect on energy, thermal and ventilation performances are reported in this review.

The last section of this chapter recapitulates the main findings from these studies, underpinning the development of a naturally ventilated base case building model and the identification of the key parameters affecting the building thermal performance. It also indicates what still need to be evaluated for a comprehensive understanding of a more effective design of DSF when applied to naturally ventilated buildings under warm and hot climate conditions.

2.1 Overview of studies on double skin façades

The studies reviewed in the following sections of this chapter allowed the development of an overall understanding of the DSF conceptual and historic aspects, what are the motivations and expectations from its use and general information concerning its requirements in modelling approaches for airflow and thermal simulations. The advantages and disadvantages regarding the DSFs applications and the real cases examples presented by some studies allowed a factual understanding of the positive aspects and the constraints that limit its use.

Key publications reviewed included the book by Oesterle et al. (2001) which presents a comprehensive description of the technology, providing both a theoretical framework for its use and numerous practical examples. It also includes design issues about acoustics, thermal insulation, smoke control systems, economic viability and construction of DSF. Additionally, reports about DSF generated from extensive research projects are reviewed such as Belgian Building Research Institute (BBRI, 2002), which resulted in the document 'Source Book for Active Façades', and the BESTFAÇADE, which was sponsored by the Energy Intelligent Europe Program of the European Union and presented the state of the art of several DSFs in European countries (Schiefer et al., 2008).

Wide range of reports and books about the advances on DSFs developments, such as by Lee et al. (2002) and Compagno (2002) in glazed building skins are studied. The extensive literature review produced by Poirazis (2006) presents reflections about the design and operation of the technology including real examples of several office buildings with DSF. Additionally, dissertations about the theme such as by Saelens (2002), Dickson (2004), Hamza (2004), Kalyanova (2008) and Azarbayjani (2010) includes literature reviews and clarifications about the evolution of the DSF. Details of these studies are reported in sections 2.3 to 2.5.

2.2 Double skin façade working principle

The DSF is a type of thermal chimney that can promote natural ventilation in the building by using solar induced thermal buoyancy and pressure variations resulting from the effects of wind around the building. Thermal stack and wind effects never act in isolation and the magnitude and pattern of natural air movement through the building depends on the strength and direction of these combined natural driving forces and the resistances to the flow paths.

The thermal buoyancy within the cavity is created mainly as a result of solar radiation reaching the DSF. Fundamentally, part of the total of shortwave solar radiations incident on the outer layer of the DSF is reflected to exterior, some is absorbed by the material and some directly transmitted into the cavity, according to the properties of the glazing used. A portion of the radiation absorbed is converted into heat energy and stored in the glazing, thereby rising its temperature. Part of this heat energy is transferred into the cavity by convection, increasing the air temperature and part of it is reemitted to outside and to the cavity as longwave radiations. Similar heat exchange processes occur with the radiations that reach the internal skin. If received on an opaque material, some of the radiations are absorbed and some are reflected back to

the cavity. The absorbed radiations increase the temperature of the inner layer and this energy is then reemitted towards the office room and the cavity by means of convection, therefore contributing to the increasing of air cavity temperature. In reality, multiple reflections occur repeatedly between the two skins and the increase of the layers' temperatures cause heat gains by convection of air within the cavity (Pérez-Grande et al., 2005). Figure 2.1 shows a schematic representation of these heat exchanges in the DSF.

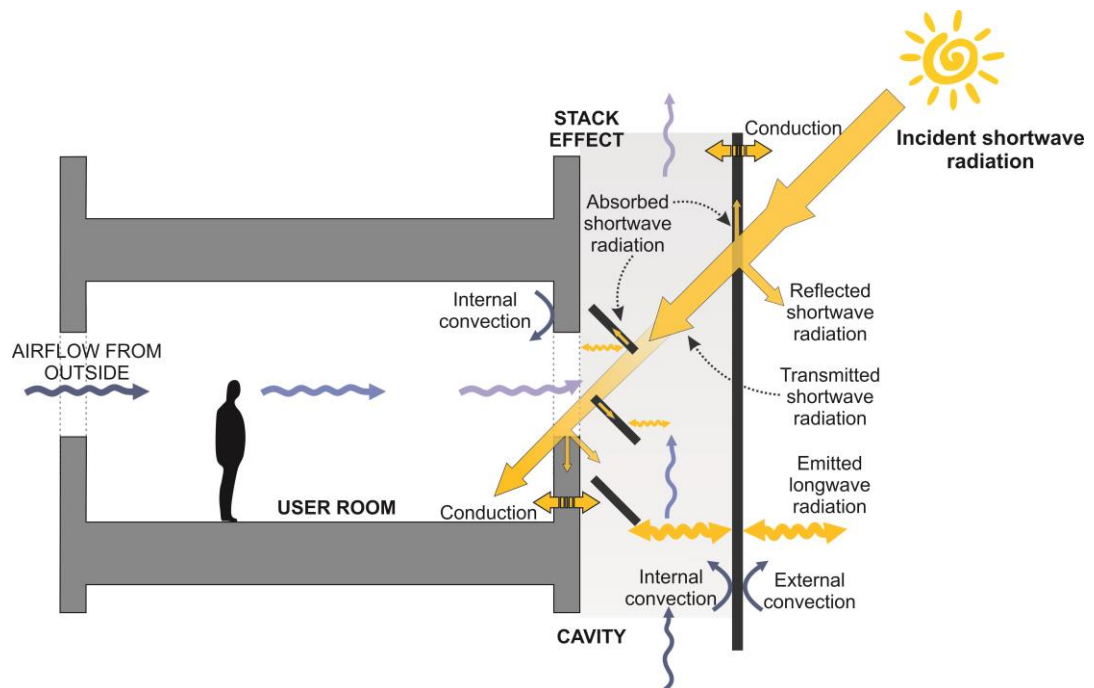


Figure 2.1 - Heat transfer and airflow mechanisms occurring in the DSF and the adjacent office floor

Shading devices are commonly placed within the cavity to reduce the amount of transmitted solar radiations into the room space that lead to increase in the room air temperature. The shading device can also contribute to the increase in air temperature within the cavity space, since part of the radiations transmitted through the outer layer is absorbed by the shading device material and released to the air cavity by convection (Pappas and Zhai, 2008).

As the warmer cavity air expands, it becomes less dense and rises to the top of the cavity, creating a stack effect within it. The increase of cavity air temperature in relation to outside air creates a difference in air density. The decrease of pressure with height creates a pressure difference between the cavity and the external air between the lower and upper ends of the DSF cavity (Figure 2.2). As a consequence, air from the cavity will be pulled out through the top opening, while air from exterior will be pushed to enter the cavity through the bottom aperture (CIBSE, 2005).

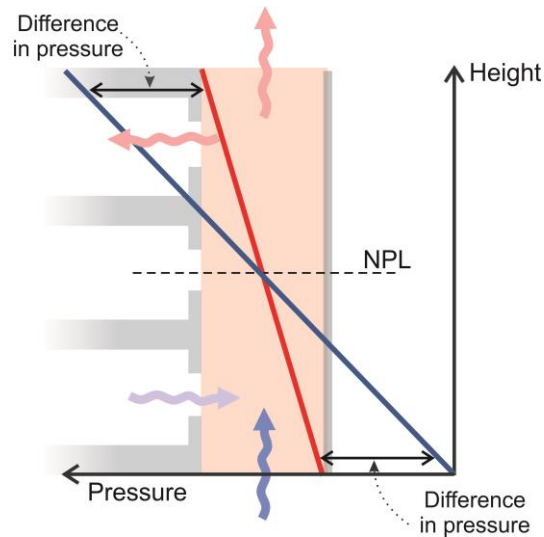


Figure 2.2 – Schematic representation of pressure gradients inside the cavity and outside the building. Source: adapted from CIBSE (2005).

In cross flow naturally ventilated buildings, the displacement of air within the cavity pulls air from the adjacent office rooms, which is replaced by outdoor fresh air from window openings in the opposite façade that passes through the occupant space before being discharged into the cavity. The air in the cavity is continuously heated by the incident solar radiations on the façade when available, thus forming a continuous convective air stream through the DSF (Radhi et al., 2013; Ding et al., 2005), as shown in Figure 2.1.

The airflow in such a thermal chimney can be quantified by the following empirical equation (ASHRAE, 2009):

$$Q = C_D A \sqrt{2g \Delta H_{NPL} (t_i - t_o) / t_i} \quad (\text{Equation 1})$$

Where: Q = air flow rate, m^3/s ; A = area of the opening, m^2 ; C_D = discharge coefficient of the opening; g = acceleration due to gravity, m/s^2 ; ΔH_{NPL} = vertical distance from the neutral pressure line (NPL) to the aperture, m ; t_i = air temperature in cavity (higher temperature), K ; t_o = outdoor temperature (lower temperature), K .

This equation shows that in buildings with DSF, the key variables determining the thermal airflow through a building are the cavity height and cross-sectional area, the position and area of the window's openings and the temperature difference between the air inside the cavity and the external air. Secondary and interacting factors such as the building compartmentation, the thermal properties of building fabric and glazing, and the internal heat gains may affect how the heat is exchanged and the consequent path of airflow in the building.

An important variable of the equation is the height of the neutral pressure line (NPL), which is defined as the point at which the inside and outside hydrostatic pressure gradients intersect, as indicated by Figure 2.2. The position of the NPL relative to the apertures defines the direction and magnitude of the airflows through the building. When the cavity air is warmer than the outside air, inflow will occur through lower openings and outflow through higher openings. As the location of the NPL is influenced by the interior compartmentation of the building, it is not unique or necessarily located at the mid-height of a building. NPL may also exist locally across the vertical height of an opening, such as a window connecting the room and the DSF cavity. This can cause local air recirculation which consequently disturbs the overall air exchange between the building and the DSF (CIBSE, 2005; ASHRAE, 2009).

Another important parameter that contributes to the resulting air movement within the building is the wind effect that varies according to the external surface pressures acting across the building envelope. When wind approaches a building, it creates a distribution of static pressures on the building's exterior surface that depends on the wind direction, wind speed, air density, surface orientation, and surrounding obstructions (ASHRAE, 2009).

Studies by Gratia and De Herde (2004a) and Lou et al. (2012) indicate that the airflows in the cavity reach their minimum when the wind direction is parallel to the façade but they increase when perpendicular, especially if the DSF is located at the leeward side of the building, which reinforces the cavity's stack effect. The wind effect should therefore be utilised to promote airflow from the user room to the cavity of DSF, although sometimes its magnitude may mask the thermal buoyancy effect. However, it is not always possible to achieve a high difference in pressure coefficient for all wind angles, and because wind direction is a varying parameter, a design that relies on a large difference in wind pressure coefficient is unlikely to be robust. For this reason, it is recommended that the building design should be based on thermal stack effects alone, and in such a way that the inclusion of wind effect is used to enhance the driving forces (CIBSE, 2005).

The following sections review the state of the art of current body of literature about the application of DSF technologies in order to provide an understanding of the individual influence of the design and site parameters on the building thermal performance. Three groups of parameters are identified as having significant impact on the DSF performance: the 'façade' parameters, which involves the features of the cavity and the external layer of the façade; the 'building' parameters, which comprises the physical configurations of the building, including the inner layer of the DSF; and the 'site'

parameters, which are related to the effects of the outdoor surrounding conditions on the building thermal behaviour. At the end of each section, a table summarizing the main findings of the cases reviewed including the major findings from each study.

2.3 Façade design parameters

This section presents the influence of the key façade parameters on the building thermal performance. It includes the height, structure, depth and openings sizes of the cavity, definition of the glazing properties applied on the outer DSF layer and the application of shading device within the cavity. These design solutions have a significant impact on several aspects of the building such as thermal exchanges, ventilation magnitude and shading control (Shameri et al., 2011).

2.3.1 Height of the cavity/number of floors

As indicated by the empirical equation determining the airflow in a thermal chimney presented in section 2.2, one of the main factors that affect the magnitude of the thermal buoyancy in DSFs is the height difference between the inlet and the outlet openings of the cavity, which determines the difference in pressure between those apertures. A taller cavity produces a stronger stack effect, creating a greater airflow rate (Oesterle et al., 2001; Mingotti et al., 2011). The magnitude of the airflow induced in the cavity is especially important in warm and hot areas, where the buoyancy force should be enough to extract excessive heat through cross ventilation from the user rooms.

Monitor points placed along the height of the cavity by Radhi et al. (2013) measured air temperatures at different heights of a 3-floor high building. A maximum difference of air temperature at the bottom and top of the cavity was 3.2°C at 9:00 when the outside air temperature registered 31°C on a summer day of Al-Ain city (24.2° N, 55.7° E). The air temperature and flow of the cavity was also compared by Pappas and Zhai (2008) in a single and a five stories building models. It was observed that, even under solar incidence as high as 500 W/m², the resulting air velocity through the cavity due to buoyancy is less than 1 m/s in both models.

Fundamentally, taller cavities tend to generate greater pressure difference between its apertures, which increases the airflow rates within it. However, studies reviewed in this section indicate that the temperature stratification in the cavity air can significantly differ between different building models and under different solar incidence. Therefore, evaluation of ventilation rates for different building geometries and under different outdoor conditions has to be individually analysed.

In addition, the influence of a residual chimney extended above the building roof (Figure 2.3) on the thermal performance of a naturally ventilated model was demonstrated by Ding et al. (2005). The results show that increasing the height of the cavity, the NPL is raised above the upper window. This results in higher airflow rates within the cavity and therefore, higher air change rate on each floor, especially in the upper floors. The study recommends that the effective cavity extension should be more than two-floor height.

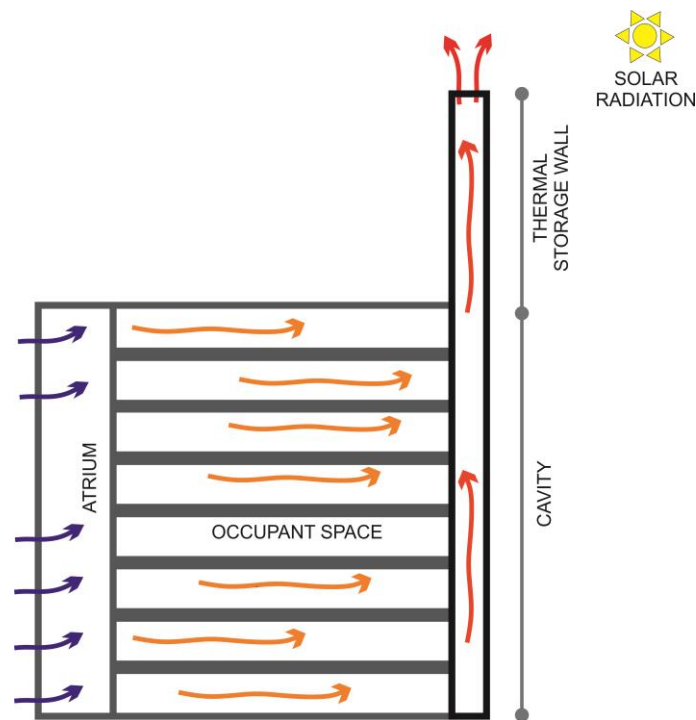
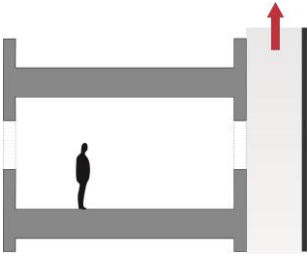


Figure 2.3 – DSF with thermal storage space above the cavity proposed by Ding et al. (2005).

However, the necessary height of the residual cavity may be different for other building geometries and needs to be calculated according to the number and area of the windows openings and the outlet area on the top of the cavity. Furthermore, the extension of cavity above the roof of the building may be limited by a number of factors such as safety, building regulation and costs. In these cases, mechanical ventilation can be used on the upper floors and the cavity height above the upper naturally ventilated floor will act as chimney extension. Table 2.1 presents the studies evaluated in this section, summarizing main findings of the cases reviewed. It contains the location/climate, the type of tool and the major findings from each study. The type of ventilation applied to the model is also presented, where A/C, N/V and M/V stand for air conditioning, naturally ventilated and mechanically ventilated models.

Table 2.1 – Summary of research on ‘cavity height’ and key findings

Param.	Author /year	Location	Variation	Tool	Ventilation	Major findings/Observations
Height of the cavity/Number of floors	Pappas and Zhai (2008)	Brussels Belgium	One and five stories	Energy Plus (BES) + Phoenix (CFD)	-	<ul style="list-style-type: none"> • A taller cavity will produce a stronger buoyancy force, creating a greater airflow rate. • The cavity air temperature increases towards the top of the cavity in a fairly linear progression.
	Radhi et al. (2013)	Al-Ain city, UAE	Monitoring points: 2.2, 6.2, 10.2 m	Design-Builder (BES) + Phoenix (CFD)	A/C	<ul style="list-style-type: none"> • A maximum difference of air temperature in 3-stories building was 3.2°C, when the outside temperature registered 31°C.
	Ding et al. (2005)	Tokyo, Japan	Residual cavity: 3.75, 7.5, 11.25m	Lab. measurements + CFD	N/V	<ul style="list-style-type: none"> • Increasing the height of the thermal storage space increases pressure difference between the top and the bottom of the cavity, resulting in higher airflow rates within it.
Impact to this study	<p>To extend the cavity above the roof of the building is a solution to increase difference between inlet and outlet flows. But it needs to be calculated for different building geometry.</p> <p>Close windows of upper floors may be a solution to increase the difference between inlet and outlet flows.</p> <p>Even under high solar incidence (500 W/m²), the resulting air velocity through the cavity due to buoyancy is less than 1 m/s.</p>					

2.3.2 Structure

The height of the cavity is not only determined by the number of floors, but it is also defined by how the cavity is internally divided. As there are numerous variations in the DSF construction types, a structural classification by Oesterle et al. (2001), according to the form in which the intermediated cavity is compartmentalised (Figure 2.4), assesses and compares the merits of the various typologies. The four types identified are as follow:

- a) The **box window** type has the cavity between the two layers divided horizontally and vertically along the constructional axes, on a room-by-room or on an individual window element basis. In this case, the windows on the inner layer can be operable to allow for natural ventilation.
- b) The **shaft-box** is a special form of box window type in which the continuous boxes form a vertical shaft that extends over a number of stories to pronounce the stack effect. The typology has a positive effect on acoustic insulation against external noise.

c) The **corridor** type closes the intermediate space between the two skins at the level of each floor and divisions are included along the horizontal length. The inlet and outlet air openings on the external façade layer are to be situated near the floor and the ceiling of each level and the exhaust air from one room should be avoided to enter in the room above. In this case, special care should be taken to avoid sound transmission from room to room.

d) The **multi-storey** style has the cavity adjoined vertically and horizontally by a number of rooms, covering the entire façade of the building. The ventilation of the cavity occurs via large openings at the bottom and top of the façade. The position of the NPL may cause weak or reverse airflow on the upper floors and therefore, mechanical ventilation may be required on such levels (Oesterle et al., 2001). This typology is suitable where external noise levels are very high.

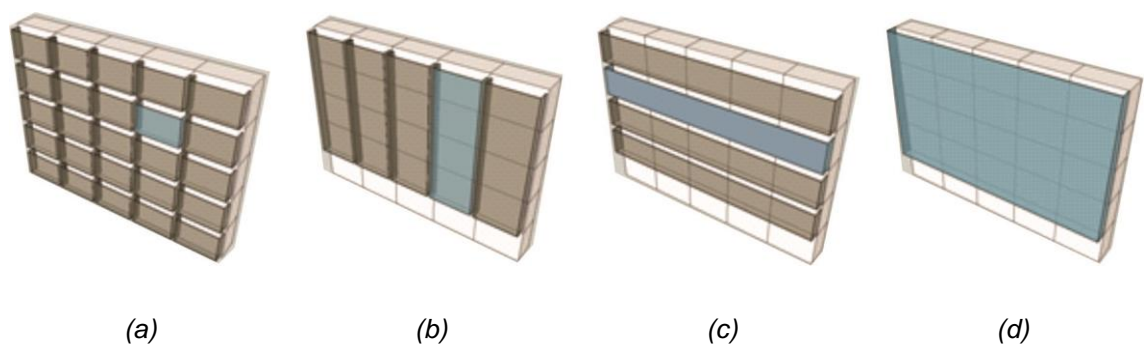
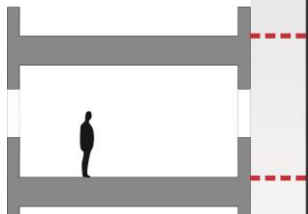


Figure 2.4 – Classification of DSF structure: (a) box window, (b) shaft-box, (c) corridor and (d) multi-storey

Comparisons of the thermal performance of types of DSF structure by Torres et al. (2007) and Hong et al. (2013) indicate that the shaft and the multi-storey styles present the greatest temperature gradient along the cavity due to its height. The pronounced stack effect accentuates the cavity ventilation rate, resulting in a lower air temperature within it, which reduces heat gain in the occupied spaces.

As the height of the façade is crucial to the DSF performance due to the enhancement of the buoyancy effect, the shaft-box and multi-storey types present suitable performance for naturally ventilated buildings. On the other hand, in the box-window and corridor cases, the height difference between the inlet and outlet openings is smaller, covering only one floor. Thus, the DSF tends to be less effective in promoting natural ventilation. Summary of the findings are presented in Table 2.2.

Table 2.2 – Summary of research on ‘structure’ and key findings

Param.	Author /year	Location	Variation	Tool	Ventilation	Major findings/Observations
Structure	Torres et al. (2007)	Barcelona, Spain	Corridor and multi-storey	TAS (BES)	A/C	<ul style="list-style-type: none"> The stack effect of multi-storey and shaft types are more accentuated, increasing its ventilation rate.
	Hong et al. (2013)	Seoul, South Korea	Box, corridor, multi-storey and shaft	Design Builder (BES)	A/C	<ul style="list-style-type: none"> The multi-storey type had the lowest cooling loads because the natural ventilation prevented the rising in air temperature due to the solar heat gains.
	Impact to this study	The shaft-box and multi-storey types presents suitable performance for naturally ventilated buildings.				

2.3.3 Cavity depth

One of the factors most studied about the DSF cavity design is its depth, which may vary from 10cm to more than 2m according to different design concept, needed space for shading device and access for maintenance and cleaning (Pappas and Zhai, 2008).

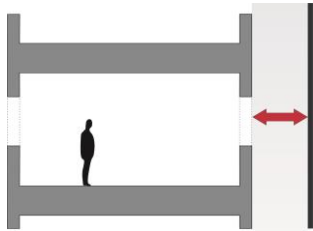
The influence of cavity depth on the amount of solar heat transferred through the DSF layers and the resulting air temperatures and ventilation rates produced in the building were evaluated by Gratia and De Herde (2007a), Torres et al. (2007), Rahmani et al. (2012) and Radhi et al. (2013). Although the studies tested different model dimensions, they all agree that narrower cavities resulted in greater air temperature, an accentuated stack effect and a stronger air speed within the cavity. As a consequence, a more effective extraction of the warmer air from the cavity was carried out and the total heat transfer towards the inner spaces was reduced. In these cases, reductions in the energy consumption during the warm periods were observed.

In naturally ventilated buildings, although narrow cavities tend to enhance the stack effect, it also creates higher resistances to the airflows. Additionally, the discharge of cooler air from the adjoining space to the cavity may influence the magnitude and pattern of airflow in both the cavity and the building. Thus, the effect of airflow from the user room into the cavity air movement needs to be investigated and adequate cavity dimensions for naturally ventilated buildings are likely to be different from air conditioned buildings.

Other aspects that can influence the cavity dimension such as additional cost due to greater use of materials, increasing weight of the additional structure and adequate

space for shading device installation were pointed out by Torres et al. (2007). Another relevant constraint is the space required if the cavity needs to be accessed for maintenance proposes. Torres et al. (2007) indicated that a 40cm wide cavity is the minimum required in those cases. On the other hand, as the cavity space is usually not occupied, loss of the internal area may be a limiting aspect of the cavity depth, which normally does not exceed one meter. Table 2.3 presents a summary of the findings of this section.

Table 2.3 – Summary of research on ‘cavity depth’ and key findings

Param.	Author /year	Location	Variation	Tool	Ventilation	Major findings/Observations
Cavity depth	Rahmani et al. (2012)	Johor Bahru, Malaysia	10, 30, 50, 100 and 150 cm	FloVENT (CFD)	A/C	<ul style="list-style-type: none"> Increasing the cavity depth up to 1m reduces solar heat gains in the building, but for lager cavities, the DSF has its efficiency reduced.
	Radhi et al. (2013)	Al-Ain city,UAE	50, 70, 100, 120, 150 cm	Design-Builder (BES) + PHONIC ES-FLAIR (CFD)	A/C	<ul style="list-style-type: none"> Heat transfer rates decrease when the cavity depth is reduced due to the higher ventilation rates. Cavity size between 0.7 and 1.2 m can give a balance between solar gain and heat transmission.
	Torres et al. (2007)	Barcelona, Spain	40, 60, 80, 100 cm	TAS (BES)	A/C	<ul style="list-style-type: none"> Narrow cavity with no horizontal partitions may demands less cooling loads due to the accentuated stack effect occurring in the cavity.
	Gratia and De Herde (2007a)	Uccle, Belgium	30, 60 120, 240 cm	TAS (BES)	A/C	<ul style="list-style-type: none"> Air temperature in deeper cavities is slightly lower than air temperature in lower DSF depth.
Impact to this study	<p>Narrow cavities enhance the stack effect, but it can create a higher resistance to the flow supplied from the user rooms.</p> <p>A minimum of 40cm is required if the cavity needs to be accessed for maintenance proposes.</p> <p>A maximum of 1m wide is recommended to avoid losing area in the office.</p>					

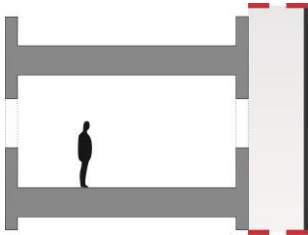
2.3.4 Cavity openings

The cavity depth limits the maximum openings areas at the bottom and the top of the cavity, which strongly affect the overall thermal performance of the building with DSF. The opening areas influence the resulting air temperature within the cavity and the buoyancy force in the DSF. The inter-relationship among the openings dimensions, air temperature and airflow rate were studied by Gratia and De Herde (2007a), Safer et al. (2005) and Torres et al. (2007). They observed that cavities with larger openings presented lower air temperatures and higher airflow rates than cavities with smaller openings, which can be attributed to the resistance created to the ventilation paths. Increase cavity opening areas from 5 to 15% led to a decrease of air temperatures of

5.6% in a corridor type façade (Torres et al., 2007). The cavity airflow observed by Gratia and De Herde (2007a) was threefold higher when the cavity top opening area increased from 8% to 20%.

Although studies by Gratia and De Herde (2007a), Safer et al. (2005) and Torres et al. (2007) present the benefits of increasing cavity opening areas, fully open top and bottom openings were not tested. This still needs to be tested as it would potentially enhance the ventilation in the cavity due to the lower resistance to air movement in wider cavity depths. The top of the cavity is especially important to the airflow rates in naturally ventilated buildings as it is likely to be the only outlet aperture. Therefore, for enhanced building ventilation, the top of the cavity is likely to be as large as possible. Although not mentioned in the literature, closing the bottom of the cavity may induce higher airflow rates from the windows opposite to the DSF, which would improve thermal comfort acceptance conditions in warm and hot climates. A summary of studies on ‘cavity openings’ is presented in Table 2.4.

Table 2.4 – Summary of research on ‘cavity openings’ and key findings

Param.	Author /year	Location	Variation	Tool	Ventilation	Major findings/Observations
Cavity openings	Safer et al. (2005)	Not specified	30 and 50% of top and bottom of cavity	Fluent (CFD)	M/V cavity	<ul style="list-style-type: none"> • Only cavity was modelled. • The air path does not have influence on the air velocity in the cavity, while the openings areas are important factors to be considered.
	Torres et al. (2007)	Barcelona, Spain	5, 10 and 15% of top and bottom of cavity	TAS (BES)	A/C	<ul style="list-style-type: none"> • Larger openings help to extract warm air from the cavity as higher air flow rates occur.
	Gratia and De Herde (2007a)	Uccle, Belgium	8 and 20% of top and bottom of cavity	TAS (BES)	A/C	<ul style="list-style-type: none"> • Null wind speed. • Cavity air temperature decrease does not vary in a linear way with the size of the openings.
Impact to this study	<p>Large openings lead to higher airflow rates within the cavity. But fully open top and bottom were not tested.</p> <p>Top of the cavity is likely to be as large as possible.</p> <p>By closing the bottom of the cavity may improve airflow ventilation through the user rooms.</p>					

2.3.5 Outer skin glazing properties

Another fundamental factor for improving airflow rates within the DSF cavity is to increase the air temperature difference between inside and outside. The properties of the glazing applied on the outer layer of a DSF have a significant influence on the

building thermal and ventilation performances, as it directly influences the solar radiation transmitted into the cavity. Due to the numerous glazing types currently available, there is an ongoing debate about the best choice considering the complex heat transfer and resulting airflow mechanisms in the DSF.

Pérez-Grande et al. (2005) investigated the influence of the several glazing optical properties on the transmission of solar radiation on both inner and outer layers of a DSF. It was found that a low transmittance and high absorptance glazing applied on the external skin combined with low emissivity glazing on the internal pane can lead to a reduction in solar heat gain to the occupied space. In this case, most part of the heat is stored in the outer glazing material before reaching the cavity. In reality, this configuration acts as a shading device and does not increase the ventilation within the cavity.

On the other hand, the application of a high-absorbing inner layer glazing in conjunction with an equal transmittance/absorptance glazing of 40% on the outer layer resulted in the highest air mass flow rate passing through the cavity (Pérez-Grande et al., 2005), as shown in Figure 2.5. In this case, the air temperature within cavity increases due to re emission of longwave radiation into cavity from the outer and inner glazing layers. This improves the stack effect and the ventilation within the system.

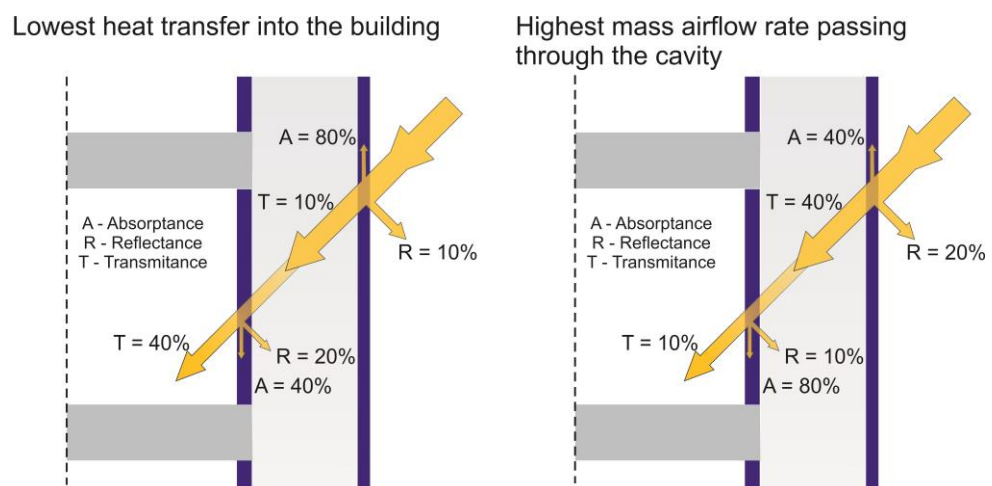


Figure 2.5 – DSF performance according to the glazing characteristics by Pérez-Grande et al. (2005)

It is a common practice to use double glazing on the inner layer and single glazing on the outer skin of DSFs. Nevertheless, two of the case scenarios tested by Chan et al. (2009) used single and double glazing on the inner and outer DSF layers, respectively (cases (c) and (d) of Figure 2.6, which presents the percentages of energy savings in

relation to a single skin façade). The resulting energy savings of cases (b) and (d) were similar, which can be explained by the use of reflective glazing on the outer layer of both cases. The reflection of shortwave radiation by the outer DSF layer avoided solar heat gain into the cavity and the room, decreasing the cooling loads. This indicates that that the optical glazing properties have more influence on the final thermal performance than the number of glass sheets.

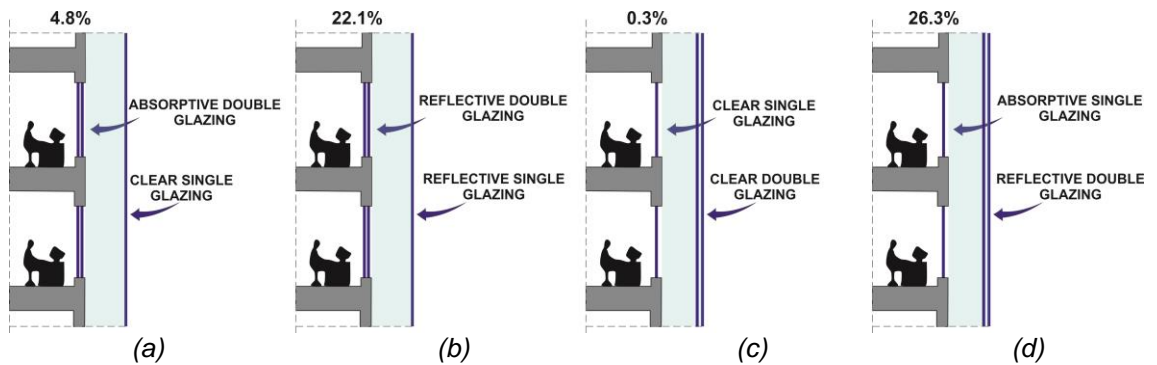
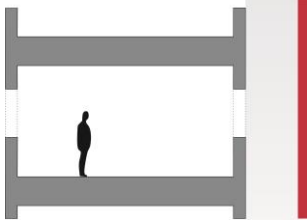


Figure 2.6 – Performance of a building with DSF under variations of the glazing properties resulting from study by Chan et al. (2009)

In naturally ventilated buildings, it is fundamental to enhance airflow rates in the cavity by increasing its air temperature. The application of a single glazing with higher transmittance on the outer layer tends to pronounce this behaviour. Section 2.4.1 continues this discussion indicating the findings about the influence of the choice of materials to the inner skin layer. Table 2.5 presents the studies evaluated in this section, summarizing main findings of the cases reviewed.

Table 2.5 – Summary of research on ‘outer skin glazing properties’ and key findings

Param.	Author /year	Location	Variation	Tool	Ventilation	Major findings/Observations
Outer skin glazing properties	Manz et al. (2004)	Duebendorf, Switzerland	Glazing thermal properties	Lab experiments	-	<ul style="list-style-type: none"> The solar energy absorbed in the DSF was efficiently removed by mechanical ventilation.
	Guardo et al. (2009)	Barcelona, Spain	Glazing transmissivity and emissivity	CFD	A/C	<ul style="list-style-type: none"> A reduction of external glazing transmissivity of 55% can lead to 40% of reduction of solar heat gain.
	Pérez-Grande et al. (2005)	-	Gazing properties	FLUENT (CFD)	-	<ul style="list-style-type: none"> Highest airflow rates are resulted for outer and inner layers with 0.2 and 0.1 of reflectance, 0.4 and 0.1 of transmittance and 0.4 and 0.8 of absorptance, respectively.
	Gratia and De Herde (2007a)	Uccle, Belgium	Material: reflective, clear, absorbing	TAS (BES)	A/C	<ul style="list-style-type: none"> Null wind speed. Clear glazing transmits most of the solar radiation (62%) and the reflective glazing returns 51% of it.
	Mingotti et al. (2013)	Cold and warm climates	Single and double glazing	Analytical model	A/C	<ul style="list-style-type: none"> In warm climates, double glazing minimises convective and radiative components of heat transfer across the façade, leading to a smaller heat gain into the user room.
	Chan et al. (2009)	Hong Kong	Glazing type and position	Energy Plus (BES)	A/C	<ul style="list-style-type: none"> Outer layer made of low transmissivity double glazing can decrease the heat gain and the building cooling energy.
Impact to this study	<p>High transmittance glazing applied to outer layer increases air temperature and stack effect in the cavity.</p> <p>The optical properties of the glazing have more influence on the energy transmitted through the DSF layers than the number of glass sheets.</p>					

2.3.6 Shading device

The primary reason for implementing shading devices in DSF building is the possibility of reducing overheating during the hottest periods as they can reduce the solar energy transmitted to the user space. In DSF buildings, shading devices are usually positioned within the cavity in order to protect them from excessive rain, sun and pollution, thus reducing maintenance costs. Furthermore, as explained in section 2.2, the application of shading device may contribute to enhance the stack effect in the cavity by increasing the air temperature. Currently, there is a number of available shading device types such as roller shades and louvered blinds, which can be fixed or controlled manually or automatically (Pappas and Zhai, 2008; Mingotti et al., 2011).

The position of the shading device, close to the inner layer, to the outer layer, and in the middle of the cavity (Figure 2.7a), was examined by Gratia and De Herde (2007b)

and Jiru et al. (2011). The results showed that the temperature of the inner glass surface became higher when the systems were positioned close to it. This caused a higher heat transfer from the cavity into the indoor space and consequently, higher cooling loads were resulted in the user rooms. On the other hand, when the blinds were placed in the middle of the cavity, the air circulation was well distributed on both sides of the blinds. In this case, a lower temperature was observed on the inner glass surface and the lower heat transfer to the user space decreased the annual cooling loads.

The influence of different blind's angle on the radiative heat transfers and on ventilation performance in the DSF system was investigated by Ji et al. (2007), Jiru et al. (2011) and Marques da Silva et al. (2015) (Figure 2.7b). They observed that when the slats are on vertical position, the air temperatures of the two side gaps approach each other more than in other cases. The lower resistance to the flow combined with the enhanced buoyancy effect, increased the natural ventilation in the cavity in up to 35%, when blind's angle was 80 degrees compared to the horizontal slates case (Ji et al., 2007).

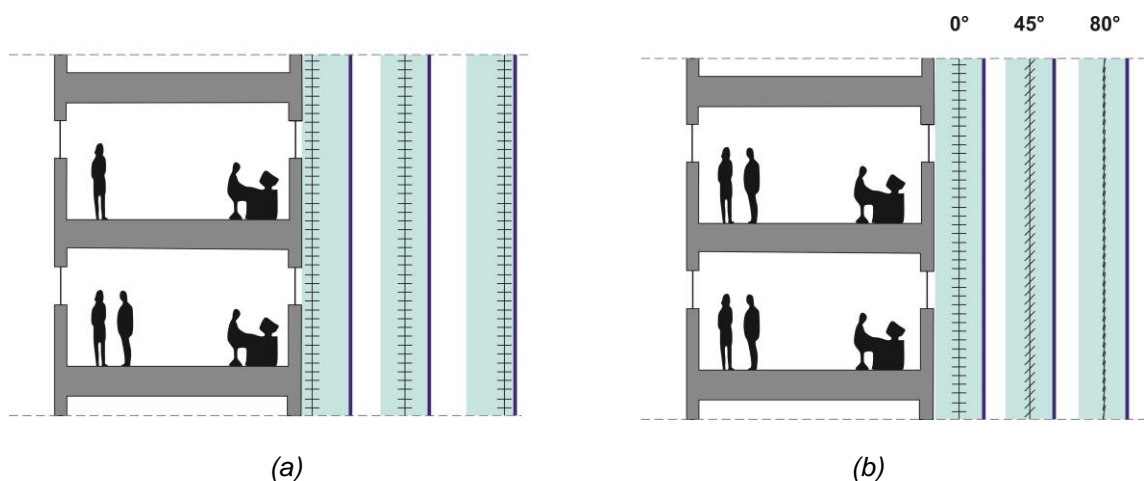
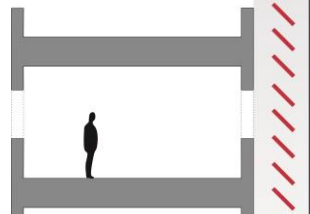


Figure 2.7- Variations of the shading device (a) position proposed by Gratia and De Herde (2007b) and (b) angle evaluate by Ji et al. (2007).

Simulations comparing the effect of colour (white and black) of the material used on the shading device were performed by Haase et al. (2009). The results showed that the cavity with black blind presented air temperature 11°C higher than with the white blind. Most of the incident solar radiation on the white material is reflected back to outdoors through the outer skin, and only a small part of the energy is absorbed by the material. In the black blind, on the other hand, a great amount of energy is stored into the material and released to the cavity air by convection and in the form of longwave radiation.

From the studies reviewed, it can be concluded that shading devices increase the air temperature, and therefore the ventilation rates inside the cavity, especially if made of dark colour or high absorptive materials. The decision about the location of the blinds has also considerable influence on the air temperature and ventilation rates within the system. Placing the shading device in the middle of the cavity allows for effective air circulation on both sides of it, but if it is placed close to the inner layer, higher heat transfer towards the internal environment may occur. Regarding the angle of the blind, it was suggested that horizontal angles act as an obstruction to the air circulation; therefore, higher angles seem to be more appropriate. Summary of the findings are presented in Table 2.6.

Table 2.6 – Summary of research on ‘shading device’ and key findings

Param.	Author /year	Location	Variation	Tool	Ventilation	Major findings/Observations
Shading device	Gratia and De Herde (2007b)	Uccle, Belgium	Position: outer, middle, inner	TAS (BES)	A/C	<ul style="list-style-type: none"> When blinds are placed in the middle of the cavity, the air movement is well established on both sides of the gap.
	Jiru et al. (2011)	Torino, Italy	Slat angle: 0°, 45°, 90° Position: outer, middle, inner	Ansys Fluent (CFD)	A/C	<ul style="list-style-type: none"> The heat transfer into the room for totally vertical slats is lower than inclined or horizontal slats cases. The inner position lead to a high temperature on the inner glass surface, increasing heat gains to the indoors.
	Ji et al. (2007)	–	Slat angles (0°, 30°, 45°, 60°, 80°)	Ansys CFX (CFD)	-	<ul style="list-style-type: none"> The presence of blinds offers the shading functions and enhances natural ventilation in the cavity (up to 35%) reduces heating loads by 75%.
	Haase et al. (2009)	Hong Kong, China	Blind colour: black, white	TRNSYS and TRNFL OW	A/C	<ul style="list-style-type: none"> The black roller blind is largely responsible for high cavity air temperatures, which achieved up 11 °C higher than the case with white coloured roller blind.
	Marques da Silva et al. (2015)	Mediterranean climate	Slat angles (0°, 45° and 90°)	Tracer gas tests		<ul style="list-style-type: none"> Vertical slats promote proximity of air temperatures of both sides of the gap. Horizontal slats resulted in lower airflow in the cavity.
Impact to this study	Dark colour or high absorptive materials increases the ventilation in the cavity Shading devices should be placed in the middle of the cavity Horizontal slates angles should be avoided as it may obstructs the up lift air circulation					

Based on the existing literature review, the building with DSF thermal performance is highly dependent on the geometry of the façade due to the ventilation mechanisms and heat transfer processes occurring inside the cavity. The airflow path, the air velocity and the air temperature distribution along the height of the cavity are affected by a number of parameters such as the shading device configurations, the cavity depth and

height and glazing properties. Incorporating all these within the chosen DSF structure and the optimized opening settings are the key factors that will determine the effectiveness of the DSF in improving the indoor thermal comfort.

The findings are useful in understanding how the individual façade parameters influence the system performance. However, the great interdependence among the parameters indicates the need for a more comprehensive investigation that identifies how the design solutions interact with each other, contributing to the building thermal and ventilation performance. Additionally to those parameters, the definition of the building design also influences the heat transfer and airflow mechanisms occurring in the DSF, as presented in the next section.

2.4 Building parameters

This section reviews studies on the impact of the key building parameters on the DSF thermal performance, which encompass the properties of the materials and the position and the size of the openings on the inner layer of the DSF.

2.4.1 Inner skin materials

Similarly to the properties of glazing applied on the outer layer, the inner layer also has a great influence on the heat transfer occurring within the cavity. If a high thermal mass material, such as concrete and masonry, is applied within the cavity of the DSF, greater amount of heat is absorbed and stored into the material. On warm summer days, walls with high thermal mass will steadily absorb heat at their surface and store it until later, when the heat is released to the cooler air. Absorption and release of heat in response to the change in thermal conditions help to stabilise the fluctuation in temperatures and maintain the airflows, thus reducing the risk of overheating and the need for mechanical cooling.

In DSFs, the application of combined concrete wall and glazed windows on the inner layer is a common design practice. The study by Radhi et al. (2013) indicate that due to the solar incidence on the glazing surfaces, it can achieve higher temperatures than concrete walls due to the low thermal mass properties of the glass. Fallahi et al. (2010) evaluated the differences in energy consumption when different materials were applied to the inner layer of the DSF. They showed that the application of thermal mass on the external layer (see Figure 2.8) presented higher cooling requirements than the amount consumed in the conventional case, in which glazing was applied in both layers (a).

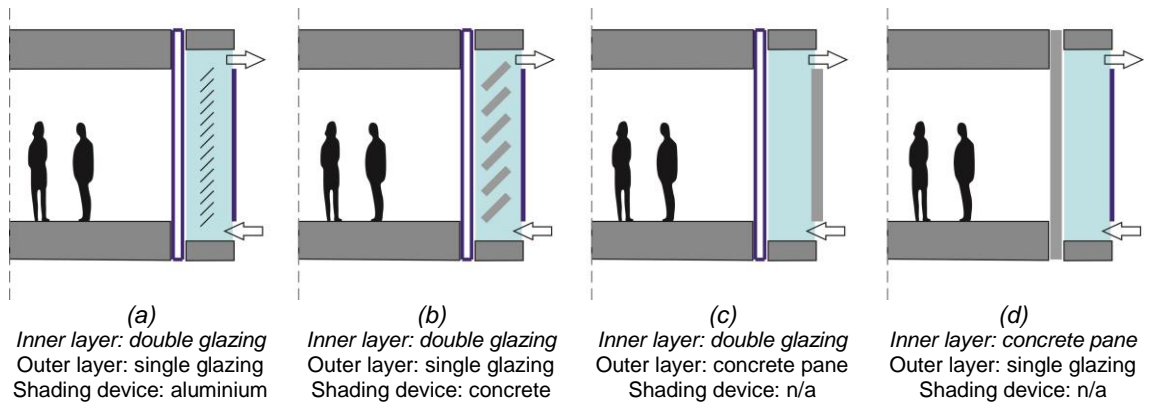
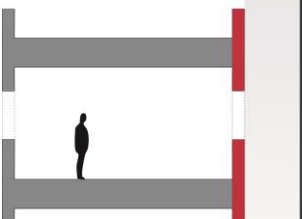


Figure 2.8 – Models using thermal mass (concrete) proposed by Fallahi et al. (2010)

For glazing in the inner layer, the study by Joe et al. (2014) suggests that the application of low-e clear double glazing of 6 mm and 3 mm in the outside and inside surfaces of the inner layer, respectively, leads to the highest reduction in energy consumption among several glazing combinations tested. The double glazing minimises the convective and radiative components of heat transfer into the room, thus reducing the building cooling loads (Mingotti et al., 2013).

Although the studies used air conditioning models, the underpinning principles of the application of thermal mass to alleviate the peak load and air temperature in naturally ventilated buildings with DSF still apply. Therefore, the application of high thermal mass materials, instead of glazing, within the cavity seems to be more appropriate when high levels of ventilation in the cavity are required. Table 2.7 presents a summary of the findings of this section.

Table 2.7 – Summary of research on ‘Inner skin materials’ and key findings

Param.	Author /year	Location	Variation	Tool	Ventilation	Major findings/Observations
Inner skin materials	Fallahi et al. (2010)	Munich, Germany	Concrete inner and outer layers and blind	BES	N/V and M/V cavity	<ul style="list-style-type: none"> The application of thermal mass on the inner skin increased the cooling loads in 12% in relation to the case with thermal mass applied to shading devices.
	Radhi et al. (2013)	Al-Ain city,UAE	Single, double, triple glazing	Design-Builder (BES) + Phoenix (CFD)	A/C	<ul style="list-style-type: none"> The optical properties of the layers are one of the most effective ways to reduce cooling loads, with a particular influence to the direct solar gain and to the cavity stack effect.
	Joe et al. (2014)	Seoul, South Korea	Glazing properties	Energy Plus (BES)	A/C	<ul style="list-style-type: none"> Modification on the glazing type of the DSF inner layer provided the highest energy savings, up to 3.8%, than variations of the outer layer glazing type.
Impact to this study	Application of high thermal mass materials on the inner DSF layer leads to an increased air cavity temperature					

2.4.2 Window to wall opening ratio

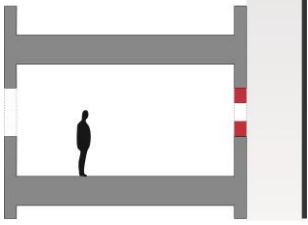
Windows provide beneficial daylight, direct sunlight and visual contact with the outside, but it may cause problems if excessive undesired heat gain occurs due to the high solar energy transmittance of glass, glare or asymmetric thermal radiation (Park et al., 2004). In naturally ventilated buildings with DSF, not only the properties of the materials used in the layers, but also the area and position of the windows openings could have a significant influence on the DSF’s thermal performance.

The effect of the window to wall opening ratio (WWR) on the solar radiation transferred through the DSF was evaluated by Chou et al. (2009) and Manz et al. (2004). They observed that the positive effect of applying DSF as a solution to reduce solar heat gains into the building seems to be mitigated if a high WWR is designed. Therefore, a balanced WWR is essential to effectively reduce building energy consumption on the hottest periods. Chou et al. (2009) observed a reduction in the overall annual heat transfer into the building located in Singapore (1.1° N, 103.5° E) when the WWR increased from 50% to 70%. However, greater heat transfer levels were observed for the model with WWR of 90%. Haase et al. (2009) complemented that in terms of energy consumption, the enhancement in the annual energy savings can achieve up to 26% for WWR of 30%, when compared to the case WWR of 90%.

Ventilation performance of a naturally ventilated model with DSF was studied by Ding et al. (2005). They found that there was an enhancement from 7 to 10 air changes per hour (ACH) on the ventilation levels on the first floor when the WWR were 15% and 30%, respectively. However, when WWR of 60% was set, the ventilation rates increased to only 11 ACH. In conclusion, they established that WWR between the occupant space and the cavity space should not be less than 30% to obtain favourable airflow conditions on all floor levels.

The studies reviewed show that there is a positive influence of high WWR on the building with DSF as it allows for higher airflow through the user rooms which enhances removal of heat gains. However, disadvantages were observed with a high WWR due to the increase in solar gain. Thus, a balanced WWR threshold should be identified considering the building's design features and the local climatic conditions. A summary of studies reviewed in this section is presented in Table 2.8.

Table 2.8 – Summary of research on 'WWR of openings' and key findings

Param.	Author /year	Location	Variation	Tool	Ventilation	Major findings/Observations
Wall-window ratio of openings	Haase et al. (2009)	Hong Kong	30, 60 and 90%	Transys	A/C and M/V cavity	<ul style="list-style-type: none"> The WWR and glazing type have great influence on annual cooling loads. DSF with large WWR (90%) has the same annual cooling load as a SSF with small window area.
	Ding et al. (2005)	Tokyo, Japan	15, 30 and 60%	Laboratory measurements + CFD	N/V	<ul style="list-style-type: none"> WWR between the occupant space and the cavity space should not be less than 30% to obtain favourable airflow conditions on the eight floor levels.
	Chou et al. (2009)	Singapore	30, 50, 70 and 90%	Experimental laboratory measurements	A/C	<ul style="list-style-type: none"> A reduction in the heat transfer through the façade was observed for WWR from 50% to 70%. But for a WWR = 90%, the heat transfer increased.
	Manz et al. (2004)	Duebendorf Switzerland	Inner layer opening positions	Experimental laboratory measurements	M/V cavity	<ul style="list-style-type: none"> The opening at the bottom of the inner layer leads to a low solar heat gain in the user room.
	Impact to this study	<p>WWR between the occupant space and the cavity space should not be less than 30% to obtain favourable airflow conditions on an eight floors building.</p> <p>If WWR = 90%, the great solar heat gain into the user room may increase thermal discomfort.</p>				

Studies in naturally ventilated office buildings (Zhang and Barrett, 2012; Herkel et al., 2008; Rijal et al., 2007) suggest that the control over the opening of windows by the

user has a strong correlation to the outdoor temperature. The variation in windows open and outdoor temperature occurred simultaneously with very little time gap, suggesting that the opening of windows by occupants is a response to short term fluctuations in outdoor temperature. They also showed that temperature band between opening and closing windows (the “deadband”) is around 4 °C. The results suggest that at 16 °C, the probability of having windows open in a building is 50%, and at a temperature of 20 °C, the highest percentage of open windows is reached.

Façade and building parameters are not the only variables contributing to the effective functioning of the building with DSF. The influence of the environmental conditions on the building thermal performance has also to be addressed in order to evaluate the adaptability of such technology to different climatic conditions.

2.5 Site parameters

This section presents existing studies on the key parameters related to the surrounding conditions; they are: levels of local solar incidence, façade orientations, external air temperatures and humidity and wind conditions (Poirazis, 2006).

2.5.1 Solar irradiance and orientation

The temperature difference between the outside and the cavity air has been identified as one of the most important factors in generating ventilation in a building with DSF (Gratia and De Herde, 2007a; Kim et al., 2009). This is not only associated to the solar radiation level and angle, which have a dominant contribution to the air cavity temperature (Hazem et al., 2015), but it is also a function of the façade orientation and the solar shading generated by the surrounding environment.

Mulyadi (2012) explains that the percentages of reflected, absorbed and transmitted solar radiation through a glazing vary according to the material selected, but also to the angle at which the solar radiation reaches the façade. When the angle of incidence is lower than 70 degrees, the percentage of reflection and absorptance gradually decreases, while the percentage of transmission increases. Figure 2.9 shows the percentages of reflection, absorption and transmission for two moments of the same day, when the solar angles are 32 degrees at 8:00 a.m. and 77 degrees at 11:00 a.m. The angle at which the solar radiation reaches the façade is not only affected by the hours of the day, but also by the building position in latitude and the season of the year. The resulting heat transfer affects the air temperature and consequently airflow within the cavity.

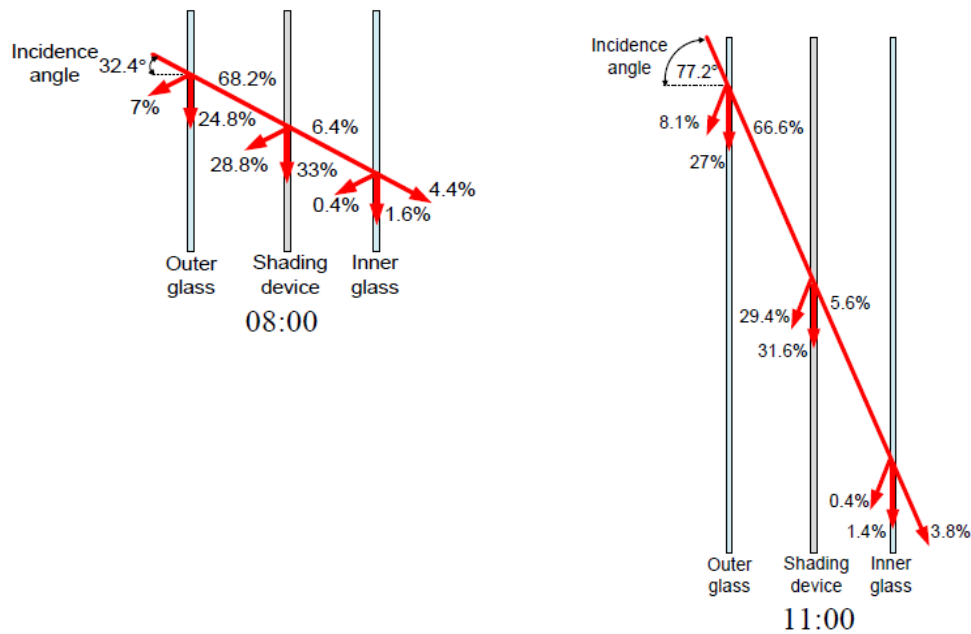


Figure 2.9 – Percentage of reflection, absorption and transmission in relation to solar angle reaching the façade by Mulyadi (2012)

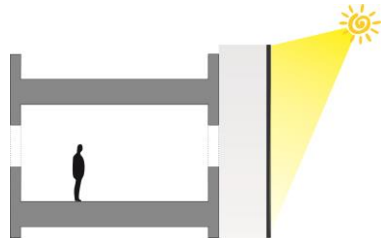
Studies by Stec and Paassen (2005), Gratia and De Herde (2007a) and Kim et al. (2009) on the effect of different levels of solar radiation on the DSF indicated that in sunny days, temperatures of cavity air of a south facing DSF (in the northern hemisphere) exceeded the surrounding air temperature by around 20°C for a system without shading device. However, under cloudy sky conditions, the DSF functioned less effectively with a maximum air temperature difference of only 10°C.

Regarding the orientation, Hamza (2008) and Gratia and De Herde (2007a) argue that for air conditioned buildings, the most unfavourable orientations for DSF were east and west as they have the undesirable effect of increased building cooling loads. When the DSF was east oriented, overheating appeared early in the morning, while for west orientation, large cooling loads were created in the afternoon. This can be due to the great difficulties to control solar radiation when it is transmitted through the glazing at low angles, which increases the building cooling loads.

On the other hand, for naturally ventilated buildings, Kim et al. (2009) suggested that the east-facing DSF did not function beneficially in practice, while the west-facing façade received enough solar radiation and succeeded in generating natural ventilation for the indoor space. In a mechanically ventilated building, Haase et al. (2009) recommend that south, southeast and south west orientations are the most efficient positions for the DSF.

Thus, if DSF is applied to east and west facings, higher solar gains in the cavity tend to induce higher airflow rates and therefore improved thermal performance under warm and hot conditions. However, if the shading device does not adequately control shortwave transmission into the user room, it may result in poor thermal comfort within the building. Thus, for overall daily solar incidence, the north facing (for southern hemisphere) presents most suitable conditions for the DSF application. It is also important to notice that in highly dense cities the sun shading created by surrounding buildings has to be considered and the resulting stack effect in the cavity may be not be enough to create adequate natural ventilation. Table 2.9 presents the studies evaluated in this section, summarizing main findings of the cases reviewed.

Table 2.9 – Summary of research on ‘orientation and solar irradiance’ and key findings

Param.	Author /year	Location	Variation	Tool	Ventilation	Major findings/Observations
Orientation and solar irradiance	Stec and Paassen (2005)	–	Solar incidence (100 - 1200 W/m ²)	Matlab/ Simulink	-	<ul style="list-style-type: none"> Only the cavity was modelled. On a sunny day, the temperature in the cavity air may exceed the surrounding temperature by more than 16°C.
	Gratia and De Herde (2007a)	Uccle, Belgium	East/West orientations Sky conditions	TAS (BES)	A/C	<ul style="list-style-type: none"> On sunny and cloudy days, the air cavity temperature for a south facing DSF exceeded the surrounding air temperature by around 20 and 10°C, respectively.
	Kim et al. (2009)	South Korea (winter)	East/West orientations Sky conditions	Laboratory experiments + CFD	N/V	<ul style="list-style-type: none"> The west-facing façade received enough solar radiation to generate ventilation. DSF does not function effectively under overcast skies since there is not enough radiation to heat up the cavity air.
	Haase et al. (2009)	Hong Kong, China	Eight orientations	TRNSYS and TRNFLOW	M/V	<ul style="list-style-type: none"> The façade orientation has been identified as having major influence on annual cooling loads. Efficiencies are highest for S, SE, and SW orientation and lowest for N orientation.
	Hamza (2008)	Cairo, Egypt	Four main orientations	IES (BES)	A/C	<ul style="list-style-type: none"> Due to the direct solar radiation intensities, the East and West orientations are to be avoided, while the North orientation provides the least cooling loads.
Impact to this study	<p>For building in south latitudes, the north facing (with 45° variations) seems to be the most effective orientation to buildings with DSF</p> <p>It is indicated that shading devices should adequately control shortwave radiation transmission into the user room</p> <p>Surrounding buildings of highly dense cities may create shading on the DSF</p>					

2.5.2 Wind speed and direction

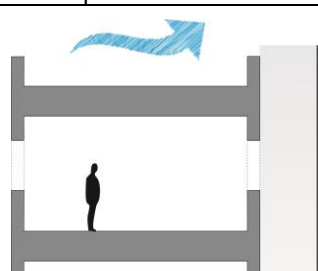
In addition to solar radiation, wind is a key climatic parameter that affects the airflow behaviour of the DSF as the front, top and bottom of the cavity are subject to different and varying wind pressures. During windy days, wind pressure plays a dominant role in driving airstreams in the DSF, thus having a significant influence on the air temperature and ventilation of the cavity (Pasquay, 2004; Stec and Paassen, 2005; Lou et al., 2012).

Gratia and De Herde (2007a) analysed the wind influence on the cavity's air temperature and suggested that on a typical clear sunny day, the difference in temperature between the cavity and the outside air can drop by up to 10.2°C from a null wind speed condition to a 4m/s wind speed. The wind direction has also a great impact on the magnitude and direction of airflow through the cavity and other building openings. Lou et al. (2012), Stec and Paassen (2005) and Nasrollahi and Salehi (2015) explained that high values of pressure coefficients occur when the DSF is located at the leeward side of the building. Thus, the airflow in the cavity achieves a minimum for the wind direction parallel to the façade but increases for the perpendicular wind direction.

More detailed studies by Gratia and De Herde (2004a) showed that when the wind was oriented perpendicular away from the face of the DSF, the airflows were similar among the floors, with air taken from outside through the user room and discharged into the cavity. In this case, the thermal stack effect was less significant than the wind effect on the upper floors.

However, because wind direction is a varying site characteristic, it is unlikely that high airflow rates due to wind effect alone will be achieved the whole time. Therefore, the conditions under which the wind effect may enhance or mask the stack effect should be identified. Table 2.10 presents the studies evaluated in this section, summarizing the main findings of the cases reviewed.

Table 2.10 – Summary of research on ‘wind speed and direction’ and key findings

Param.	Author /year	Location	Variation	Tool	Ventilation	Major findings/Observations
Wind speed and direction	Gratia and De Herde (2004b)	Uccle, Belgium	Wind orientations: protected and facing DSF	TAS (BES)	N/V	<ul style="list-style-type: none"> If the DSF is protected from or facing the wind direction, the wind effect will dominate over the stack effect.
	Gratia and De Herde (2007a)	Uccle, Belgium	Wind speed: 0, 2 and 4m/s	TAS (BES)	-	<ul style="list-style-type: none"> The case with null wind speed resulted air cavity temperature 10°C higher than the case which wind speed was 4m/s.
	Lou et al. (2012)	-	Various wind orientations	Wind-tunnel and numerical modelling	-	<ul style="list-style-type: none"> Inner layer sealed. Peak values of pressure coefficients occur when the DSF is located at the leeward side of the building.
	Stec and Paassen (2005)	-	Wind speed and direction	Matlab/ Simulink + CFD	-	<ul style="list-style-type: none"> Only the cavity was modelled. The air velocity in the cavity is directly proportional to the wind speed; around 4 times lower than the wind speed.
Impact to this study	Improved airflow rates in the cavity are created when DSF is protected from wind direction.					

2.5.3 Outdoor air temperature and humidity

Another significant aspect that influences the building thermal performance is the occurrence of high external air temperatures. As in naturally ventilated buildings air from outside is drawn into the user room, the necessary ventilation rates to meet comfort expectations of occupants are determined by the external air temperature.

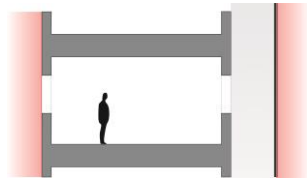
An evaluation of a naturally ventilated building with DSF in the subtropical climate of Ningbo in China was undertaken by Darkwa et al. (2014) who reported the thermal performance during the cold period, when the air temperature dropped to -5°C, and also during the hot seasons, when air temperatures of up to 39°C were experienced. The difference of temperature between the DSF cavity and the outside air was, on average, 8°C and 3°C, during winter and summer, respectively. These differences in air temperatures between the seasons are related to the solar angle, which are lower during winter time. The results indicated that on average, during winter, air temperature of the user space increased by 8.4 °C, whereas in summer, the room air temperatures reduced by approximately 0.5 °C in relation to the exterior.

Another important factor related to the site conditions is the air humidity, which can affect thermal comfort in a building and it is highly correlated to the outdoor air temperature. Although the following studies are not specifically related to buildings with DSF, they were included in this section in order to address the influence of air humidity on the occupant’s thermal expectations under hot and humid areas.

According to Fountain et al. (1999), occupants in the tropics are thermally comfortable at wide range of air relative humidity. The field study conducted in the tropical hot-humid environment of Kota Kinabalu city, Malaysia (5.9° N, 116.1° E) did not indicate clearly differences regarding the thermal comfort preferences among the building occupants when exposed to various air humidity conditions. Recently, an extensive field investigation by Djamila et al. (2014) confirmed occupants’ tolerance to high humidity levels when performing sedentary activities, such as office work. Studies by Farghal and Wagner (2010) and Toe and Kubota (2013) indicated that humidity influences the predicted neutral air temperature in hot–dry climates but not in hot–humid climates.

From the findings, it can be concluded that due to lower solar angles reaching the building façade, the DSF tends to be more effective in enhance the building ventilation during the winter period. However, the challenge of increasing ventilation rates in hot periods may be achieved with the application of effective combined façade and building design parameters. Summary of the findings are presented in Table 2.11.

Table 2.11 – Summary of research on ‘outdoor air temperature and humidity’ and key findings

Param.	Author /year	Location	Variation	Tool	Ventilation	Major findings/Observations
Outdoor air temperature and humidity	Darkwa et al. (2014)	Ningbo, China	Summer and winter	Fluent (CFD)	N/V	<ul style="list-style-type: none"> During winter, air temperature of the user space increased 8.4 °C, whereas in summer, there was a reduction of 0.5 °C.
	Fountain et al. (1999)	-	-	-	-	<ul style="list-style-type: none"> Occupants in the humid tropics are thermally comfortable at wide range of air relative humidity.
	Impact to this study	<p>The higher solar angles in the summer are unfavourable to the inducement of high air temperatures and consequently stack effect within the cavity</p> <p>Occupants in the tropics have higher tolerance to a wide range of humidity levels when performing sedentary activities</p>				

2.6 Chapter summary

This chapter has reviewed the parameters that influence the thermal behaviour of buildings with DSF. Relevant studies from the existing body of literature that can

contribute to the study of DSF in naturally ventilated buildings were categorized and grouped under the headings of 'façade', 'building' and 'site' parameters. The main deductions from this critical review are summarized as follows:

- 1) The taller the cavity, the greater the buoyancy effect and therefore, higher airflow rates tend to occur in the building. However, studies demonstrated that even under high solar incidence, as much as 500 W/m^2 , the resulting air velocity through the cavity due to buoyancy force is lower than 1 m/s . A possible solution to increase the difference between inlet and outlet flows, and therefore the stack effect, is to extend the cavity above the roof of the building to raise the NPL or to close windows of upper floors and use mechanical ventilation in those levels.
- 2) The continuous height of the cavity, which is necessary to the creation of the buoyancy effect, is crucial to the DSF performance. As a consequence, the shaft-box and multi-storey types seem to be the most suitable DSF structures for naturally ventilated buildings.
- 3) In air conditioned buildings, narrow cavities are preferred as they accentuate the stack effect and enhance ventilation rates within them. However, the proximity of the second skin to the inner layer may create a high resistance to the flow supplied from the user rooms in naturally ventilated buildings. Considering the need to access the cavity for maintenance purposes and the office space requirements, a minimum of 40 cm and a maximum of 1 m are recommended for the cavity depth.
- 4) As large openings lead to higher airflow rates within the cavity, due to the reduced resistance to airflow, the top of the cavity is likely to be as large as possible to promote higher airflow rates through the building. Additionally, by closing the bottom of the cavity airflow ventilation through the user rooms may be improved.
- 5) The properties of the glazing materials selected for the DSF layers impact on the heat transfer rates, particularly the solar heat gains. The use of single glazing with high transmittance enhances the buoyancy force within the cavity and therefore the building natural ventilation. For the inner skin, application of high thermal mass materials leads to an increased air cavity temperature.
- 6) Apart from reducing direct solar gains into the user rooms, the heat absorption and re-emission by the shading device can increase the air temperature and

pronounce the stack effect within the cavity. Additionally, dark colour or high absorptive materials enhances the ventilation in the cavity. When placed in the middle of the cavity, the shading device allows smoother vertical air flow through either side of the gap, as low flow resistance is created. If placed closer to the inner layer, there is a risk of high heat transfer to the user room. Regarding the blind angles, horizontal angles may cause obstruction to the air circulation; therefore, near vertical positions seem to be more appropriate to reduce hindrance to the airflow in the cavity.

- 7) Increasing WWR usually improves the building thermal conditions, as it increases ventilation through the system. However, for WWR as high as 90%, the great solar heat gain into the user room may increase thermal discomfort.
- 8) For naturally ventilated buildings located in the northern hemisphere, the south facing façade (with 45° variations) seems to be the most effective orientation in capturing the solar gains needed to facilitate the natural ventilation in buildings with DSF. The DSF design should consider the density and height of surrounding buildings as they may create shading on the DSF.
- 9) The wind speed may counteract the influence of the thermal buoyancy effect created within the DSF cavity. When applied to naturally ventilated buildings, the DSF tends to perform better if the wind direction is perpendicular and away from the façade. However, it is important to evaluate the performance of the DSF with other wind directions that are occurring at the site.
- 10) Higher solar angles in summer are unfavourable to the occurrence of high temperatures within the cavity, but ventilation rates needs to be addressed for optimized design models. Regarding the air humidity, studies indicate that occupants have higher tolerance to a wide range of humidity levels when performing sedentary activities, such as in office buildings.

The study of DSF on naturally ventilated buildings can be considered still at its infancy as this review highlighted most studies are based on air-conditioned models and many of them focused on the DSF cavity as an 'isolated' structure, which is often treated as a local thermal feature without taking into account its influence on the user space. Although there is a lacking of comprehensive studies on the application of DSF in naturally ventilated buildings, some of the generic principles identified on the studied models can be applied to naturally ventilated buildings. They are therefore adapted as

guidance in defining a reference model and the key design parameters affecting the thermal performance of building with DSF, presented in the chapter 4.

Chapter Three

Climatic context and performance evaluation

The aim of this chapter is to provide supportive references for the methodology defined for this study in the following chapter. It presents an overview of the different climate conditions in the Brazilian territories in order to identify the requirements of natural ventilation as a viable passive strategy to meet the thermal comfort requirements in buildings. Additionally, a discussion about the comfort criteria is presented in order to establish the reference indicator for evaluating the thermal performance of naturally ventilated buildings. It also introduces the use of computational simulation tools as viable means for thermal evaluation of the building design.

3.1 The climatic context

Analysis of the climate context is the initial fundamental assessment of the proposed building's surrounding environment conditions that can help the designer to identify the seasons or periods during which a person may experience comfortable or uncomfortable conditions. The climatic analysis enables identification of possible passive design strategies that can be applied in buildings in order to reduce energy demand for mechanical systems. The climate is essentially characterised by the following variables: solar radiation, ambient temperature, air humidity, precipitation, wind and sky condition (Nayak and Prajapati, 2006). The following sections summarise the climatic characteristics of the Brazilian territories, identifying their differences among the regions.

3.1.1 The Brazilian climates

Brazil is the largest country in South America situated between the parallels of 5°16'19" latitude north and 33°45'09" latitude south. Because of its great extension, different regions in the country experience accentuated differences in their climate characteristics. A climate classification system proposed by the Brazilian Association of Technical Standards (2003) divides the territory into eight relatively homogeneous climate areas, as shown in Figure 3.1. The zones were defined according to the climate characteristics of 330 cells across Brazil, considering the local maximum and minimum temperatures and relative humidity. Figure 3.2 presents the population distribution over the country in order to show the occurrence of the main cities. Most of the population occupies the coastal area and the south-east regions, while sparse population is found in areas in the interior of the country and northwest region.

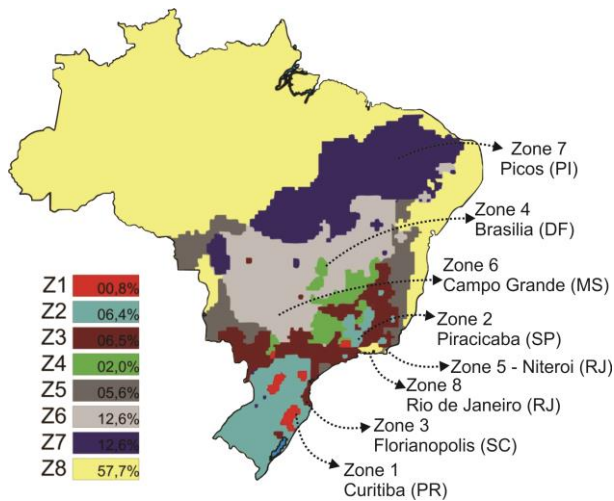


Figure 3.1 - Brazilian map with the incidence of eight bioclimatic zones

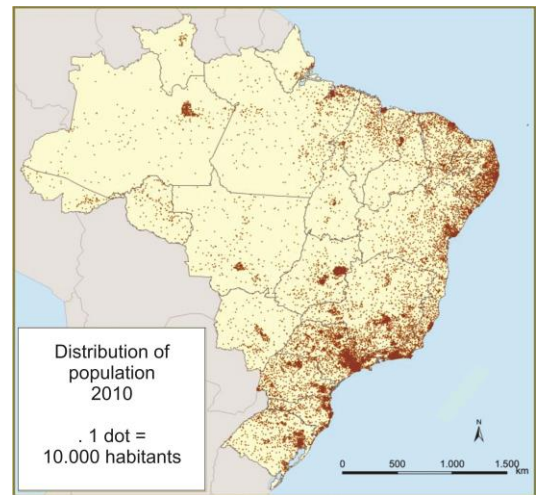


Figure 3.2 - Brazilian map with population distribution in 2010

For each of these bioclimatic zones, a set of passive design strategy recommendations for winter and summer periods is given by the National Construction Guidelines Standard (ABNT, 2003), as shown in Table 3.1. Those strategies give an indication of the country's diverse climatic conditions and the main strategies recommended in each zone.

Those recommended passive design strategies are based on the psychometric chart developed for non-air-conditioned buildings in developing countries by Givoni (1992). Fundamentally, the chart indicates the alternatives to expand the comfort zone through the adoption of architectural solutions to improve the user's thermal sensation. Although there are numerous approaches to define strategies for adaptation of the building to the local climate, the Givoni's method was adopted because the methodology considered countries with similar climatic conditions to Brazil. The chart is based on calculations that project the expected internal temperatures for buildings adequately designed for their environment, with sun protection and adequate natural ventilation (Bogo et al., 1994).

Among the recommended passive strategies, natural ventilation is clearly identified and divided into 2 different types: 'Selective cross-ventilation', which is indicated to be used only in the hottest times of day for zones 2, 3, 4, 5, 6 and 7 and 'Permanent cross ventilation', which is indicated exclusively for zone 8.

Table 3.1 - Passive strategies recommendations for the 8 bioclimatic zones in Brazil

	Recommended strategies	Bioclimatic zone							
		1	2	3	4	5	6	7	8
Winter	Solar heating of the building	X	X	X	X				
	Heavy internal walls	X	X	X	X	X	X		
	Artificial heating	X	X						
	Insulation materials to façades	X	X						
Summer	Selective cross ventilation		X	X	X	X	X	X	
	Permanent cross ventilation								X
	Evaporative cooling				X		X	X	
	Materials with thermal inertia							X	
	Artificial cooling							X	X
	Shade devices on openings							X	X

3.1.2 Climate characteristics of representative cities

Assessments of one representative city in each of the eight bioclimatic zones are presented in this section in order to highlight the differences in climatic conditions and to evaluate their climatic potential for natural ventilation. Considering the key site parameters that influence the DSF thermal performance defined in section 2.5, the analysed characteristics of the selected cities are: monthly maximum, average and minimum dry-bulb temperatures, global radiation levels and wind conditions. Detail analysis of air relative humidity is not included in the zones descriptions because, as described in section 2.5.3, this variable has low influence on the occupant's thermal sensation, when performing sedentary activities, such as office work.

Moreover, psychometric analysis for each climatic zone were performed using the software Analysis Bio (Schuch et al., 2010) developed by the Federal University of Santa Catarina in Brazil (Figure 3.3). By applying suitable weather files, the tool plots a series of climatic data points onto the Givoni's psychometric chart and indicates the percentages of annual hours of thermal comfort and the appropriate design solutions to be applied during the discomfort periods in order to improve thermal conditions within the building.

ZONES:

1. Thermally Comfortable
2. Natural Ventilation
3. Evaporative Cooling
4. Mechanical cooling
5. Humidification
6. High Thermal Mass/Passive Solar Heating
7. Passive Solar Heating
8. Mechanical Heating
9. Nat. Vent./Thermal Mass/Evap. Cool.
10. Thermal Mass/Evap. Cool.

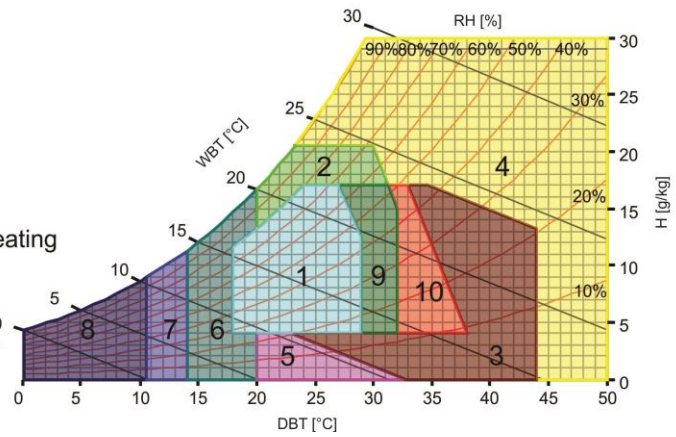


Figure 3.3 – Givoni's psychrometric chart used by Analysis Bio software

The representative cities selected are state capitals or cities with the highest number of habitants among those classified in each bioclimatic zone. They are: Curitiba-PR (zone 1), Piracicaba-SP (zone 2), Florianopolis-SC (zone 3), Brasilia-DF (zone 4), Niteroi-RJ (zone 5), Campo Grande-MS (zone 6), Picos-PI (zone 7) and Rio de Janeiro-RJ (zone 8). The data used are based on the weather test reference year (TRY) databases obtained from the US department of energy website and from the energy efficiency laboratory of the Federal University of Santa Catarina. For each zone, the city climatic characteristics and the results from the psychrometric analysis are presented. Graphs to demonstrate the seasonal variations in air temperature and global radiation are included. Wind conditions are also presented showing the predominant direction and velocities in each city. Additionally, variations of daily temperatures of a month in summer and in winter are included for each city to show the magnitude of their thermal amplitudes.

Zone 1 - Curitiba city

Localization: 25.4° S, 49.2° W. Zone 1 is mainly localized in the south region of Brazil.

Temperature and humidity: This zone presents the lowest temperatures (Figure 3.4) and fairly constant and high relative humidity, with averages of 21°C and 86% throughout the year.

Wind: The wind direction is predominantly distributed between east and east southeast and the speeds are lower than 6m/s in 92% of the time (Figure 3.5). During the summer, the dominant wind direction varies from 0° (north) to 135° (south east) in 85% of time.

Psychometric chart analysis:

Acceptable thermal comfort: 20% of the year, with the most comfortable months occurring during the summer.

Main strategies recommended: Although mechanical heating is not discarded during the winter, solar heating is one of the main recommended strategies for both winter and summer periods. The city presents a relative small annual demand for natural ventilation, 7% in average, and it occurs mainly during the summer season.

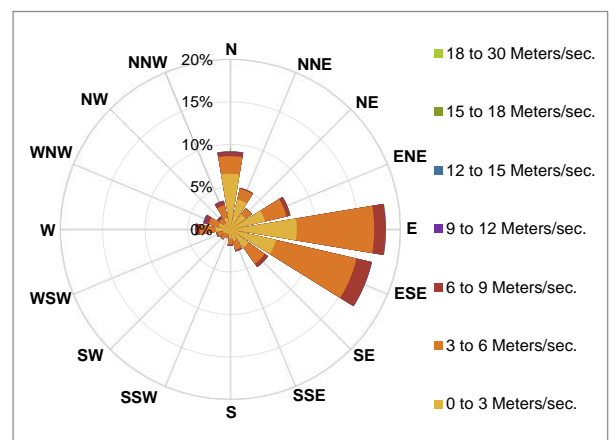
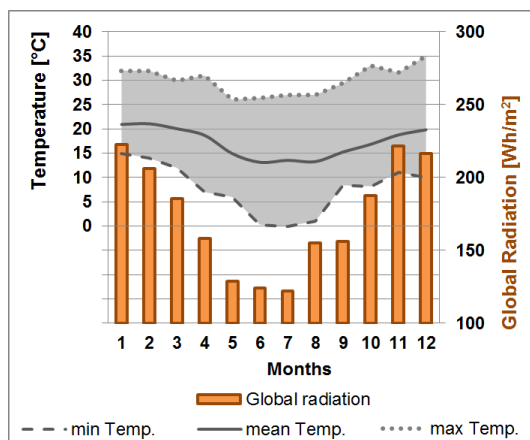


Figure 3.4 - Monthly average temperature and global radiation of Curitiba (zone 1)

Figure 3.5 - Wind rose of Curitiba (zone 1)

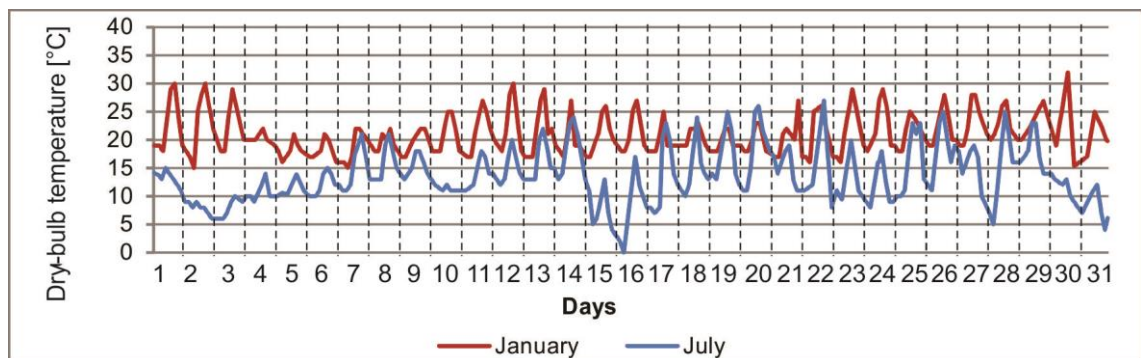


Figure 3.6 – Dry-bulb temperatures during January and July for Curitiba (zone 1)

Zone 2 - Piracicaba city

Localization: 22.7° S, 47.6° W. The zone occurs predominantly in the south and southwest areas of the country.

Temperature and humidity: The city presents the annual mean relative humidity of 74%, with lower ranges of approximately 65% occurring during the winter.

Wind: The predominant wind incidence occurs mainly from east and south-east and speeds lower than 6 m/s are recorded in 98% of the year. However, during the hottest months, the wind direction is well distributed, with 48% of time occurring from 90° (east) and 135° (south east.)

Psychrometric chart analysis:

Acceptable thermal comfort: 40% of the year.

Main strategies recommended: Similarly to Curitiba, this city presents a strong dependence on solar heating to keep the internal environment comfortable, especially during winter, when the strategy is indicated in 49% of time. Cross ventilation is recommended, in average, 21% of the year to achieve thermal comfort.

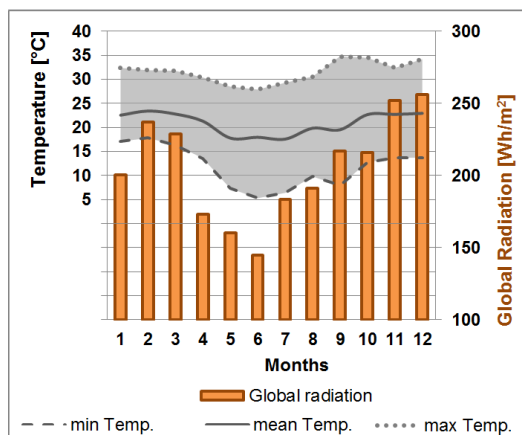


Figure 3.7 - Monthly average temperature and global radiation of Piracicaba (zone 2)

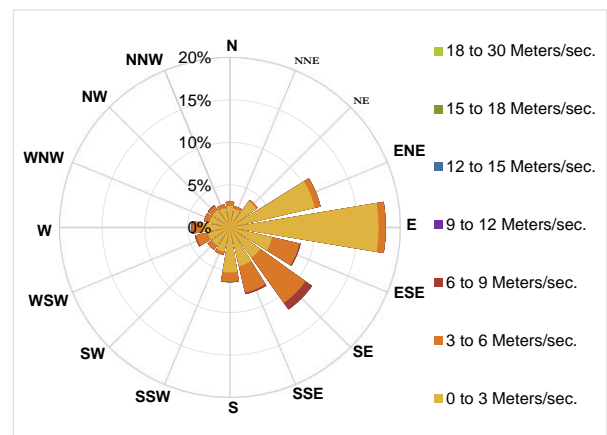


Figure 3.8 - Wind rose of Piracicaba (zone 2)

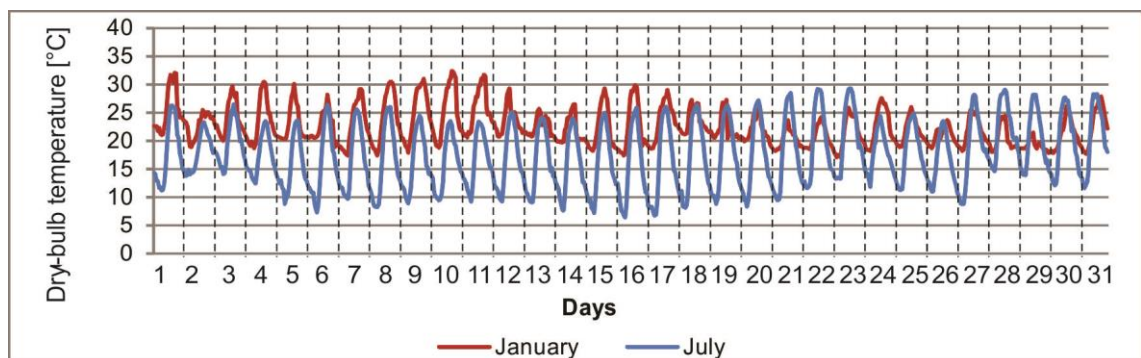


Figure 3.9 – Dry-bulb temperatures during January and July for Piracicaba (zone 2)

Zone 3 - Florianopolis city

Localization: 27.5° S, 48.5° W. The zone is mainly localized in south and southeast regions.

Temperature and humidity: The city is characterized by mild and low temperatures in the summer and winter, respectively (Figure 3.10), and mean relative humidity of 85%.

Wind: Florianopolis presents predominant wind direction from north and wind speeds lower than 6 m/s in 88% of the time for the whole year, being calm conditions experienced in 13% of the time (Figure 3.11).

Psychrometric chart analysis:

Acceptable thermal comfort: 21% of the year.

Main strategies recommended: During the warmest periods, the need of mechanical cooling is not discarded. But cross ventilation is the main passive strategy suggested during the summer, especially from November to April, when it is required, in average, in 67% of time. During the winter, the use of passive solar heating is the key strategy to keep the environment thermally comfortable, being indicated in 65% of the time from May to September.

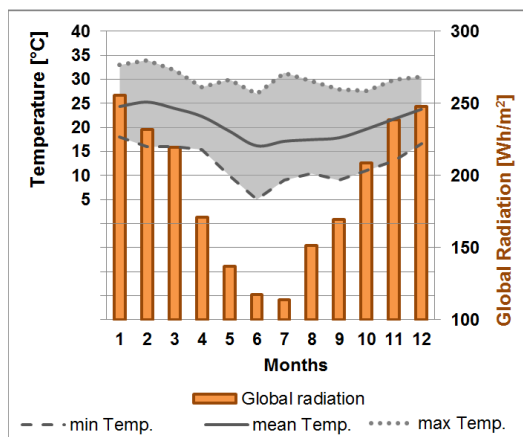


Figure 3.10 - Monthly average temperature and global radiation of Florianopolis (zone 3)

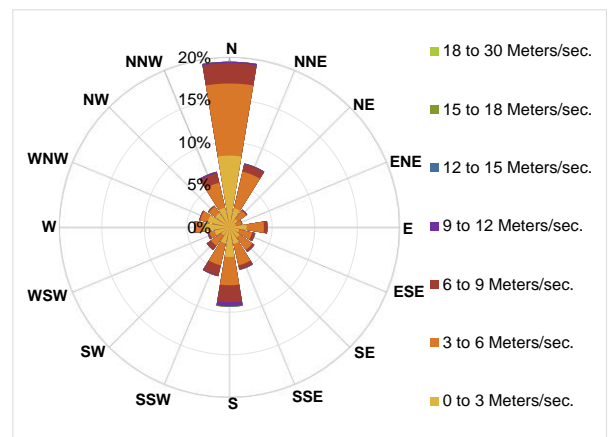


Figure 3.11 – Wind rose of Florianopolis (zone 3)

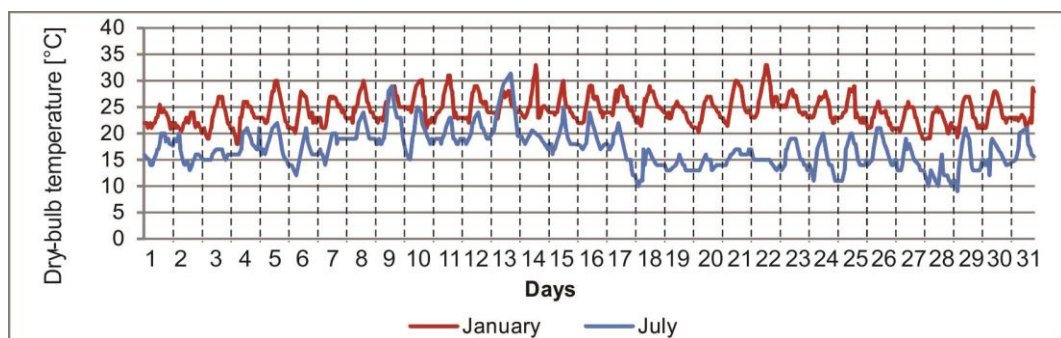


Figure 3.12 – Dry-bulb temperatures during January and July for Florianopolis (zone 3)

Zone 4 – Brasilia city

Localization: 15.7° S, 47.8° W. The zone is mainly localized in the centre west region. Although it covers only 2% of the country’s territory, it includes the national capital.

Temperature and humidity: The annual average temperature is 22.8°C and the monthly mean temperature varies from 16 to 30°C in 90% of the year (Figure 3.13). The annual relative humidity is 75%, with the driest periods occurring from July to September when the relative humidity drops to about 63%.

Wind: In 95% of the year, wind speeds are lower than 6m/s and predominantly from east, as shown in Figure 3.14. The wind directions are mainly from 0° (north) to 90° (east) in 63% of time during the summer. Calm conditions represent 35% of the time.

Psychometric chart analysis:

Acceptable thermal comfort: 41% of the year.

Main strategies recommended: The application of passive solar heating is indicated as the main passive solution for 42% of the time from March to September. From December to March, the warmer period, selective cross ventilation is indicated in 32% of the time.

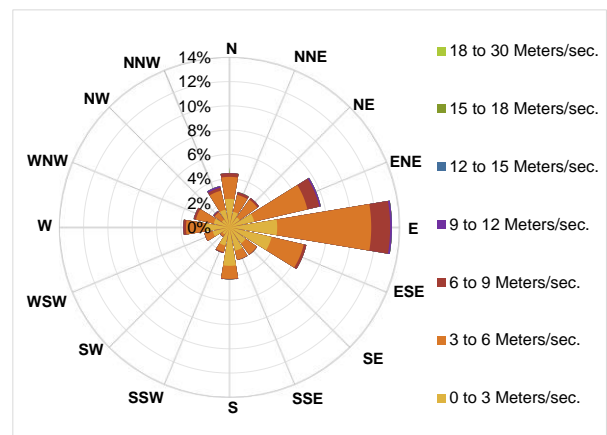
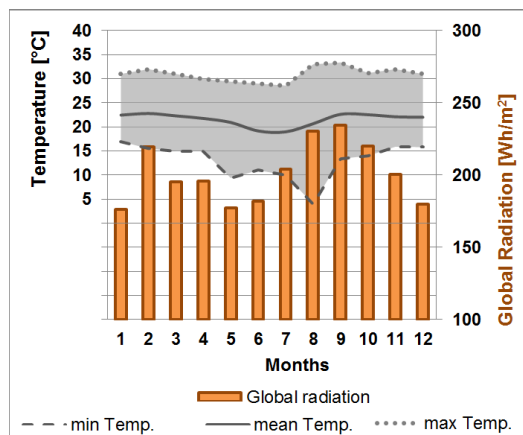


Figure 3.13 - Monthly average temperature and global radiation of Brasilia (zone 4)

Figure 3.14 – Wind rose of Brasilia (zone 4)

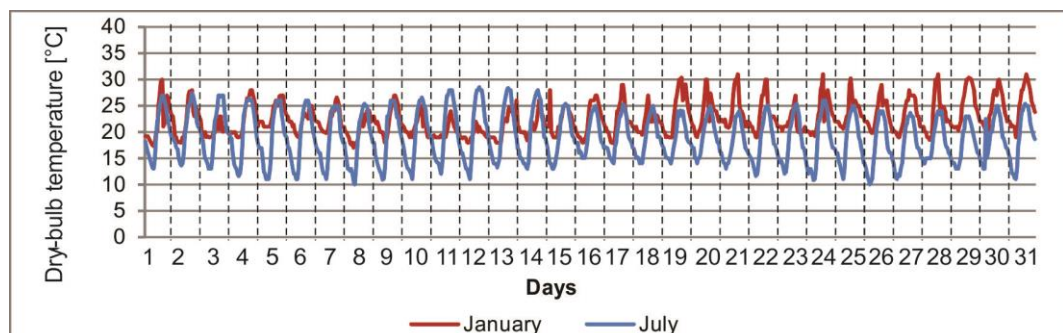


Figure 3.15 – Dry-bulb temperatures during January and July for Brasilia (zone 4)

Zone 5 – Niteroi city

Localization: 22.8° S, 43.1° W. The zone is present in some areas of the south east and the centre west regions.

Temperature and humidity: Niteroi is characterized by monthly average temperatures lower than 26 °C (Figure 3.16) and 78% of annual mean relative humidity.

Wind: In 98% of the time, the wind speeds are lower than 6m/s and the wind direction is predominantly from south, which is experienced in 48% of time during the hottest months (Figure 3.17).

Psychrometric chart analysis:

Acceptable thermal comfort: 50% of the year.

Main strategies recommended: For the winter season, one of the main strategies suggested is the use of solar heating, especially from June to September, when it is required in 30% of time. Cross ventilation is indicated all over the year, especially during the summer, being recommended in more than 30% of the time from November to May and up to 71% during February.

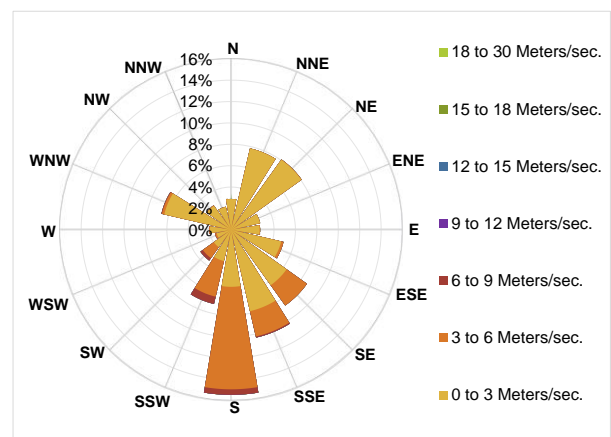
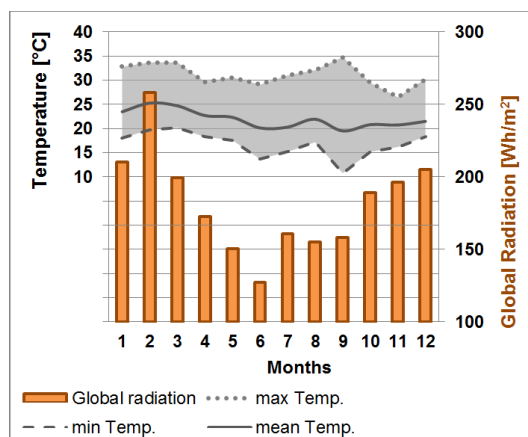


Figure 3.16 - Monthly average temperature and global radiation of Niteroi (zone 5)

Figure 3.17 – Wind rose of Niteroi (zone 5)

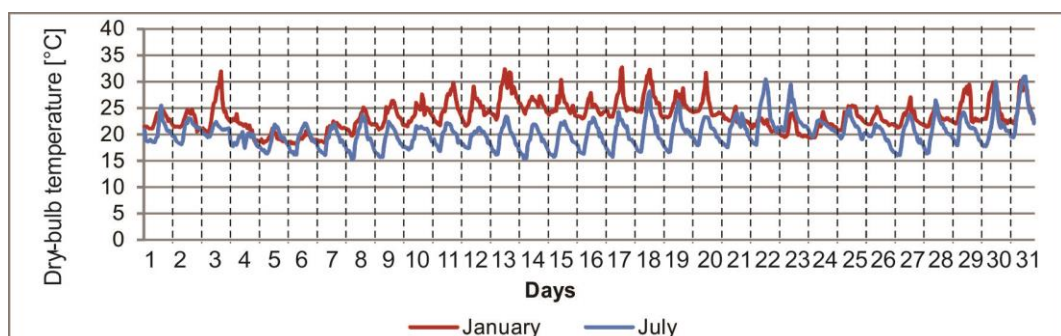


Figure 3.18 – Dry-bulb temperatures during January and July for Niteroi (zone 5)

Zone 6 – Campo Grande city

Localization: 20.4° S, 54.6° W. The cities with the climate characteristics of bioclimatic zone 6 are mainly localized in the centre-west of the country.

Temperature and humidity: The climate of Campo Grande presents annual mean temperature of 26°C (Figure 3.19) and 68% of mean relative humidity over the year, being the winter the drier season, when it drops to a minimum of 55%.

Wind: The wind conditions examination shows that in 83% of the time the wind speeds are lower than 6m/s and mostly directed from north and east (Figure 3.20), representing 46% of time during summer time.

Psychometric chart analysis:

Acceptable thermal comfort: 46% of the year.

Main strategies recommended: The main strategies recommended for this zone are selective cross natural ventilation, recommended in 26% for the year, and evaporative cooling.

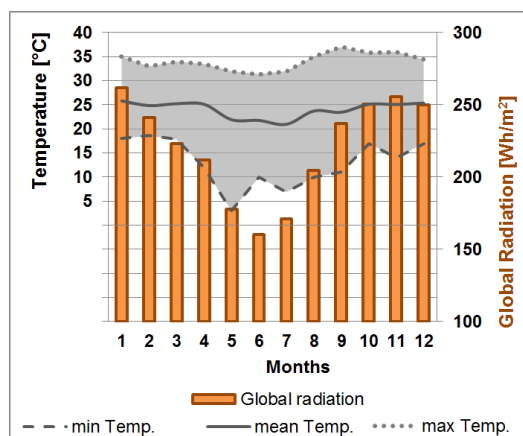


Figure 3.19 - Monthly average temperature and global radiation of Campo Grande (zone 6)

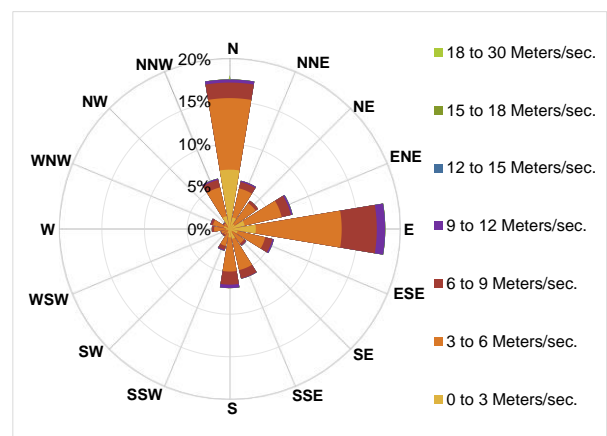


Figure 3.20 – Wind rose of Campo Grande (zone 6)

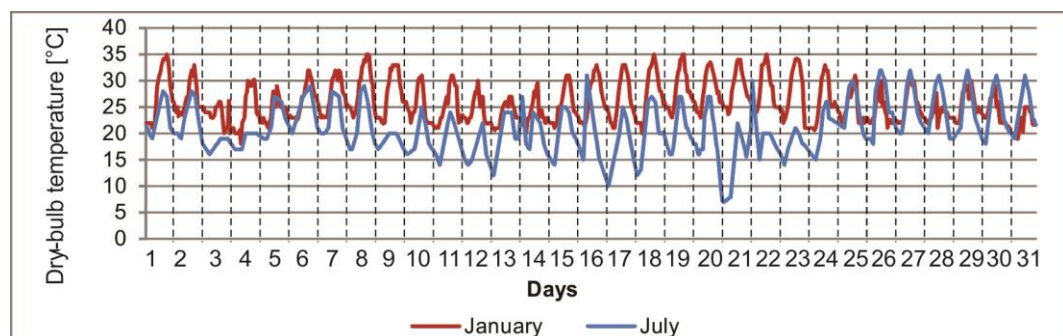


Figure 3.21 – Dry-bulb temperatures during January and July for Campo Grande (zone 6)

Zone 7 – Picos city

Localization: 7.1° S, 41.4 W. It is the hottest and driest climate among the zones and it is present in the arid region of the north-east.

Temperature and humidity: The city of Picos presents temperatures above 31°C in 33% (Figure 3.22) of the year combined with low annual relative humidity, 57% in average.

Wind: The wind analysis indicates that the speeds are lower than 6m/s in 100% of the time and directions mainly distributed from north-east to south-east, representing 69% of the time during the summer, as shown in Figure 3.23.

Psychometric chart analysis:

Acceptable thermal comfort: 33% of the year.

Main strategies recommended: The psychometric graph indicates that although the use of air conditioning is necessary, especially during the summer, natural ventilation is recommended in 39% of the time, reaching a peak of 55% in August.

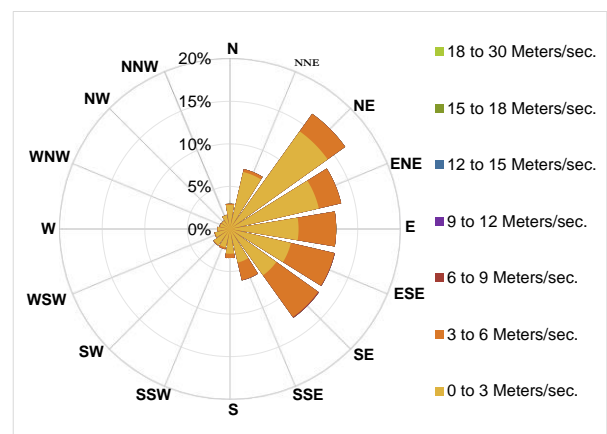
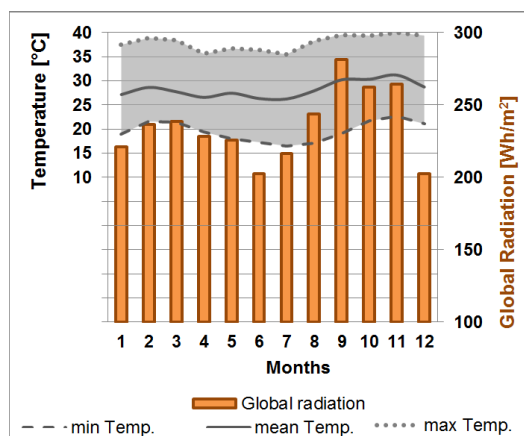


Figure 3.22 - Monthly average temperature and global radiation of Picos (zone 7)

Figure 3.23 – Wind rose of Picos (zone 7)

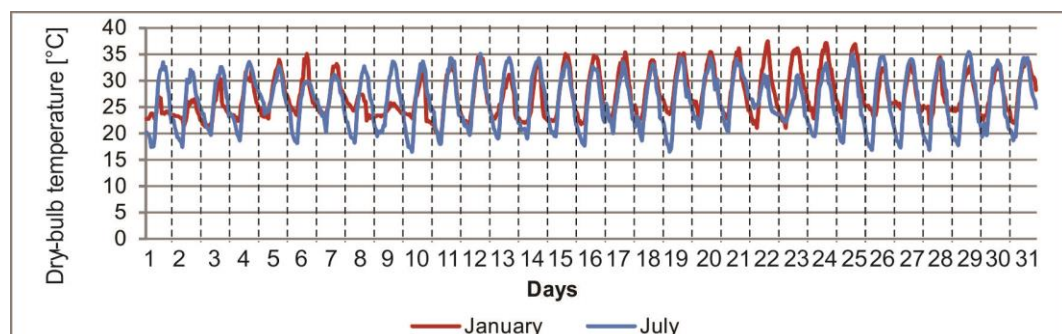


Figure 3.24 – Dry-bulb temperatures during January and July for Picos (zone 7)

Zone 8 – Rio de Janeiro city

Localization: 22.9° S, 43.1° W. The zone covers the biggest part of the territory (58%) and contains most of the coastal areas, including important state capitals such as Rio de Janeiro (RJ), Belem (PR), Natal (RN) and Vitoria (ES).

Temperature and humidity: The climate is characterized by high temperatures (Figure 3.25) and relative humidity; with averages equal 27°C and 80%, respectively, throughout the year.

Wind: As can be seen in Figure 3.26, the city presents wind direction well distributed with a slightly predominance to west and speeds lower than 6m/s in 99% of the year.

Psychrometric chart analysis:

Acceptable thermal comfort: 21% of the year.

Main strategies recommended: Although mechanical cooling is not discarded during the summer, one of the main passive strategies recommended is the permanent natural ventilation, which is indicated in 61% of the year.

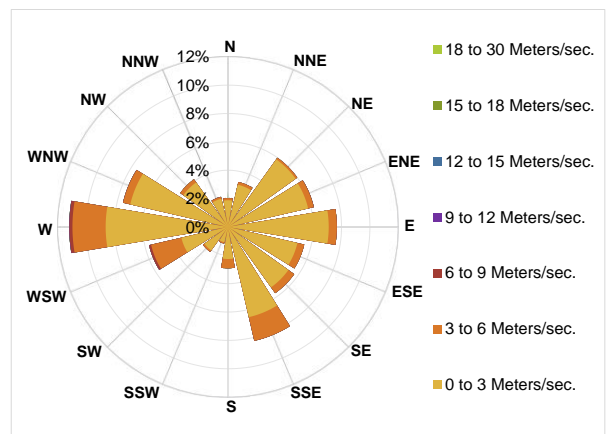
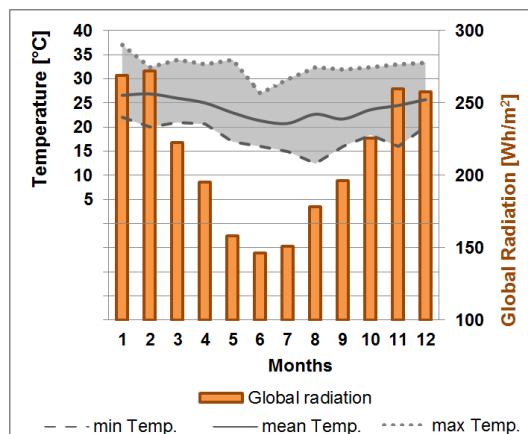


Figure 3.25 - Monthly average temperature and global radiation of Rio de Janeiro (zone 8)

Figure 3.26 – Wind rose of Rio de Janeiro (zone 8)

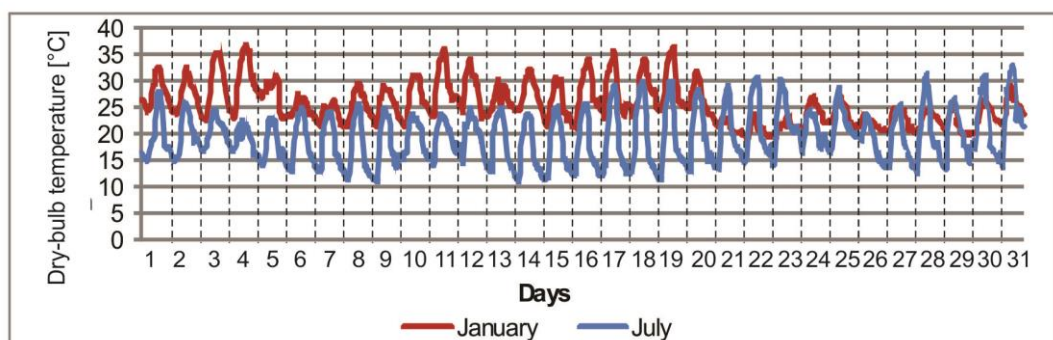


Figure 3.27 – Dry-bulb temperatures during January and July for Rio de Janeiro (zone 8)

3.1.3 Climatic potential for natural ventilation

Brazil presents a range of different climates, varying from low temperatures as in zone 1 to very hot areas as in zones 7 and 8. In terms of the solar incidence, the highest values are detected in the arid areas of northeast and centre west regions, whereas the lowest values are observed in the south region. In approximately 80% of the year, the temperatures experienced by the representative cities range from 16 to 30°C, which indicate favourable conditions for the use of natural ventilation as a passive design strategy. Apart from zone 1, the use of natural ventilation is strongly encouraged in all bioclimatic zones as a strategy to improve the thermal comfort (ABNT, 2003).

Table 3.2 shows monthly percentages of time in which natural ventilation is recommended according to the results of psychometric analysis for all representative cities. While ventilation is recommended during the whole year for zones 7 and 8, lower levels of ventilation is required during the coldest months for bioclimatic zones 1 to 6. This evidences the need to decrease airflow rates for the coldest cities, especially in bioclimatic zones 1 to 4.

Table 3.2 – Monthly percentages of time in which natural ventilation is recommended according to psychometric analysis

	Cities	Months												% of time	
		1	2	3	4	5	6	7	8	9	10	11	12	0 to 10%	
1	Curitiba	16	37	13	1	0	0	0	0	0	2	11	4	11 to 20%	
2	Piracicaba	43	56	40	29	0	2	1	4	5	22	21	29	21 to 30%	
3	Florianopolis	77	82	75	36	14	4	3	5	16	28	49	51	31 to 40%	
4	Brasilia	41	36	29	14	7	1	0	4	15	14	19	30	41 to 50%	
5	Niteroi	35	71	60	51	31	13	7	14	11	28	32	32	51 to 60%	
6	Campo Grande	84	65	60	46	6	3	10	14	8	26	44	49	61 to 70%	
7	Picos	59	45	66	77	40	38	26	17	17	25	23	36	71 to 80%	
8	Rio de Janeiro	75	73	68	58	39	28	32	32	61	85	81	62	81 to 90%	
														91 to 100%	

Another strategy able to improve the thermal conditions of building in hot areas is by employing a night ventilation strategy. The cooling benefit can be further enhanced by this approach that takes advantage of the lower external night-time temperature to pre-cool the building structure. Some of the advantages of this operational strategy are described by CIBSE (2005) such as cooling of the building fabric will reduce the mean radiant temperature, which enhances the occupant's perception of thermal conditions during the following day. Furthermore, the lower night-time temperature, the inside–outside temperature differences will be greater, enhancing both the stack driven flow

rates and the cooling capacity of the outside air. Additionally, by ventilating during unoccupied periods, the potential problems of draught and noise in the occupied space are avoided.

The local climate characteristics are crucial to ensure that appropriate strategies are applied to the building design. Moreover, another important phase of the building conception consists of predicting its thermal behaviour which allows modification and incorporation of variable design solutions to improve the thermal performance. The next section presents a discussion about the existing thermal performance evaluation criteria in order to establish an indicator for predicting the indoor thermal performance of naturally ventilated buildings with DSF under Brazilian climates.

3.2 Building thermal performance evaluation

Prediction of a building's thermal performance refers to the characterization of human requirements of thermal comfort based on the heat transfer between the building and its surroundings. For air-conditioned buildings, it influences the heating and cooling loads and hence determines the amount of energy required for heating and cooling to maintain optimal thermal comfort conditions for occupants. For non-air-conditioned buildings, it represents how the building continually responds to the changing of outdoor climatic conditions, regulating the indoors conditions in order to provide the thermal comfort requirements of occupants (Nayak and Prajapati, 2006). In warm areas thermal performance is usually measured against a benchmark temperature, related to the likelihood of discomfort, which should not be exceeded for more than a certain length of time, usually expressed as a designated numbers of hours or a percentage of the annual occupied period (CIBSE, 2006). Determined by selected materials and design solutions, the building thermal performance analysis not only determines how effective the solutions applied are, but it also guides the determination of more suitable design strategies, from the identification and quantification of moments of thermal discomfort (Nayak and Prajapati, 2006).

Achieving acceptable thermal performance in naturally ventilated buildings under warm climates requires adequate definition of solutions in the design according to the use and operation of the building such as application of suitable fabric materials (density, specific heat, thermal conductivity, transmissivity, etc.), size and orientation of glazing areas and openings and incorporation of shading devices. Additionally, local weather data, which are represented by solar radiation, ambient temperature, wind speed, humidity, etc., and internal heat gains produced by occupants, lighting and equipment can influence the heat transfer processes and affect levels of thermal acceptance

within a building. Increase of air movement and use of evaporative cooling are also suitable strategies that can remove internal heat and therefore, enhance the building thermal performance in warm and hot areas.

A key criterion when assessing a building's thermal performance is to define the conditions which are considered acceptable by occupants and consequently the thermal comfort experienced by them (CIBSE, 2005; Nayak and Prajapati, 2006). The next section introduces the thermal comfort concept and discusses the available methodologies to evaluate its perception.

3.2.1 Thermal comfort

Thermal comfort is defined by ASHRAE (2013) as the condition of mind that expresses satisfaction with the thermal conditions. It is usually used to indicate whether or not an individual feels thermally comfortable in an environment. This is generally perceived as a combination of several factors such as the level of activity performing by the occupant, the ambient air and surrounding surfaces temperatures, and air's relative speed and humidity. These aspects influence the way in which heat is exchanged from our body to the environment and our thermal satisfaction (Nicol et al., 2012).

Thermal comfort is a subjective sensation resulting from a combination of environmental and personal factors. The former includes air temperature, which is measured by the dry bulb temperature, air velocity, which defines the level of heat exchange between the person and the air, radiant temperature, which is related to the temperature of the surroundings surfaces, heat generating equipment placed in the user room, and the air relative humidity. The personal factors are related to occupants' clothing and metabolic rate. Clothing insulates a person from exchanging heat with the surrounding air and surfaces and affects the loss of heat through evaporation of sweat and the metabolic rate measures the level of activity performing by the occupant, which is related to the body's heat production. Other contributing but less significant factors can include access to food and drink and state of health (Treeck, 2011).

A number of different approaches and methodologies for estimating the likely thermal comfort perceived by the user have been developed to combine the environmental variables into a single index for the assessment of thermal comfort. There are two main models to evaluate the thermal acceptability of indoor environments, which describe how the building microclimatic conditions can be evaluated (Nicol et al., 2012).

The first model, known as static thermal heat balance, is an analytical evaluation of human thermal sensation that considers the individual as a passive recipient of the

thermal environment. This approach was developed by Fanger in the late 1960s and it is based on the predicted mean vote (PMV) model. It consists of a numerical index that combines physical and personal variables to predict the perception of occupants in relation to the thermal conditions in the building (Hoof et al., 2010). The International Standard ISO 7730 (2005) is the main thermal comfort regulation based on PMV/PPD method. However, the use of this model has become globally questionable, especially when applied in naturally ventilated buildings, as it does not consider the change in indoor thermal comfort in relation to the season variations and does not account for human adaptation under different temperatures (Yau and Chew, 2012).

The second model, known as the adaptive approach, considers the human body as an active agent that interacts with the environment in response to one's preference and thermal sensation. In this model, the variations in the indoor environmental conditions under different seasons and climates change the limits of the acceptable comfortable temperatures. The local social conditions and past thermal history thus modify the occupant's thermal expectations and preferences (Nicol et al., 2012; Race, 2006). Thus, people in warm climate zones tend to tolerate higher indoor temperatures than people living in cold climate zones (Halawa and van Hoof, 2012).

The two main standards specifying the adaptive approach are ANSI/ASHRAE 55 (2013) and EN 15251 (CEN, 2007). They present conceptually similar methodologies, though some differences exist such as the number and type of buildings measured and the outdoor temperature definition (Nicol and Humphreys, 2010). The ASHRAE 55 (2013) method is based on more than 21,000 measurements taken around the world, primarily office buildings, and it is applied only to naturally ventilated buildings. The dark shaded regions in Figure 3.28 illustrate the limits within which the indoor operative temperatures are considered thermally acceptable. The outdoor temperature (T_{out}) used in this methodology is defined by the prevailing mean outdoor air temperature, which is calculated by the average of daily mean temperature of the previous days. Acceptability limits for typical building applications, in which the thermal comfort range satisfies 80% of people, are represented by the following equations:

- **Lower temperature limit** ($^{\circ}\text{C}$): $0,31 * T_{out} (^{\circ}\text{C}) + 14.3$ (equation 2)
- **Upper temperature limit** ($^{\circ}\text{C}$): $0,31 * T_{out} (^{\circ}\text{C}) + 21.3$ (equation 3)

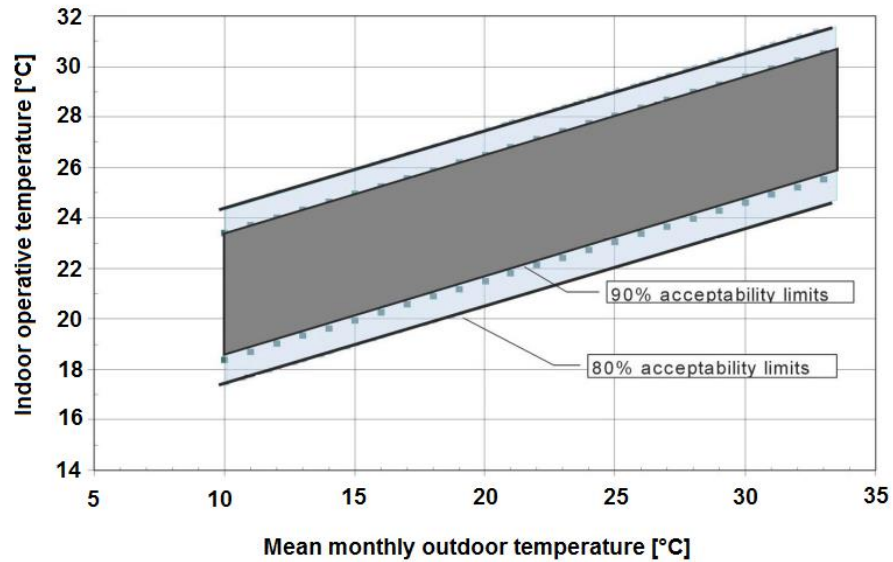


Figure 3.28 - Acceptable operative temperature ranges for naturally ventilated spaces from ASHRAE 55 (2013)

The 90% acceptability limits are used only when higher levels of thermal comfort are desired. The standard indicates that the upper acceptability temperature limit increases when the room air speed is above 0.3m/s. In this case, the modified acceptable temperature limits are calculated according to the corresponding air speed, as shown in Table 3.3. This calculation is based on the Standard Effect Temperature (SET) method, which enables a calculation for determining the cooling effect of air movement.

Table 3.3 – Increase in acceptable operative temperature limits in the adaptive comfort approach resulting from increasing air speed above 0.3m/s.

Air speed = 0.6m/s	Air speed = 0.9m/s	Air speed = 1.2m/s
1.2°C	1.8°C	2.2°C

Operative temperature used in the standard is defined mathematically as (ASHRAE, 2009):

$$T_{op} = \frac{t_i \sqrt{10v} + T_r}{1 + \sqrt{10v}} \quad (\text{Equation 4})$$

where t_i is the indoor air temperature [°C], T_r is the mean radiant temperature [°C], and v is the air speed [m/s].

Regarding the effect of relative humidity, the standard highlights that no humidity limits are required in this model. According Nicol and Humphreys (2010) humidity is insignificant in the model as it plays a minimal influence on thermal sensation and perceived air quality by users performing sedentary activities.

The ASHRAE 55 standard also specifies that the operative temperature graph is specifically applicable to naturally conditioned spaces where near sedentary physical activity levels as those typical of office work, with metabolic rates ranging from 1.0 to 1.3 met. The method also specifies that occupants may freely adapt their clothing to the indoor and /or outdoor thermal conditions within a range at least as wide as 0.5–1.0 clo.

Thermal comfort analysis can be applied at the building design stage in order to check levels of acceptable comfort conditions that can be achieved. In this case, calculations of the building heat transfers and airflow process, considering the geometry and materials applied on the building model, are performed to identify the resulting internal conditions. Nowadays, those calculations are embedded within the computer simulation design software, which have been widely used to examine the thermal performance of a building design. The following section introduces the use of computational simulation tools as a viable method for thermal assessment of the building design and defines the software used in this study.

3.2.2 Computational simulation

Computational simulation is nowadays one of the most used analysis tools based on numerical methods that aim to provide an approximate solution of a building's thermal behaviour based on a realistic model (Hensen and Lamberts, 2011). It is the most advanced method that the industry has at its disposal to assess the performance of a building before it is built (CIBSE, 2015). It is an alternative to controlled experimental measurements in laboratory or experiments in-situ, which in the case of DSFs, is not only subject to uncertainties in controlling the complex thermo-fluid phenomenon, but it also generally demands high cost, specific equipment and considerable time to execute (De Gracia et al., 2013).

Although recent advances in simulation tools have attempted to address the complexity of reality to provide more comprehensive and detailed behaviour of a building, the computational modelling is an idealised version of reality. Therefore, the building will not perform exactly in the same way that a real building performs. To introduce consistency into the implementation of modelling work and design calculations and to provide confidence in the results, some quality assurance procedures must be followed according to CIBSE (2015). They include the following procedures.

- **Establishment of the aim of the simulation task:** frequently, modelling is used to predict trends and to compare different design options. In these cases,

analyses comparing the impact of various design measures in relation to the reference model are performed.

- **Software selection:** The definition of an adequate model needs to take into consideration the level of accuracy and details required, time and computational resources available. More detailed models are usually more time and computational resource consuming, and, therefore, appropriate and suitable models have to be selected based on the specific design objectives (Hand et al., 1998).
- **Software training:** the training process involves workshops, use of manuals with training examples, support by online training resources and use of documented performance assessment methods.
- **Design processes:** the design process and its stages provide the context to all decisions to be made. These include information available, selection of calculation methodologies and software, strategy for modelling, and the level of risk and accuracy of results required.

It is important to be aware of the approximations and underlying assumptions in the mathematical models of the software tools and calculation procedures. It is also necessary to appreciate the implications these assumptions have on the analysis. To acquire a good qualitative understanding is considered to be more important than a quantitative assessment of the theoretical models (CIBSE, 2015). De Gracia et al. (2013) reviewed different typologies of numerical modelling and available computational resources for the study of DSFs, highlighting their benefits and limitations. The models are associated with methods of calculation and their accuracy demonstrates the differences among the levels of detail of the results. Simple tools such as analytical and lumped models, non-dimensional analysis and control volume models provide information in the design phase of the DSF without consuming high computational resources. However, simplified modelling inputs such as linear vertical temperature gradient in the cavity, constant surface temperatures and convective heat transfer coefficients were assumed (De Gracia et al., 2013). Those assumptions may affect the basic premises of the DSF functioning, such as the lack of air temperature gradient within the cavity and the variability of airflow according to solar incidence on the façade, resulting in a poor evaluation of the building thermal performance.

Computational fluid dynamic (CFD) simulation software

One of the main current approaches used to study the thermal performance of the DSF is the computational fluid dynamic (CFD). In the CFD technique, arguably the most complex ventilation modelling technique in use today, the external atmosphere and the

air space in the interior of the building are divided into domain geometries. Solid boundary layers, such as walls, ceilings, windows, are then defined and a material U-value, which relates the inside to outside temperature difference to the heat flux through the material, can be defined. A mesh of small cells is included in the spaces, creating a grid, which the cell dimensions can be defined by the modeller. The typical elements used in CFD packages are tetrahedral, pyramids, prismatic wedges and hexahedral. Although being a time costly procedure, regions of refinement (smaller cells) can be applied in certain parts of the building to capture details with more accuracy (CIBSE, 2015).

From that, basic fluid dynamics equations for conservation of mass, momentum and thermal energy are solved for all nodes of the grid. For the conservation of mass, the equation used is derived by considering a fixed volume in space and assuming that the flow of air into the volume is equal to the flow of air leaving the volume. For the conservation of momentum, the equation used is derived from Newton's second law, which states that force = mass \times acceleration. The conservation of energy equation (or the first law of thermodynamics) states that the rate of change of internal energy of a volume of air is equal to the heat supplied to that air minus the work done by the volume of air on its surroundings. All these calculations give a detailed picture of the flow pattern (temperature, air velocities and pollutant distribution) in each room.

The CFD tools also consider the turbulent nature of the flow in the building, regardless whether the flow is caused by mechanical, ventilation or natural ventilation. Turbulent flows mean that they exhibit a random, fluctuating, time dependent behaviour. There are various methods available for calculating this including the k-epsilon family of models, the k-omega model and the SST (shear stress transport) model. Much research has been done to help CFD practitioners to make an informed decision about which model is most suitable for their application. Regarding the modelling of a building with DSF Pasut and De Carli (2012) has highlighted which factors are important in the simulation and indicated that the results are more stable for the models with k-epsilon turbulent model.

Other settings in the CFD simulation are the buoyancy effect and the nature of the simulation. In CFD models involving building ventilation, especially natural ventilation, representation of the small forces created by buoyancy effects, which is the density of the air at some reference temperature, is of paramount importance. It is usual to adopt the Boussinesq approximation for modelling buoyancy effects. Regarding the nature of the simulation, two possible options are steady state and transient. For most CFD modelling, a steady state simulation is sufficient (CIBSE, 2015).

Although CFD simulations provide details about the nature of the flow field inside the building rooms, some limitations also need to be considered. The key limitation of the CFD use is related to the highly demanding computing resources, which often restrict the calculation to steady-state cases or very short simulation periods. Other limitations are the dependency of finer grid definition to effectively capture the thermal and flow effects, which usually increases time demand and limits size of geometry modelled (Ji et al., 2007), (Jiru et al., 2011).

Building dynamic thermal simulation software

In the airflow network technique, the building is divided into thermal zones which are treated as a network of nodes representing rooms and system components. These internodal connections represent the distributed flow paths associated with temperatures and airflows resulted from many simultaneous thermal and fluid flow processes, which interact and vary with time. This allows analysis of the thermal performance of a building with DSF and predicts air temperatures and airflow rates for each thermal zone normally at hourly intervals or less for the period of a whole year. Usually, a thermal comfort analysis model, such as PMV/PPD and adaptive assessment method, is embedded within the algorithm allowing definition of periods of comfort and discomfort on a yearly basis.

The advantages of this approach include less time required for modelling and simulation processes compared to the CFD models and enabling of the study of transient thermal behaviour (Treeck, 2011). This technique is commonly used in building thermal evaluations to examine the interactions between the building's envelope, its occupants and the external environment, and to predict the relative performance among design alternatives, where there is less demand for absolute accuracy (Augenbroe, 2011).

The main limitation of this approach lies in the assumption that the air within each thermal zone is well mixed. It is assumed that air temperature is uniformly distributed over the whole thermal zone and the air momentum effect from an inflow opening is neglected. Thereby the room temperature distribution cannot be determined and the results of multizone models could be inaccurate (Wang and Chen, 2008). This may affect the predicted thermal comfort, as different spaces within a thermal zone may experience different thermal conditions, depending on the openings location and the thermal transmittance of the materials applied to different walls, for example. Moreover, this technique does not provide details about profiles of air flows inside the rooms (Hand et al., 1998), but only the amount of air flowing in and out of a thermal zone.

IESVE and FloVENT simulation tools: the model verification

Four techniques for validating a building simulation tool are given by CIBSE (2015). They include:

- code checking, in which the computer code is checked line by line;
- analytical tests, which predictions for a simple situation are compared with expected results that can be calculated analytically;
- empirical validation, which predictions are compared with real building measurements and;
- inter-program comparisons, where predictions are compared with those from other simulation programs supplied with equivalent data input.

Although the empirical validation is claimed to be, in principle, the most powerful validation technique, it is used to address 'how well' the program is able to predict reality. Moreover, the results are dubious due to the uncertainty in measurements (as it should take into account occupant variant behaviour) and data supplied to the program. More weaknesses related to this method are the difficulty to carry out, high cost and time consuming. The last method, on the other hand, is specially indicated for exploration of the sensitivity of building design changes. Moreover, it is an accessible test to undertake and allows the solution of less conventional building modelling to be validated. Although both software to be used will have inaccuracies, uncertainty is an intrinsic weakness of any validation process.

The validation of a software can be defined as the testing of the theoretical correctness of a program and of the mathematical and numerical solution procedures used in a software (CIBSE, 2015). Verification of a building thermal model, on the other hand, is related to the procedure of checking whether the results obtained from simulations matches the expectations when different design variations are applied to the model. Due to the lack of knowledge on the thermal and flow behaviour of a naturally ventilated building with DSF, this thesis did not aimed to validate any available software, but to verify the consistency of the results of building models with DSF using two different tools. For this, the inter-program comparison method was used as a verification process of the thermal and flow behaviour of a building with DSF.

It is known that dynamic simulation software has limitations in specific predictions. In the case of DSFs, there is an uncertainty of the software in predicting the stratification of air within a space linked to the network model that simulates the airflow between spaces and the external environment (CIBSE, 2015). This type of software assumes

that a space has a single temperature no matter how large the space is. This is commonly described as the 'well mixed' or 'stirred tank' model, referring to the assumption that the temperature in a space is uniform because the air is suitably mixed. Therefore, a CFD software was used to overcome this limitation as it has a specific calculation algorithm to provide more accurate assessments of the thermal environment. In this study, CFD modelling was used for computing the airflow path of different designs of naturally ventilated building models with DSF.

Similarly to thermal dynamic models, CFD programs exhibit several important limitations which result from the way CFD programs have been developed and the assumptions made in this process. One of the most commonly recognised limitations is the high computational resources required, especially for time dependent flows. Thus, it is unfeasible to simulations that the aim to predict the variations of the building thermal behaviour with time of the day and seasons of the year.

The thermal dynamic simulation software IESVE was used as a main tool to compare the impact of various design measures in relation to a reference model. The CFD tool FloVENT was used to perform a comparative verification on predictions of the DSF's airflow results from IESVE. The capability of modelling and simulating the DSF thermal and airflow mechanisms, the usability of navigation and control systems and the presentation and visualization of the results analysis were considered in these selections.

The IESVE is a dynamic thermal simulation software based on principles of mathematical modelling of the heat transfer processes occurring in and around a building. The tool is composed of integrated analysis modules with features to calculate dynamic conduction and convection heat transfers. It also incorporates models for calculating short and long-wave radiation exchanges and external solar shading according to solar angle and glazing properties (IESVE, 2014).

The airflow network approach addresses infiltration, single-sided and cross ventilation, which are driven by pressures arising from the combined wind and buoyancy forces (stack effect) calculated at each simulation time step. The flow through each opening is calculated as a function of the buoyancy pressures, which are dependent on the aperture positions in height and air densities, providing two-way flow that may occur through a single opening either side of a neutral pressure plane. The software has been used on simulation of models with DSF (Hamza, 2008; Shameri et al., 2013), in which bulk air temperature and stratification that occur within the cavity can be modelled and simulated using horizontally divided thermal zones.

FloVENT is a CFD air flow modelling analysis software designed to simulate air flow and heat transfer mechanisms specifically for rooms or buildings. In the software, the overall dimensions and materials specifications of the enclosure are defined, over which a computational grid is applied. The software includes the application of solar boundary conditions and automatically calculates radiation exchange. With ability to simulate either turbulent or laminar flow, FloVENT solves the relevant differential conservation equations at each computational grid cell. It provides solution for convective, conductive and radiative heat transfers through glazing and walls (Mentor, 2014). FloVENT has also been used to simulations of models with DSF (Rahmani et al., 2012; Manz, 2003; 2004; Wong et al., 2005). In these cases, although different design aspects were tested, steady state condition solutions were used and the transient effect of heat transfer was not taken into account.

3.3 Chapter summary

This chapter provides the background knowledge for simulation and thermal performance analysis of building models in order to underpin the methodology defined for this study, presented in the next chapter. Analyses of 8 cities in Brazil highlighted the contrast of the different bioclimatic zones and the potential to use natural ventilation to improve thermal comfort conditions in these climates. Differences regarding radiation level, outdoor air temperature, wind conditions and daily thermal amplitude are also presented. Based on the climate analysis, maximization of airflow rates through the building appears as a viable complementary strategy to improve the thermal performance of Brazilian buildings in many regions. Natural ventilation is strongly indicated for zones 2 to 6 during the warmest months and during the entire year for bioclimatic zones 7 and 8. The high temperature and levels of solar radiation in the Brazilian territories indicate the need for application of additional solutions such as control of solar gains, application of construction materials with high thermal mass and provision of night ventilation to improve the thermal comfort, especially during the summer.

The ASHRAE 55 (2013) standard method was identified as a suitable indicator for predicting the indoor thermal performance of naturally ventilated buildings under Brazilian climate conditions. It uses the adaptive approach, which considers the indoor acceptable temperature as a function of the outdoor air temperature. In this approach, especially developed for naturally ventilated buildings, the individual is supposed to have some degree of control over the thermal environment. This results in a wider comfort temperature range in which occupants will feel comfortable. For this evaluation, outdoor and operative indoor temperatures are combined into a chart to indicate

whether or not the user is thermally comfortable. These calculations are performed by thermal simulation computer software, which provide detailed hourly results over the whole year.

The network airflow model algorithm is used in the IESVE to predict the effect of ventilation and thermal details of the building that enable comparatively evaluation of design alternatives. The complexity of heat transfer and airflow processes in the DSF are studied using CFD FloVENT software and the results are used to verify findings obtained from the integrated dynamic thermal simulation software IESVE.

Chapter Four

Research methodology

This chapter presents the methodology for achieving the aim of the research. Firstly, it describes and justifies the characteristics defined for the base case model. Then, the modelling and simulation processes are described and the procedures to the analysis of the resulting data are presented. Furthermore, findings from the simulation of the base case model are presented, indicating the issues of the model thermal performance. Lastly, the definition of the key design and site parameters are presented.

4.1 Research methodology outline

This study aims to determine the thermal performance of office buildings with DSF under Brazilian climate conditions. The methodology, linked to the objectives defined in Chapter 1, involves literature search, computer simulation and data analysis. The overall structure is presented in Figure 4.1 and described under 6 main stages as follow.

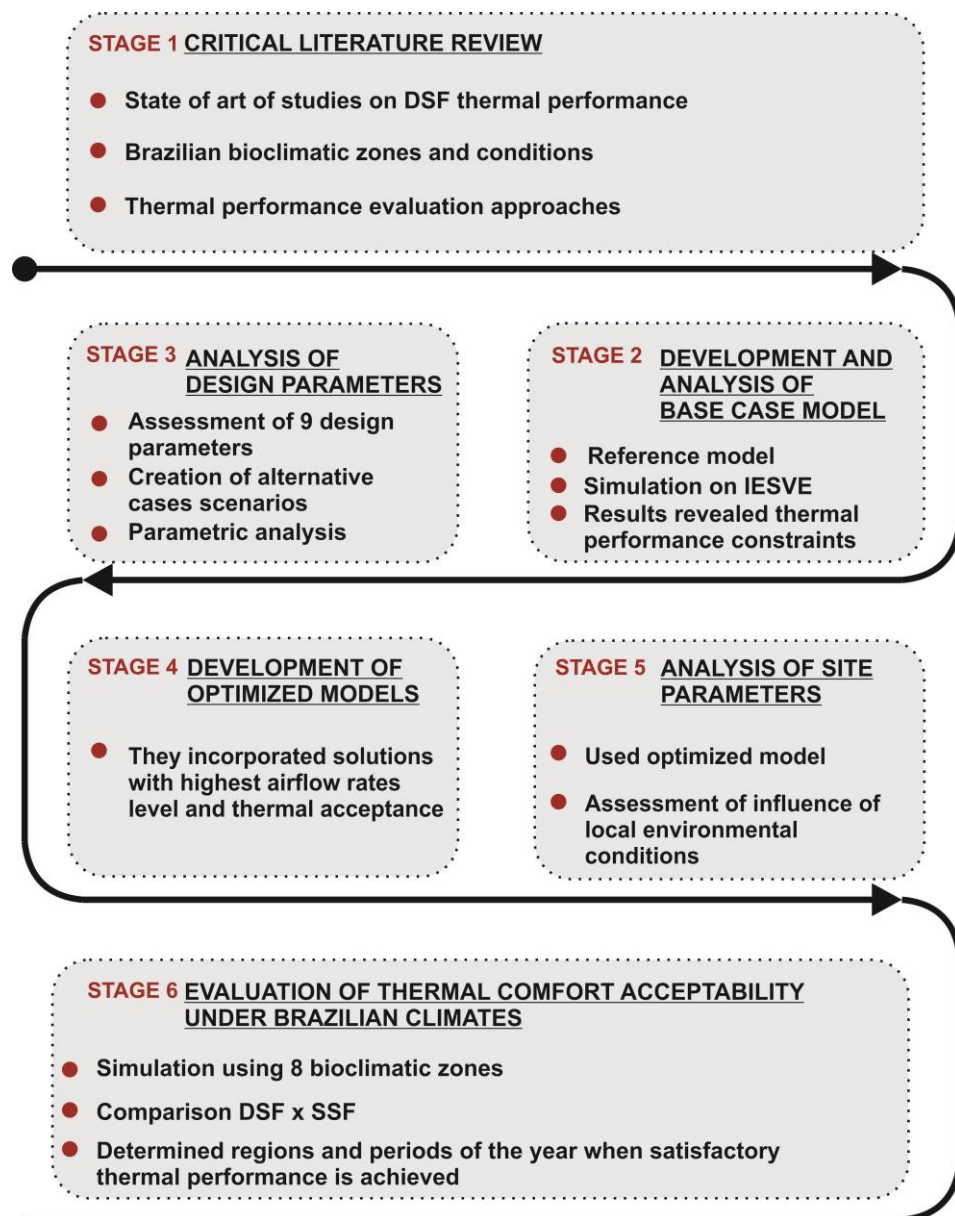


Figure 4.1 - Methodology scheme

Stage 1 Critical literature review – In order to have a comprehensive understanding on the state of art of thermal performance of building with DSF, a systematic critical review of the existing body of knowledge was

performed and presented in Chapter 2. Deductions of the main design solutions and site conditions required for an effective functioning of the DSF in naturally ventilated buildings were derived from this review. Additionally, in order to establish the requirements of natural ventilation as a viable passive strategy to improve thermal comfort in Brazilian buildings, an overview of the country's climate conditions was carried out and presented in section 3.1 of Chapter 3. Moreover, to identify a suitable method to assess the thermal performance of naturally ventilated buildings with DSF, a discussion on the existing thermal comfort evaluation approaches was conducted and presented in section 3.2 of Chapter 3.

Stage 2 Development and analysis of base case model – To demonstrate the fundamental thermal and air movement behaviour of a naturally ventilated building with DSF, a reference model was developed and simulated using IESVE software, which was selected based on the discussion presented in section 3.2.2. The simulation results revealed the building thermal performance constraints, assisting the development of design parameters to be tested in the simulations. The model detail characteristics are presented in section 4.3.1 and the results of simulation are presented in section 4.4 of this chapter.

Stage 3 Analysis of design parameters – In order to demonstrate the individual influence and relative importance of the design parameters on the building and DSF's thermal performance, a parametric analysis was performed through computational simulations. A total of 9 design parameters groups were individually applied on the base case model, creating alternative case scenarios which were tested in IESVE. These alternative cases were also simulated in the CFD software FloVENT, allowing a comparative verification of results. The results mainly indicate the airflow magnitude and profile and improvements of thermal comfort of each case and are presented in Chapter 5.

Stage 4 Development of optimized models – In order to establish the highest airflow rate levels achievable in the building to maximise thermal comfort acceptance, two models that incorporated the optimum variables selected from tests performed in stage 3, were developed and further studied. In addition, the influence of building dimensions on the DSF thermal performance was also evaluated.

Stage 5 Analysis of site parameters – To assess the influence of local environmental conditions on the thermal performance of naturally ventilated office building with DSF, variants of solar intensity and wind direction and speed were evaluated through simulation of a selected optimized model and presented in Chapter 5.

Stage 6 Evaluation of thermal comfort acceptability under Brazilian climates - To evaluate the viability of the DSF's operation under the Brazilian weather conditions, simulations using the optimized case developed in stage 4 were performed for each bioclimatic zone characterized in Chapter 3. This determined the regions and periods of the year when satisfactory thermal acceptance is achieved in the Brazilian territories and the results are presented in Chapter 6.

The next sections detail the model characteristics and the procedures for modelling, simulations and analysis of resulting data. Then, findings from simulation of base case model are presented followed by the definitions of design and site parameters to the development of the alternative cases.

4.2 Development of base case model

The base case model comprises of a computational building model used as a benchmark reference for evaluating the influence of different parameters on the DSF thermal performance. Definitions related to the model features considered the climate and regional contexts and are based on a topology study of non-residential buildings in Brazil by Carlo (2008). In the study, the most common characteristics of different building typologies in Brazil, including office buildings, were identified. Approximately 300 office buildings distributed over 5 state capitals were evaluated and the results indicated data related to volumetry, window to wall ration of the façades, presence of shading devices, among others. The study consists of a database for creating reference models of buildings of different typologies in Brazil with focus on developing representative models for thermal assessments by using computational simulation. Additionally, the study covered a large amount of data and it is based in the national construction reality. Therefore, some of the data presented by Carlo (2008) were considered in the definitions of the building model design characteristics in thus study. The model fabric material features followed recommendations of Brazilian regulations for thermal performance and design parameters for office buildings (ABNT, 1980; ABNT, 2003).

4.2.1 Building characterization

This section describes and justifies the geometric configuration and dimensions defined for the building model. It also includes definition of the internal layout, materials applied to the building fabric, windows open/close patterns and open area and the internal heat gains profiles.

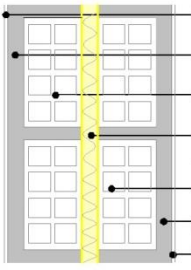
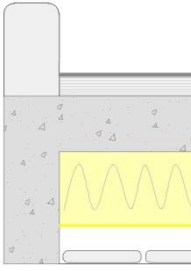
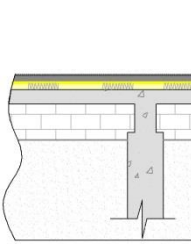
Building geometry - Building shape and dimensions have a significant influence on the thermal performance of the DSF as the degree of exposure of the façade to solar radiation and wind pressures may enhance natural ventilation through the user space. The size defined for the building model also considered the modular dimensions of furniture systems and tenant spaces, which are usually multiple of 0.3m. The American and European modular dimensions, for example, are 1.5m (Kohn and Katz, 2002). Regarding a suitable depth of the building for an effective ventilation, although there is a discrepancy among authors, the dimensions between 11 and 13.5m are usually indicated for naturally cross ventilated spaces (Lorand et al., 2013). The narrow plan depth has the additional benefit of enhancing potential for the use of natural lighting. In buildings with DSF, the airflow pattern is similar along its length, thus the resulting ventilation performance is generally independent of the building extension, except for some variation at the end of the building. Moreover, according to the study by Carlo (2008), the rectangular format represents the most common shape of offices buildings in Brazil. Therefore, based on the requirements for the use of the DSF as a thermal chimney, the adequate dimension for naturally ventilated buildings and considering the characteristic of the common shape of buildings in Brazil, dimensions of 12 x 16m were defined for the base case model.

Building layout - The building internal compartmentation is another important factor as in principle, for naturally ventilated buildings, the design of the rooms should have a minimum of obstructions that would block the airflow and create friction, decreasing the airflow rates through the building (Hyde, 2000). The study by Voordt and Maarleveld (2006) indicated that the future tendency of layout in office buildings indicates interest in spaces that fits companies organisational changes, such as less hierarchical organisational structures and a growing number of part-time workers. Such modifications require more flexible use of the space, encouraging communication and exchange of information and knowledge. Therefore, open plan layout with no internal partitions presented an appropriate design for the base case model.

Fabric materials - Selection of envelope composition draws on recommendations from the Brazilian code for thermal performance of buildings (ABNT, 2003). The model

preserved the typical Brazilian construction typology, which consists of an insulation material sandwiched between two layers of ceramic block, plastered and finished in white. For roof and ground floor surfaces, low thermal transmittance materials were selected in order to minimize the conductive heat transfer. Table 4.1 specifies the thermal properties of envelope fabric defined for the base case model.

Table 4.1 – Building model characterisation

	Envelope	Description (from outside to inside)	Overall U value [W/(m ² .K)]
Walls	 <ul style="list-style-type: none"> White painting External plaster (2.5cm) Ceramic block (9 x 14 x 24cm) Thermal insulation: stone wool (2.5cm) Ceramic block Internal plaster (2.5cm) White painting 	External plaster (2.5 cm) Ceramic block (9.0 cm) Thermal insulation: stone wool (2.5 cm) Ceramic block (9.0 x 14.0 x 24.0 cm) Internal plaster (2.5 cm) Internal painting ($\alpha = 0.3$) Total thickness = 27 cm	0.61
Roof	 <ul style="list-style-type: none"> Stone chipping (1cm) Felt and bitumen layers (0.5cm) Concrete (15cm) Insulation material: glass fibre quilt (20cm) Cavity (5cm) Ceiling tiles (1cm) 	Stone chippings (1 cm) Felt and bitumen layers (0.5 cm) Concrete (15 cm) Insulation material: glass fibre quilt (20 cm) Cavity (5 cm) Ceiling tiles (1 cm) Total thickness = 42 cm	0.18
Ground floor	 <ul style="list-style-type: none"> Synthetic carpet (1cm) Chipboard (5cm) Insulation material: dense EPS (5 cm) Cast concrete (10 cm) Brickwork (25cm) Clay (75 cm) 	Clay (75 cm) Brickwork (25 cm) Cast concrete (10 cm) Insulation material: Dense EPS (5 cm) Chipboard (5 cm) Synthetic carpet (1 cm) Total thickness = 121 cm	0.28

Windows area – Regarding the definition of the window aperture areas, Carlo (2008) identified that the predominant WWR among the office buildings in Brazil varies from 40% and 60%. On the other hand, the studies reviewed in section 2.4.2 of Chapter 2, indicated a broader range of windows area on the façade, suggesting that the WWR in DSF buildings should be between 30 and 90%. In the base case model defined for this study, horizontal windows placed at mid-height of the floor with WWR of 50% on both south and north façades were incorporated to the model. They are set open 24 hours/day allowing for natural night ventilation, which offers the advantage of reducing the mean radiant temperature of the room by cooling the building fabric.

Internal heat gains – Internal activities influence the thermal and airflow processes within the building. The three most important sources of heat gains are people, lights and office equipment (computers, printers, copying machines etc.). Although it is crucial to manage light and equipment according to the user need, a profile from 8 a.m. to 6 p.m. for all internal gains was set for the whole year. The occupancy density was defined as medium capacity, which is 14 people per 100m², indicated by the regulation for Brazilian design parameters (ABNT, 1980). Thus, each thermal zone was set with occupation of 26 people from 8 a.m. to 6 p.m. Heat gains related to people, equipment and lighting are shown in Table 4.2.

Table 4.2 – Profile of internal heat gains

	Internal gains			Total [W/m ²]
	People	Equipment [W/m ²]	Lighting (500lux) [W/m ²]	
Occupancy 8 am – 6 pm	9.8 (70 W/person)	8.4 (55 W/equip.)	18.7 (3.75 W/m ² /100lux)	36.9

4.2.2 Double skin façade characterization

The façade structure selected for the base case model is the multi-storey type (Oesterle et al., 2001) in which the cavity is vertically and horizontally open covering the entire face of the building. It delivers a greater absolute temperature difference along the cavity due to its height, accentuating the stack effect and the ventilation through the building, as indicated in section 2.3.2. To prevent resistance to the flow of air, as mentioned in section 2.3.4, and to reproduce the majority of real examples of DSFs, the top and bottom of the cavity were modelled as fully open.

The DSF was modelled oriented to the north with 50cm of width, covering the height of the building from the first floor. The ground floor was modelled without the second skin to allow air entrance through the bottom of the cavity, if required. The glazing material used for the outer layer is clear single glass (transmittance = 0.64 and reflectance = 0.06) of 12mm with thermal transmittance of 5.3 W/m²K. The base case model has no shading devices or mechanical systems in order to provide a baseline to assess what extent the provision of natural ventilation for thermal comfort can be exploited merely due to the DSF.

Figure 4.2 shows the base case model, which comprises of a 11 storey open plan office building with dimensions of 12 x 16m and 3.5m floor-to-floor height. The longest side faces north/south orientations and the DSF was applied to the north facing.

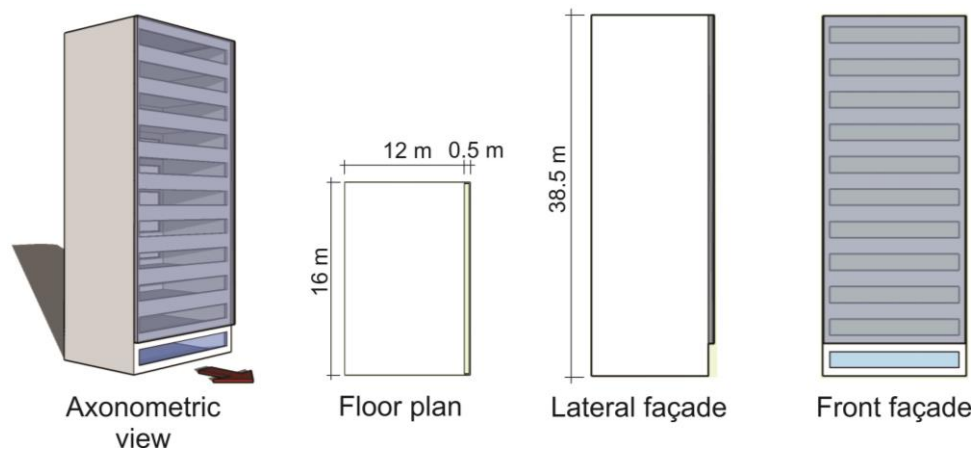


Figure 4.2 – Building model

4.3 Simulations and analyses procedures

This section describes and justifies the modelling processes and presents the specifications of both IESVE and FloVENT simulations. Limitations and necessary adjustments of the model on preliminary simulations on IESVE are also included. Then, procedures for the simulations and analysis of data for the base and the alternative cases are explained followed by a description of the procedures for the presentation of results.

The quality issues procedures specified by CIBSE (2015) and presented in section 3.2 were followed in the modelling process of both software. Firstly, from the literature review the aim of the simulations were defined. In this study, the computational simulations aimed to predict trends in the building with DSF and to compare the thermal behaviour of different design options. Based on the level of accuracy and details required and on the uncertainty of the airflow and thermal behaviour of a naturally ventilated building with DSF, two software were used in conjunction in this study. While the dynamic thermal simulation software provided an prediction of the building models behaviour during the entire year, the CFD software increased the confidence of the qualitative results when different design parameters were applied. For the use of both software training processes were carried out involving workshops, use of manuals with training examples, support by online training resources and use of documented performance assessment methods. On both software, the simulations started from initial models with basic design and a sequential and iterative processes were performed and complex inputs were progressively included. More robust answers and precision were then obtained from a gradually sophisticated model. Decisions made regarding the strategies and stages of modelling and the simplifications of the

design took into account the aim of this study and level of accuracy required at this stage of understanding of the DSF behaviour in naturally ventilated buildings.

4.3.1 Modelling processes

Modelling on IESVE

The geometry of the computational model was created in the IESVE (2014) plug-in for SketchUp, in which thermal zones and position and areas of solid and transparent surfaces were defined. The geometry was then exported to IESVE, where building fabric materials, window types and openings profile, internal heat gains profile, building orientation, surrounding exposure type and location, which is defined by the selected weather file, were applied to the model.

The thermal zoning of the cavity was conducted in accordance with the software guides and manuals. The DSF cavity was divided into several horizontal zones which are associated with an airflow network node. Several possibilities of the cavity division were tried and the most appropriate zone subdivision was the application of one zone at the section of the cavity in front of each floor. With this arrangement, the cavity zones are interconnected by openings and multizone airflow calculations are performed at each time step, accounting for the gradient of temperature occurring over the height of the cavity (Figure 4.3). This provides an indication of the stratified temperatures, rather than assuming a simple average for the volume. For cases in which the shading device was applied within the cavity, the 'curtains' type was used as it takes into account the absorbed and transferred heat to the cavity by convection and long-wave radiations. The values of the material resistance and shading coefficient were manually introduced to the software calculations.

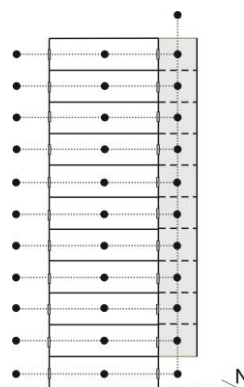


Figure 4.3 - Airflow network node diagram

The main simulation outputs obtained from IESVE were hourly airflows in and out of each window, cavity air temperatures and rooms' operative temperatures of each case. The results tables were converted into Excel sheets to facilitate the analysis of data.

IESVE initial analysis and modelling modifications

Each office room of the base case model was initially modelled as a single thermal zone. As explained in section 3.2.2, network airflow models assume that each thermal zone represents a space of fully mixed air and therefore, temperature distribution across the room width and the locally generated airflows at the openings are not considered.

However, preliminary results from the base case model revealed that recirculation of air occurred at the north window apertures (near the DSF) from the cavity towards the office spaces. This indicated that the space close to the DSF in reality experiences higher air temperatures than the spaces away from the DSF. In this case, considering the variances in heat transfer and airflow mechanisms of the different sides of the building with DSF, the outputs from the single thermal zone may not well reflect the thermal behaviour of the user space. To capture the distribution of temperature within the room, the office space was divided into 6 thermal zones, as shown in Figure 4.4. The graph shows an example of operative temperature distribution resulted over the width of the 1st floor of the model. The difference of operative temperature between two ends of the office zone is in average 3.2°C, reaching a maximum of 8.1°C on the top floor in sunny days.

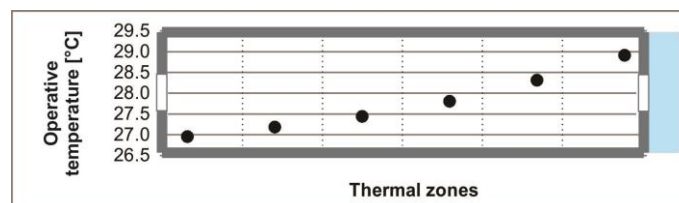


Figure 4.4 – Operative temperatures resulted for office room on the 1st floor, when 6 thermal zones are applied

This indicated that fully mixing air is not occurring in reality and there is a considerable difference of temperature between the north and south sides of the building, as heat gains by convection and radiation contribute to increase the air temperature close to the DSF. Thus, considering the level of accuracy required by this study and to avoid the use of a single thermal zone leading to overestimation of the room temperatures due to the recirculation close to the DSF, an extra zone of 1m was implemented on the north side of each level of the model. Figure 4.5 shows the operative temperatures of

the main and the extra zones. This procedure addressed the recirculation phenomena and prevented unrealistic heat propagation across the whole office, thus allowed a better representation of the levels of thermal comfort in the room.

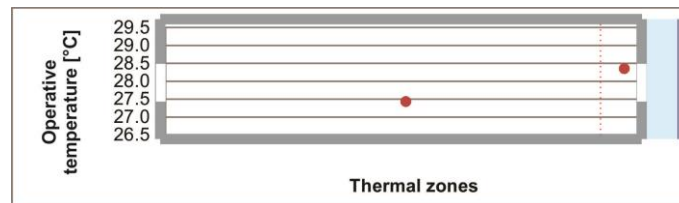


Figure 4.5 - Operative temperatures resulted for office room on the 1st floor, when 2 thermal zones are applied

Modelling on FloVENT (CFD)

Due to the complexity of the physical phenomena involved in the DSF behaviour, qualitative results of base case and some of the alternative cases performed on IESVE were compared to CFD results. Although a number of discrepancies may exist between both simulation software due to the type of solution algorithms and modelling assumptions, comparison of their results enhanced the confidence of the outcomes obtained from IESVE towards the thermal buoyancy, heat transfer and airflow mechanisms in naturally ventilated building with DSF.

Simulations considering the dynamic nature of thermal storage effects during an entire year, which influence the air movement in a building, are still beyond the capability of CFD software currently accessible, hence only steady state snapshot scenarios were applied. Lessons learned by Pasut and De Carli (2012) for CFD simulation on DSFs and the software user guides were consulted on the modelling and simulation in FloVENT.

The building geometry was modelled into FloVENT algorithm, including the components and materials that define the design structure. Solid boundary layers representing walls, ceilings and windows were firstly defined and the material U-values were set. Heat sources inside each room were set to simulate the presence of people, lighting and equipment. The default of the properties of the initial air flow (air at 20°C with 50% relative humidity) was maintained. The solutions of the variables were calculated within a solution domain represented by the cuboid of fluid. This domain represents the external atmosphere and it was modelled large enough beyond the building perimeter so that the boundaries did not affect the airflow at the building openings. Moreover, the external domain was set without boundaries on the laterals and top of the domain and only the ground was set with a border.

The k-ε standard turbulence model was applied to the building model, as it is able to simultaneously deal with laminar and turbulent flow patterns and it is well validated for different building temperatures and flows. The effects of the sun on the model were also included in the solution. A specified sun position and intensity were calculated during the program solution. It was defined by the description of the building orientation and local latitude, the position of the sun in the sky and the solar intensity from which the solar radiation was calculated. Short wave radiation is absorbed, reflected (and transmitted by transparent objects) thus increasing solid temperatures where the solar beam impacts. It also raises the mean radiant temperature. Table 4.3 shows the specifications of the radiation defined for FloVENT.

Table 4.3 – Specifications of the solar radiation defined for the FloVENT model

Model orientation	The DSF was oriented to north
Solar position (time of year)	Winter solstice
Latitude	Rio de Janeiro latitude (22°54')
Solar time	12:00
Solar intensity	500W/m ²

Then, a computational grid was superimposed to the model. The hexahedron mesh was automatically spaced by the software and the cells size required close to the edges of the surfaces were automatically adjusted to better fit the region. The more grid cells in the model meant more number of points to be calculated and consequently the better the resolution of the case. However, this refinement in the solution added additional computer time to calculate the results. Therefore, a balance between the mesh level of refinement required and the computational cost defined the grid size selected for the model. Preliminaries tests were used to establish the level of mesh refinement required to capture regions of complex flow or high gradients such as the DSF cavity and outer layer. The model was divided into 'mesh regions', where limited values for the maximum size of the cells were applied, as indicated in Table 4.4.

Table 4.4 – Maximum cell size defined for each region

'Mesh region'	Maximum size of cell
External domain	50 cm
Office rooms	50 cm
Cavity	7 cm
Outer skin	0.3 cm

Due to the great number of cells required for the entire building, the solution was limited by the computational resources available. In order to maintain the solution for all the building floors, the depth of the model was reduced to a representative section of 1m length (Figure 4.6). This allowed the application of a fine grid definition to improve the resolution of the calculations and the accuracy of the results. The internal heat gains included on each floor were calculated for 1m length of the building model.

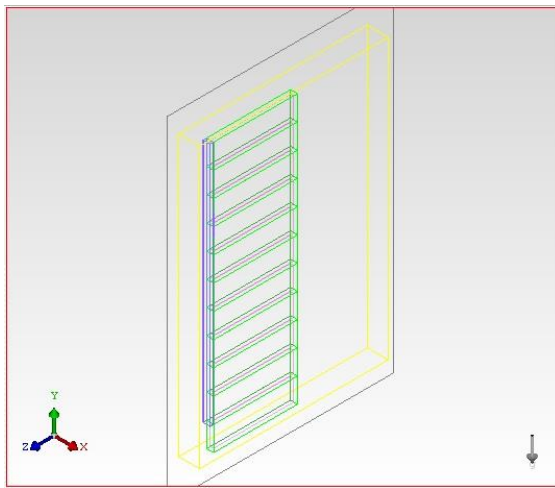


Figure 4.6 – CFD base case model in perspective

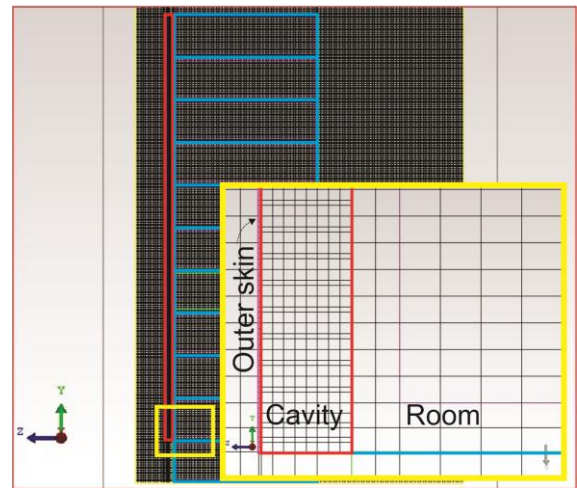


Figure 4.7 – CFD base case model with grid definition

During the FloVENT simulation, the solution activated the CFD algorithms which provided an integration of the fluid flow and heat transfer equations within the solution domain. The progress of the solution was monitored in profile plots of convergence of residual errors and variable values at monitored points. The conservation equations were solved in an iterative manner, until the errors in the conservation equations were at an acceptable level. All the solutions were automatically stopped when the convergence was reached.

The post processing of results were performed using the Visual Editor window. Graphics mode planes of results (contours and vectors of air speeds, temperatures and pressures) were displayed to evaluate the model thermal and airflow behaviours. Additionally, tables of setup and quantitative results were viewed and exported to excel sheets to manipulation of data. The airflow profiles across the floors of the base case model were compared to the IESVE model and presented in section 4.4.3 of this chapter. The results of the alternative cases are presented in section 5.5 of the next chapter.

Modelling simplifications

This section describes the simplifications and limitations of both software due to the tool capabilities and the modelling design assumptions. The implications of these assumptions are appreciated on the analysis of the next chapter. They are described in topics as follow.

- **Building occupant behaviour:** Assumptions with regard to the occupation pattern over the day were made considering the likely working hours of an office building. However, occupants will never operate a building precisely as

assumed in the model and a precise estimation of the occupant profile is almost impossible for predicting the thermal performance of a building. Although the pattern of occupation from 8 a.m. to 6 p.m. was assumed, a more detail definition of the hours of occupancy of a real case may influence the identification of the building uncomfortable hours. The same way, a specific profile for the utilization of lighting and office equipment throughout the day were not considered in the simulation.

- **Climate data:** Climate is the most unpredictable driver that affects the behaviour of a building (CIBSE, 2015). In this study, test reference year (TRY) data were used. These datasets represent averages of several years and do not contain extreme periods. However, it is important to note that there will always be variation between these datasets and the actual weather. Future weather datasets are not yet available for Brazilian territories and therefore, extreme weather conditions caused by climate change were not considered in this study.
- **Simplified design details:** Although all models, by definition, are always a simplified view of the real world, some details of the model design were absent considering the level of accuracy required by this research.
 - The window frames definitions were set for the automatic calculations of the thermal behaviour of the materials, including definitions of U-values, percentage in relation to the window area, absorbance and resistance. However, these frames were not physically modelled on the building.
 - As the IESVE software does not allow a physical detailed designing of the shading devices, they were attached to glazing panes by an input dialogue window in which resistance, shading coefficient and shortwave radiation fraction values of these systems are defined.
 - No specific window opening type was defined, but a sharp edge/orifice was set. Given the aim of this study of understanding the general behaviour of a DSF when applied to naturally ventilated buildings, a simple window frame was defined in order to avoid any influence of air resistance through the openings.
 - The wind pressure coefficients were specified from the extensive list available in the software algorithm according to the height and level of exposure of the opening and no data from wind tunnels were obtained.
 - The degree of opening profile was set according to the outside temperature in the different climatic conditions as specified in chapter 6. A more realistic prediction would also consider the internal air speed as in

office buildings it is likely that users would close the windows to avoid papers blowing off the desks. However, the software does not allow the creating of an opening profile according to the internal air speed.

- In the CFD simulation the modelling of a reduced length of the building was due to the impossibility of having an adequate fine grid if the model were designed in full size. Simulation of all floors was a priority as it influences the airflow path and magnitude of the building. Additionally, as the airflow pattern is similar along its length, the resulting ventilation performance is generally independent of the building extension.

A performance gap will inevitably exist between model and the actual measured thermal performance. These simplifications include a level of risk that was assumed as permissible considering the aim of this study of evaluating different architectural parametric inputs on the airflow and thermal behaviour of the DSF in naturally ventilated buildings. In order to reduce the effect of these limitations, progressively inclusion of more details were added to the models and the variation of results gradually assessed.

4.3.2 Simulations procedures

Results of base case model not only demonstrated the general functioning of the DSF system, showing the airflow profiles and the resulting thermal comfort distributions over the building floors, but also the building thermal performance constraints. The issues observed informed the development of design parameters to be tested through the parametric analysis.

In the parametric analysis, for each design parameter evaluated, a single variable was modified in the base case, while the rest of the studied parameters remained constant. The base and the alternatives cases used weather data of Rio de Janeiro (bioclimatic zone 8), as it not only covers more than 50% of the Brazilian territories, representing the most common climatic characteristics of the territories, but it also includes a number of capital cities in Brazil. Additionally, considering that the DSF functioning is greatly influenced by the solar availability, the city's latitude (22.9° S), which is approximately at middle locality of the territories where most part of population is concentrated, represents a typical scenario to the evaluation of thermal performance of the DSF. The weather file used was modified and wind speeds were made zero for the whole year, in order to detach the DSF buoyancy effect and remove any influence of wind pressures.

Following a multitude of tests based on the outcomes of the evaluation on individual design parameters, two optimized models utilising a combination of parameters that maximize the building airflow and thermal comfort were developed. One of the optimized models was then selected for the evaluation of the site parameters.

The selected optimized model was also used to the simulations performed with weather data of different Brazilian bioclimatic zones. In these cases, original weather files of the cities presented in section 3.1.2 were used. The building model exposure was set to an urban and suburban surrounding context, which regulates the wind speed of the weather file according to the degree of obstructions nearby. Results of the DSF building models were compared to single skin façade (SSF) cases, in which, except for the additional outer skin, all the building characteristics were similarly modelled. Additional cases with modifications in the façade orientation and/or window openings profile were also performed according to the local climatic conditions such as temperatures during the winter and wind prevailing direction.

4.3.3 Presentation of results

For the base and each alternative case, the resulting airflow magnitude and pattern through each level of the building were generated from simulations using IESVE. Although each simulation generates hour-by-hour data for the entire period of the representative year (8760 hours), annual mean net airflow through the north windows are shown graphically to provide an effective summative presentation in particular when used to compare the relative differences among the cases tested. More detailed results for all cases tested are presented in Appendix A. They include mean monthly cavity airflow and air temperatures and mean monthly airflow across the levels of the building. Although not included on the main body of this study, they were also used to gain a broader understating of the DSF functioning throughout the year.

The results are also presented in terms of thermal comfort acceptability of the alternative scenarios, highlighting their relative effectiveness in improving the building and DSF thermal performance. Thermal acceptability limits based on the methodology of ASHARE-55 (2013) were adopted in this study. The particular conditions applied to this method are presented in section 3.2.1. The method calculates thermal acceptability based on the prevailing outdoor air temperature and the indoor air speed and operative temperature, which was extracted directly from the IESVE software. The prevailing mean outdoor temperatures were calculated based on the average of the mean daily outdoor temperatures of the previous fifteen days.

4.4 Findings from base case model

This section presents the results of the simulations of the base case model, including airflow and thermal acceptance at different floors levels. The results of this case show the airflow and thermal behaviours of a naturally ventilated building with DSF and revealed some issues that assisted the development of design parameters to be tested in the parametric analysis.

4.4.1 Results of base case model

The results of the base case analyses establish benchmarks for thermal performance based on airflow profiles and operative temperatures across each floor of the building model. In this section, air temperature differences between the cavity and outside according to the solar radiation incidence on the façade are presented. Additionally, airflow distribution across different building levels and the position of the NPL (neutral pressure line) in the model are graphically illustrated. Finally, thermal acceptability across the building floors are included indicating the main issues and potential improvements of the building and DSF designs.

Figure 4.8 shows the hourly mean direct solar radiation incident on the north façade during the whole year and the corresponding outside and cavity temperatures for the base case. The increase in cavity temperature bears a direct but non-linear relationship to the amount of solar radiation reaching the façade. The annual average difference between these temperatures reaches a maximum of 5.7°C at midday, while on a sunny day this can reach up to 9.8°C. These values are lower than those indicated by literature review in section 2.5.1, in which the differences of temperature between the cavity and the outside air were reported to be between 10°C and 20°C for cloudy sunny and days, respectively. As the studies reviewed used a sealed inner skin, this difference can be explained by the contribution of cooler air from the rooms, which decreases the cavity air temperature in the base case model.

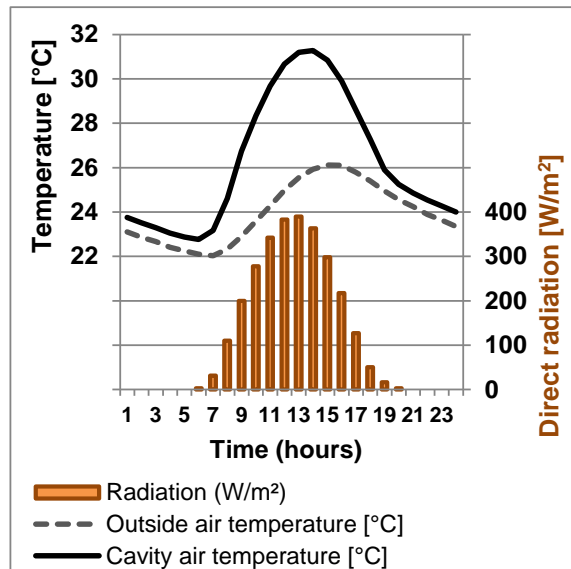


Figure 4.8 - Annual mean outside and cavity temperature distributions and direct radiation on the north façade

The solar intensity reaching the façade not only varies in relation to the hours of the day, but also according to the periods of the year. This results in differences in airflow within the cavity, as shown in Figure 4.9. From April to August, the mean airflow was slight higher (3.6 - 3.8 m³/s) than those recorded for the warmer months November to February (3.2 – 3.3 m³/s). This is related to the solar angle reaching the façade as observed by Hazem et al. (2015) and Mulyadi (2012), described in section 2.5.2. The highest percentages of transmitted solar radiation during the coldest months increased the air temperature and airflow within the cavity.

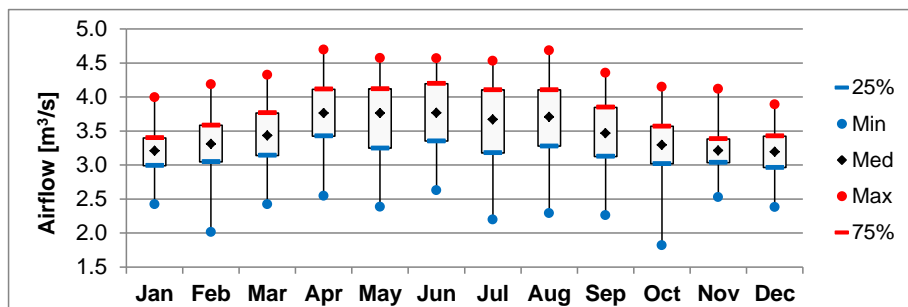


Figure 4.9 – Graphical representation of descriptive statistics for the airflow through the cavity in each month

The airflow distribution through north windows of the rooms of the base case scenario is indicated in Figure 4.10, in which the positive values indicate airflows moving from the offices towards the cavity, whereas the negative values represent reverse flows. The mean annual net airflows for each floor is shown in Figure 4.11, which also presents the mean annual airflows entering the cavity through the bottom and leaving it

though the top outlet. The diagrams show the occurrence of reverse flow on the top floor, represented by the negative net airflow as a result of the recirculation phenomena, which is indicated by air movement from the cavity towards the rooms occurring in all floor levels.

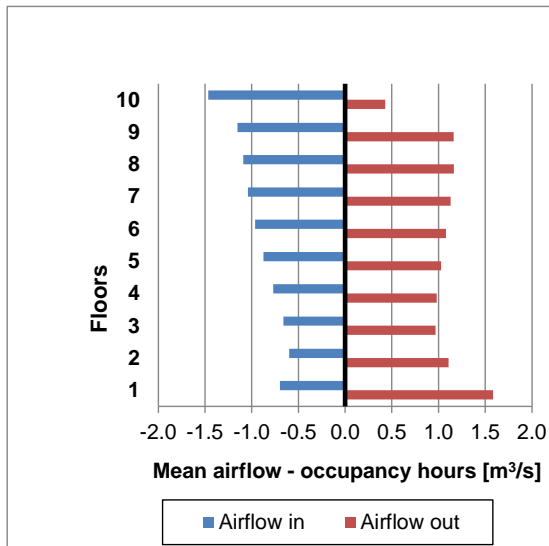


Figure 4.10 – Annual mean airflows in and out of each floor for the base case

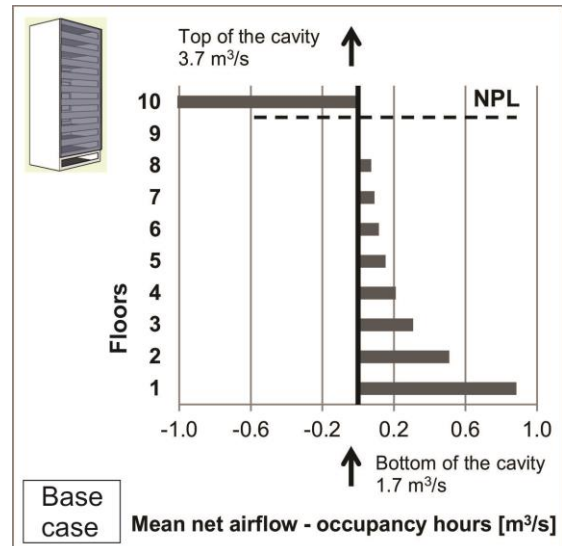


Figure 4.11 – Annual mean net airflow for each floor for the base case

The airflow profile distribution over the floors is a result of the pressure differences at different levels of the building. The driving pressure at the first floor level is greater than that at the second, which is correspondingly greater than that at the third, due to the difference in height between the inlet and outlet openings. Thus, net airflows across each floor gradually reduce from 1st level up to the neutral pressure line (NPL). For the base case scenario, the NPL occurs on the 9th floor and the net airflow changes from the cavity towards the occupied space on the 10th floor, where the pressure in the cavity is higher than the adjacent office space.

The air speed achieved at the top of the cavity is on average 0.45m/s for the occupied hours, reaching a peak of 0.61m/s on a sunny day. These results agree with those observed by Pappas and Zhai (2008) presented in section 2.3.1, which demonstrated that the air speed in the cavity was less than 1m/s for all cases tested. As the ventilation through the rooms is essentially related to the magnitude of airflow in the cavity, but less pronounced, application of solutions to maximize the cavity absolute airflow may prove useful to enhance office ventilation rates.

Figure 4.12 is a plot of thermal comfort matrix based on the method by ASHARE 55 (2013). It compares the annual operative temperatures that fall within and outside the acceptable limits for 1st and 10th floors only. Using yearly percentages in terms of

comfortable and uncomfortable sensations during occupied hours (both due to too hot/too cold conditions) for each floor, Figure 4.13 shows the gradual reduction in thermal acceptability as a result of the decreasing of air speed in each floor. The base case achieved an average of 62% of occupied hours of acceptable thermal comfort, varying between 44% on the top floor and 70% on the bottom floor. Although the net airflow on the 10th level is negative, the higher air speed and moderate cavity temperatures during milder seasons explain the thermal comfort acceptability over 40% of the time.

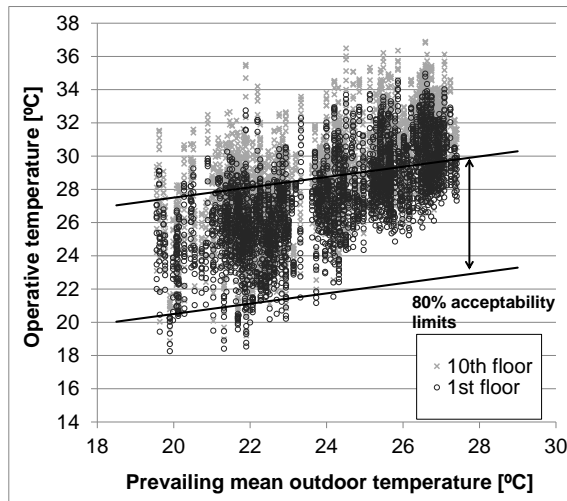


Figure 4.12 – Annual operative temperatures of the base case (1st and 10th floors)

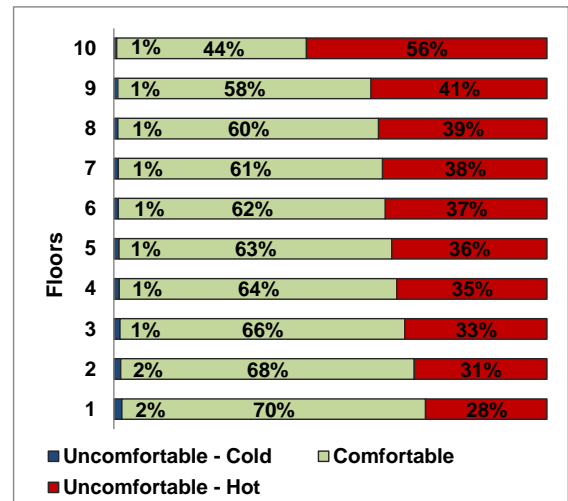


Figure 4.13 - Annual distribution of thermal comfort (%) on each floor of the base case model

The base case model demonstrated the general functioning of the DSF system, showing the airflow profile and the resulting thermal comfort distribution over the building floors. Some of the findings show agreement with previous predictions identified from the literature review such as low air speed within the cavity demonstrated by Pappas and Zhai (2008), lower airflow levels resulted on upper floors in relation to the others, as identified by Ding et al. (2005), and high levels of airflow within the cavity in period of low solar angles, as indicated by Hazem et al. (2015). In conclusion, the issues observed from the simulation of the base case model are:

- Low air speed in the cavity, which results in low airflow through the rooms. Strategies to maximize absolute airflow within the cavity and consequently in the rooms are required.
- High level of uncomfortable conditions due to high temperatures. Solar gains control may enhance acceptable temperatures and minimize the periods of uncomfortable conditions.

- Compromised ventilation levels on the upper floors and reverse airflow occurring on the upper floor. Solutions to increase the NPL above the upper open window should be applied.
- Local recirculation phenomena occurring on the north windows. This should be avoided as it can cause overheating, especially during the hottest months.
- Difference in airflow rates at different building levels. Similar comfort levels are likely to be achieved for all levels of the building.

4.4.2 Verification of base case model results

This section presents the results of the base case from the CFD software FloVENT. Due to the differences in modelling process, i.e. reduction of the building length on CFD to a representative slice of the building model in order to keep the adequate grid refinement and the simulation to all floors of the model, and the steady/transient nature of the two simulation approaches, the resulting absolute values of airflow through the cavity and the rooms could not be directly compared. However, in the view of the complexity of airflow mechanisms involved in the simulation of buildings with DSF, comparisons are focused on the resulting airflow profile across the floors when different design solutions are modified from the base case.

Figure 4.14 shows the CFD image of vectors of air speed on the first, second and third floors. No reverse airflow is occurring on the first floor where the driving pressure is greater than the other floors. From the colour scale presented it is possible to observe that the air speed on the third floor is lower and a small reverse flow is occurring. It is consistent with the observed in the IESVE simulations reinforcing the confidence of the results.

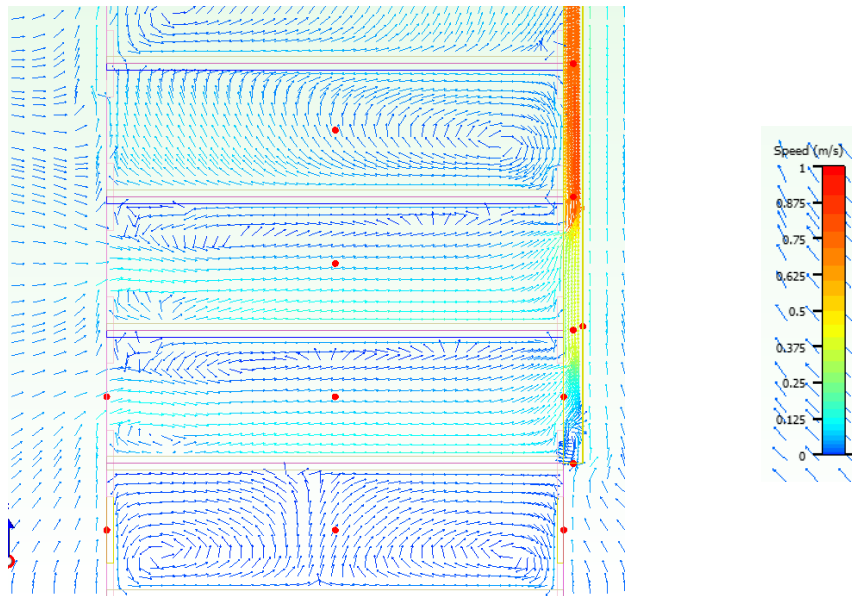


Figure 4.14 – CFD image of vectors of air speed with detail of the 1st, 2nd and 3rd floors.

Figure 4.15 presents the CFD results of the base case model. Similarly to the results by IESVE model, the airflow gradually decreases on the upper floors of the building indicating that the pressure distributions across the building levels were effectively estimated by IESVE. The results are comparable to those obtained from IESVE indicating that the tool is adequate for the purpose of simulating the airflows of naturally ventilated building with DSF in this study.

On the other hand, there is a clear difference of airflow on the top of the building between the IESVE and CFD models, as the last did not present reverse airflow from cavity towards the room. This can be explained by the nature of the CFD simulation, in which thermal mass is saturated with solar heat in a steady state model, pronouncing the buoyancy force within the cavity, and the consequent suction of air from the rooms. Additionally, in the CFD simulation, the transient condition of the exterior air temperature is not considered and the case is simulated under a stable external environmental condition. Another possible reason for this effect is that the reduced length of the cavity may have increased the stack effect within it by concentrating and directing the flow of air towards the top of the cavity. This increased the buoyancy force in relation to the IESVE model, in which the full length of the façade is modelled.

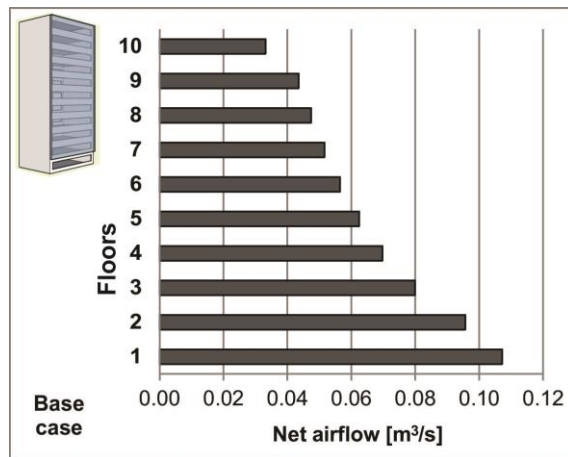


Figure 4.15 – Results of base case model simulated on FloVENT

The inter-program comparisons technique used in this study shows that the IESVE software tested performs in agreement with the CFD simulation, which nowadays is one of the most reliable computational estimation of the resulting natural ventilation in a building. As the level of knowledge about the DSF performance in a naturally ventilated building is still at its early stages, this study aimed to compare the impact of various design measures in relation to a reference model. Thus, no absolute accuracy of airflow values was required and therefore, the results were adequate to the study.

However, it is important to note that the methodology used in this study presents constraints. The lack of real measurements in cell tests or real buildings is a limitation as it would benefit the accuracy of the results provided by the software. The model results represent a specific scenario testing a particular aspect of the building thermal performance that may not be replicated in reality, e.g. due to varying weather conditions, differences in the assumed occupancy and occupant behaviour in using the building and modelling assumptions resulting in missing design information. The estimated outcomes of the simulation software are results of defined climatic and operational conditions to satisfy certain requirements, whereas in real buildings, the systems operate under a variety of dynamic conditions that may not be considered by the simulation algorithm.

4.5 Design parameters definitions

Based on the issues observed from the simulation of the base case model listed at the end of section 4.4.1, specific objectives to improve the building thermal performance were identified as presented in Table 4.5. The key design parameters and variables defined and applied to the alternative cases are divided into four main groups (A to D), as summarised in Table 4.7. The variables defined are described as follow.

Table 4.5 – Issues and strategies identified from the simulation of the base case model

	Issue	Strategy objective
Group A	Low air speed in the cavity, which results in low airflow through the rooms	Maximization of absolute airflow in the cavity and the rooms
Group B	High solar gain and high level of uncomfortable conditions due to high temperatures	Application of high thermal mass materials within the cavity
Group C	Compromised ventilation levels on the upper floors and reverse airflow occurring on the upper floor	Reposition of the NPL in order to reduce risk of severe overheating
Group D	Difference in airflow rates at different building levels	Achieve even horizontal airflows across each floor

Group A tests the parameters that maximize the absolute air flow of the cavity and consequently the rooms as a strategy to improve the heat removal during the hot periods. The design strategies defined include variation of the cavity width, closing of the cavity bottom aperture and reposition of the windows in each floor. Increasing the cavity extension above the building roof may also have effect on the airflow rates through the building, but it is dealt with in group C. In relation to the cavity width variables (cases A1 according to Table 4.7), it was assumed that larger cavities of more than 1m are not desirable as useful office area would be displaced by unoccupied cavity space, as indicated by studies of section 2.3.3. Thus, two extra cavity widths of 25 and 100cm were modelled and simulated. In case A2, the bottom of the cavity was fully closed in order to induce higher airflow through the offices. The north windows (close to the DSF) of case A3 were placed towards the top of the room, while the south windows were positioned at the bottom of each floor, in order to increase the pressure difference between inlet and outlet by enhancing the height difference between openings.

Group B investigates the effect of the application of high thermal mass materials on the cavity's air temperatures and airflow rates. The cases were defined based on the Kirchhoff's law of thermal radiation that relates to the absorptivity and emissivity of surfaces. As highly absorptive materials are also highly emissive, during the day, when the office building is occupied, high absorptance surfaces tend to absorb and release heat into the cavity air, which warms faster compared to the low absorptance/emissive surfaces. At night, the high absorptance/emissivity material sends radiation towards the outer glazing layer and some of which is transmitted to outside. In cases B1, aluminium and concrete, low and high absorptive materials, respectively, were applied to shading

devices placed within the cavity. Details of the properties of the materials used are presented in Table 4.6.

Table 4.6 - Properties of the materials applied to the shading device

	Absorptance	Resistance [$\text{m}^2\text{K/W}$]	Shading coefficient (SC)
Aluminium	0.14	0.150	0.12
Concrete	0.70	0.014	0.61

In case scenario B2, a black painted wall facing the DSF was set to the inner skin. This included a single layer of brick on the internal surface, followed by a thick layer of insulation (20cm) and cover plaster painted in black. With this arrangement, it was expected that during the day the black surface would rapidly absorb and release the heat it into the cavity, enhancing the air temperature and the stack effect. The insulation material applied on the inner surface would reduce the heat conduction towards the interior of the building.

Group C attempts to raise the NPL and resolve the low or unintentional reverse flows through the upper floors of the building in order to reduce the risk of severe overheating. This can be achieved by extending the cavity above the roof of the building, which corresponds to cases C1 tested. However, if extension of the cavity above the building roof is not viable, closing the building upper windows and service them by separate mechanical ventilation system will be necessary. Three cases scenarios, showing the building airflow performance when the windows of the 10th floor only, 9th and 10th or 8th, 9th and 10th floors are closed, are studied (cases C2).

Group D includes two possible designs to achieve even horizontal airflows across each floor by introducing a gradual increase in cavity width with floor height (cases D1). The outer layer of the DSF was inclined, creating a wider gap of 100cm at the top of cavity and 20cm at the base, in order to balance the resistance from the bottom to the top floors (case D1.2). A second option gradually decreases the depth of the floors from 1st to 10th (case D1.3). In case D2, using the empirical equation that quantifies airflow in a thermal chimney by ASHRAE (2009), the window apertures were sized according to the height level of each window and the top of the cavity position and size, which resulted in a gradual increase of the windows size from the bottom to the top floor.

A total of 16 variables are gathered into 9 groups of design parameters according to their purpose in improving the airflow and thermal conditions of the model. Graphical representations of the corresponding scenarios are shown in Figure 4.16. The purpose of such grouping is to show the most effective strategies in achieving the objective

proposed. The results are presented following the same grouping in order to and to compare the airflow magnitude and pattern through each level of the building and the thermal performance among the cases tested.

Some of the alternatives solutions have been previously tested in mechanically ventilated building models such as cavity width by Gratia and De Herde (2007a), Torres et al. (2007), Rahmani et al. (2012) and Radhi et al. (2013) and inclusion of thermal mass materials on the shading device and on the inner layer of the DSF, by Fallahi et al. (2010). However, due to the peculiar behaviour of naturally ventilated buildings, those cases are additionally tested in this study.

Table 4.7 - Parameters and variables defined for simulations

Case	Design parameter	Scenario	Variables	
Group A	A1	Cavity width	A1.1	• 25 cm
			*A1.2	• 50 cm
			A1.3	• 100 cm
A2	Cavity bottom opening	*A2.1	• Bottom open	
		A2.2	• Bottom closed	
A3	Windows positions	*A3.1	• North and south windows in the middle of the wall	
		A3.2	• South windows on the bottom, north windows on the top of the wall	
Group B	B1	Shading devices	*B1.1	• No shading device
			B1.2	• Concrete
			B1.3	• Metal
B2	Inner skin material	*B2.1	• Masonry (white wall)	
		B2.2	• Insulation applied to the inner surface and black painting on the outer surface	
Group C	C1	Cavity extension above roof	*C1.1	• Cavity height = building height
			C1.2	• 1.75m above roof
			C1.3	• 3.5m above roof
			C1.4	• 5.25m above roof
C2	Upper windows closed	*C2.1	• All windows open	
		C2.2	• Top floor closed	
		C2.3	• Two top floors closed	
		C2.4	• Three top floors closed	
Group D	D1	Tapered cavity	*D1.1	• Equal cavity width over the floors
			D1.2	• Inclined outer skin (base = 20cm; top = 100cm)
			D1.3	• Inclined inner skin (base = 20cm; top = 100cm)
D2	Windows sizes	*D2.1	• Equal windows size over the floors	
		D2.2	• Calculated window sizes	
*Base case				

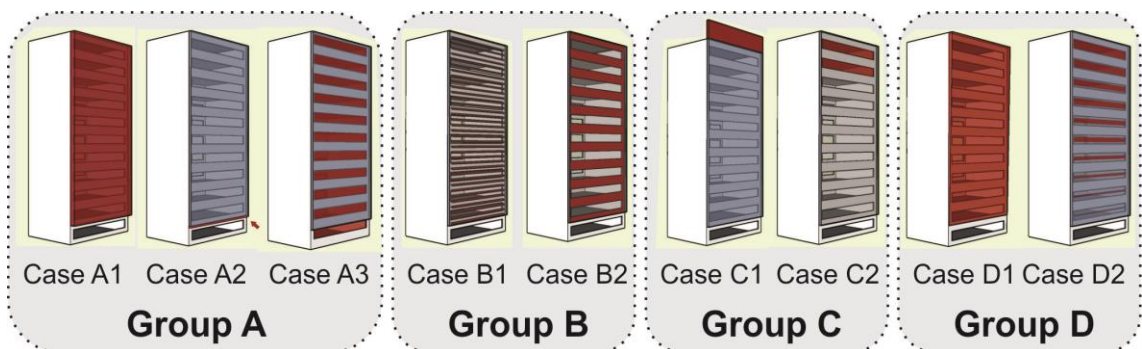


Figure 4.16 - Pictorial diagrams of the design parameters simulation scenarios of groups A to D

In addition, resilience of the optimized model under different building dimensions are evaluated. Cases of **Group E** (Table 4.8), establishes the influence of height and depth of the building on the DSF thermal performance.

Table 4.8 - Parameters and variables defined for simulations of group E

Case	Design parameter	Scenario	Variables	
Group E	E1	Number of floors	E1.1	• 5 floors covered by DSF
			*E1.2	• 10 floors covered by DSF
			E1.3	• 20 floors covered by DSF
	E2	Building depth	E2.1	• 6 m
			*E2.2	• 12 m
			E2.3	• 18 m
*Base case				

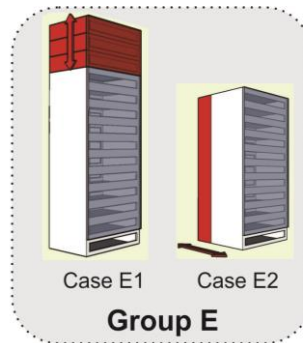


Figure 4.17 - Pictorial diagrams of the building shape parameters simulation scenarios

4.6 Site parameters definitions

The site parameters, specified in Table 4.9, are represented by two main groups of variables: the solar incidence (**Group F**) and the wind conditions (**Group G**). For the first group, a detailed analysis of the influence of hours of the day, solar angle, sky conditions (cloudy and clear) and façade orientation on the building behaviour is performed. For the façade orientation parameter, the DSF was applied to north, northwest and northeast faces as these are indicated as the most efficient orientations to increase the cavity stack effect by studies in section 2.5.1. Similarly to base and alternative design cases, the weather file used in this simulation did not include application of wind on the environment.

The wind variables consist of speed and direction and several combinations of both have been specified and analysed. For group G, which evaluates the influence of wind conditions on the model performance, different and constant wind speeds and directions were altered in the weather file. Definitions for the maximum wind speed tested considered the prevailing conditions of the cases presented in section 3.1.2.

IESVE software estimates the wind pressure coefficients using correlations based on wind tunnel experiments combined with an adjustment for wind turbulence.

Table 4.9 - Parameters and variables defined for simulations

	Case	Design parameter	Scenario	Variables
Group F	F1	Level of solar incidence	F1.1	• Solar angle
			F1.2	• Hours of the day
			F1.3	• Sky conditions (cloudy and clear)
			F1.4	• Façade orientation (N, NW, NE)
Group G	G1	Wind speed	G1.1	• 2 m/s
			G1.2	• 4 m/s
			G1.3	• 6 m/s
	G2	Wind direction	G2.1	• 0°
			G2.2	• 90°
			G2.3	• 180°
			G2.4	• 225°
			G2.5	• 315°

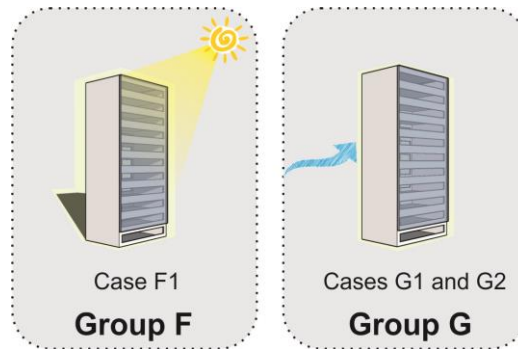


Figure 4.18 - Pictorial diagrams of the site parameters simulation scenarios

The design and site variables defined in this chapter were used to the development of the alternative models. Using the modelling and simulation procedures described in this chapter, all cases were individually tested and the results are presented in the next chapter.

Chapter Five

Parametric analysis: results and discussions

This chapter presents the results of the simulations of alternative case models. Firstly, results of the design parameters are presented. They consist of airflow magnitude and pattern and thermal acceptability levels on all floors of the building. Results of CFD simulations are also included to verify consistence of IESVE results. The analyses indicated the development of optimized models that incorporated design solutions to improve airflow rates in the building and the results of those simulations are also presented. Lastly, the influence of the 'site' parameters on the thermal performance of the optimized model is assessed.

5.1 Introduction

The analyses presented in this chapter aims to demonstrate the individual influence and relative importance of the design and site parameters on the building and DSF's thermal performances. Firstly, the results of the design parameters tested on IESVE are presented. The results are discussed according to their specific purpose in improving the airflow and thermal conditions of the model. The alternative cases used a modified weather data of Rio de Janeiro (bioclimatic zone 8), in which wind speeds were made zero for the whole year in order to detach the DSF buoyancy effect and remove any influence of wind pressures.

For each parameter evaluated, airflow magnitude and pattern across all levels of the building are presented. The resulting annual average net airflow through the north windows of all floors is demonstrated by using a bar graph with positive values indicating net airflows moving from the offices towards the cavity and negative values representing reverse flows. Variables of the same parameter are presented on the same graph to highlight the relative differences among the cases. Thermal acceptance levels for each case tested are also discussed based on the resulting air movement in the building model. Then a summary table, including the acceptable percentage of thermal comfort resulted on each floor for the cases simulated, is presented which compares the thermal comfort acceptability of the alternate options.

Results of the CFD simulations are presented. Similar to base case model results presented in 4.4.2, the absolute airflow values between IESVE and FloVENT were not directly compared, but only the airflow profiles across the floors when different design solutions were modified from the base case. Characterization and results of the optimized models are then presented. They also include annual average net airflow through the north windows of all floors and additionally, a plot of operative temperatures resulted on the 5th floor of the building based on the ASHRAE (2013) thermal comfort matrix is presented. This indicates the improvements in thermal comfort in relation to the base case. The building dimensions parameters were then included, indicating the resilience of the optimized model under different building shapes. These cases established the influence of height and depth of the building on the DSF thermal performance. Finally, the results of the site parameters are presented. They mainly include the variations of airflow rates in the building under different surrounding environmental conditions.

5.2 Design parameters

Table 5.1 reminds the design parameters developed in section 4.5. They are divided into 4 main groups and consist of a total of 9 design parameters. These parameters were individually applied on the base case model, creating 16 alternative case scenarios.

Table 5.1 - Parameters and variables tested (Groups A to D – Design parameters)

Case	Design parameter	Scenario	Variables	
Group A	A1	Cavity width	A1.1	• 25 cm
			*A1.2	• 50 cm
			A1.3	• 100 cm
	A2	Cavity bottom opening	*A2.1	• Bottom open
			A2.2	• Bottom closed
	A3	Windows positions	*A3.1	• North and south windows in the middle height of the wall
A3.2			• South windows at the bottom, north windows at the top of the wall	
Group B	B1	Shading devices	*B1.1	• No shading device
			B1.2	• Concrete
			B1.3	• Metal
	B2	Inner skin material	*B2.1	• Masonry (white wall)
			B2.2	• Insulation applied to the inner surface and black painting on the outer surface
Group C	C1	Cavity extension above roof	*C1.1	• Cavity height = building height
			C1.2	• 1.75m above roof
			C1.3	• 3.5m above roof
			C1.4	• 5.25m above roof
	C2	Upper windows closed	*C2.1	• All windows open
			C2.2	• Top floor closed
			C2.3	• Two top floors closed
			C2.4	• Three top floors closed
Group D	D1	Tapered cavity	*D1.1	• Equal cavity width over the floors
			D1.2	• Inclined outer skin (base = 100cm; top = 20cm)
			D1.3	• Inclined inner skin (base = 100cm; top = 20cm)
	D2	Windows sizes	*D2.1	• Equal windows size over the floors
			D2.2	• Calculated window sizes
*Base case				

5.2.1 Group A: maximization of airflow

Cavity width

Two cavity widths of 25cm (case A1.1) and 100cm (case A1.3) were tested. The results show that higher air cavity temperatures occurred in the narrower cavity in relation to the wider one, as confirmed by studies by Rahmani et al. (2012), Torres et al. (2007) and Radhi et al. (2013). In the climate analysed, the annual average difference is 0.8°C, reaching up to 1.8°C on a sunny day. However, because wider cavities resulted in lower flow resistance to the airflow path, the airflow rates through the user space of the 100 cm-case were higher than the base case, which were respectively higher than the 25 cm-case, as shown in Figure 5.1. As consequence, heat gains by convection in the room offices due to the occurrence of reverse flows decreased by approximately 40% for the 100cm-cavity case compared to the 25cm-cavity.

Although improvement of 115% in airflow was observed in the wider cavity in relation to the narrower one, in the offices this increase was less pronounced and a minor improvement of only 2% on the overall acceptable level of thermal comfort was observed on the wider cavity in relation to the base case. As wider cavity promoted higher airflow rates in both positive and negative directions, top floor presented a slightly lower thermal acceptance level than the narrower cavity.

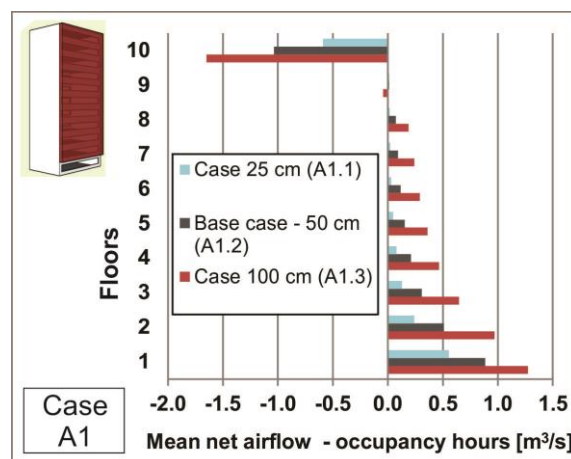


Figure 5.1 - Annual mean of the net airflow for each floor for parameter 'cavity width'

Cavity bottom opening

In order to increase the airflow drawn from the offices, case scenario A2.2 had the aperture of the cavity bottom closed. Figure 5.2 shows that this change resulted in a threefold increase in the net airflow on the 1st floor compared to the base case, but only small differences in the other floors. The reduction of air supplied by the bottom cavity

aperture caused a drop in pressure in this region, which created a higher pressure difference between the first floor and the section of the cavity in front of it. On the upper floors, this pressure differential is balanced and airflow rates similar to the base case are observed. The mean annual increase in air speed on the 1st floor enhanced the acceptable thermal comfort level on this floor by 5% in relation to the base case.

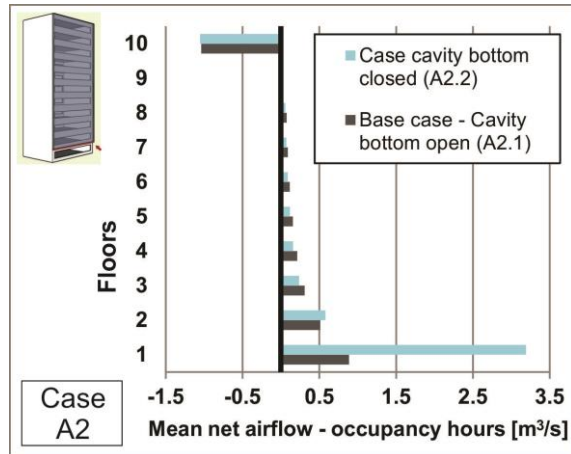


Figure 5.2 - Annual mean of the net airflow for each floor for parameter 'cavity bottom opening'

Windows opening position

In order to enhance the buoyancy force through greater height difference between their inlet and outlet apertures, in case scenario A3.2, the south windows were placed to the bottom and the north windows to the top of the walls. The results are particularly noticeable on the 1st and 10th floors, as shown in Figure 5.3. On the middle floors, the pressure differential created between each aperture and the cavity section in front of it is balanced and similar flow rates to the base case are observed.

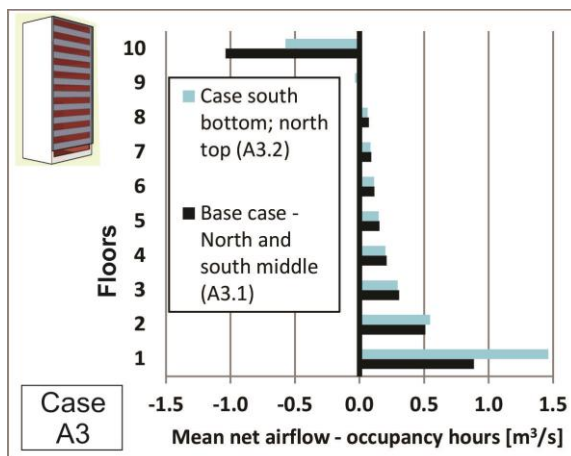


Figure 5.3 - Annual mean of the net airflow for each floor for parameter 'windows position'

5.2.2 Group B: shading device and skins materials

Shading device

Case scenario B1.2, in which shading device made of concrete (high thermal mass material) was applied within the cavity, presented higher cavity temperatures during the day. Figure 5.4 illustrates these cases on the winter solstice day (21st June), when the differences among the cases are likely to be more pronounced. This can be explained by Kirchoff's law, which says that the fraction of incident radiation that is absorbed by a surface is equal to its emissivity, ϵ . As concrete material is highly absorptive, it is also highly emissive ($\epsilon \sim 0.9$). During the day, it absorbs the solar radiation and releases it by convection and longwave radiation into the cavity air, which warms faster compared to the base case (no shading device) and to the aluminium case ($\epsilon \sim 0.1$). Therefore when concrete is applied as a shading device, there is an increasing of the resulting stack effect and airflow rates within the cavity during the day. After sunset, the high emissivity property of concrete send radiation towards the outer glazing layer, which is lost to the cold night sky.

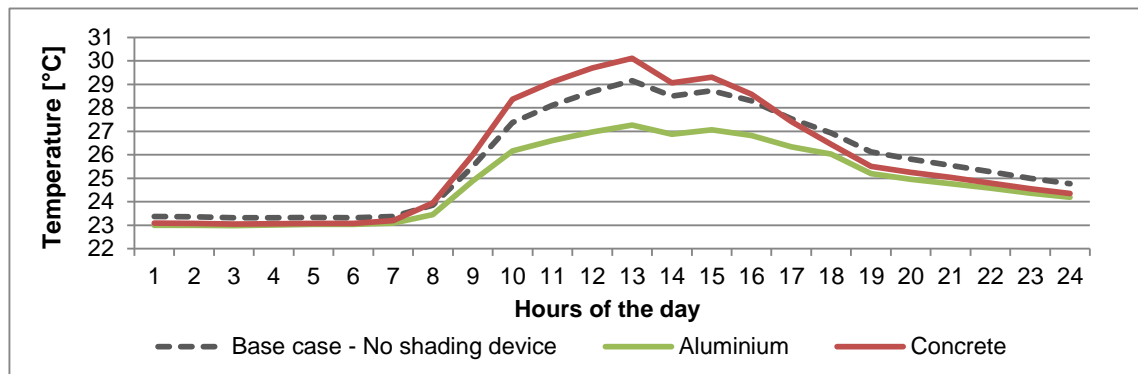


Figure 5.4 - Cavity temperature for the alternatives of case scenario B.1 'shading device'

Although the application of metal shading device within the cavity reduced the overall airflow in the offices as shown in Figure 5.5, this option improved the thermal comfort in the building by 9% in relation to the base case, due to the reduction in direct solar heat gains from the cavity. On the other hand, the improvement in the overall building thermal comfort of the concrete case relative to the base case was only 4%. As the concrete case experiences higher air temperature within the cavity during the day, higher convective heat gains into the rooms due to the recirculation flow occurring in all floors decreases acceptance levels of this case in relation to the aluminium case.

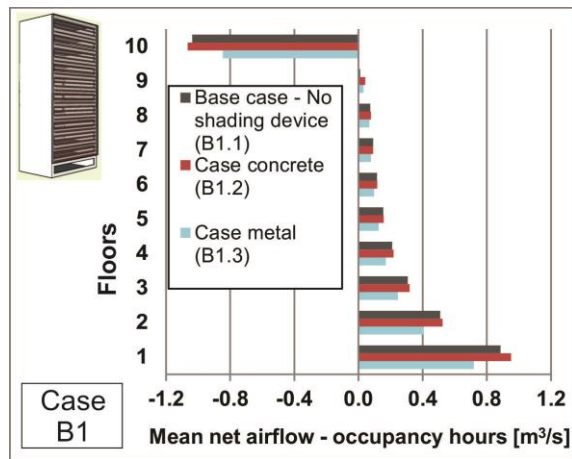


Figure 5.5 - Annual mean of the net airflow for each floor for parameter 'shading device'

With fixed shading devices applied to the model, the fully efficient solar protection of the office spaces is not guaranteed at all solar angles. Thus, the application of automatized blinds according to the solar angle may increase the acceptance levels in the model.

Inner skin material

Figure 5.6 shows the net airflow through the offices when high insulated material was applied on the inner surface of a black wall (scenario B2.2). The configuration promoted a marginal enhancement in airflow through the floors compared to the base case. Although the black wall was applied to the inner layer, during the day the increase in the cavity air temperature is in average only 0.5°C in relation to the base case, reaching a maximum of 1.1°C. This can be explained by the radiation transmission to outside through the outer glazing. Therefore, the solution was not considerably effective in increasing airflow through the offices.

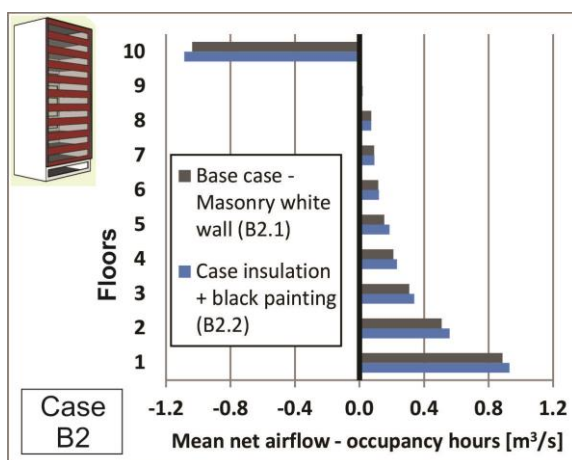


Figure 5.6 - Annual mean of the net airflow for each floor for parameter 'inner skin material'

5.2.3 Group C: reverse flows on top floors

Cavity extension above roof

Cases in group C1 were used to resolve the reverse flow direction on the top floor of the building model by extending the height of the cavity (175, 350 and 525cm above the roof) to raise the NPL above the highest window of the building (from the law of conservation of mass, the sum of all inflows has to balance with the outflow at the top of the cavity). For the model defined in this study, the extension of 525 cm (one and half floor heights) achieved the intended ventilation flow paths on all floors with thermal comfort enhancement of 9% on the top floor compared to the base case (Figure 5.7). However, the height of the residual cavity above the roof is intrinsically related to the number, position and size of windows and the area of the top of the cavity, thus different height extension may be necessary for other building configurations.

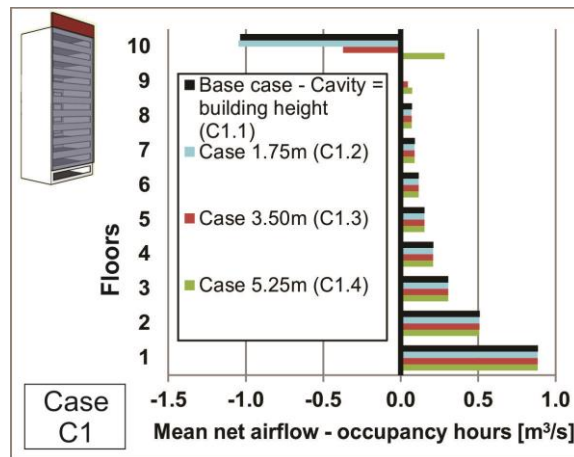


Figure 5.7 - Annual mean of the net airflow for each floor for parameter 'cavity extension above roof'

Upper windows closed

When extending the cavity height above the top of the building is not viable, mechanical ventilation for the upper floors with windows closed should be considered, as tested in case scenarios C2. Results in Figure 5.8 shows that closing windows on the top three floors would be necessary to ensure no reverse flow to occur in the model studied.

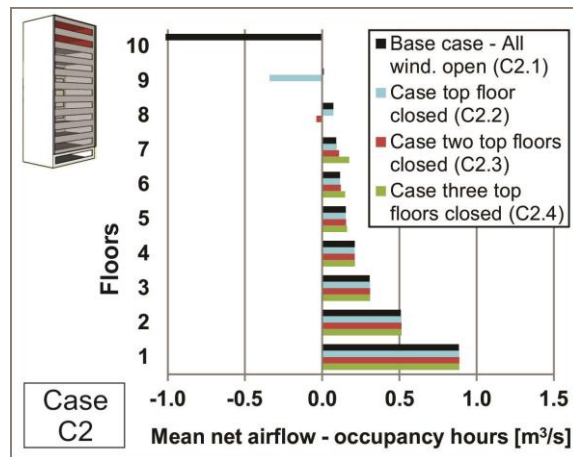


Figure 5.8 - Annual mean of the net airflow for each floor for parameter 'upper windows closed'

5.2.4 Group D: balanced flows on all floors

Tapered skin

Cases in group D1 aimed to achieve even flow through each floor by modifying the cavity width over the height of the building. As shown in Figure 5.9, both cases tapered inner and outer layers resulted in similar net airflows from the 1st to 9th floors, where acceptable annual comfort levels of approximately 65% were achieved. The airflow resistance increased on the bottom floors and decreased on the top floor, resulted in a balanced flow resistance among the levels. However, for the top floor of both cases, only 45% of thermal acceptance was accomplished due to the occurrence of reverse flow.

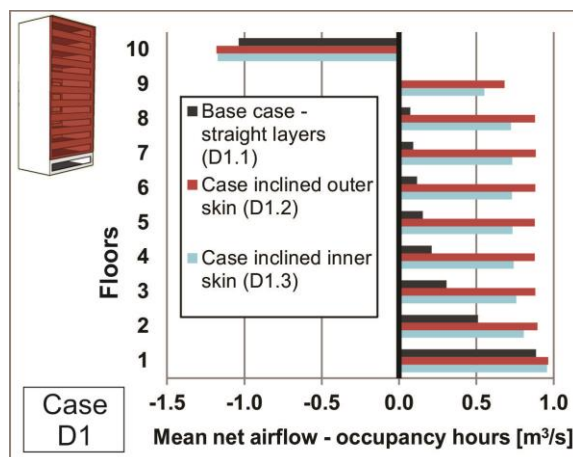


Figure 5.9 - Annual mean of the net airflow for each floor for parameter 'tapered skin'

Windows size

In case scenario D2.2, the size of the windows were calculated according to their position in height such that the neutral pressure line occurs at a point above the highest

window and the flows from each floor are balanced, as illustrated in Figure 5.10. Windows position in height, calculated area and position of NPL are presented in appendix B. This strategy appeared to be effective in evening out airflows and consequently similar acceptable annual comfort levels of approximately 65% were achieved over all the floors. However, the thermal comfort acceptability of top floor reached 55% due to slightly higher solar heat gains and small heat gains by conduction from the roof.

In this case, the resulting stack effect overcame the recirculation flow in the north windows and no flow from cavity into the rooms in those apertures was observed. In the model, only the north windows (close to the DSF) were sized whereas the south windows remained 100% opens to take advantage of the single sided ventilation on the south facing façade. Although higher airflow levels occurred on cases D1, similar overall acceptable thermal comfort levels of around 64% were achieved in those cases due to the absence of reverse airflow over the floors of case D2.

A motorized system could be applied to the north windows to control the aperture sizes in order to balance the airflow in all floors, while the rooms benefit from higher amount of fresh flow entering from the south side of the building. Under cold conditions, the windows opposite to the DSF could be also regulated to reduce the airflow through the building.

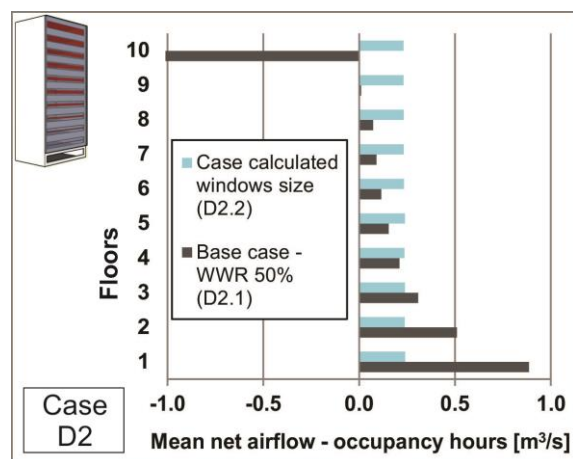


Figure 5.10 - Annual mean of the net airflow for each floor for parameter 'windows size'

As noted in section 4.3.3, mean monthly cavity airflow and air temperatures and mean monthly airflow across the levels of the building for all cases tested are presented in Appendix A. They were also used to gain a broader understating of how the DSF functions throughout the year.

5.2.5 Thermal comfort acceptance

This section presents and compares the thermal acceptability among the base and alternative cases. It shows the relative influence of the design parameters on the building thermal performance and identifies the most important parameters to be considered on the design of naturally ventilated buildings with DSF. Table 5.2 presents the acceptable percentage of thermal comfort delivered on each floor for the cases simulated. It compares the thermal comfort acceptability of the alternate options applied in the models and highlights their relative effectiveness in improving thermal comfort.

Some alternative cases improved the overall thermal comfort of the building, such as increasing the cavity width and applying shading devices, which enhanced the annual thermal comfort by up to 9% in comparison to the base case. Impacts of other parameters such as the cases of 'bottom closed' and 'windows position' were more specific to the bottom floor, where improvements of approximately 4% in the thermal acceptability were observed. By extending the cavity above the roof of the building, the problem of reverse flow on the top floor was resolved, which resulted in 9% of thermal comfort improvement on that floor. The strategies of inclining the outer skin and adjusting the flow resistances through calculation of window sizes according to their positions relative to the building height achieved the desired outcome of similar airflows on each floor, providing approximately 65% of thermal acceptability from the 1st to the 9th floor.

Except for the windows size calculation case, all scenarios presented a local recirculation between the room and the cavity. This is explained by the difference in temperature between room air and the section of the cavity in front of it, which creates a pressure difference on each window. Thus, local NPLs occur between the cavity and the occupied space generating a recirculation phenomenon on the openings, where air will tend to flow in at the bottom and out at the top in each window of the inner layer of the DSF. This results in increase of air temperatures in the occupied spaces, especially close to the windows. For the 'windows size calculation' scenario, the low height of the north windows and the stack effect resulted in the cavity prevented those local recirculation flows.

Table 5.2 – Effect of design parameters to annual thermal comfort

Design parameter	Scenario	Variable	Annual thermal comfort acceptance (%)										Mean Overall
			1 st floor	2 nd floor	3 rd floor	4 th floor	5 th floor	6 th floor	7 th floor	8 th floor	9 th floor	10 th floor	
	Base case	Refer to Table 3	70	68	66	64	63	62	61	60	59	44	62
Cavity width	A1.1	25 cm	67	64	62	61	60	59	59	58	57	45	59
	A1.3	100 cm	72	71	69	67	66	65	64	63	59	42	64
Bottom closed	A2.2	Bottom cavity closed	75	68	65	64	62	61	61	60	58	44	62
Windows position	A3.2	Up north, bottom south	71	67	64	62	61	60	59	58	55	43	60
Shading device	B1.2	Concrete	77	73	71	69	67	66	66	65	63	47	66
	B1.3	Aluminium	74	74	73	72	72	71	71	70	69	59	71
Inner skin material	B2.2	Reflective glazing	69	66	64	62	61	60	59	58	56	41	60
Cavity extension	C1.2	1.75 m	70	67	65	64	62	61	61	60	58	44	61
	C1.3	3.50 m	70	67	65	64	62	61	61	60	59	48	62
	C1.4	5.25 m	70	67	65	64	62	61	61	60	59	53	62
Windows closed	C2.3	9 th and 10 th	70	68	66	64	63	62	59	41	-	-	62
Tapered cavity	D1.2	Inclined inner skin	68	67	66.1	66	66	66	66	65	63	45	64
	D1.3	Inclined outer skin	69	68	67	66	66	65	66	65	63	45	64
Calculated windows size	D2.2	Calculated WWR	65	64	64	64	64	64	64	63	63	55	63

5.3 Results of CFD verification

This section presents the results of CFD models. As explained in section 4.3.1, the verification procedures aim to compare overall predictions of airflow trends in order to ensure consistency of the thermal and airflow behaviour of the DSF building model generated from IESVE and FloVENT, but no quantitative data was compared given the reduced building length modelled in the CFD package. Cases in which the airflow through the building is affected by the transient nature of thermal transfers of materials were not performed in the steady state CFD simulation. Therefore, the cases simulated in FloVENT are cavity depth', 'cavity bottom opening', 'windows position', 'cavity extension above roof' and 'tapered skin'.

The cavity depth cases simulated with CFD showed a similar airflow profile to the IESVE models. The wider cavity case presented higher airflow rates than the narrower cavities due to less resistance within the flow path, as shown in Figure 5.11. As in the IESVE simulation, the airflow of the 100 cm-case was approximately double the 25 cm-case. As verified on the base case model, the CFD simulations for the cavity depth cases did not revealed reverse airflow on the upper floor. The reasons for this are explained in section 4.4.2.

The cavity bottom opening case also presented similarities with the IESVE simulation. By closing the bottom aperture of the cavity, the lower floor presented higher airflow rate in relation to the other floors, while the other levels presented similar airflow rates to the base case (Figure 5.12).

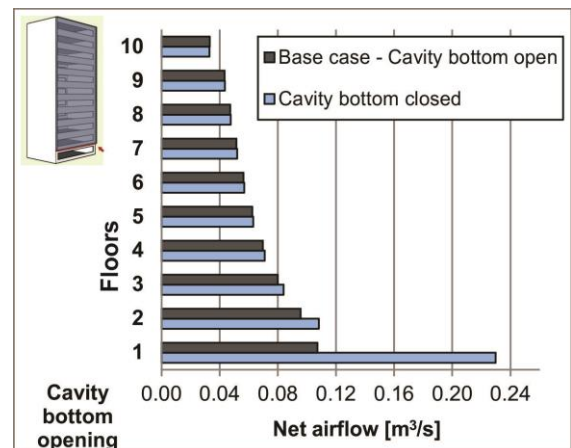
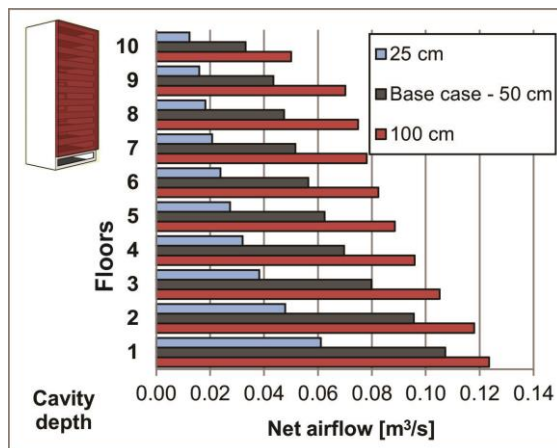


Figure 5.11 – Net airflow for each floor for parameter 'cavity depth' simulated on CFD

Figure 5.12 – Net airflow for each floor for parameter 'cavity bottom opening' simulated on CFD

The case in which south and north windows were positioned at the bottom and top of walls respectively, presented higher airflow levels on the first and top floors, as shown in Figure 5.13. Although differently from results of the IESVE model, which presented lower reverse flow on the top floor, the CFD simulation showed an improvement of airflow from the room towards the cavity on this level. Essentially, an enhancement in airflow rates from the rooms towards the cavity was captured by both software when the windows were repositioned.

For the case in which the cavity is extended 3.5m above the building roof, the CFD model indicated an enhancement on airflow from the upper office towards the cavity (Figure 5.14). This demonstrates an increase in the airflow rate from the upper room towards the cavity, which is conceptually similar to the IESVE results.

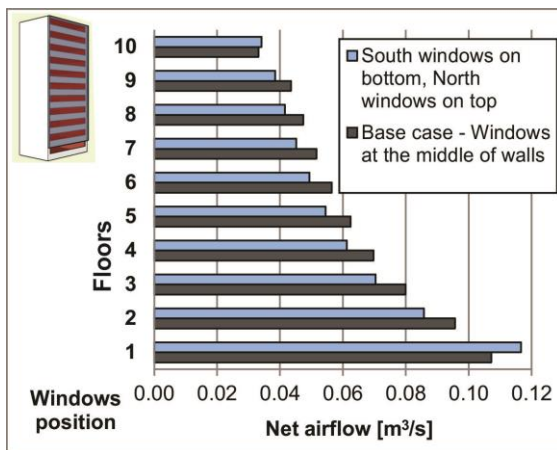


Figure 5.13 – Net airflow for each floor for parameter ‘windows position’ simulated on CFD

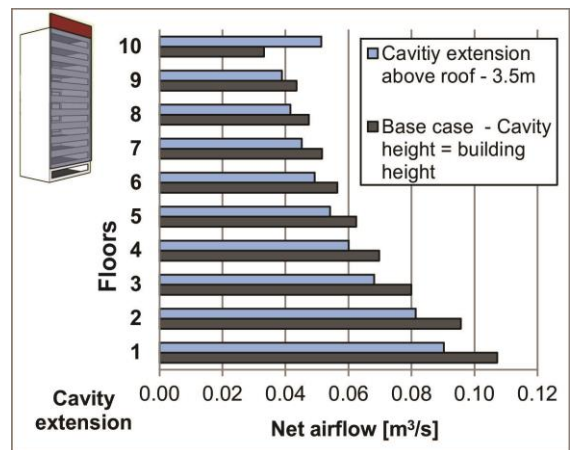


Figure 5.14 – Net airflow for each floor for parameter ‘cavity extension above the building roof’ simulated on CFD

The case with the outer glazing layer inclined outwards, increasing the cavity width with floor level, also indicated good agreement with IESVE model results. As seen in Figure 5.15, in this case, similar flow rates were achieved across all floors, which is explained by the increased resistance on the bottom floors and decreased on the top floors. It is also clear that the upper floors presented lower airflow rates than the others. This is also comparable with the IESVE results, in which an increase of reverse flow on the top floor was observed.

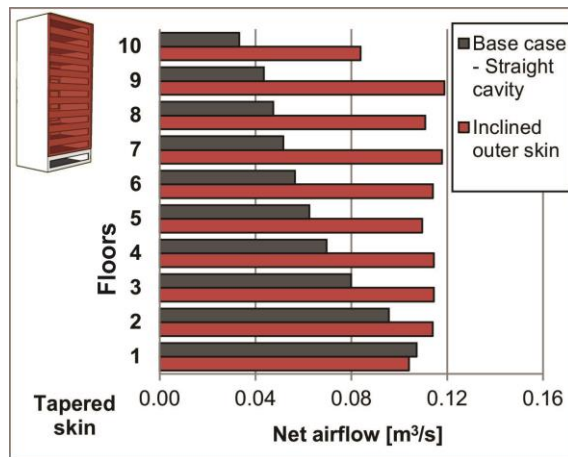


Figure 5.15 – Net airflow for each floor for parameter 'tapered skin' simulated on CFD

Although the case in which the window sizes increased with floor is not influenced by the transient nature of thermal transfers of materials, this case was not included in the CFD simulations. The size of the lower windows would require an extremely fine mesh to effectively capture airflow through them, which was not supported by the computer resources available.

Although the absolute airflow values could not be compared between the software, the cases verified presented similar tendency in airflow trends over the floors when different design parameters were applied. IESVE was able to replicate the general profile of airflow rates from CFD simulations, which is known for the increased accuracy of ventilation simulations. This strengthened the confidence of the findings described in section 5.2.

5.4 Optimized cases

Based on the outcomes of the evaluation of individual design parameters presented in section 5.2 of this chapter, two optimized models that utilise a combination of variables to maximize thermal comfort were developed. These models incorporated the parameters that maximized the absolute flow rates while resolving the reverse flow through the upper floors and attained even airflows at each floor level. The characteristics of the two optimized models proposed are:

Optimized model 1 - the DSF cavity bottom is closed and the top is extended 3.5m (equivalent to one floor) above the roof of the building. A concrete shading device is placed inside the cavity and white masonry wall is applied to the DSF inner layer. The outer DSF glazing is inclined outward such that there are similar horizontal flow rates across all floor levels. Windows with a WWR of 50% are positioned at the bottom and on the top of the south and north walls, respectively.

Optimized model 2 – a fixed vertical DSF cavity of 1m width has its bottom closed. The top of the cavity is extended 3.5m above the roof of the building. North windows, placed at the top of the walls, are sized to achieve similar flow rates across all floors levels. South windows, positioned at the bottom of the walls, are fully open. A concrete shading device is positioned within the cavity and a white masonry wall is used on the inner layer of the DSF.

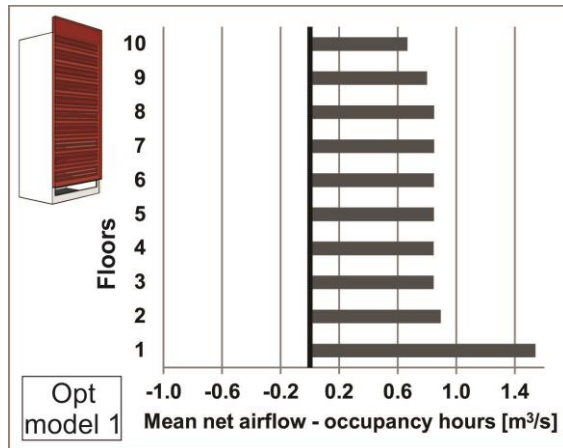


Figure 5.16 – Annual mean of the net airflow for each floor of 'Optimized model 1'

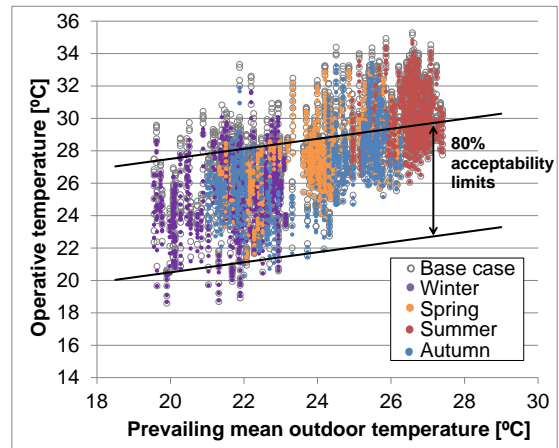


Figure 5.17 - Annual operative temperatures of 'Optimized model 1' (5th floor)

Figure 5.16 to Figure 5.19 show that higher levels of thermal comfort acceptance were achieved by both models compared to the base case, while similar airflows were generally maintained on all floors. Net flow rates in optimized model 1 are marginally higher than optimized model 2, but the overall thermal comfort levels are similar, approximately 68%, in both cases. The top floor presented the lowest hours of thermal comfort acceptance, 58% in case 1 and 62% in case 2, due to the higher heat gain by conduction from the roof. Hourly operative temperatures for the whole year are plotted in the adaptive comfort charts (Figure 5.17 and Figure 5.19) in colour to highlight the thermal acceptability according to the seasonal variations. It shows that most of the uncomfortable hours occur when the prevailing mean outside temperature is above 24°C. Although summer presents the highest levels of excessively hot conditions, uncomfortable moments can occur all over the year, including the winter season.

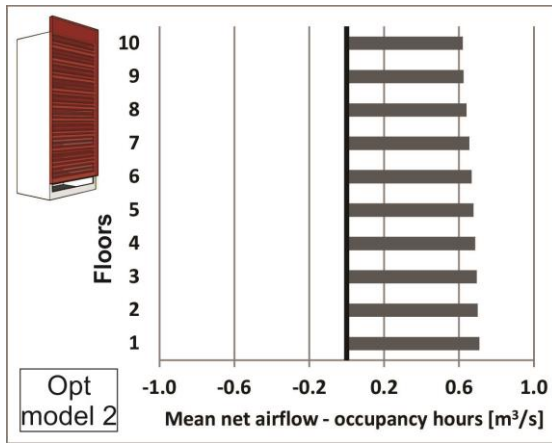


Figure 5.18 – Annual mean of the net airflow for each floor of 'Optimized model 2'

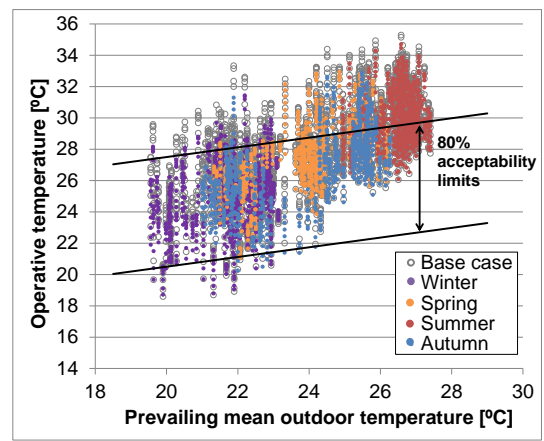


Figure 5.19 - Annual operative temperatures of 'Optimized model 2' (5th floor)

5.5 Building dimension parameters

A combination of design variables that maximize the airflow rates and consequently the thermal comfort in the building was applied in the optimized models. This section tests the sensitivity of these design solutions for other building geometries. Table 5.3 summarizes the building dimension variables that influence the thermal performance. Cases within E1 tested the influence of number of floors, including two models with 5 and 20 floors. Cases within E2 verified the effect of the building depth on the acceptance level. As Brazil does not have an official typical modular dimension for office buildings, the American and European dimensions, described in section 4.2.1, were considered and cases of building depth of 6 and 18m were tested in addition to the base case.

Different from the design parameters of group A to D, the building dimensions parameters cases used the optimized model 2 as the reference. In these cases, the windows sizes were recalculated considering the number and position of openings in each model. Windows position in height, calculated areas and positions of NPL of those cases are presented in the appendix B.

Table 5.3 - Parameters and variables tested (group E – Building dimension parameters)

Case	Design parameter	Scenario	Variables	
Group E	E1	Number of floors	E1.1	• 5 floors covered by DSF
			*E1.2	• 10 floors covered by DSF
			E1.3	• 20 floors covered by DSF
	E2	Building depth	E2.1	• 6 m
			*E2.2	• 12 m
			E2.3	• 18 m
*Base case				

5.5.1 Group E: building shape

The model with 5 floors presented airflow rates approximately threefold higher in relation to the 20 floors-model, as shown in Figure 5.20. Considering that according to the physical law of conservation of mass the inflow has to match the outflow, keeping the top of the cavity opening area constant, for a greater number of inlets, the airflow through each floor will decrease. However, similar acceptable annual comfort levels were achieved in those cases with the difference from the highest to the lowest building of only 3%. This can be explained by the relatively low difference in air speed among the cases.

Cases E.2, in which changes to the depth of the building were evaluated, delivered similar airflow rates, as the inlet opening areas remained the same in all models (Figure 5.21). However, the shallower building case presented higher overall acceptance levels, 4.2% and 9.6%, than the 12m and 18m cases, respectively. This can be related to the more effective removal of internal heat by ventilation in the office spaces, as lower heat gains are set for the narrow model. In this case, cooler air is discharged into the cavity in relation to the wide models. This can induce lower stack effect in the cavity and therefore, can explain the gradual small decreasing in airflow in the narrower models in relation to the wider one.

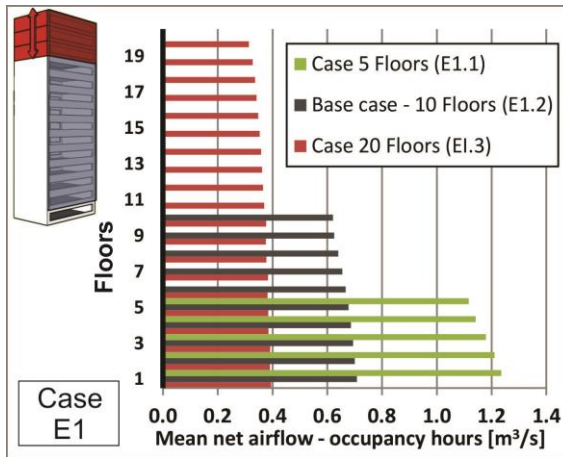


Figure 5.20 - Annual mean of the net airflow for each floor for parameter 'number of floors'

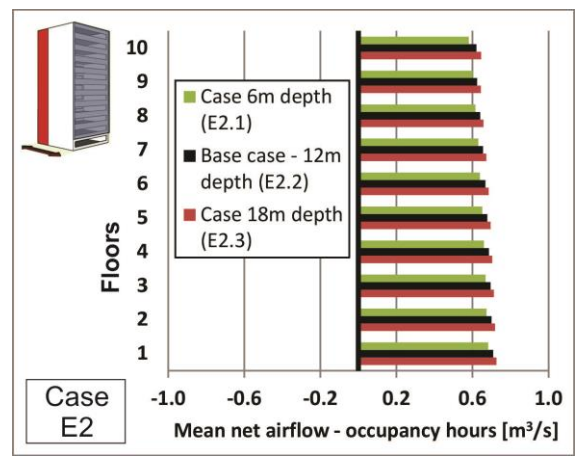


Figure 5.21 - Annual mean of the net airflow for each floor for parameter 'building depth'

5.6 Site parameters

The site parameters are represented by two main groups of variables: the solar incidence and the wind conditions. For the first group, analysis of the influence of hours of the day, solar angle, sky conditions (cloudy and clear) and façade orientation on the building behaviour is performed using data of Rio de Janeiro city. In those cases, the weather file used was modified and wind speeds were made zero for the whole year. The wind variables consist of speed and direction and several combinations of both have been specified and analysed. In those simulations, manipulated weather files were set with specific wind speed and direction, as shown in Table 5.4.

Table 5.4 - Parameters and variables tested (Groups F and G – Site parameters)

Case	Design parameter	Scenario	Variables	
Group F	F1	Level of solar incidence	F1.1	• Solar angle
			F1.2	• Hours of the day
			F1.3	• Sky conditions (cloudy and clear)
			F1.4	• Façade orientation (N, NW, NE)
Group G	G1	Wind speed	G1.1	• 2 m/s
			G1.2	• 4 m/s
			G1.3	• 6 m/s
	G2	Wind direction	G2.1	• 0°
			G2.2	• 90°
			G2.3	• 180°
			G2.4	• 225°
			G2.5	• 315°

5.6.1 Group F: Level of solar irradiance and angle

The amount of solar incidence reaching the façade is a function of the angle at which solar radiation strikes the surface, which is determined by latitude, the time of the day and year and also the level of cloud cover. The functioning of the DSF is intrinsically related to the solar incidence, as it increases the cavity air temperature, generating the buoyancy effect that will function as a ventilation driver for naturally ventilated buildings. The results presented in this section are from Rio de Janeiro city (22.9°S, 43.1°W), where the solar altitude varies from about 45 degrees on the coldest months to 88 degrees over the hottest periods. However, cities closer to the equator line, such as Brasilia (15.7° S, 47.8° W, bioclimatic zone 4) and Picos (7.1° S, 41.4° W, bioclimatic zone 7), may have the potential ventilation reduced as higher solar altitude decreases the percentage of solar radiation transmitted through the outer DSF layer.

The relationship between the cavity/outside air temperature differences in relation to the amount of solar radiation reaching the façade is broadly linear, as shown in Figure 5.22. In the climate analysed, the solar incidence on the north façade is below 500 W/m² in 86% of the daylight time and reaches a maximum of approximately 730 W/m² on brighter days, when the difference of temperature between the cavity and the outside air can achieve 12°C. This value is slightly lower than those observed on the study by Gratia and De Herde (2007a), which used an air conditioned building model, presented in section 2.5.1 of chapter 2. The lower difference of temperatures in this study can be explained by the discharge of cooler air from rooms into the cavity, which contribute to the decrease the air cavity temperature.

Figure 5.23 shows the resulting airflow at the middle level of the model (5th floor) according to the solar incidence on the north DSF. The airflow rates varies from 0.45m³/s to approximately 0.8m³/s on brighter days. The airflow rates through the office space during moments of low solar incidence can be explained by the buoyancy ventilation promoted by the internal heat gains and the re-radiation of the absorbed heat by thermal mass materials applied on the inner layer and shading device within the cavity.

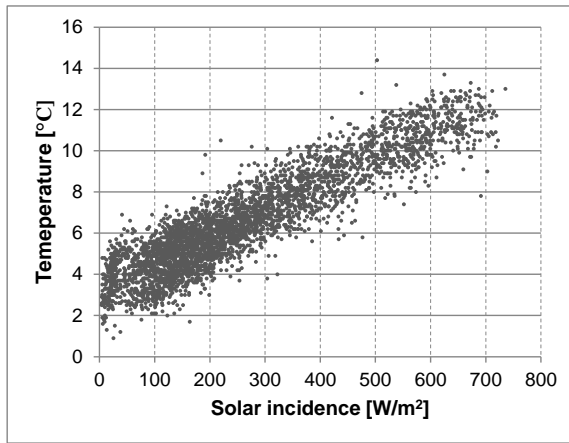


Figure 5.22- Difference of temperature between the cavity and the outside air in relation to the solar incidence on the DSF

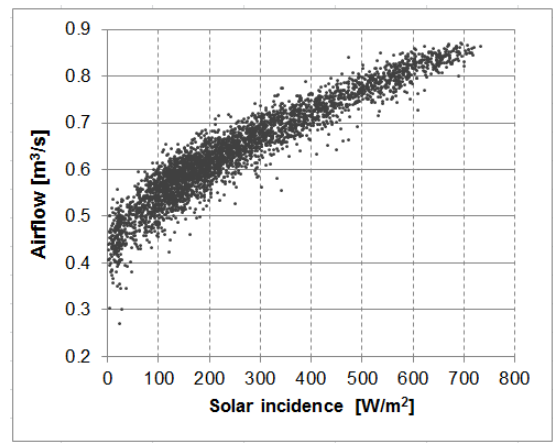


Figure 5.23 - Airflow on the 5th floor of the model as a result of the solar incidence on the DSF

Figure 5.24 indicates the average of solar incidence on the façade surface for solar angles 15 - 20°, 45 - 50° and 85 - 90°. The diagram shows that the lowest levels of solar incidence on the façade occur under low solar altitudes. This happens because those moments tend to occur at the beginning and end of the daylight hours, when the levels solar radiation are the lowest. Therefore, although according to Mulyadi (2012) the percentage of transmitted solar radiation through the outer DSF layer tends to increase at lower solar altitudes, it may not correspond to the moments of higher ventilation in the building because of the low solar incidence to warm the cavity air. On the other hand, the highest levels of solar radiation reaching the façade occur close to midday, when the solar angle varies from about 45 - 50° and the solar incidence levels are high. Finally, the highest solar altitudes occur during the summer and close to the midday and explain the relatively high levels of solar radiation reaching the DSF.

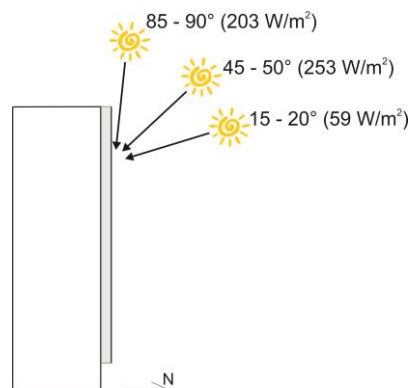


Figure 5.24 - Average of solar incidence on the façade surface for solar angles 15 - 20°, 45 - 50° and 85 - 90°.

Orientation

In order to identify the potential of airflow promoted by the DSF when it is applied at different faces of the building, three cases were tested. Based on the discussion presented in section 2.5.1, north, northwest and west demonstrated to be the most suitable orientations for the DSF as the south and east facings do not receive enough solar radiation to generate ventilation for the indoor space.

Figure 5.25 shows the annual mean net airflow of the 5th floor in the three orientations tested. The solar radiation transmitted through the outer layer of the DSF is symmetrically distributed over the day when it is north oriented, generating higher levels of ventilation around midday. In contrast, the northwest and west orientations provided the highest levels of airflow in the cavity during the afternoon, which is explained by the low solar angle and the consequent highest radiation levels transmitted through the outer skin.

The maximum difference in the annual mean airflow rates between the west and north orientations occur at 5 p.m., when the west case presented 17% higher airflow than north case. As a consequence of the induced airflow in the office rooms, the building models reported 62%, 66% and 69% of thermal acceptability for the west, northwest and north orientations, respectively. Although higher airflow rates are observed in the afternoon for the cases northwest and west, the difficulty in promoting sun protection against low solar angles explains the lowest levels of thermal comfort.

Therefore, because of the distributed solar incidence on the north facing façade during the day (for buildings located in the southern hemisphere), this orientation presented the most adequate conditions to promote natural ventilation for office buildings in breezeless days under warm climates. It is important to notice however that in highly dense cities the sun shading created by surrounding buildings may affect the resulting stack effect within the cavity.

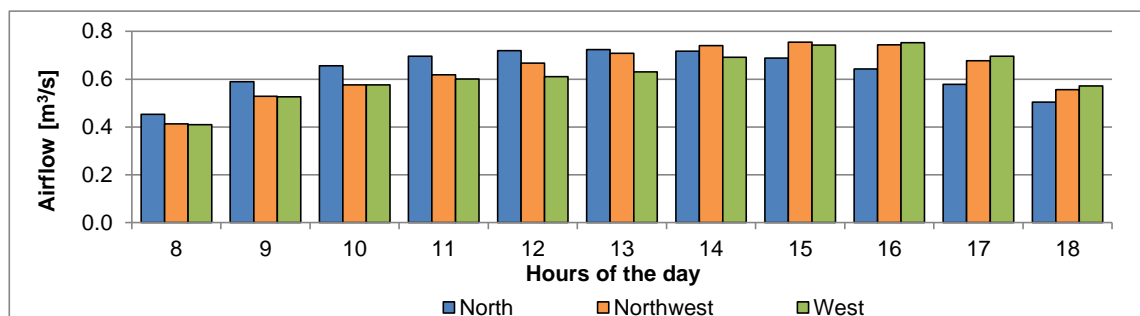


Figure 5.25 - Annual mean net airflow of the 5th floor in three orientations

Hours of the day and sky conditions

As the internal heat gains are constant during the occupancy hours, the variation of the induced ventilation at different hours of the day relies on the temperature difference between the outside and the cavity air. Figure 5.26 shows how the potential of natural ventilation in a DSF building differs throughout the day. Following the solar incidence pattern, the peak of airflow tends to occur around midday. It also shows that the highest airflow rates remains until around 2 p.m., which can be related to the thermal delay in heat transfer through the layers and shading device of the DSF. Thereafter, a decrease in ventilation is observed, reaching its minimum at 6 p.m. when the annual average of airflow decreases 40% in relation to the value observed at 1 p.m. The minimum values registered can be related to the cloud sky conditions.

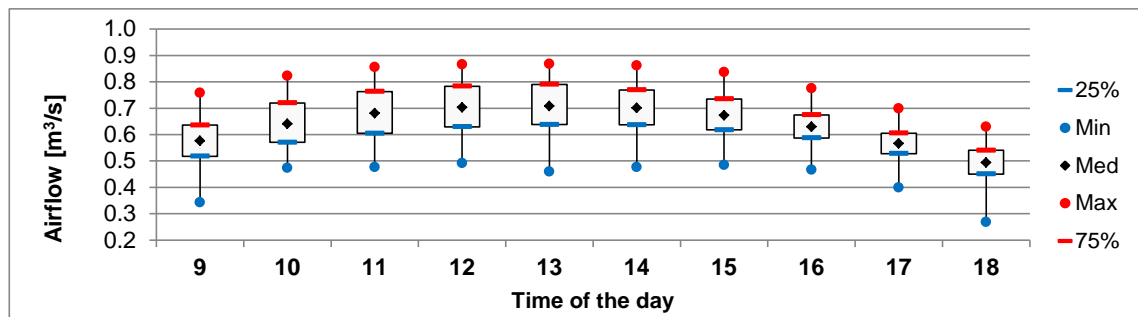


Figure 5.26 - Airflow occurring on the 5th floor according to the time of the day during the occupancy hours

A cloudy day (07-Sep) and a sunny day (17-Sep) were selected for the evaluation of the effects of the sky conditions on the DSF. The weather file indicates that the mean direct radiations of the selected sunny and cloudy days (from 8 a.m. to 6 p.m.) are 571 W/m² and 6 W/m², respectively. This resulted in an addition of up to 11.6°C for the sunny day, and 6.1°C for the cloudy day, to the cavity temperature relative to the outdoor air. Therefore, on average, an increase of 0.6m³/s in the cavity airflow is observed from a cloudy to a sunny day. However, this difference is less accentuated in the offices where an increase of approximately 0.1m³/s on the induced airflow rates was observed, as shown in Figure 5.27.

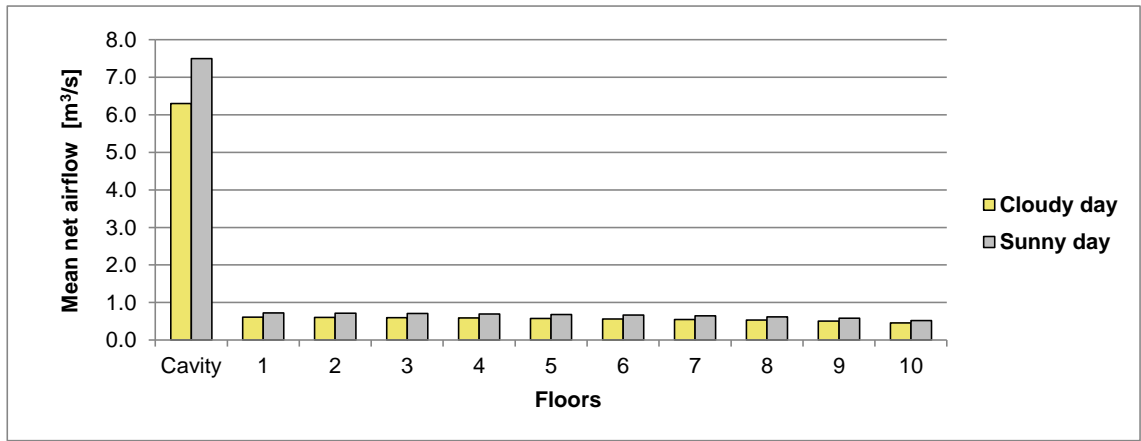


Figure 5.27 - Difference in airflow rates for the cavity and the rooms in a cloudy (07-Sep) and a sunny days (17-Sep) during the occupancy hours

5.6.2 Group G: Wind conditions

As explained in section 2.2, from Bernoulli's principle, wind induced pressures on the surfaces of a building are related to local air speed, with lower speeds causing relatively higher static pressures and faster speeds causing relatively lower static pressures. As wind approaches the building, it collides with the façade surface and local air speed is reduced generating recirculation zones that results in an increase of the static pressure. Conversely, the air speed on the top and sides of the building increases, resulting in a reduction in local static pressure. As a result, a pressure differential through the building is created, whose magnitude is affected by the wind direction relative to the building orientation, determining the sides and openings of the building that are exposed to the low/high pressures. Additionally, higher wind speed at roof level causes a lower static pressure on the upper part of the building surface than near the ground. Figure 5.28 shows a diagram of static pressures created at different sides of the building according to wind direction.

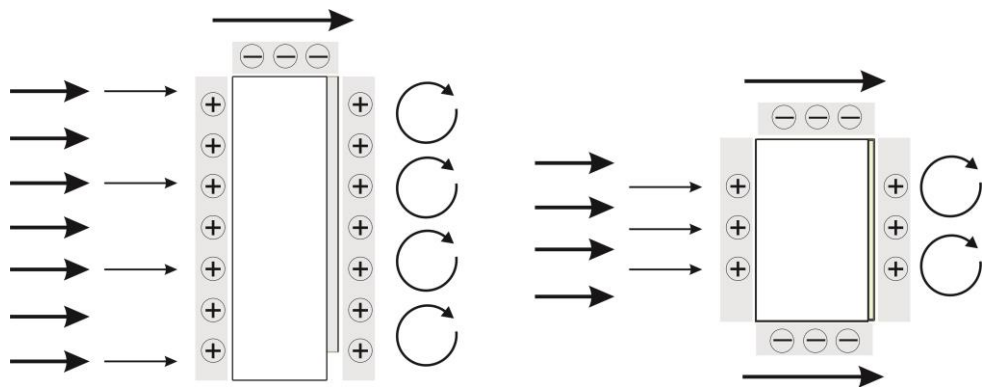


Figure 5.28 - Diagram of static pressures created at different sides of the building according to wind direction

Due to the un-aerodynamic nature of the building analysed, not only air movement is slowed on the façade facing the wind, resulting in a higher relative static pressure, but separation of the flow on the leeward side of the building generates a relatively slow moving recirculation zone that also results in a relatively high static pressure. This means that positioning the DSF either on the leeward or windward side of the building results not only in a lower pressure at the roof level but also a relatively high pressure at some of the window inlets opposite the DSF. Flow rates through the system are therefore improved, as shown in Figure 5.29 and Figure 5.30, which present the airflow rates in each floor for the DSF in the windward and leeward directions, respectively, for different wind speeds. For wind speeds of 6 m/s, the natural cross-ventilation in the offices is improved by up to 140% and 300% on the upper floors when the DSF is facing and protected from wind, respectively.

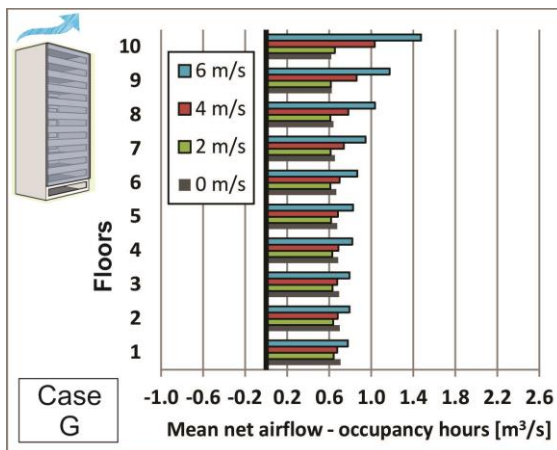


Figure 5.29 – Difference in airflow for winds speed varying from 2 to 6 m/s, for DSF facing the wind

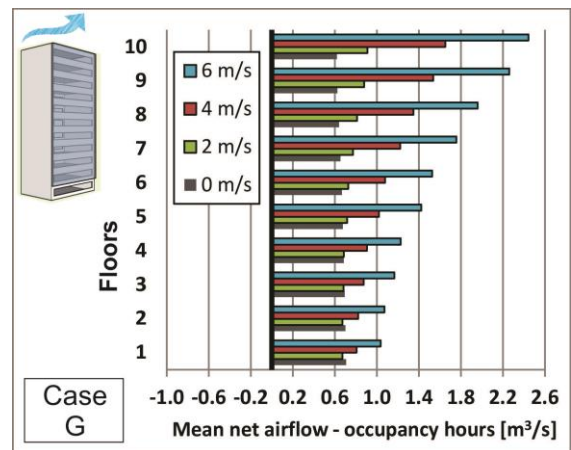


Figure 5.30 – Difference in airflow for winds speed varying from 2 to 6 m/s, for DSF protected from wind

Figure 5.31 shows that there is a reduction in the net amount of airflow through the office spaces when wind direction is parallel to the DSF. Its occurrence is due to the decreasing in pressures differences between the top of the cavity and the window openings. While air speeds outside windows at lower floors are not significantly modified, higher speeds on other floors would result in lowering the local pressures. These differences in pressure lessen the existing stack effect at higher wind speeds, especially where the stack effect is already weak such as on the upper floors. When the wind blows parallel to the DSF and for air speeds higher than 6 m/s, reverse airflow will start to occur on the top floor.

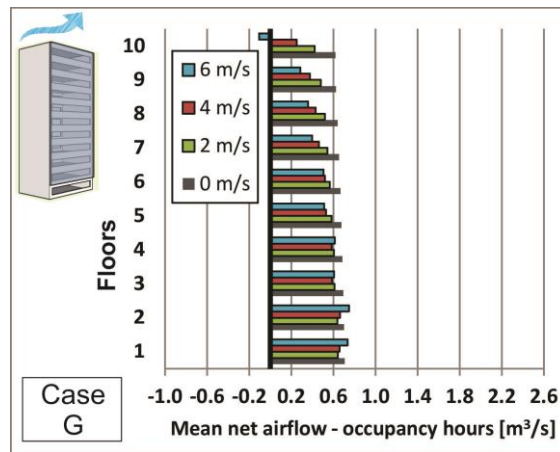


Figure 5.31 – Difference in airflow for winds speed varying from 1 to 4m/s, for DSF parallel to the wind

Complementary, Figure 5.32 and Figure 5.33 shows airflow rates when wind is blowing from northeast (45°) and southwest (135°). Small improvements in airflow can be observed in the 45° case on the top floors, especially with higher wind speeds. When wind is blowing from southeast, the airflow on the top floor increases up to 340%, for wind speeds of 6m/s.

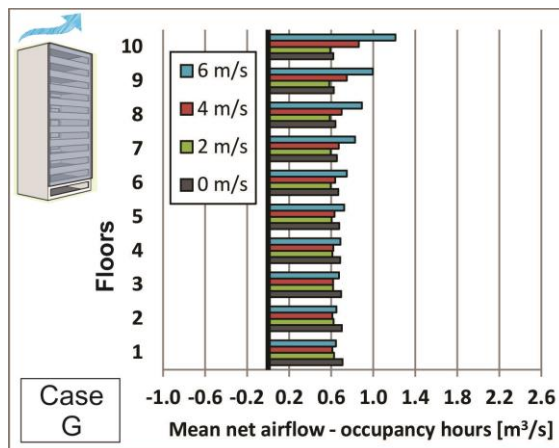


Figure 5.32 – Difference in airflow for winds speed varying from 2 to 6 m/s, for wind blowing at 45°

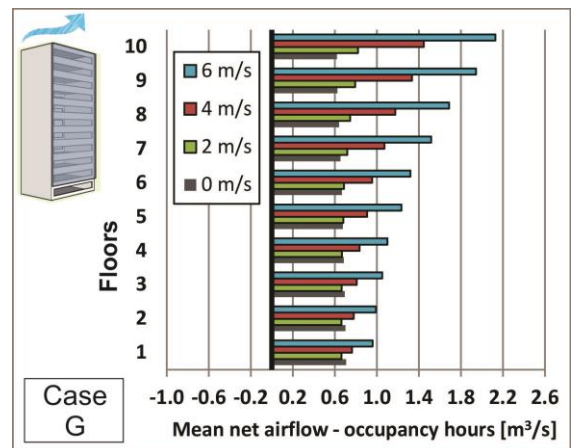


Figure 5.33 – Difference in airflow for winds speed varying from 2 to 6 m/s, for wind blowing at 135°

The wind pressures acting on the surfaces of the building may multiply the effectiveness of the stack effect when DSF is correctly applied according to the dominant wind direction. As already reported in section 2.5.2, maximum benefit of wind is observed when the DSF is oriented perpendicular to the wind direction, which results in an additional increase in airflow rates through the cavity. To the offices this may represent a threefold increase in airflow for wind speeds at 6m/s. On the other hand, application of DSF parallel to the prevailing wind direction must be avoided in warm

climates as it may lessen the cavity stack effect and may cause reverse flow on the top floor even though the windows sizes are adjusted to avoid it.

Variations of wind direction and its speed are related to the sites conditions. For this reason, it is important that the DSF design is based on stack effect and it should consider the effect of wind as an enhancement to the driving forces. As the local wind speed is affected by the type of terrain surrounding the building (e.g. open country or city centre), slower speeds will in reality occur relative to the quoted meteorological wind speed in dense terrains.

5.7 Chapter summary

This chapter has presented the results of the identified alternative case models. The findings have enabled not only definitions regarding the design of the building and the DSF to maximise the system airflows, but also identification and evaluation of environmental factors that affect the component and system thermal performance.

Regarding the design parameters, the results show that wider cavities result in higher absolute airflow rates through the user space due to lower flow resistance to the airflow path. By repositioning the windows apertures to increase the height difference between inlets and outlets, results found improvements in airflow rates mainly on the lowest and upper floors of the building. The application of high thermal mass materials on the shading devices within the cavity not only contributes to the decreasing of solar heat gains to the rooms, but it also enhances the heat absorption and therefore, enhances the buoyancy effect to the air within the DSF. Options to avoid reverse net airflow occurring on the upper floor are to raise the NPL above the window openings by extending the cavity above the building roof or closing the windows of the upper floors. Inclining the outer DSF skin outwards from the bottom to the top balances airflow resistances over the building levels, creating relatively even airflow rates on the floors. Another option to balance airflow rates is to calculate the windows sizes according to their position in height, opening areas and the top of the cavity dimensions. The results indicate that only the north windows (close to the DSF) should be adjusted, so the fully open south windows would take advantage of single sided ventilation. This solution prevents the recirculation effect in the windows close to the DSF.

The local environmental conditions also have a significant impact on the overall system thermal performance. The magnitude and angle of solar incidence reaching the façade, which vary according to location, time of day, façade orientations and seasons, determine the increase of temperature within the cavity in relation to the outside air.

These factors define the airflow levels in the cavity and in the building, especially at low or null wind speeds. The airflow of the system is also dictated by the wind pressures created around the building faces, which may enhance the effectiveness of the stack effect when DSF is correctly applied to exploit such wind effects. Positioning the DSF on either the windward or leeward side of the building results in a relatively high pressure at some of the window inlets opposite the DSF, and flow rates through the system are therefore improved. On the other hand, a reduction in the net amount of airflow through the office spaces is observed when wind direction is parallel to the DSF.

The interdependence of the building design aspects, such as the number, size and positions of the inlet windows and the cavity dimensions and openings, should be carefully considered for different building configurations as they directly affect the overall profile of airflows, hence the ventilation within the building. Regional climates have also a great influence on the building thermal performance. Next chapter determines representative Brazilian regions and periods of the year when satisfactory thermal acceptance can be achieved in naturally ventilated buildings with DSF.

Procedures to improve the quality assurance of the results were applied to the modelling and simulations processes. The aim of the simulations task was clearly previously defined to the modelling procedures. In this study, trends of airflow and the consequent thermal performance of the buildings model were compared by using two different software codes. The selection of the software used considered the level of accuracy and details required, time and computational resources available. Software training was also performed of both software used and a careful modelling evolution defined the decisions made in relation to the design details incorporated. This provided the ability to check whether the outputs were consistent and plausible.

The similarity of the airflow trend results of both codes used provided confidence that the effects observed on the simulations are likely to occur in reality. The aim of determining which design and site parameters would reduce the possibility of overheating issue by improving airflow through the cavity and the rooms as manner to overcome the reverse flow on the floors of the building was achieved.

However, the absolute accuracy of the quantitative results was not possible to address because of the simplifications set in the models. More detailed models would provide a more precise prediction of the building thermal performance. For example, a more realistic occupancy profile would influence the hours in discomfort during the lunch time or at the end of the day when the number of people would be in fact lower than it was modelled. Extreme climatic conditions were also not considered as the typical

reference year dataset was used. More detailed models would give to further studies more reliability in terms of quantitative results.

Chapter Six

Thermal acceptance under Brazilian climates: results and discussions

This chapter presents the results from simulations of the optimized model of naturally ventilated offices with DSF for all bioclimatic zones of Brazil, determining periods of the year when satisfactory thermal acceptance can be achieved. According to the characteristics of the climate conditions presented in Chapter 2 and the understanding of the influence of site parameters on the DSF thermal behaviour, different orientation and application of openings profile for the windows are applied to the selected cases. The results of these models are compared to those with single skin models.

6.1 Introduction

This chapter presents the thermal performance of naturally ventilated office building with DSF under Brazilian climatic conditions. Thermal comfort levels delivered by the optimized model 2 defined in section 5.4 are established for each bioclimatic zone. The following sections present the results for the cities of Curitiba (zones 1), Piracicaba (zone 2), Florianopolis (zone 3), Brasilia (zone 4), Niteroi (zone 5), Campo Grande (zone 6), Picos (zone 7) and Rio de Janeiro (zone 8). Detail descriptions of their climatic conditions are presented in section 3.1.

Based on the understanding and findings from the influence of the site parameters on the DSF thermal performance presented in section 5.6, decisions about inclusion/exclusion of shading devices, DSF orientation in relation to solar incidence and dominant wind and windows opening control according to exterior temperatures are determined and justified for the models to be studied in each Brazilian bioclimatic zone. All cases were firstly simulated with DSF oriented to north as it considers the fundamental principle applied in the generation of ventilation in a building with DSF.

For bioclimatic zones 6, 7 and 8, night time ventilation was set to the models considering the additional benefits for reducing thermally uncomfortable moments. For bioclimatic zones 1 to 5, which experience mild and low temperatures, especially during the winter, window opening profiles are applied to the south side of the building model in order to control airflow and to avoid high levels of discomfort due to cold conditions. Based on the discussion presented in section 2.4.2 about the window openings control according to outside temperature, the opening regulator was set to start to open the south windows when the outside temperature is above 16°C and modulates the degree of opening linearly until it is fully open at 20°C. The north windows and the top of the cavity are set open the whole time to maintain some ventilation rate, even in cold days. Figure 6.1 indicates the airflow mechanisms when south windows are closed, during the coldest moments and when they are open.

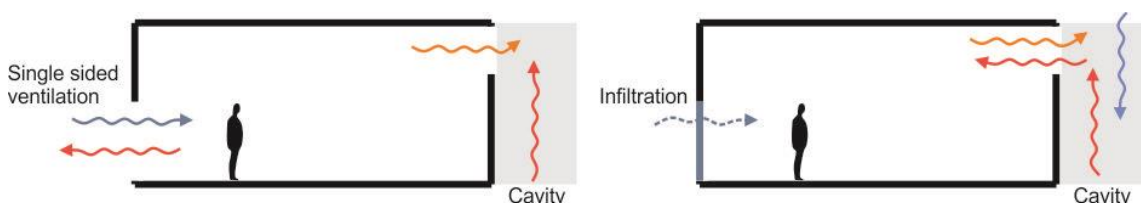


Figure 6.1 - Airflow mechanisms when south windows are open or closed

Typical results are illustrated using annual operative temperatures for the occupancy hours of the 5th floor, according to the different seasons of the year, plotted on the

ASHRAE (2013) thermal comfort matrix. In addition, monthly totals in terms of comfortable and uncomfortable occupied hours (both due to too hot/too cold conditions) are also presented for each case. Comparisons with single skin façade (SSF) models, which preserved the same geometric and fabric materials characteristics of the base case model, are also included. For each bioclimatic zone, a table summarizes the thermal acceptance results for each case tested.

6.2 Bioclimatic zone 1 – Curitiba

General climate characteristics: Curitiba is localized in the south region of Brazil and is characterized by the occurrence of the lowest temperatures among the zones with constant and high relative humidity, having annual averages of 21°C and 86%. Solar heating is the main passive strategy recommended throughout the year to maintain acceptable temperatures in the internal environment, especially during winter. As the city is localized in the lowest latitude among the cities tested, the incidence of low solar altitudes on the façade is beneficial to the building thermal performance. Natural ventilation, on the other hand, is recommended in less than 8% over the year.

DSF proposed: Considering these characteristics, two cases with DSF facing north, with and without shading devices, which allow higher levels of incident solar radiation into the offices, were tested. The opening profile described previously was applied for the windows opposite to the DFS in order to decrease the convective heat losses due to the single sided ventilation.

DSF thermal performance: Both cases, with and without shading devices, presented similar thermal acceptability of approximately 90% over the year (Table 6.1). Figure 6.2 and Figure 6.3 show periods of acceptable temperatures for the case with shading device. The removal of shading devices marginally decreased the periods of thermal discomfort due too cold conditions, which can be due to the difficulty of promoting sun protection for low solar altitudes. Few moments of thermal discomfort due too cold conditions occur from September to March, when windows opposite to the DSF are open as the outside temperatures are above 16 °C. For the periods in which the outside temperatures are below 16 °C, when north windows and top of the cavity are open and south windows are closed, the ventilation rate in the office is, on average, 25 l/s*person, 5 times more than the minimum ventilation rate recommended for office buildings by ASHRAE (2001) for provision of outside air intake, dilution and removal of airborne pollutants and control of excessive humidity.

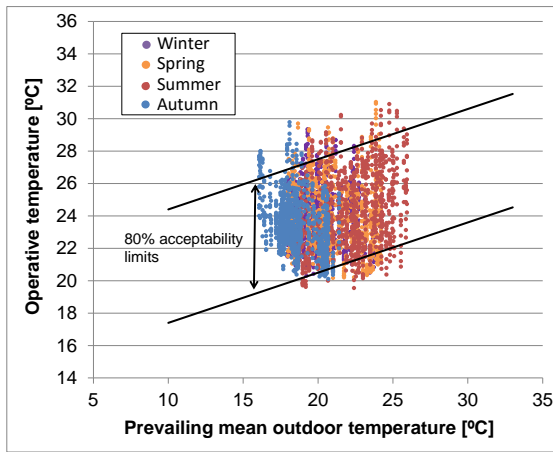


Figure 6.2 - Annual operative temperatures of optimized model under bioclimatic zone 1 plotted on the ASHRAE (2013) thermal comfort matrix

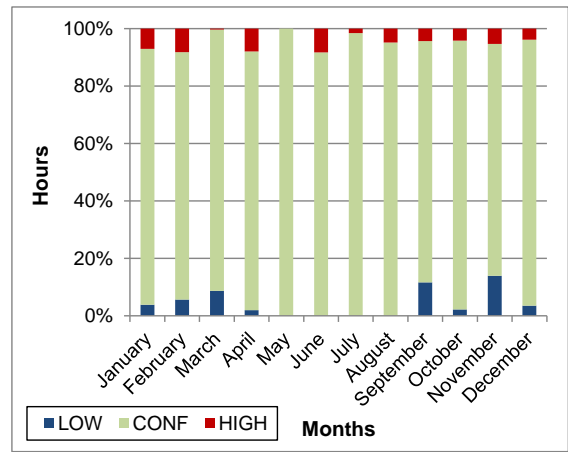


Figure 6.3 - Hourly thermal acceptance in the optimized building model with DSF in bioclimatic zone 1

SSF thermal performance: Figure 6.4 and Figure 6.5 present the results of the SSF model. Although windows opening profile were applied to both sides of the single skin case, it presented 12% more uncomfortable periods due to cold conditions than DSF case. The application of DSF regulated the air speeds in the offices, increasing the operative temperatures throughout the year.

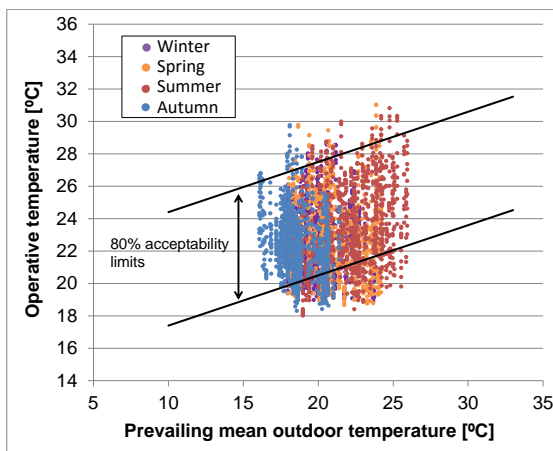


Figure 6.4 - Annual operative temperatures of single skin model under bioclimatic zone 1 plotted on the ASHRAE (2013) thermal comfort matrix

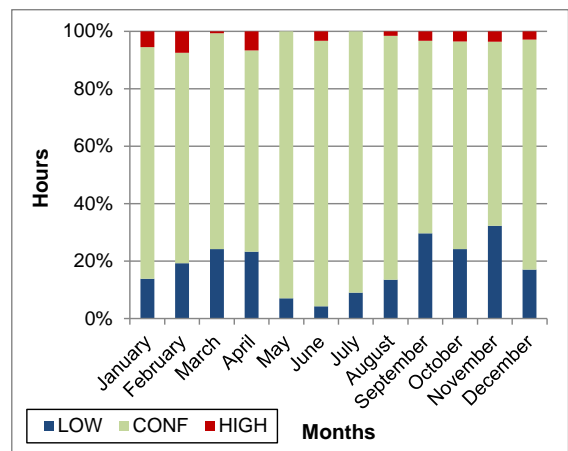


Figure 6.5 - Hourly thermal acceptance in the single skin façade building model in bioclimatic zone 1

Outcomes: The application of DSF as a solution to preheat the building is not a novel finding and improvements in the thermal comfort due to the air exchanges between the warmer cavity air and the room air has been confirmed by a significant number of examples in cold climates. Although, closing the top of the cavity have been indicated as a possible arrangement for cold seasons (Oesterle et al., 2001; Saelens et al., 2008), in the cases simulated under the climate of Curitiba, the north windows and the

top of the cavity remains open the whole time, allowing for adequate natural ventilation through the occupied spaces even in cold periods. The control strategy applied to the windows opposite to the DSF has considerable implications on the magnitude of airflow allowed in the building and consequently on the levels of discomfort during winter. The deficiency of ventilation in the SSF case when outside temperature is below 16 °C can be unfavourable to the indoor air quality conditions. This reinforces the beneficial use of the DSF as a passive heating system that promotes ventilation through the building.

Table 6.1 – Summary of thermal acceptance conditions of cases under bioclimatic zone 1

Façade type	Orientation	Window profile operation applied	Thermal acceptance (%)		
			Too cold	Comfortable	Too hot
DSF	North	Yes	8	89	3
	North - no shading device	Yes	5	90	5
SSF	North/South	Yes	20	77	3

6.3 Bioclimatic zone 2 – Piracicaba

General climate characteristics: Piracicaba experiences mild temperatures throughout the year, which result in a strong dependence on solar heating to keep the internal environment comfortable, especially during winter. The annual mean relative humidity varies from 80% during the summer to 65% during the winter and the predominant wind incidence occurs mainly from east and southeast.

DSF proposed: Based on those conditions, two different DSF orientations were defined for this bioclimatic zone. In order to take advantage of the distributed potential of ventilation over the day, a north oriented DSF was tested. Additionally, a case with DSF oriented to west, at the leeward of wind direction was also tested as this increases airflow rates in the building, which are especially required during the summer. In both models, considering the low temperatures of the coldest months, the opening profile was applied for the windows opposite to the DSF and shading devices were maintained to avoid excessive solar heat gains.

DSF thermal performance: Figure 6.6 and Figure 6.7 show the thermal acceptability for DSF facing north. It reached 84% over the year with the most uncomfortable periods occurring due to hot conditions. Slightly increasing of discomfort due to excessively high temperatures was observed for the case in which DSF is west oriented (Table 2.1). Although the perpendicular predominant wind direction reinforces the stack effect within the cavity, the increasing in temperatures is explained by the higher solar heat gains during the afternoons. The use of fixed shading devices and

their poor protection under low solar altitudes contribute to the decreasing of thermally comfortable periods.

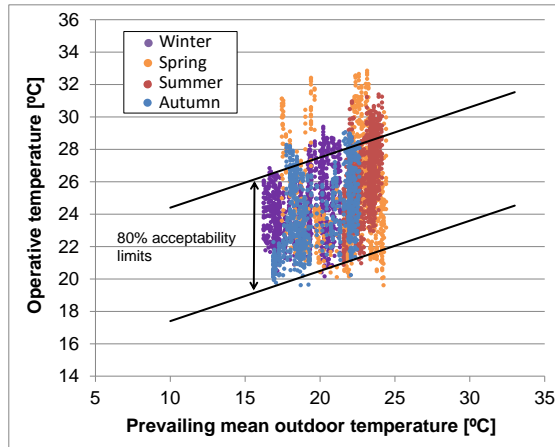


Figure 6.6 - Annual operative temperatures of optimized model under bioclimatic zone 2 plotted on the ASHRAE (2013) thermal comfort matrix.

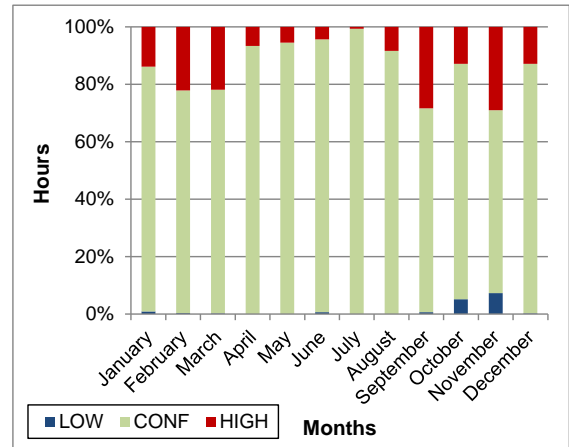


Figure 6.7 - Hourly thermal acceptance in the optimized building model with DSF in bioclimatic zone 2

SSF thermal performance: SSF models with window openings oriented to north/south and east/west were tested considering the prevailing wind direction. Although the east-west orientation case presented slightly higher levels of cold conditions due to the perpendicular direction of wind to the building openings, the DSF and SSF models presented similar periods of comfortable conditions. The SSF cases, however, experienced a marginal increase in periods of ‘too cold’ conditions due to the less resistance to airflow through the office rooms.

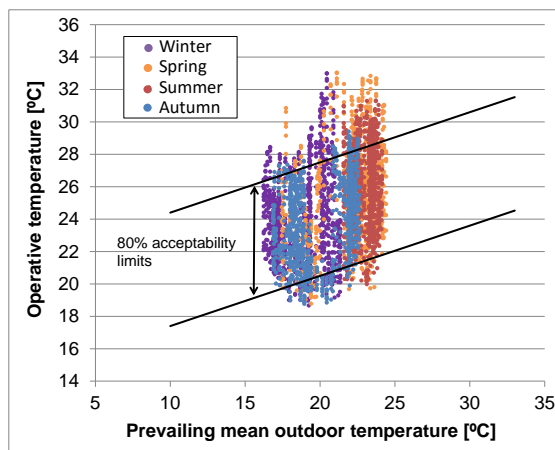


Figure 6.8 - Annual operative temperatures of single skin model under bioclimatic zone 2 plotted on the ASHRAE (2013) thermal comfort matrix

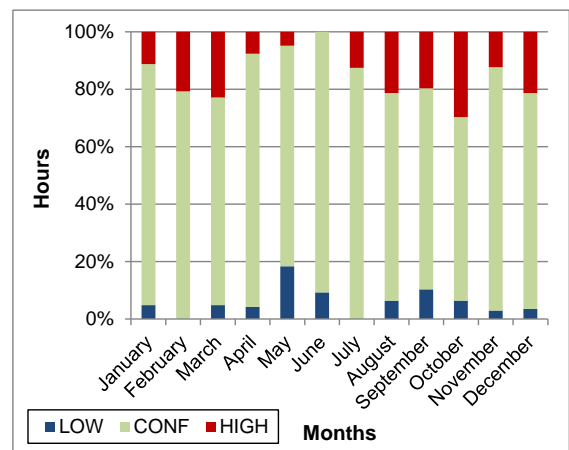


Figure 6.9 - Hourly thermal acceptance in the single skin façade building model in bioclimatic zone 2

Outcomes: The enhancement in airflow when the DSF was oriented protected from the prevailing wind direction was not effective in improving the thermal comfort

because the west orientation provided higher solar heat gains into the offices. As discussed in section 5.5, due to the fixed configuration of shading device applied in the model and the difficulty of sun protection under low solar altitudes, solar protection cannot be fully guaranteed in the offices. Therefore, an effective solar protection would, not only enhance the stack effect in the cavity, but also avoid solar heat gains in the office, which may improve the acceptance levels in this bioclimatic zone.

Table 6.2 – Summary of thermal acceptance conditions of cases under bioclimatic zone 2

Façade type	Orientation	Window profile operation applied	Thermal acceptance (%)		
			Too cold	Comfortable	Too hot
DSF	North	Yes	2	84	14
	West	Yes	1	80	19
SSF	North/South	Yes	6	78	16
	East/West	Yes	10	78	13

6.4 Bioclimatic zone 3 – Florianopolis

General climate characteristics: Florianopolis is characterized by mild and low temperatures in the summer and winter, respectively, with the dominant wind direction being from north. During the summer, cross ventilation is the main passive strategy suggested, while in winter, solar gains are required to keep the indoor environment thermally comfortable.

DSF proposed: Considering these climatic characteristics, the optimized model was simulated with DSF oriented to north as it not only is the most effective orientation to improve stack effect during the day, but it does not prejudice the needed cross ventilation, as the prevailing wind direction reinforces the cavity stack effect. Considering the mild climate conditions of the winter season, two cases with and without windows opening control applied to the south windows were tested in order to evaluate whether the airflow resistance created by the DSF was enough to avoid moments of too cold conditions.

DSF thermal performance: The case which south windows remain open the whole time presented 17% of uncomfortable hours due to cold conditions more than the case with windows control. This demonstrates the importance of regulating the airflow through to the offices in this climate. Figure 6.10 presents the operative temperatures for the case in which the opening profile was applied to the south windows. The model achieved acceptable thermal comfort conditions in 92% of occupied hours. Most of the discomfort moments are due to hot conditions, which account for 7% of time, occurring mostly in January and February, as can be seen in Figure 6.11.

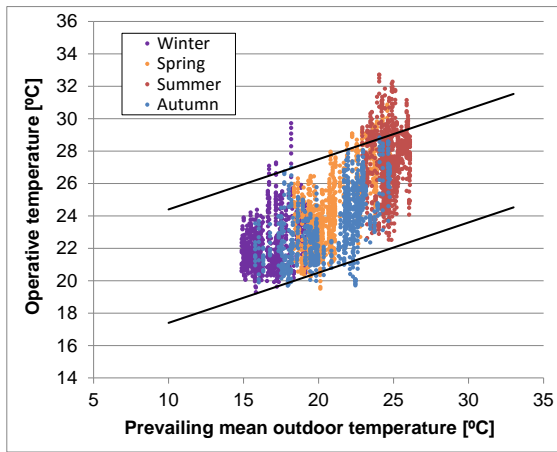


Figure 6.10 - Annual operative temperatures of optimized model under bioclimatic zone 3 plotted on the ASHRAE (2013) thermal comfort matrix

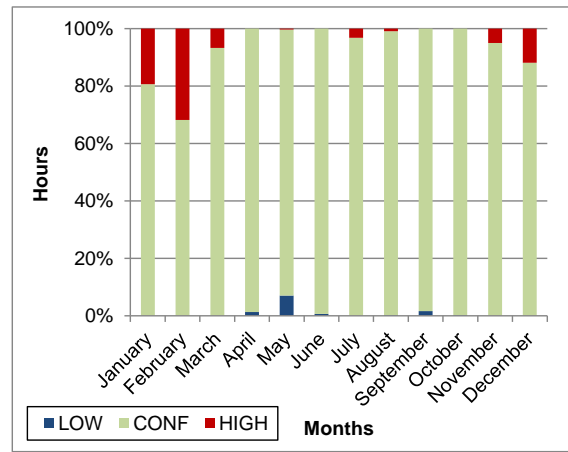


Figure 6.11 - Hourly thermal acceptance in the optimized building model with DSF in bioclimatic zone 3

SSF thermal performance: Figure 6.12 presents the operative temperatures for the SSF model, in which the same opening profile applied to the optimized model was set to both north and south windows. The results show that in 18% of the time, the office spaces are in thermal discomfort, being 16% due to 'too cold' conditions. Percentages of cold periods higher than 20% of time are experienced from September to November (Figure 6.13). In these months, in 13% of time, air speeds, which were calculated from the net airflow in the office space, are higher than 0.8m/s. This is the maximum air speed recommended by ASHRAE (2013) for office spaces, as it might blow papers on the desks. The windows opening area in IESVE cannot be controlled according to the thermal zones air speed. Therefore, the results may not correspond to a real situation.

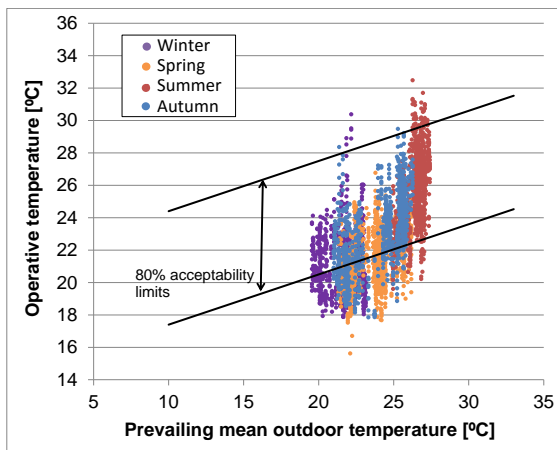


Figure 6.12 - Annual operative temperatures of single skin model under Bioclimatic zone 3 plotted on the ASHRAE (2013) thermal comfort matrix

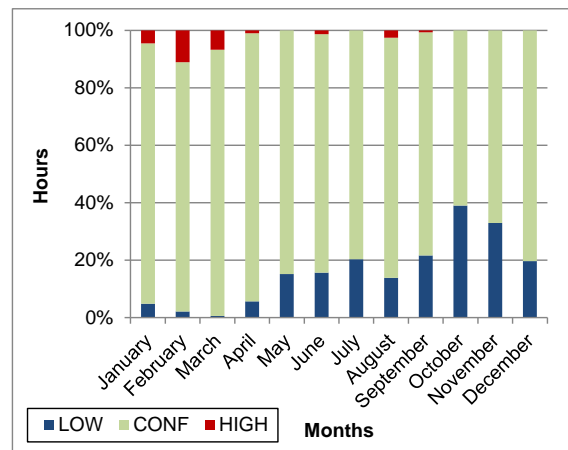


Figure 6.13 - Hourly thermal acceptance in the single skin façade building model in bioclimatic zone 3

Outcomes: The implementation of DSF combined with a control of openings appears as a satisfactory strategy for bioclimatic zone 3, as it increased the annual thermal comfort conditions by 17% in relation to the case which windows are fully open the whole time. In relation to a SSF case, the model with DSF proved to deliver approximately 10% more periods of comfortable temperatures, as shown in Table 6.3 that compares the thermal acceptance levels for the cases tested under bioclimatic zone 3. Thermal acceptability can be achieved in 92% of the year with the application of DSF, with uncomfortable periods due too hot conditions occurring mainly between January and February.

Table 6.3 – Summary of thermal acceptance conditions of cases under bioclimatic zone 3

Façade type	Orientation	Window profile operation applied	Thermal acceptance (%)		
			Too cold	Comfortable	Too hot
DSF	North	No	18	75	7
	North	Yes	1	92	7
SSF	North	Yes	16	81	2

6.5 Bioclimatic zone 4 – Brasilia

General climate characteristics: Brasilia presents mild climatic conditions over the year with an average temperature of 22.8°C. The dominant wind is from east and in 35% of the time the city presents low wind speeds; hence stack effects will dominate the pressure distribution in the building. It experiences a relative low humidity, 75% on average, which drops to 63% during the winter, when passive heating is typically recommended. During the summer, cross ventilation is effective in 32% of the time.

DSF proposed: Based on general climatic characteristics, a model with DSF facing north was tested in order to take advantage of the stack effect to promote natural ventilation in the building, considering the low wind speeds characteristics of the city. Different from the models performed for bioclimatic zones 1 to 3, this model was set without any window opening control, since the predominant wind is parallel to the window openings and temperatures in winter are not extremely low. Additionally, as the predominant wind direction is from the east, another case in which the DSF is facing west was tested, in order to take the maximum advantage of the available wind conditions. In this case, as the wind is perpendicular to the windows, openings profile for the windows opposite to the DSF were applied in order to avoid high airflow rates through the user space during moments of temperatures lower than 16°C, which occur in 13% of the year.

DSF thermal performance: The resulting thermal acceptance conditions of both cases tested are similar. The case with DSF facing north presented 84% of annual thermal

acceptance, 3% higher than the case with west DSF. The west DSF presented higher levels of discomfort due 'too hot' conditions, which can be explained by the highest levels of solar heat gains during the afternoons. Figure 6.14 and Figure 6.15 present the annual operative temperatures and the hourly thermal acceptance for the case in which DSF is facing west. Although uncomfortable temperatures are experienced all over the year, the spring season presents the highest levels of uncomfortably hot conditions.

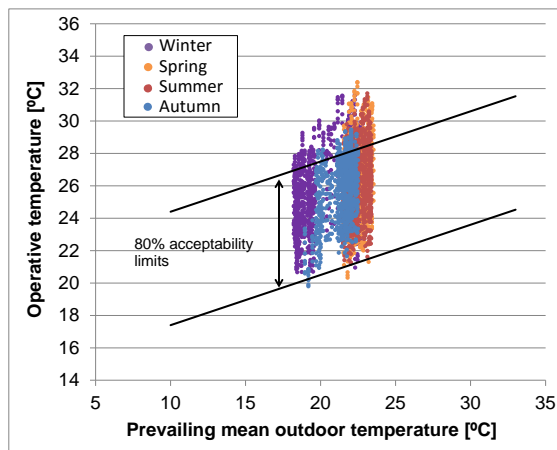


Figure 6.14 – Annual operative temperatures of optimized model under 'Bioclimatic zone 4' plotted on the ASHRAE (2013) thermal comfort matrix

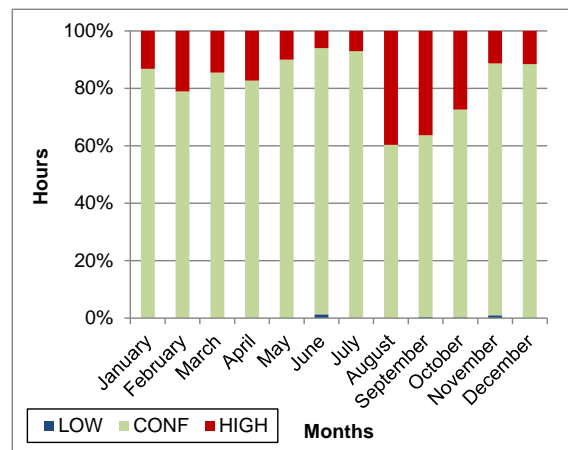


Figure 6.15 - Hourly thermal acceptance in the optimized building model with DSF in bioclimatic zone 4

SSF thermal performance: In order to compare the differences in thermal comfort conditions regarding the wind direction when using SSF, two cases with windows oriented to north/south and east/west were tested and results indicate that both cases presented similar thermal conditions. As the city experiences low wind speeds, the application of windows perpendicular to the dominant wind did not improve thermal comfort conditions during the hottest days. Those cases presented similar percentages of thermal performance to the case in which DSF is facing north (Figure 6.16). The single skin case presented 85% of hours of thermal acceptance, being August and September the most uncomfortable periods (Figure 6.17).

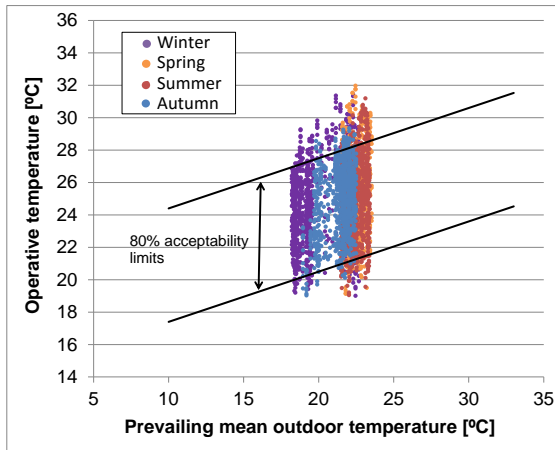


Figure 6.16 – Annual operative temperatures of single skin model under Bioclimatic zone 4 plotted on the ASHRAE (2013) thermal comfort matrix

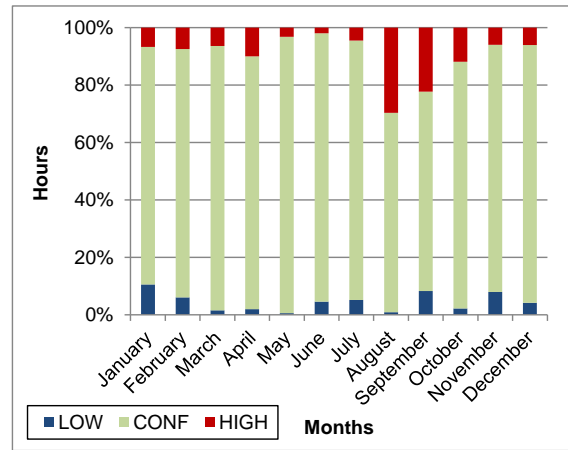


Figure 6.17 – Hourly thermal acceptance in the single skin façade building model in bioclimatic zone 4

Outcomes: Table 6.4 summarizes the thermal acceptance levels resulting from the cases simulated under bioclimatic zone 4. The DSF models presented similar thermal performance to the model with SSF. Although when DSF was oriented to west, the airflow rates were in average 11% higher than when it was facing north, the high solar heat gains in the afternoons decrease the thermal acceptability in the building. Due to the high number of periods of low or zero wind speeds, in which the buoyancy effect of the DSF will be the main ventilation driver in the building, and the higher levels of solar heat gains when glazing areas are facing west, north facing presented to be an adequate orientation for the DSF, when considering its application to Brasilia.

Table 6.4 – Summary of thermal acceptance conditions of cases under bioclimatic zone 4

Façade type	Orientation	Window profile operation applied	Thermal acceptance (%)		
			Too cold	Comfortable	Too hot
DSF	North	No	5	84	11
	West	Yes	0	81	18
SSF	North/South	Yes	5	85	10
	East/West	Yes	6	84	10

6.6 Bioclimatic zone 5 – Niteroi

General climate characteristics: Niteroi is characterized by high and mild temperature in the summer and winter, respectively. The lowest temperatures occur in September, when the monthly average drops to 19.5°C. The city presents a high relative humidity, with monthly averages varying from 70% to 80%. Those characteristics indicate cross natural ventilation as a passive strategy to be applied during the whole year, especially during summer, when the predominant wind direction is from south.

DSF proposed: To take advantage at both the wind and stack effects, a model with DSF oriented to north was tested in order to meet the demands for cross ventilation all over the year. Since the predominant wind is perpendicular to the window openings, automated windows opening control according to the outside temperature was applied in order to avoid discomfort during the coldest days.

DSF thermal performance: The model presented 92% of annual thermal acceptance (Figure 6.18). The uncomfortable moments due to too hot conditions occur mainly during January and February, as shown in Figure 6.19, although unacceptable temperatures resulted for only 15% of the time during the summer (from December to March). September is the month with the highest levels of uncomfortable conditions, which reaches approximately 12% of the time due to the lowest temperatures experienced during the period.

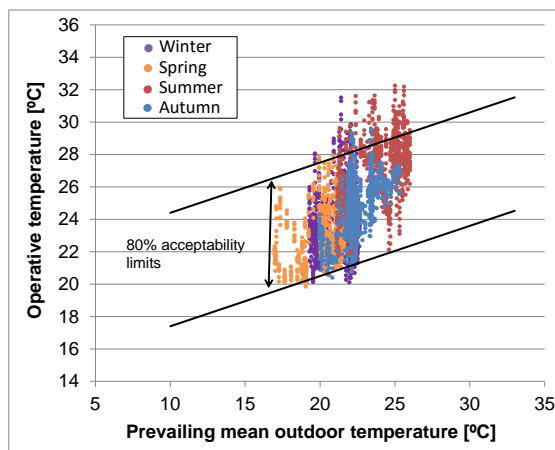


Figure 6.18 – Annual operative temperatures of optimized model under 'Bioclimatic zone 5' plotted on the ASHRAE (2013) thermal comfort matrix

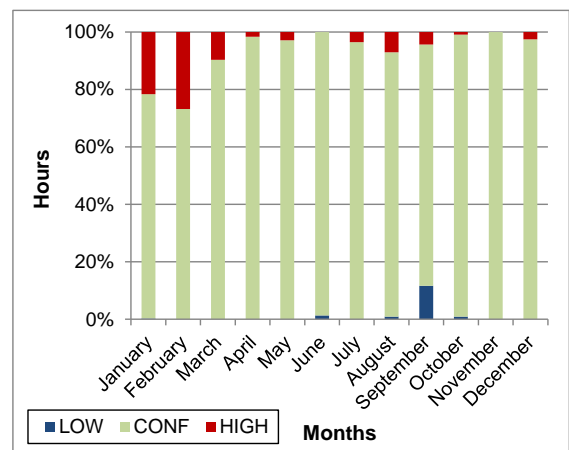


Figure 6.19 - Hourly thermal acceptance in the optimized building model with DSF in bioclimatic zone 5

SSF thermal performance: The SSF model presented 85% of acceptable temperatures (Figure 6.20 and Figure 6.21). Although the case was modelled with widows opening control profile to avoid high levels of airflow under cold conditions, it presented 10% more hours in uncomfortable conditions due low temperatures than the DSF case, as shown in Table 6.5.

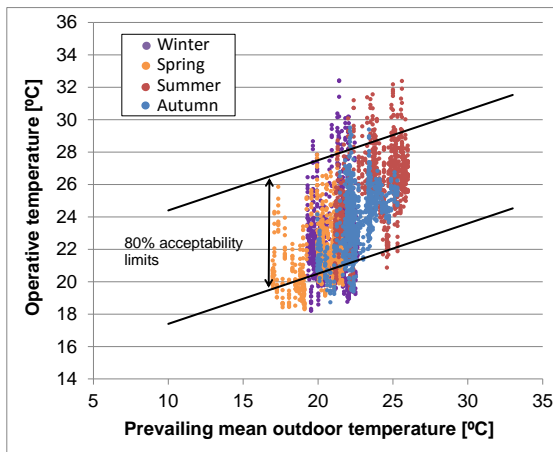


Figure 6.20 – Annual operative temperatures of single skin model under Bioclimatic zone 5 plotted on the ASHRAE (2013) thermal comfort matrix

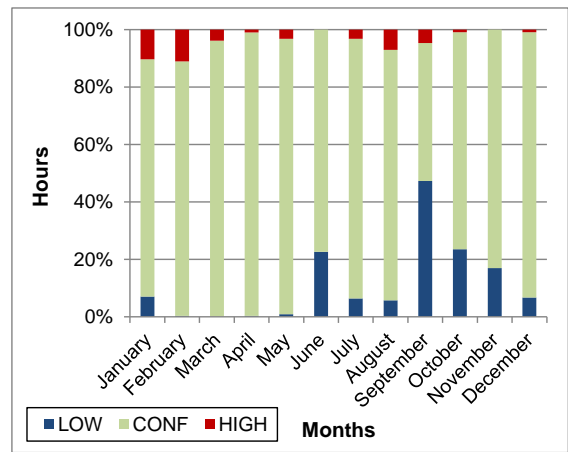


Figure 6.21 – Hourly thermal acceptance in the single skin façade building model in bioclimatic zone 5

Outcomes: The application of DSF decreases the uncomfortable periods due to too cold conditions, but marginally increased moments of ‘too hot conditions’. This indicates that the application of DSF is an optional solution regarding thermal comfort conditions to be applied under bioclimatic zone 5, where thermal comfort can be achieved in more than 90% of the year.

Table 6.5 – Summary of thermal acceptance conditions of cases under bioclimatic zone 5

Façade type	Orientation	Window profile operation applied	Thermal acceptance (%)		
			Too cold	Comfortable	Too hot
DSF	North	Yes	1	92	7
SSF	North	Yes	11	85	4

6.7 Bioclimatic zone 6 – Campo Grande

General climate characteristics: The representative city of bioclimatic zone 6 is characterized by high temperatures, with annual mean of 26 °C, combined with low relative humidity over the year, 68% in average. Natural cross ventilation and evaporative cooling are the main passive strategies indicated. In Campo Grande, the dominant wind directions are mostly divided between from north and east.

DSF proposed: To combine the benefits of the ventilation promoted by buoyancy effect of the DSF and the wind pressures, a case with DSF oriented to north was tested. Additionally, a model with DSF oriented to south was also evaluated as the ventilation is improved when DSF is at the leeward side of the wind direction. Although there is a considerable prevalence of wind directions from east, a case with DSF on the west facing of the buildings was discarded in order to avoid high solar heat gains during the hottest periods of the day, considering the high temperatures experienced

by the city. In both models simulated, no windows opening profile were applied due to the climate conditions experienced in this city and night time ventilation was considered.

DSF thermal performance: Although similar thermal acceptance levels, of approximately 57%, were resulted for the orientations tested, the model with DSF facing south presented 5% more uncomfortable temperatures due too hot conditions than the case with DSF oriented to north. When DSF is south oriented, the wind forces are the main ventilation driver through the building, whereas when the DSF is north oriented, not only the DSF stack effect drives the airflow, but there is also a contribution from wind effects. Additionally, the south oriented DSF may have higher solar heat gains through the windows opposite to the DSF, which may contribute to the increasing of temperature in the offices. Figure 6.22 shows the plotted annual operative temperatures according to the seasons when DSF is north oriented. The moments of discomfort by excessive heat account for 35% of time with the lowest unpleasant time occurring from May to July, as shown in Figure 6.23.

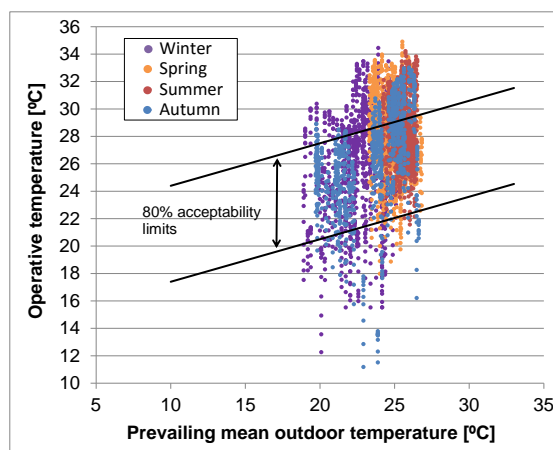


Figure 6.22 – Annual operative temperatures of optimized model under ‘Bioclimatic zone 6’ plotted on the ASHRAE (2013) thermal comfort matrix

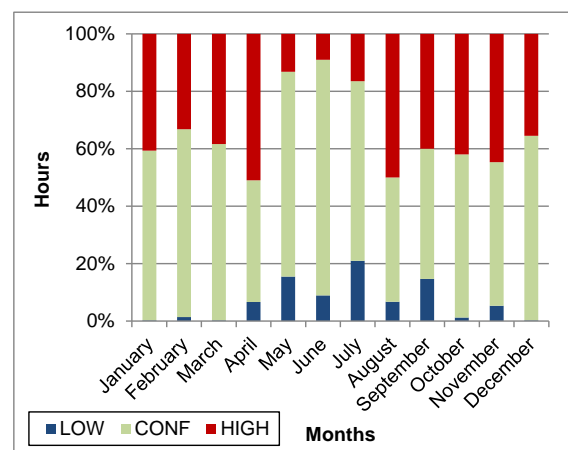


Figure 6.23 – Hourly thermal acceptance in the optimized building model with DSF in bioclimatic zone 6

SSF thermal performance: Enhanced acceptance levels were resulted from the SSF case in comparison to the DSF model. Discomfort due to ‘too hot’ conditions increases approximately 10% with the application of DSF, which can be explained by the decrease in air speed in the room due to greater air resistance promoted by the application of the second skin.

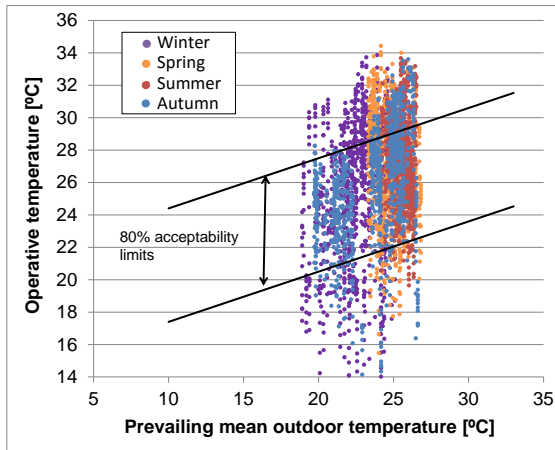


Figure 6.24 – Annual operative temperatures of single skin model under Bioclimatic zone 6 plotted on the ASHRAE (2013) thermal comfort matrix

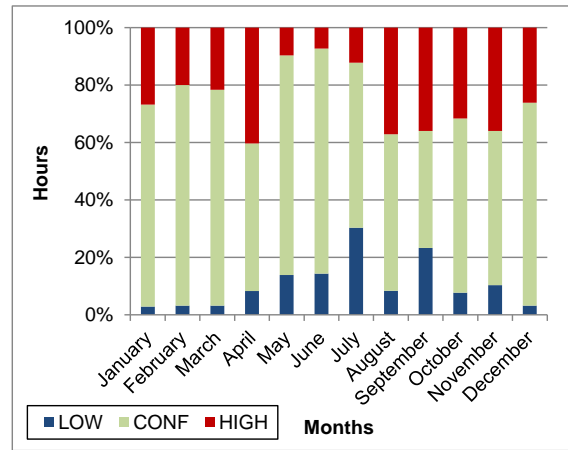


Figure 6.25 – Hourly thermal acceptance in the single skin façade building model in bioclimatic zone 6

Outcomes: Table 6.6 shows the thermal acceptability of the cases simulated. Although the application of DSF provides positive aspects to the building thermal conditions, such as the promotion of shade on the north facing and enhancement of air speeds during calm conditions, the free cross ventilation allowed in the SSF case presented better results for the model applied under the bioclimatic zone 6. Considering the low relative humidity of the city, the application of DSF combined with an evaporative cooling strategy may improve the thermal acceptance levels.

Table 6.6 – Summary of thermal acceptance conditions of cases under bioclimatic zone 6

Façade type	Orientation	Window profile operation applied	Thermal acceptance (%)		
			Too cold	Comfortable	Too hot
DSF	North	No	7	58	35
	South	No	5	55	40
SSF	North	No	11	63	26

6.8 Bioclimatic zone 7 – Picos

General climate characteristics: Picos, situated in the hot and arid region of the north-east, experiences temperatures above 31°C in 33% of the year and low annual relative humidity, 57% in average. Although natural ventilation may improve thermal comfort in some moments of the year, air conditioning is highly recommended, especially during spring and summer seasons when the prevailing wind is from the east.

DSF proposed: A case with DSF facing north was tested with the view that the stack effect ventilation is promoted by the DSF. Cases with DSF oriented to east or west were discarded to avoid glazing areas on those orientations, as it would increase solar

heat gains into the office rooms. In the model, all windows remain open the whole year (including night time) and shading devices are always on.

DSF thermal performance: Figure 6.26 and Figure 6.27 show the results for the case with DSF. Acceptance levels of only 20% were achieved in the model and no cold conditions were indicated due to the extremely high outside temperatures throughout the year.

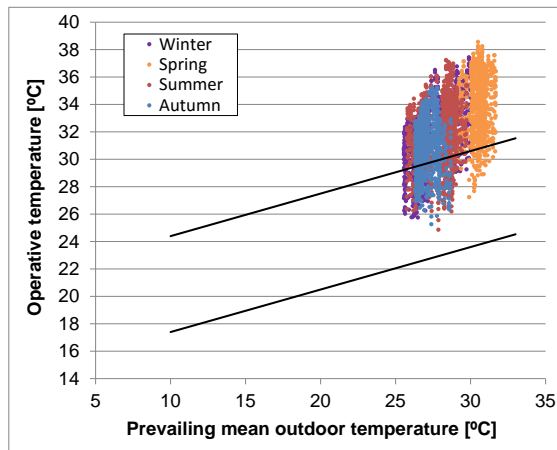


Figure 6.26 – Annual operative temperatures of optimized model under bioclimatic zone 7 plotted on the ASHRAE (2013) thermal comfort matrix

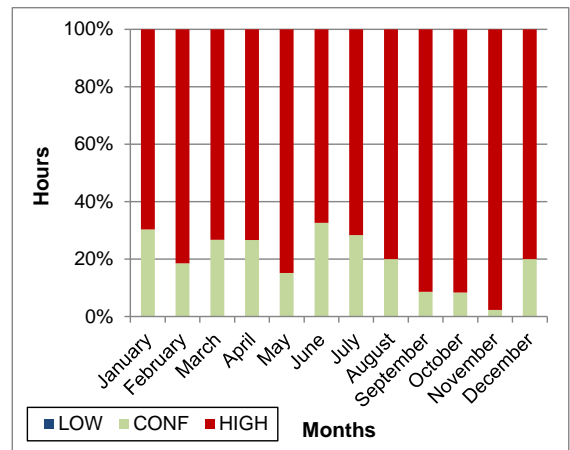


Figure 6.27 – Hourly thermal acceptance in the optimized building model with DSF in bioclimatic zone 7

SSF thermal performance: The single skin model presented slightly better results as comfortable periods are indicated in 24% of the year. Higher levels of free ventilation through the offices result in a decrease in the operative temperatures experienced by users.

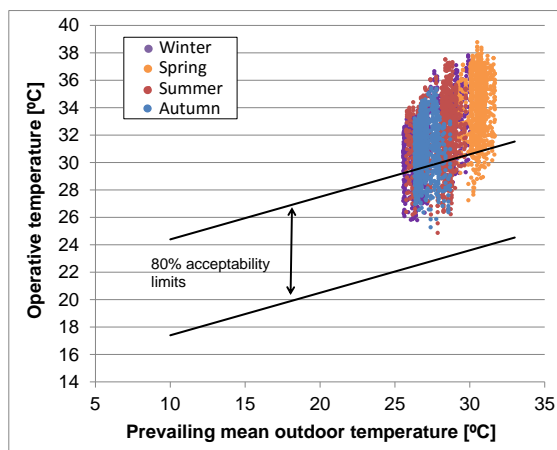


Figure 6.28 – Annual operative temperatures of single skin model under bioclimatic zone 7 plotted on the ASHRAE (2013) thermal comfort matrix

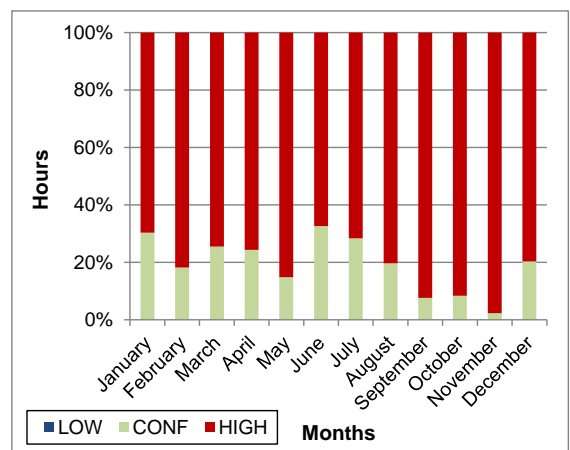


Figure 6.29 – Hourly thermal acceptance in the single façade skin building model in bioclimatic zone 7

Outcomes: The models under bioclimatic zone 7 presented the lowest thermal acceptability throughout the year showing inappropriate conditions for the use of naturally ventilated buildings. Due to the low relative humidity experienced by this city, it is possible that the application of evaporative cooling may be effective in improving thermal comfort during some periods of the year.

Table 6.7 – Summary of thermal acceptance conditions of cases under bioclimatic zone 7

Façade type	Orientation	Window profile operation applied	Thermal acceptance (%)		
			Too cold	Comfortable	Too hot
DSF	North	No	0	20	80
SSF	North	No	0	24	76

6.9 Bioclimatic zone 8 – Rio de Janeiro

General climate characteristics: Permanent and cross natural ventilation is recommended for cities in bioclimatic zone 8 due to the high temperatures and high levels of humidity. The Rio de Janeiro city presents annual mean temperature of 27°C and natural ventilation is considered to be effective in 61% of the time throughout the year, reaching a peak of 85% in October.

DSF proposed: Considering the variability of wind directions, a case with DSF facing north was tested in order to take advantage of stack effect promoted by the DSF. The model was set with windows open day and night time and shading devices always on.

DSF thermal performance: The model presented 71% of thermal comfort (Figure 6.30 and Figure 6.31) with the lowest acceptance levels occurring from January to March, when the discomfort due to too hot conditions reaches more than 60%.

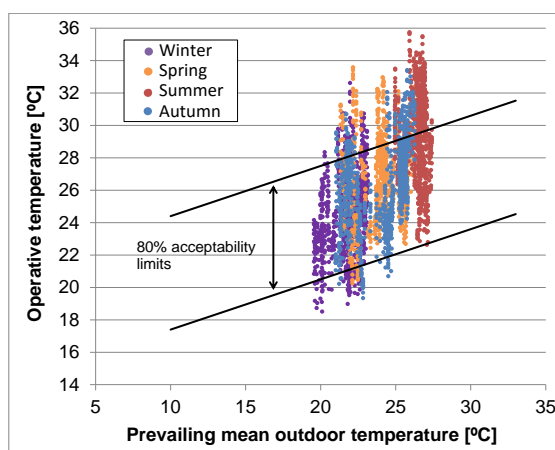


Figure 6.30 - Annual operative temperatures of optimized model under 'Bioclimatic zone 8' plotted on the ASHRAE (2013) thermal comfort matrix

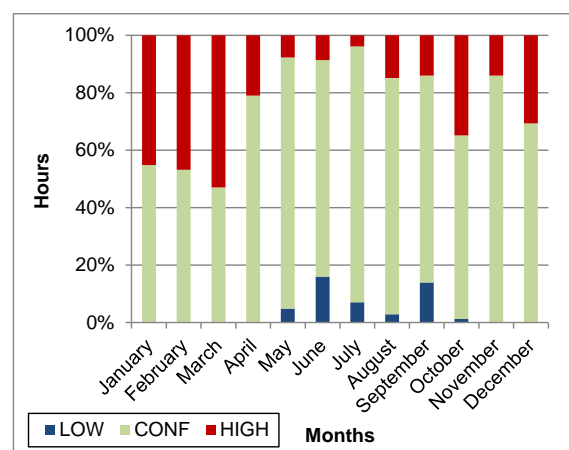


Figure 6.31 - Hourly thermal acceptance in the optimized building model with DSF in bioclimatic zone 8

SSF thermal performance: SSF case (Figure 6.32 and Figure 6.33) presented similar periods of comfortable hours to the case with DSF. Considering the critical hot moments, SSF proved to be thermally slightly better as it presented 5% reduction in periods of unpleasantly hot temperatures.

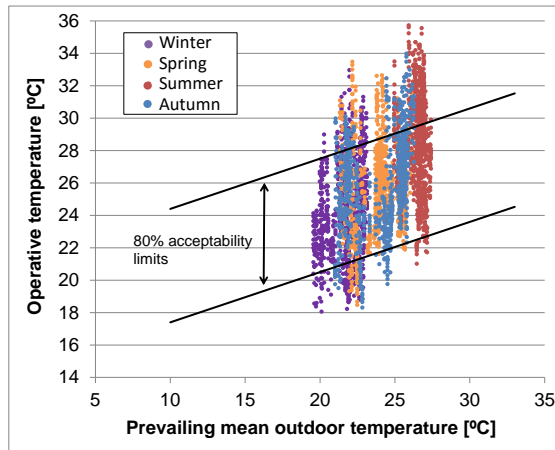


Figure 6.32 - Annual operative temperatures of single skin model under bioclimatic zone 8 plotted on the ASHRAE (2013) thermal comfort matrix

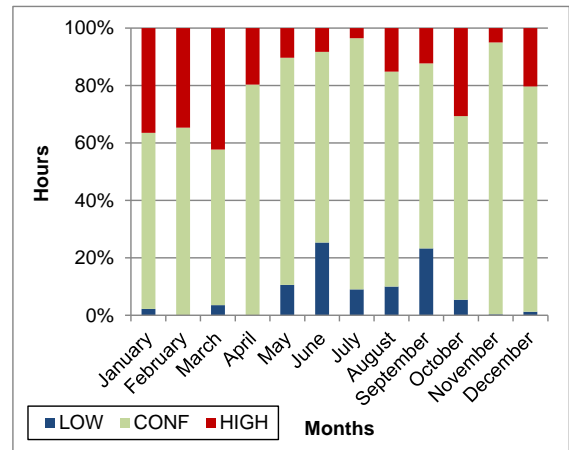


Figure 6.33 - Hourly thermal acceptance in the single skin building model in bioclimatic zone 8

Outcomes: Table 6.8 presents the thermal acceptability of cases with and without DSF under bioclimatic zone 8. Those results indicate that the application of DSF provides similar comfort conditions as a SSF model when operating under bioclimatic zone 8. The DSF case presented more hours of ‘too hot’ conditions, while the SSF case presented more moments of ‘too cold’ conditions.

Table 6.8 – Summary of thermal acceptance conditions of cases under bioclimatic zone 8

Façade type	Orientation	Window profile operation applied	Thermal acceptance (%)		
			Too cold	Comfortable	Too hot
DSF	North	No	4	71	25
SSF	North	No	8	72	20

6.10 Chapter summary and remarks

Table 6.9 summarizes the thermal acceptability levels of the cases tested, showing the design choices made for each case scenario. These definitions are based not only on the climatic characteristics describe in chapter 3, but also on the findings and outcomes from chapter 5 which show the influence of the design and site parameters on the thermal performance of naturally ventilated building with DSF.

Table 6.9 – Summary of thermal acceptance conditions of all cases under all bioclimatic zones

Zone	Façade type	Orientation	Window profile operation	Thermal acceptance (%)		
				Too cold	Comfortable	Too hot
1	DSF	North	Yes	8	89	3
		North (no shading device)	Yes	5	90	5
	SSF	North/ south	Yes	20	77	3
2	DSF	North	Yes	2	84	14
		West	Yes	1	80	19
	SSF	North/south	Yes	6	78	16
		East/west	Yes	10	78	13
3	DSF	North	No	18	75	7
		North	Yes	1	92	7
	SSF	North/south	Yes	16	81	2
4	DSF	North	No	5	84	11
		West	Yes	0	81	18
	SSF	North/south	Yes	5	85	10
		East/west	Yes	6	84	10
5	DSF	North	Yes	1	92	7
	SSF	North	Yes	11	85	4
6	DSF	North	No	7	58	35
		South	No	5	55	40
	SSF	North/south	No	11	63	26
7	DSF	North	No	0	20	80
		East	No	0	19	81
	SSF	North/south	No	0	24	76
8	DSF	North	No	4	71	25
	SSF	North/south	No	8	72	20

Results from simulations of the optimized model of naturally ventilated offices with DSF for the bioclimatic zones of Brazil indicated that thermal acceptance varies between 60% and 90% of the annual occupancy hours in the territories, except for zone 7, where acceptance level is approximately 20% over the year. This demonstrates that for significant portions of the year, the DSF can provide comfortable indoor conditions without any need for mechanical heating or cooling. Apart from zone 7, the lowest thermal acceptance levels occur mainly in regions of centre-west, north-west and coastal areas, characterized by cities located in the bioclimatic zones 6 and 8. On the other hand, the highest satisfactory thermal conditions are experienced by south and southeast regions. Figure 6.34 presents the levels of acceptability of DSF projected for all regions based on the climatic zones of the whole country.

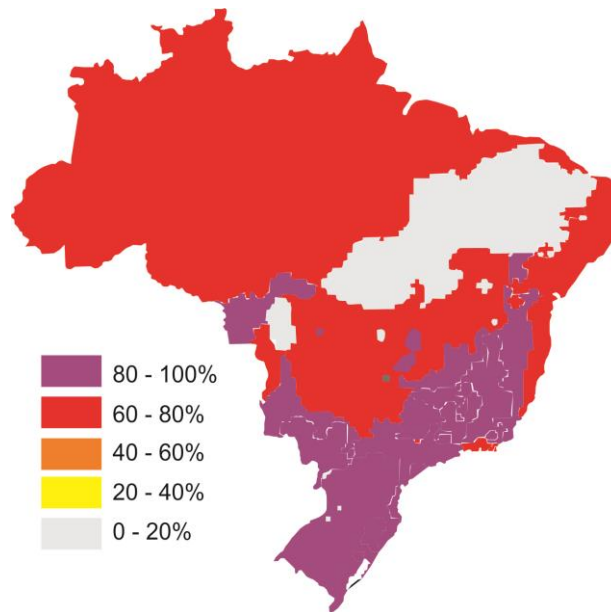


Figure 6.34 – Brazilian bioclimatic zones with indication of level of thermal acceptability

For the coldest bioclimatic zones 1, 2 and 3, the results indicate higher thermal acceptability levels for the cases with DSF when compared to SSF cases. Those levels reached up to 90% when DSF is north oriented. Better thermal conditions occur when the DSF is associated with the application of the window opening profile according to the outside temperature, which reduces the airflow when outside temperature is below set value. When defining the DSF orientation, not only the wind prevailing direction must be considered, but also the adequate solar protection, as it has a considerable influence on the likelihood of overheating during the hottest periods.

For climates with mild temperatures over the year and hot summers, as in zones 4 and 5, the single skin cases presented similar thermal acceptability to the model with DSF. This indicates that, during the hottest periods, the cooling potential of natural ventilation promoted by DSF is limited by the warm air temperature entering the building. Under hot conditions, although little or no improvements in terms of thermal performance may be achieved with the addition of the second skin, it does not negatively affect the thermal conditions when compared to a single skin case.

In hot and tropical climates of zones 6 and 8, the models presented thermal acceptance levels of around 65%, which can be explained by periods of high temperatures occurring all the year. Although night time ventilation, shading devices and fully open south windows were included, these cases presented slightly lower thermal acceptability when compared to single skin models. For the uncomfortable periods, additional mechanical ventilation within the DSF cavity may improve the airflow through the offices and improve the thermal comfort under these conditions.

As weather files are often based on data measured from open spaces, it is important to consider that temperatures may vary in urban central areas, which tend to experience higher temperatures due to the nature of materials usually applied to buildings and roads. Additionally, street canyons may modify wind magnitude and direction and therefore, wind pressure coefficients experienced in different building faces can either pronounce or decrease the airflow through the building. Moreover, the assumptions proposed and the limitations related to the building models may not capture with accuracy the real operation of the building. Therefore, thermal acceptability percentages presented may not precisely predict the real building behaviour.

Apart from achieving a thermally comfortable environment for some periods of the year, the application of DSF can bring other benefits such as aesthetics, improved acoustics, easier maintenance and security. But it is paramount to be conscious about the thermal advantages and shortcomings resulting from its application during different season of the year and time of day.

Chapter Seven

Conclusions

This Chapter summarises and concludes the study based on reflections upon the findings. It also highlights any research limitations and proposes further studies needed to enable viable implementation of DSF under Brazilian climates.

7.1 Introduction

This thesis presents a fundamental study on the thermal performance of naturally ventilated office buildings with double skin façade (DSF) under Brazilian climate conditions. Motivated by the lack of comprehensive studies relevant to the existing and prospective DSF buildings developments in Brazil, this study aims to provide a holistic insight into the design of the technology with a focus on its application in naturally ventilated buildings.

The study identified and evaluated 9 design parameters, divided under 4 groups, affecting the thermal performance of buildings with DSF. Using a reference model of an office building, the influence of these design parameters on the building's thermal behaviour was studied making use of the capability of computational simulation. From the findings of the parametric analysis at the initial stage of the study, optimized models that exploit a combination of solutions to maximize the building thermal performance were developed and analysed. The effects of the site conditions, local solar radiation and wind availability, on the DSF and building's thermal performances were also evaluated in order to provide references for improving the functioning of the DSF. Thermal comfort levels of the optimized model in different Brazilian climate zones were established in order to determine periods of the year when satisfactory thermal acceptance can be achieved.

The following sections overview the objectives identified in Chapter 1 and discuss their accomplishments. The research contributions and impacts to the design of buildings with DSFs under Brazilian climates are also presented and the two research questions proposed are answered. Lastly, limitations identified and directions for future research are presented.

7.2 Reviewing the objectives

Discussions of the objectives accomplished are presented below:

Objective 1: *To differentiate the characteristics of the Brazilian climates and to identify the corresponding thermal comfort requirements in naturally ventilated office buildings.*

An overview of different climate conditions in the Brazilian territories is presented in Chapter 3. Analyses of 8 cities showed the contrasts among the climates, highlighting periods of the year when natural ventilation is an appropriate strategy for achieving thermal comfort conditions. Differences regarding solar radiation levels, outdoor temperatures and wind conditions of the bioclimatic zones in Brazil are also addressed.

Conclusions from the analysis indicate that maximization of airflow rates through the building is a fundamental strategy to increase thermal acceptance in many regions. In the hot and arid region of the north-east and coastal areas, natural ventilation is recommended for the whole year, reaching up to 85% of the time during the summer. In the centre west region, it is applicable from September to April, while in the south and some parts of southeast regions, the passive strategy is only limited to the summer periods.

The ASHRAE 55 (2013) adaptive standard method was identified as a suitable indicator for predicting the indoor thermal performance of naturally ventilated buildings under Brazilian climate conditions. The method used data derived from simulations performed in the IESVE software. The network airflow algorithm used was demonstrated as an appropriate method to predict the airflow effects of the naturally ventilated building with DSF and to comparatively evaluate design alternatives.

Objective 2: *To develop a reference model of a naturally ventilated office building appropriate for the DSF application.*

The definition and justification of the characteristics of a computational base case building model is presented in Chapter 4. Building geometry and dimensions, internal layout, heat gains and fabric materials are based on topology studies of non-residential buildings, on the construction practice of Brazil and on the recommendations for naturally ventilated buildings. The model comprises an 11 storey open plan office building with dimensions of 12 x 16m and 3.5m floor-to-floor height. The longest sides face north/south orientations and the DSF was applied to the north facing.

Objective 3: *To identify and evaluate the key parameters governing the building thermal performance.*

A critical review of the state of the art of current body of literature on experimental and computational simulation studies about the thermal performance of DSF, presented in Chapter 2, identified the key design and site parameters affecting the system behaviour. Three groups of parameters were identified as having significant impacts on the building performance: the 'façade' parameters, the 'building' parameters and the 'site' parameters. The review established a set of assumptions for the design of naturally ventilated buildings with DSF in warm areas, which contributed to the development of the building model and the identification of the key parameters affecting the building thermal performance. Results from the base case scenario also

contributed to the identification of the alternative scenarios, as they revealed the performance constraints and potential improvements to the building model with DSF.

Influences of the identified design and site parameters on the building thermal behaviour were evaluated through parametric analysis and presented in Chapter 5. Airflow magnitude and pattern across all floors of the building indicated the improvements of the alternative cases in relation to the reference model. Dimensional parameters that maximise the system airflows were defined and the significance of material selections and design decisions were investigated. Resilience of the optimized model under different building dimensions was also evaluated establishing the influence of height and depth of the building on the DSF's thermal performance. The influence of solar incidence and wind conditions on the DSF heat transfer and airflow mechanisms was also evaluated demonstrating the impact of local environmental conditions on its thermal performance.

Objective 4: *To develop optimized naturally ventilated building models with DSF to operate under Brazilian climatic conditions.*

Based on the findings of the parametric analysis, optimized models that utilise a combination of solutions to maximize the building thermal performance were developed and analysed in Chapter 5. These models were configured to maximize the absolute flow rates while resolving the reverse flow through the upper floors and attaining even airflows at each floor level.

Objective 5: *To establish the annual thermal comfort acceptability of an optimized model under different Brazilian climates.*

Thermal comfort levels of the defined optimized building model under different Brazilian climate conditions at different periods of the year were established. Periods of thermal acceptance, examined using the adaptive comfort criteria of different regional and seasonal variations in Brazil were examined and presented in Chapter 6.

7.3 Research contributions and impacts

The contribution and impacts are highlighted through addressing the research questions set out at the start of this research, as described below.

What are the influences of architectural configurations and external climates on the thermal performance of naturally ventilated office buildings with DSF?

The results showed that one of the strategies that most influences the performance of the DSF in naturally ventilated buildings is the application of shading device within it. The application of high thermal mass materials on the shading devices within the cavity not only contributes to the reduction of solar heat gains to the rooms, but it also improves the heat absorption enhancing the buoyancy effect created by the air within the DSF. Option to avoid reverse airflow occurring on the upper floors also proved to have great influence in raising the NPL above the window openings such as extending the cavity above the building roof and adjusting the openings of windows on the upper floors. The solutions tested to balance airflow rates across each building level provided a greater understanding of air balancing effect on the building's thermal performance. Innovative features studied included inclining the outer DSF skin outwards from the bottom to the top created relatively even airflow rates on the floors. Another tested option is to balance airflow rates through adjusting windows sizes according to their position relative to the building height, opening areas and cavity configuration. Other solutions, although less effective, to improve the building thermal performance were investigated, they included the application of wider cavities, use of reflective glazing on the inner skin and reposition of windows apertures.

The local environmental conditions also proved to have a substantial impact on the overall performance of the DSF. The magnitude and angle of solar incidence reaching the façade determined the increase of temperature within the cavity in relation to the outside air. The ability of the DSF to influence the solar energy captured defines the levels of airflow that can be drawn from the building to the cavity, especially at low or null wind speeds. On the other hand, the airflow of the system is influenced by the wind pressures created around the building surfaces, which may enhance the effectiveness of the stack effect if DSF is correctly applied to exploit such effects.

To what extent will naturally ventilated office buildings with DSF meet the thermal comfort requirements in different climate regions of Brazil?

Based on the results of the thermal acceptance levels of naturally ventilated buildings with DSF in Brazil, three distinct demarcations have been identified as dominating the territories. Firstly, for the regions with 0-20% acceptance levels, mainly present in the hot arid region in the northeast, the DSF may be incorporated in buildings that are fully air-conditioned and the use of natural ventilation will have very little benefit. Secondly, for the regions with 60-80% acceptance levels, located in centre-west, coastal areas and north of the country, the DSF can maintain thermal comfort during the cooler seasons. On the other hand, during the hot seasons, the cases with DSF presented slightly lower thermal acceptability when compared to single skin models and therefore,

this technology will not benefit the building thermal performance. In this case, adoption of mixed mode ventilation strategies in which the DSF will operate in conjunction with the air-conditioning system will be necessary. Thirdly, there are regions in the south where the thermal acceptance levels are above 80% and can be as high as 90%. In these cases, moments of too cold or too hot conditions can be mitigated by a mixed mode ventilation strategy but there are also possibilities of applying other design options – depend on the site and building design - such as use of living plants, wind catcher and phase change thermal storage, to eliminate the reliance on air-conditioning.

The hypothesis defined in Chapter 1 - **Enhancing the natural ventilation through the suitably applied double skin façade can improve the thermal performance of office buildings under Brazilian climates** – is invalid for a majority of areas in Brazil. In the tropical areas of the country, the building thermal performance did not prove to enhance with the application of the double skin façade. Although the DSF works as a thermal chimney promoting air movement under low wind speeds, the solution was not able to improve the building thermal performance in most part of the year. This is due to the high outside temperatures and the airflow resistance caused by the application of the second skin. Therefore, a conventional single skin façade is more appropriate.

DSFs are promoted through the internationalization of design solutions of large corporate buildings that have a tendency in highlighting their positive aspects. Such design feature is often seen as a strategy with potential to reduce energy demands and to improve buildings' overall thermal performance. The motivation for iconic and 'green' image interests has stimulated the use of DSF. However, the performance of a naturally ventilation building could be enhanced even with the application of conventional, simpler and less costly strategies such as the use of shading devices, adequate openings and appropriate fabric materials. In conclusion, DSFs in naturally ventilated buildings under Brazilian climates generally presented lower thermal acceptability when compared to their single skin counterparts; the limited benefits to the thermal performance alone can therefore not fully justify their applications.

7.4 Limitations of the research

Assumptions made on the modelling and simulations processes and shortcomings of the research are acknowledged in this section.

Computational simulation tool - Although the resulting airflow profile of the thermal dynamic simulation software IESVE has demonstrated to be similar to the CFD models,

the computational simulation has its limitations for this study. Possible inconsistencies between the simplified computational model and a real building cannot be precisely captured by the software. The complex multiple and random driving forces acting on the building envelope may compromise the prediction of the thermal behaviour of a real building. Additionally, although the multi-zone airflow network approach demonstrated to be a viable tool to predict the relative performance of design alternatives, it assumes uniform temperature distribution and fully mixing air in the thermal zone. This also generates uncertainties regarding the 'micro' airflow and heat transfer mechanisms within the building and the façade.

Simulation assumptions - Irregular occupancy and utilization of lighting and office equipment throughout the day were not considered in the simulations. These are dynamic variables that may affect internal gains and the heat transfer interactions between the building and the façade. Furthermore, the increment of general or local mechanical ventilation on the hottest days would possibly increase the airflow rates and therefore increase thermal acceptability in the rooms.

Climate assumptions - Regarding the evaluation of thermal acceptance in different Brazilian climates, those assessments were carried out using weather data of only one city of each bioclimatic zone. However, due to the large extension of the Brazilian territory and the low number of climatic zones, the diversity in climate conditions may not be well reflected and simulations using specific climatic data would be required for more precise results.

Thermal comfort criteria - The adoption of an international standard to assess the thermal performance of buildings may not fully meet the Brazilian requirements considering the diversity of climate conditions, social and economic aspects.

7.5 Directions for future research

This research has attempted to cover an appropriate scope to produce valuable outcomes in the application of double skin façades with natural ventilation in warm and tropical climate conditions. However, due to the complexity of the issues involved in this topic, many areas of research could be further studied contributing to the understanding of the applicability of the DSF technology in the tropics, helping to reduce the energy usage by office buildings. There are described as follow:

Model refinement and additional features - Detailing of computational models is needed to provide more reliable and representative performance of the building. Finer zoning for air distribution study and an accurate design and positioning of shading

devices within the cavity may have a significant effect on the overall airflow resistances created and consequently on the resulting ventilation.

Software development and support - Although window openings control based on the internal and/or external temperatures are available in IESVE, adjusting window openings based on the thermal zone air speed would effectively indicate periods of year that users would close the windows due to high air speeds. Additionally, an output option in the software to indicate the amount of solar radiation transmitted through the layers of the DSF would improve the understating of the relationship between solar angle and transmittance in the DSF.

Experimental measurements and visualization techniques - Comparisons of computational simulations with experimental measurements of cavity and rooms of naturally ventilated buildings with DSF would increase credibility of the absolute flow rates through the system provided by the simulation software. Additionally, significant improvements on the study of airflow profiles within the cavity and recirculation phenomena close to the inner façade can be achieved with visualization technique methods of cell tests such as tracer gas method.

Extension of this study to mixed mode ventilation strategies – It will be realistic to explore the inclusion of mechanical systems operating in the building, such as the use of mechanical fan or centralized cooling plant. Incorporation of mechanical ventilation within the DSF cavity is another line of investigation that could enhance the airflow rates for moments of low solar incidence and/or inadequate wind conditions of naturally ventilated buildings. This should be arranged in such a way that the fans do not provide significant resistance to flow when the cavity is operating under the buoyancy effect only.

Building model design - Application of different window configurations on the inner DSF layer, such as the use of a bottom hang window, may contribute to maintain an uni-directional flow to prevent the recirculation phenomenon on the inner skin. A shaded atrium on the south facing side of the building could be beneficial to moderate air temperature, especially during the hottest periods. Detailing of the offices furniture and cellular partitions would further enhance details of the resulted ventilation profile within the user space.

Occupant and building interaction – In naturally ventilated buildings, occupants usually have autonomy to control window openings. However, in DSF buildings, the modification of apertures areas may have significant effect on the airflow mechanisms

of all floors. Therefore, further studies on the interaction between the DSF building and occupants are needed to investigate the user preferences on the building operation control.

Climate change - Investigation of the potential impact of global climate change on the thermal performance is also needed. Possible change in wind speed and temperature can affect how DSF and building perform and how people perceive the comfort acceptance of the work space. Thinking more broadly, a reanalysis on the building transparency philosophy and possible changes in building design standards may also be undertaken.

REFERENCES

- ABNT 2003. Desempenho térmico de edificações Parte 3: Zoneamento bioclimático brasileiro e diretrizes construtivas para habitações unifamiliares de interesse social. Associação Brasileira de Normas Técnicas.
- ABNT 2010. RTQ-C Regulamento Técnico da Qualidade do Nível de Eficiência Energética de Edifícios Comerciais, de Serviços e Públicos. *In: INMETRO INSTITUTO NACIONAL DE METROLOGIA, N. E. Q. I. (ed.) Portaria nº 163, de 08 de junho de 2009.* Brasília, DF: Associação Brasileira de Normas Técnicas.
- ABNT 2013. Residential buildings — Performance: General requirements. *NBR 15.575.* Associação Brasileira de Normas Técnicas.
- ABNT, B. A. O. T. S. 1980. Air-conditioning system - Central air units - Basic parameters for design - Procedure.
- AFLAKI, A., MAHYUDDIN, N., AL-CHEIKH MAHMOUD, Z. & BAHARUM, M. R. 2015. A review on natural ventilation applications through building façade components and ventilation openings in tropical climates. *Energy and Buildings*, 101, 153-162.
- ANĐELKOVIĆ, A. S., GVOZDENAC-UROŠEVIĆ, B., KLJAJIĆ, M. & IGNJATOVIĆ, M. G. 2015. Experimental research of the thermal characteristics of a multi-storey naturally ventilated double skin façade. *Energy and Buildings*, 86, 766-781.
- ASHRAE 2001. ASHRAE 62 Ventilation for Acceptable Indoor Air Quality. *Standard 62/2001.* Atlanta.
- ASHRAE 2009. Handbook—Fundamentals. Atlanta, GA: American Society of Heating, Refrigerating and Air Conditioning Engineers.
- ASHRAE 2013. ASHRAE 55 - Thermal Environmental Conditions for Humam Occupancy. Atlanta: Ame.
- AUGENBROE, G. 2011. The role of simulation in performance based building. *In: HENSEN, J. L. M. & LAMBERTS, R. (eds.) Building performance simulation for design and operation.* Spon press.
- AZARBAYJANI, M. 2010. *Beyond arrows: energy performance of a new, naturally ventilated double-skin façade configuration for a high-rise office building in Chicago.* University of Illinois at Urbana-Champaign.
- BBRI 2002. Source book for a better understanding of conceptual and operational aspects of active façades.: Department of Building Physics, Indoor Climate and Building Services.
- BOGO, A., PIETROBON, C. E., BARBOSA, M. J., GOULART, S., PITTA, T. & LAMBERTS, R. 1994. Bioclimatologia aplicada ao projeto de edificações visando o conforto térmico. *In: 2 (ed.).* Federal University of Santa Catarina.
- CARLO, J. C. 2008. *Desenvolvimento de Metodologia de Avaliação da Eficiência Energética do Envoltório de Edificações Não-residenciais.* Doctoral, Federal University of Santa Catarina.
- CEN 2007. Indoor environmental input parameters for design and assessment of energy performance of buildings- addressing indoor air quality, thermal environment, lighting and acoustics.
- CHAN, A. L. S., CHOW, T. T., FONG, K. F. & LIN, Z. 2009. Investigation on energy performance of double skin façade in Hong Kong. *Energy and Buildings*, 41, 1135-1142.

- CHOU, S. K., CHUA, K. J. & HO, J. C. 2009. A study on the effects of double skin façades on the energy management in buildings. *Energy Conversion and Management*, 50, 2275-2281.
- CIBSE 2005. Applications Manual AM10. *Natural ventilation in non-domestic buildings*. Great Britain: Chartered Institution of Building Services Engineers (CIBSE).
- CIBSE 2006. Knowledge series. *Comfort*. Great Britain: Chartered Institution of Building Services Engineers (CIBSE).
- CIBSE 2010. Knowledge series. *How to manage overheating in buildings: A practical guide to improving summertime comfort in buildings*. Great Britain: Chartered Institution of Building Services Engineers (CIBSE).
- CIBSE 2015. Applications Manual AM11. *Building performance modelling*. Great Britain: Chartered Institution of Building Services Engineers (CIBSE).
- COMPAGNO, A. 2002. *Intelligent Glass Façades : Material, Practice, Design*, Birkhauser, Basel.
- DARKWA, J., LI, Y. & CHOW, D. H. C. 2014. Heat transfer and air movement behaviour in a double-skin façade. *Sustainable Cities and Society*, 10, 130-139.
- DAY, J. K. & GUNDERSON, D. E. 2015. Understanding high performance buildings: The link between occupant knowledge of passive design systems, corresponding behaviors, occupant comfort and environmental satisfaction. *Building and Environment*, 84, 114-124.
- DE GRACIA, A., CASTELL, A., NAVARRO, L., ORÓ, E. & CABEZA, L. F. 2013. Numerical modelling of ventilated façades: A review. *Renewable and Sustainable Energy Reviews*, 22, 539-549.
- DICKSON, A. 2004. *Modelling Double-Skin Façades*. MSc, University of Strathclyde, Glasgow UK.
- DING, W., HASEMI, Y. & YAMADA, T. 2005. Natural ventilation performance of a double-skin façade with a solar chimney. *Energy and Buildings*, 37, 411-418.
- DJAMILA, H., CHU, C.-M. & KUMARESAN, S. 2014. Effect of Humidity on Thermal Comfort in the Humid Tropics. *Journal of Building Construction and Planning Research*, 2, 109-117.
- EICKER, U., FUX, V., BAUER, U., MEI, L. & INFIELD, D. 2008. Façades and summer performance of buildings. *Energy and Buildings*, 40, 600-611.
- FALLAHI, A., HAGHIGHAT, F. & ELSADI, H. 2010. Energy performance assessment of double-skin façade with thermal mass. *Energy and Buildings*, 42, 1499-1509.
- FARGHAL, A. & WAGNER, A. Studying the Adaptive Comfort Model a Case Study in a Hot Dry Climate, Cairo, Egypt Adapting to Change: New Thinking on Comfort, 2010 Windsor, UK.
- FOUNTAIN, M., ARENS, E., XU, T., BOUMAN, F. & MASSAYUKI, O. 1999. An Investigation of Thermal Comfort at High Humidities. *SHRAE Transactions*, 105, 1-10.
- GIVONI, B. 1992. Comfort, climate analysis and building design guidelines. *Energy and Buildings*, 18, 11-23.
- GRATIA, E. & DE HERDE, A. 2004a. Is day natural ventilation still possible in office buildings with a double-skin façade? *Building and Environment*, 39, 399-409.

- GRATIA, E. & DE HERDE, A. 2004b. Natural cooling strategies efficiency in an office building with a double-skin façade. *Energy and Buildings*, 36, 1139-1152.
- GRATIA, E. & DE HERDE, A. 2007a. Greenhouse effect in double-skin façade. *Energy and Buildings*, 39, 199-211.
- GRATIA, E. & DE HERDE, A. 2007b. The most efficient position of shading devices in a double-skin façade. *Energy and Buildings*, 39, 364-373.
- GUARDO, A., COUSSIRAT, M., EGUSQUIZA, E., ALAVEDRA, P. & CASTILLA, R. 2009. A CFD approach to evaluate the influence of construction and operation parameters on the performance of Active Transparent Façades in Mediterranean climates. *Energy and Buildings*, 41, 534-542.
- HAASE, M., MARQUES DA SILVA, F. & AMATO, A. 2009. Simulation of ventilated façades in hot and humid climates. *Energy and Buildings*, 41, 361-373.
- HALAWA, E. & VAN HOOF, J. 2012. The adaptive approach to thermal comfort: A critical overview. *Energy and Buildings*, 51, 101-110.
- HAMZA, N. 2008. Double versus single skin façades in hot arid areas. *Energy and Buildings*, 40, 240-248.
- HAMZA, N. A. 2004. *The Performance of Double Skin Façades in Office Building refurbishment in Hot Arid Areas*. PhD, University of Newcastle upon Tyne.
- HAND, J. W., IRVING, S. J., LOMAS, K. J., MCELROY, L. B., PARAND, F., ROBINSON, D. & STRACHAN, P. 1998. Building energy and environmental modelling. In: AM11 (ed.) *Applications Manual*. The Chartered Institution of Building Services Engineers London.
- HAZEM, A., AMEGHCHOUCHE, M. & BOUGRIOU, C. 2015. A numerical analysis of the air ventilation management and assessment of the behavior of double skin façades. *Energy and Buildings*, 102, 225-236.
- HENSEN, J. L. M. & LAMBERTS, R. 2011. Introduction to building performance simulation. In: HENSEN, J. L. M. & LAMBERTS, R. (eds.) *Building performance simulation for design and operation*. Spon press.
- HERKEL, S., KNAPP, U. & PFAFFEROTT, J. 2008. Towards a model of user behaviour regarding the manual control of windows in office buildings. *Building and Environment*, 43, 588-600.
- HONG, T., KIM, J., LEE, J., KOO, C. & PARK, H. 2013. Assessment of Seasonal Energy Efficiency Strategies of a Double Skin Façade in a Monsoon Climate Region. *Energies*, 6, 4352-4376.
- HOOF, J. V., MAZEJ, M. & HENSEN, J. L. M. 2010. Thermal comfort: research and practice. *Frontiers in Bioscience*, 15, 765-788.
- HØSEGGEN, R., WACHENFELDT, B. J. & HANSSSEN, S. O. 2008. Building simulation as an assisting tool in decision making: Case study: With or without a double-skin façade? *Energy and Buildings*, 40, 821-827.
- HYDE, R. 2000. *Climatic responsive design: a study of buildings in moderate and hot humid climates*, E & FN Spon.
- IEA, I. E. A. 2013a. Technology Roadmap Energy Efficient Building Envelopes *Energy Technology Perspectives* France: International Energy Agency.
- IEA, I. E. A. 2013b. Transition to Sustainable Buildings: Strategies and Opportunities to 2050. *Energy Technology Perspectives*. International Energy Agency.

- IESVE 2014. Integrated Environmental Solutions. Integrated Environmental Design Solutions Ltd
- ISO7730, I. O. F. S.-. 2005. Ergonomics of the thermal environment — Analytical determination and interpretation of thermal comfort using calculation of the PMV and PPD indices and local thermal comfort criteria. Switzerland.
- JI, Y., COOK, M. J., HANBY, V. I., INFIELD, D. G., LOVEDAY, D. L. & MEI, L. CFD modelling of double-skin façades with venetian blinds. The 10th International Building Performance Simulation Association (IBPSA) Conference and Exhibition, 2007 2007 Beijing, China. 1491-1498.
- JIRU, T. E., TAO, Y.-X. & HAGHIGHAT, F. 2011. Airflow and heat transfer in double skin façades. *Energy and Buildings*, 43, 2760-2766.
- JOE, J., CHOI, W., KWAK, Y. & HUH, J.-H. 2014. Optimal design of a multi-story double skin façade. *Energy and Buildings*, 76, 143-150.
- KALYANOVA, O. 2008. *Double-Skin Façade – Modelling and Experimental Investigations of Thermal Performance*. Aalborg University.
- KIM, Y.-M., KIM, S.-Y., SHIN, S.-W. & SOHN, J.-Y. 2009. Contribution of natural ventilation in a double skin envelope to heating load reduction in winter. *Building and Environment*, 44, 2236-2244.
- KOHN, A. E. & KATZ, P. 2002. *Building type basics for office buildings*, New York.
- KRAGH, M. Monitoring of advanced façades and environmental systems. In: KEILLER, A. & LEDBETTER, S., eds. *Whole-life performance of façades*, 2001 Bath, UK.
- LEÃO, M., HUCKEMANN, V., LEÃO, É. B., FISCH, M. N. & KUCHEN, E. 2009. Energy efficiency of double skin façades: an approach to Brazilian climates. *Bauphysik*, 31, 8.
- LEE, E., SELKOWITZ, S., BAZJANAC, V., INKAROJRIT, V. & KOHLER, C. 2002. High-Performance Commercial Building Façades. University of California.
- LORAND, R., COHEN, J., MELLO, J. & PANICH, D. 2013. Renewable Energy Guide for Highway Maintenance Facilities. In: 751, N. R. (ed.) *National cooperative highway research program*. Washington, D.C.
- LOU, W., HUANG, M., ZHANG, M. & LIN, N. 2012. Experimental and zonal modeling for wind pressures on double-skin façades of a tall building. *Energy and Buildings*, 54, 179-191.
- MANZ, H. 2003. Numerical simulation of heat transfer by natural convection in cavities of façade elements. *Energy and Buildings*, 35, 305-311.
- MANZ, H. 2004. Total solar energy transmittance of glass double façades with free convection. *Energy and Buildings*, 36, 127-136.
- MANZ, H., SCHAEELIN, A. & SIMMLER, H. 2004. Airflow patterns and thermal behavior of mechanically ventilated glass double façades. *Building and Environment*, 39, 1023-1033.
- MARCONDES, M. P. 2010. *Soluções Projetuais de Fachadas para Edifícios de Escritórios com Ventilação Natural em São Paulo*. Universidade de São Paulo.
- MARQUES DA SILVA, F., GOMES, M. G. & RODRIGUES, A. M. 2015. Measuring and estimating airflow in naturally ventilated double skin façades. *Building and Environment*, 87, 292-301.

- MARTINS, F. R., ABREU, S. L. & PEREIRA, E. B. 2012. Scenarios for solar thermal energy applications in Brazil. *Energy Policy*, 48, 640-649.
- MARTINS, F. R. & PEREIRA, E. B. 2011. Enhancing information for solar and wind energy technology deployment in Brazil. *Energy Policy*, 39, 4378-4390.
- MENTOR 2014. Computational Fluid Dynamics (CFD) software. 10.1 ed. <http://www.mentor.com/products/mechanical/products/FloVENT>: Mentor Graphics Corporation.
- MINGOTTI, N., CHENVIDYAKARN, T. & WOODS, A. W. 2011. The fluid mechanics of the natural ventilation of a narrow-cavity double-skin façade. *Building and Environment*, 46, 807-823.
- MINGOTTI, N., CHENVIDYAKARN, T. & WOODS, A. W. 2013. Combined impacts of climate and wall insulation on the energy benefit of an extra layer of glazing in the façade. *Energy and Buildings*, 58, 237-249.
- MULYADI, R. 2012. *Study on naturally ventilated double-skin façade in hot and humid climate*. Nagoya University.
- NASROLLAHI, N. & SALEHI, M. 2015. Performance enhancement of double skin façades in hot and dry climates using wind parameters. *Renewable Energy*, 83, 1-12.
- NAYAK, J. K. & PRAJAPATI, J. A. 2006. *Handbook on energy conscious buildings*.
- NICOL, F. & HUMPHREYS, M. 2010. Derivation of the adaptive equations for thermal comfort in free-running buildings in European standard EN15251. *Building and Environment*, 45, 11-17.
- NICOL, F., HUMPHREYS, M. & HUMPHREYS, M. 2012. *Adaptive thermal comfort : principles and practice*, London, Routledge.
- OCHOA, C. E. & CAPELUTO, I. G. 2009. Advice tool for early design stages of intelligent façades based on energy and visual comfort approach. *Energy and Buildings*, 41, 480-488.
- OESTERLE, E., LIEB, R.-D., LUTZ, M. & HEUSLER, W. 2001. *Double Skin Façades – Integrated Planning*, Munich, Prestel.
- PAPPAS, A. & ZHAI, Z. 2008. Numerical investigation on thermal performance and correlations of double skin façade with buoyancy-driven airflow. *Energy and Buildings*, 40, 466-475.
- PARK, C.-S., AUGENBROE, G., SADEGH, N., THITISAWAT, M. & MESSADI, T. 2004. Real-time optimization of a double-skin façade based on lumped modeling and occupant preference. *Building and Environment*, 39, 939-948.
- PASQUAY, T. 2004. Natural ventilation in high-rise buildings with double façades, saving or waste of energy. *Energy and Buildings*, 36, 381-389.
- PASUT, W. & DE CARLI, M. 2012. Evaluation of various CFD modelling strategies in predicting airflow and temperature in a naturally ventilated double skin façade. *Applied Thermal Engineering*, 37, 267-274.
- PÉREZ-GRANDE, I., MESEGUER, J. & ALONSO, G. 2005. Influence of glass properties on the performance of double-glazed façades. *Applied Thermal Engineering*, 25, 3163-3175.
- POIRAZIS, H. 2006. Double Skin Façades: A Literature Review. Sweden: IEA SHC Task 34 ECBCS Annex 43.

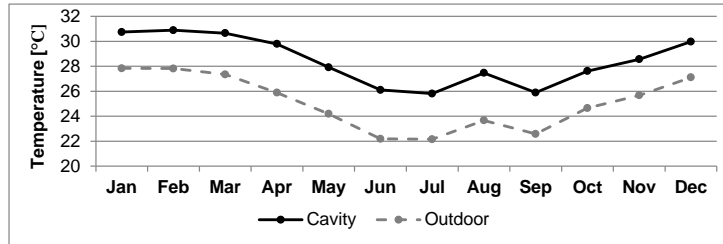
- RACE, G. L. 2006. Comfort. In: 6 (ed.) *CIBSE Knowledge series*. Great Britain: CIBSE - Chartered Institution of Building Services Engineers.
- RADHI, H., SHARPLES, S. & FIKIRY, F. 2013. Will multi-façade systems reduce cooling energy in fully glazed buildings? A scoping study of UAE buildings. *Energy and Buildings*, 56, 179-188.
- RAHMANI, B., KANDAR, M. Z. & RAHMANI, P. 2012. How Double Skin Façade's Air-Gap Sizes Effect on Lowering Solar Heat Gain in Tropical Climate? *World Applied Sciences Journal* 18, 774-778.
- RIJAL, H. B., TUOHY, P., HUMPHREYS, M. A., NICOL, J. F., SAMUEL, A. & CLARKE, J. 2007. Using results from field surveys to predict the effect of open windows on thermal comfort and energy use in buildings. *Energy and Buildings*, 39, 823-836.
- SADINENI, S. B., MADALA, S. & BOEHM, R. F. 2011. Passive building energy savings: A review of building envelope components. *Renewable and Sustainable Energy Reviews*, 15, 3617-3631.
- SAELENS, D. 2002. *Energy Performance Assessments of Single Storey Multiple-Skin Façades*. PhD, Catholic University of Leuven.
- SAELENS, D., ROELS, S. & HENS, H. 2008. Strategies to improve the energy performance of multiple-skin façades. *Building and Environment*, 43, 638-650.
- SAFER, N., WOLOSZYN, M. & ROUX, J. J. 2005. Three-dimensional simulation with a CFD tool of the airflow phenomena in single floor double-skin façade equipped with a venetian blind. *Solar Energy*, 79, 193-203.
- SCHIEFER, C., HEIMRATH, R., HENGESBERGER, H., MACH, T., STREICHER, W., SANTAMOURIS, M., FAROU, I., ERHORN, H., ERHORN-KLUTTIG, H., MATOS, M. D., DUARTE, R. & BLOMSTERBERG, Å. 2008. Best Practice for Double Skin Façades Intelligent Energy Europe.
- SCHUCH, M., MATUSO, C. A., BUDAG, K. H. & ONO, E. T. 2010. Analysis Bio. Laboratório de Eficiência Energética em Edificações.
- SHAMERI, M. A., ALGHOUL, M. A., ELAYEB, O., ZAIN, M. F. M., ALRUBAIIH, M. S., AMIR, H. & SOPIAN, K. 2013. Daylighting characteristics of existing double-skin façade office buildings. *Energy and Buildings*, 59, 279-286.
- SHAMERI, M. A., ALGHOUL, M. A., SOPIAN, K., ZAIN, M. F. M. & ELAYEB, O. 2011. Perspectives of double skin façade systems in buildings and energy saving. *Renewable and Sustainable Energy Reviews*, 15, 1468-1475.
- SINGH, M. K., MAHAPATRA, S. & ATREYA, S. K. 2011. Adaptive thermal comfort model for different climatic zones of North-East India. *Applied Energy*, 88, 2420-2428.
- STEC, W. & PAASSEN, D. V. Sensitivity of the double skin façade on the outdoor conditions. International conference on air quality and climate; Indoor Air 2005 Beijing.
- STREICHER, W., HEIMRATH, R., HENGESBERGER, H., MACH, T., WALDNER, R., FLAMANT, G., LONCOUR, X., GUARRACINO, G., SANTAMOURIS, H., FAROU, I., ZEREFOS, S., ASSIMAKOPOULOS, M., DUARTE, R., BLOMSTERBERG, A., SJOBERG, L. & BLOMQUIST, C. 2007. On the Typology, Costs, Energy Performance, Environmental Quality and Operational Characteristics of Double Skin Façades in European Buildings. In: SANTAMOURIS, M. (ed.) *Advances in building energy research* Earthscan.
- TOE, D. H. C. & KUBOTA, T. 2013. Development of an adaptive thermal comfort equation for naturally ventilated buildings in hot-humid climates using ASHRAE RP-884 database. *Frontiers of Architectural Research*, 2, 278-291.

- TORRES, M., ALAVEDRA, P., GUZMÁN, A., CUERVA, E., PLANAS, C., CLEMENTE, R. & ESCALONA, V. Double skin façades - Cavity and exterior openings dimensions for saving energy on Mediterranean climate. *Building Simulation*, 2007 Beijing, China.
- TREECK, C. V. 2011. Indoor thermal quality performance prediction. *In: HENSEN, J. L. M. & LAMBERTS, R. (eds.) Building performance simulation for design and operation*. Spon Press.
- VOORDT, T. J. M. V. D. & MAARLEVELD, M. 2006. Performance of office buildings from a user's perspective *Ambiente Construído*, 6, 7-20.
- WANG, L. & CHEN, Q. 2008. Evaluation of some assumptions used in multizone airflow network models. *Building and Environment*, 43, 1671-1677.
- WONG, P. C., PRASAD, D. & BEHNIA, M. Methodology for natural ventilation design for high-rise buildings in hot and humid climate. *World Sustainable Building Conference*, 2005 Tokyo.
- WOOD, A. & SALIB, R. 2013. Natural ventilation in high-rise office buildings. *Council on Tall Buildings and Urban Habitat*
Illinois Institute of Technology.
- YAU, Y. & CHEW, B. 2012. A review on predicted mean vote and adaptive thermal comfort models. *Building Services Engineering Research and Technology*.
- ZHANG, Y. & BARRETT, P. 2012. Factors influencing the occupants' window opening behaviour in a naturally ventilated office building. *Building and Environment*, 50, 125-134.
- ZHANG, Y., WANG, J., CHEN, H., ZHANG, J. & MENG, Q. 2010. Thermal comfort in naturally ventilated buildings in hot-humid area of China. *Building and Environment*, 45, 2562-2570.

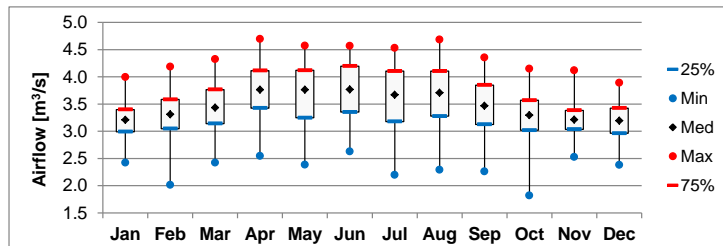
APPENDIX A - Mean monthly airflow across the cavity and floors of the building

The following figures summarize the mean monthly cavity airflow and air temperatures and mean monthly airflows across the different floors of the building for all cases tested.

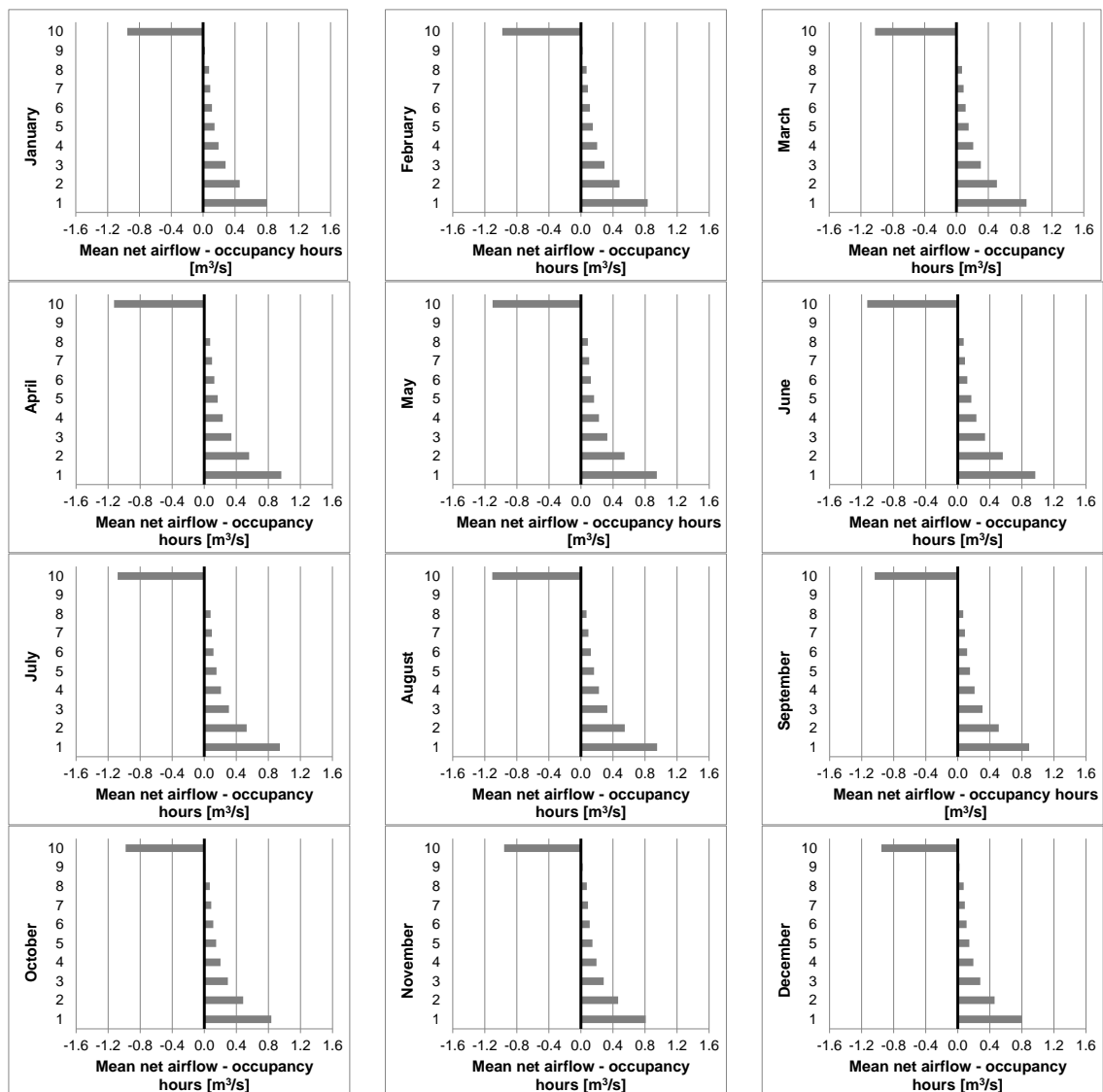
Base case



Appendix A. 1 - Monthly mean of difference of temperature between the cavity and the outside air – Base case

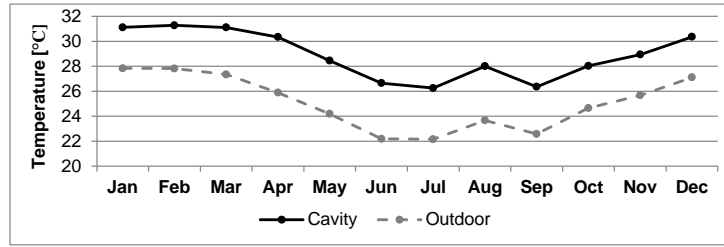


Appendix A. 2 - Monthly mean of airflow on the top of the cavity – Base case

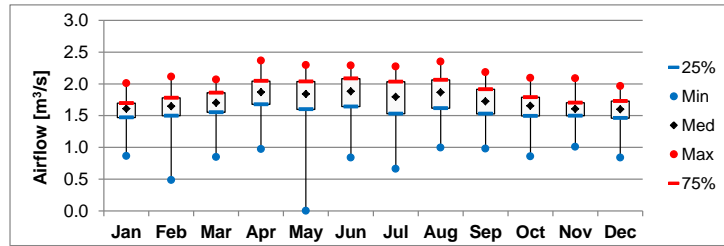


Appendix A. 3 - Monthly mean of the net airflow for each floor – Base case

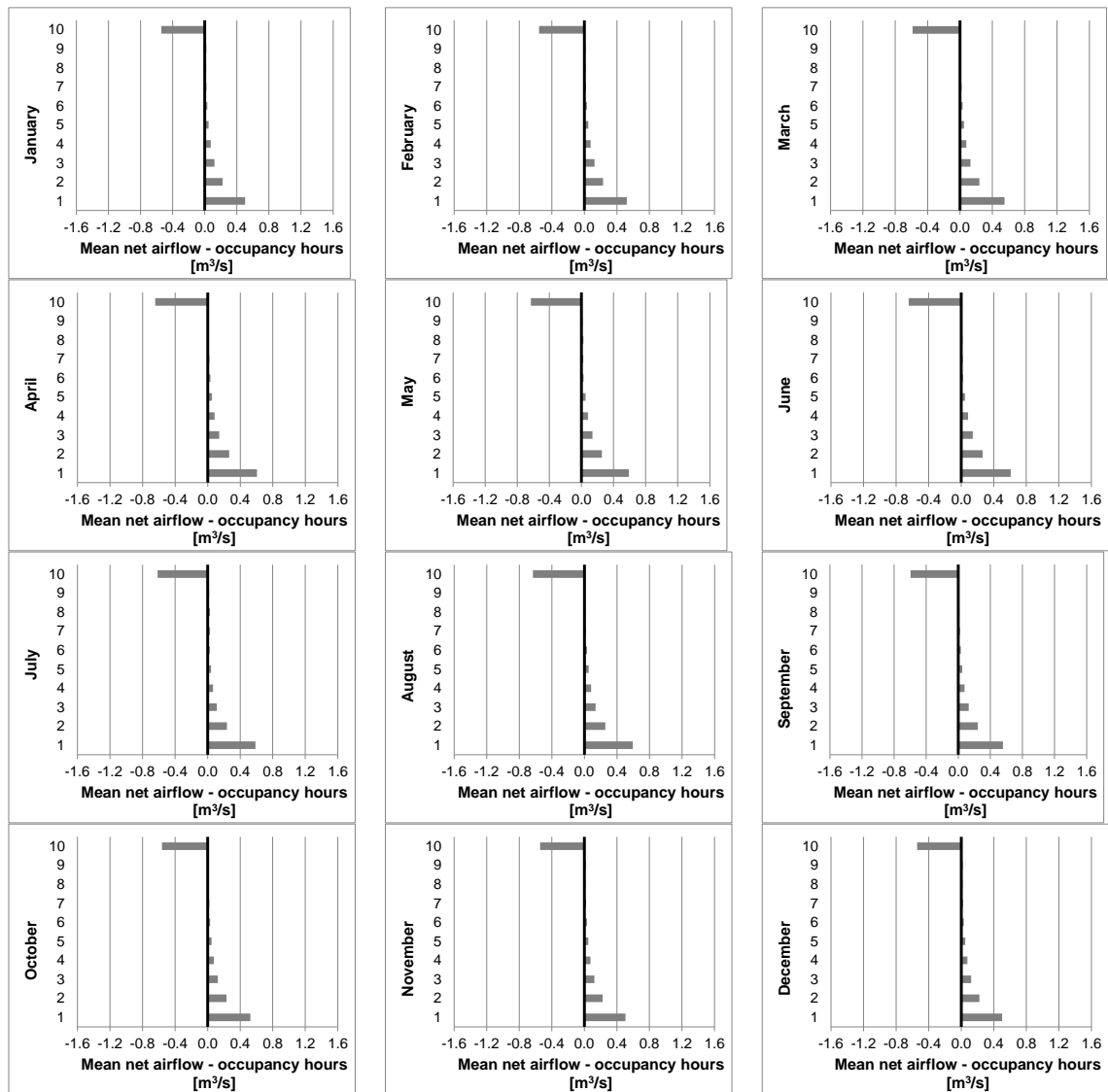
Case A1.1 Cavity depth – 25cm



Appendix A. 4 - Monthly mean of difference of temperature between the cavity and the outside air - Case Cavity depth – 25cm

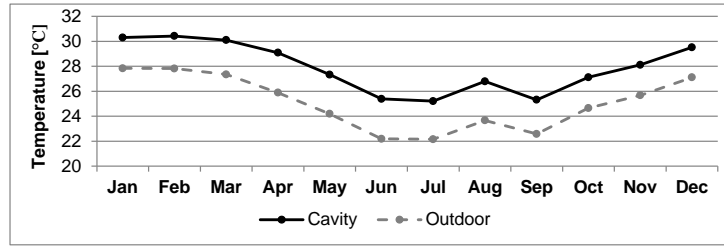


Appendix A. 5 - Monthly mean of airflow on the top of the cavity – Case Cavity depth – 25cm

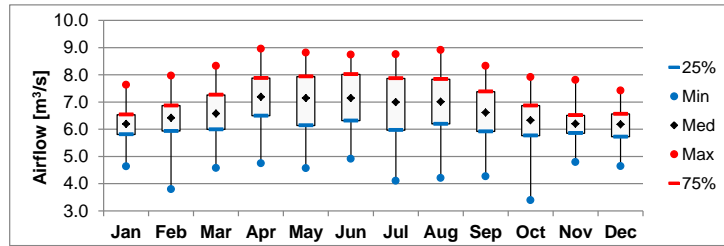


Appendix A. 6 - Monthly mean of the net airflow for each floor – Case Cavity depth – 25cm

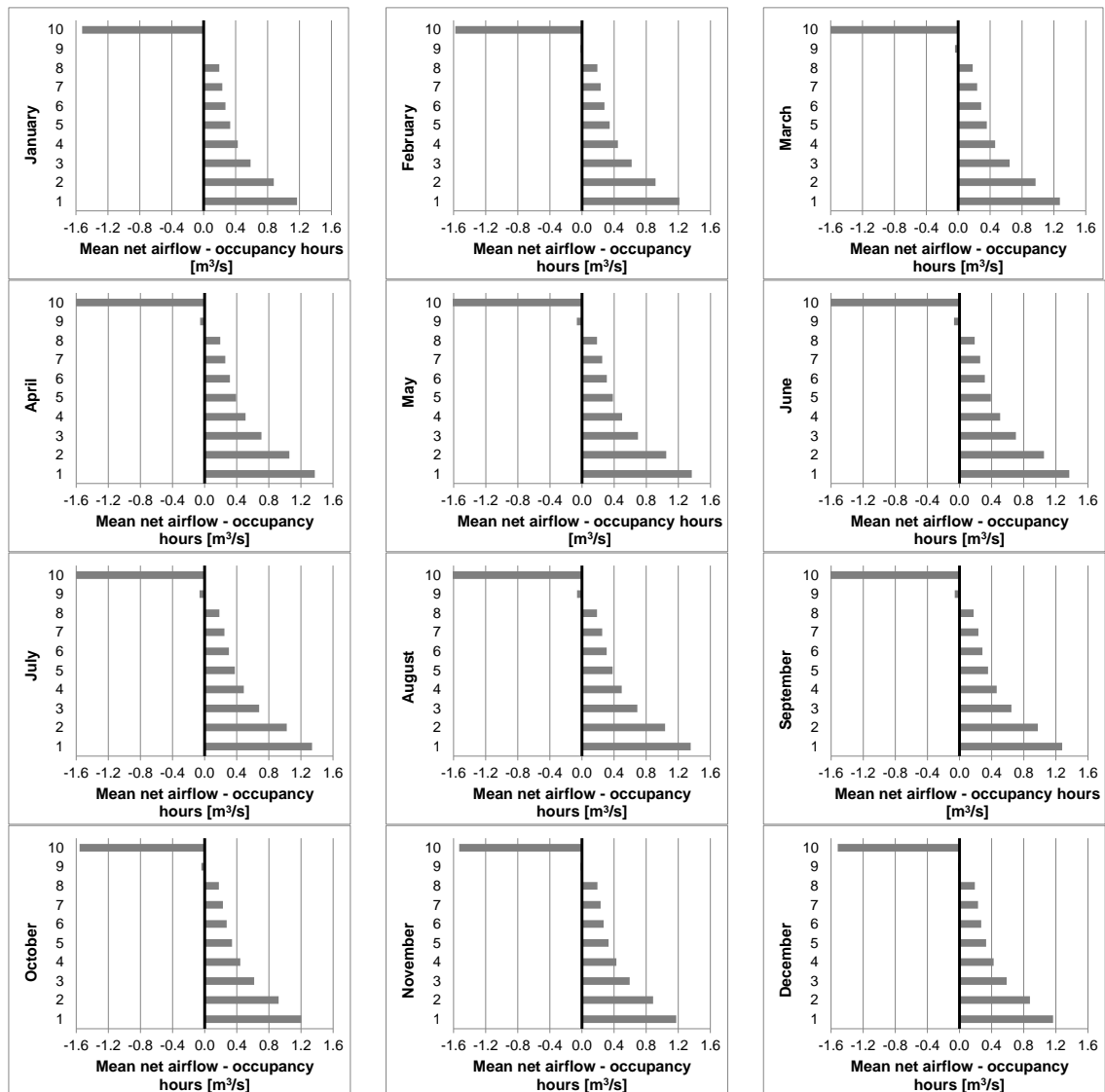
Case A1.3 Cavity depth – 100cm



Appendix A. 7 - Monthly mean of difference of temperature between the cavity and the outside air– Case Cavity depth – 100cm

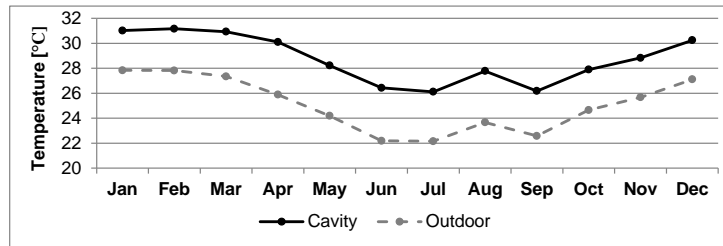


Appendix A. 8 - Monthly mean of airflow on the top of the cavity – Case Cavity depth – 100cm

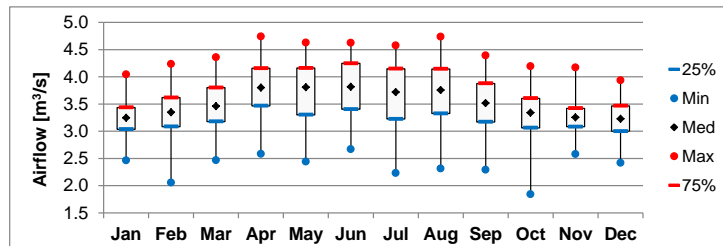


Appendix A. 9 - Monthly mean of the net airflow for each floor – Case Cavity depth – 100cm

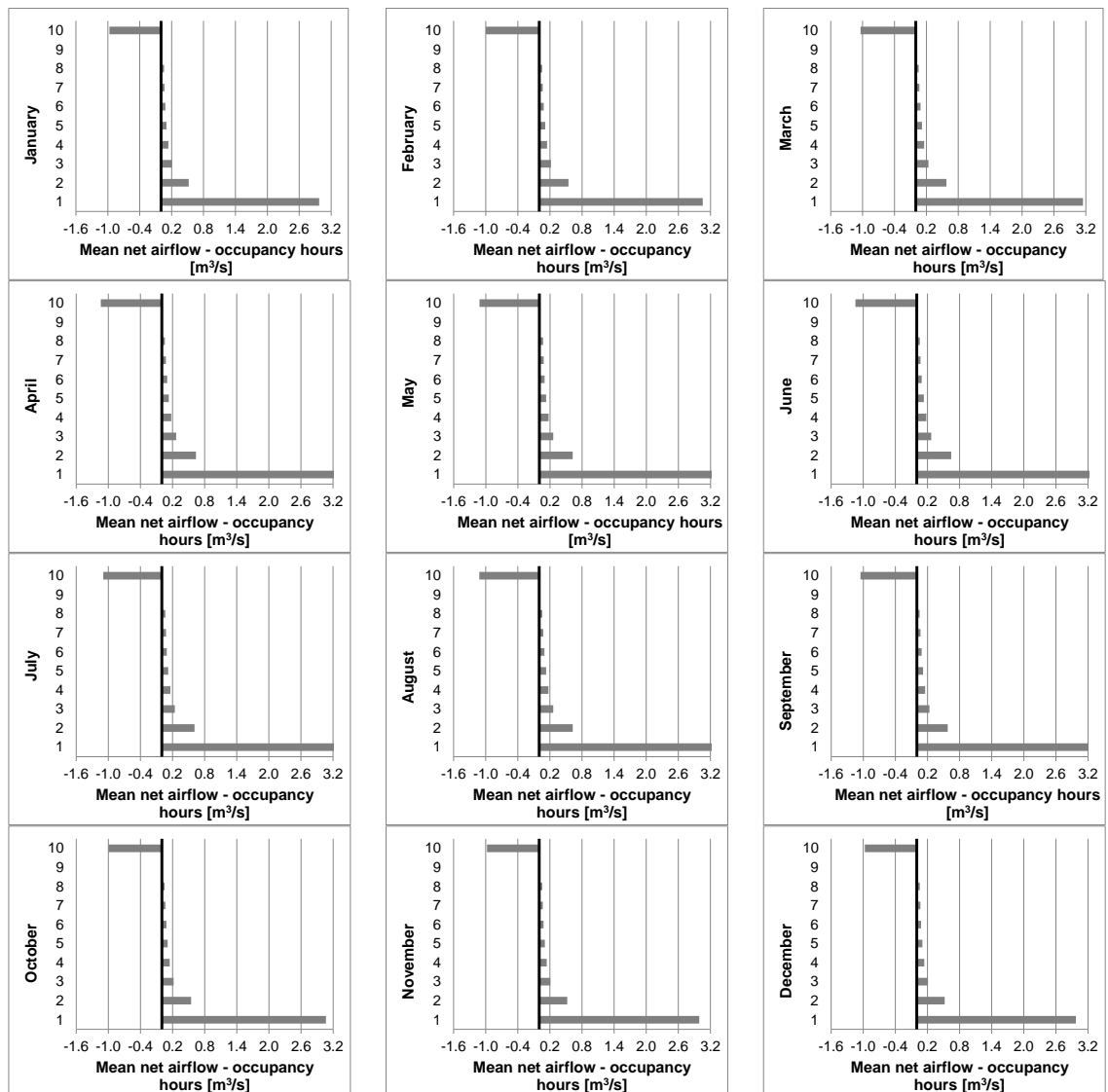
Case A2.2 Cavity bottom opening – Bottom closed



Appendix A. 10 - Monthly mean of difference of temperature between the cavity and the outside air – Case Cavity bottom opening – Bottom closed

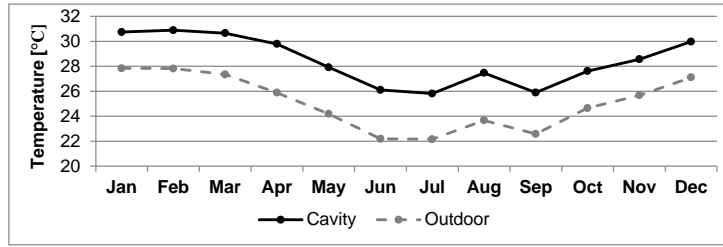


Appendix A. 11 - Monthly mean of airflow on the top of the cavity – Case Cavity bottom opening – Bottom closed

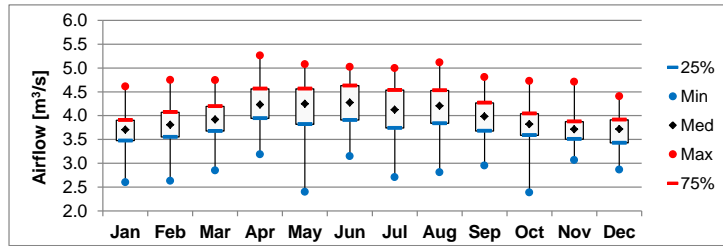


Appendix A. 12 - Monthly mean of the net airflow for each floor – Case Cavity bottom opening – Bottom closed

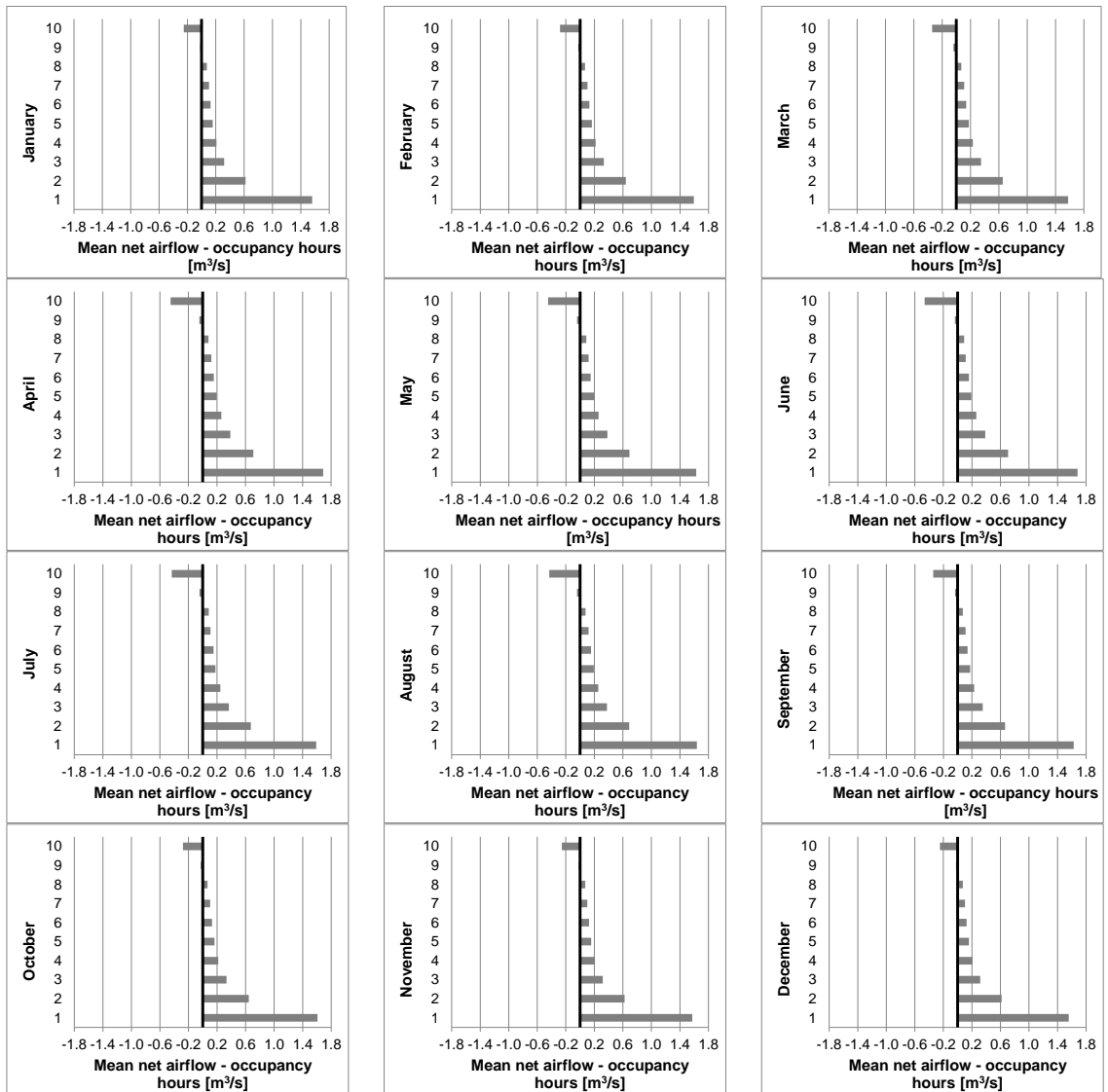
Case A3.2 Windows position – South windows on the bottom, north windows on the top of the wall



Appendix A. 13 - Monthly mean of difference of temperature between the cavity and the outside air – Case Windows position – South windows on the bottom, north windows on the top of the wall

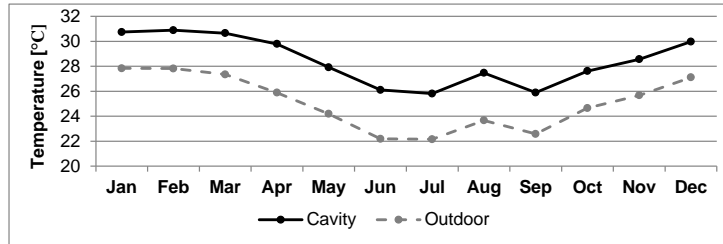


Appendix A. 14 - Monthly mean of airflow on the top of the cavity – Case Windows position – South windows on the bottom, north windows on the top of the wall

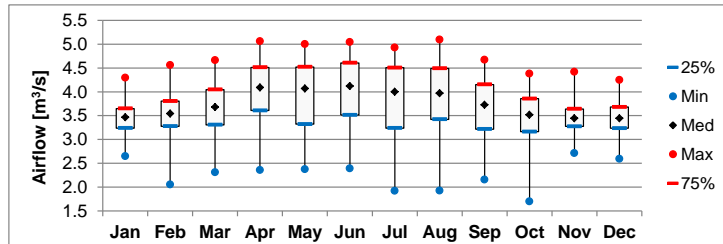


Appendix A. 15 - Monthly mean of the net airflow for each floor – Case Windows position – South windows on the bottom, north windows on the top of the wall

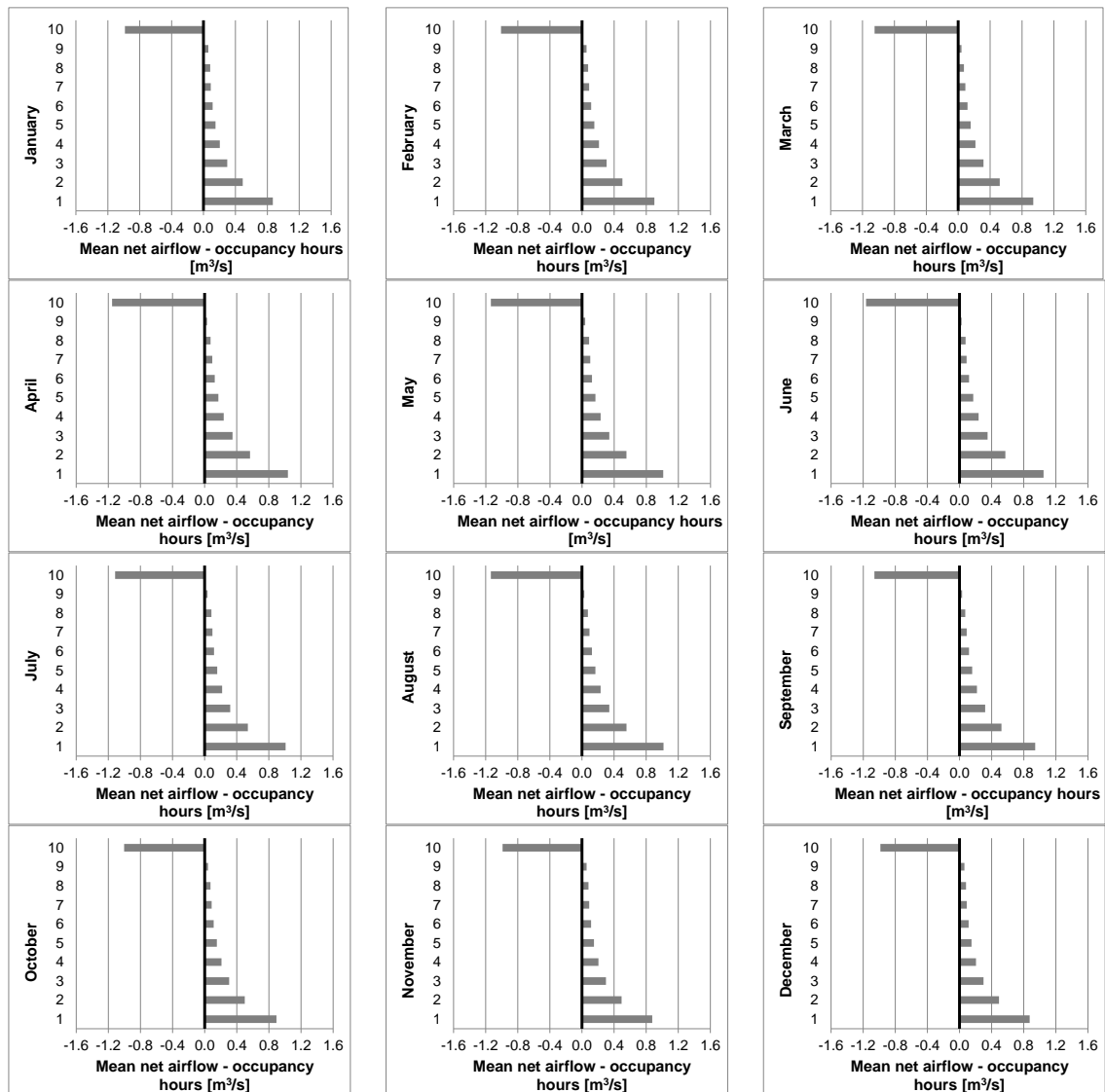
Case B1.2 Shading devices - Concrete



Appendix A. 16 - Monthly mean of difference of temperature between the cavity and the outside air – Case Shading devices - Concrete

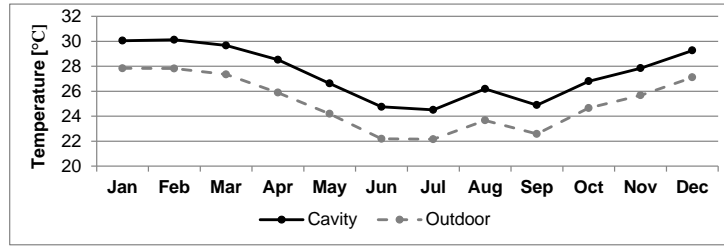


Appendix A. 17 - Monthly mean of airflow on the top of the cavity – Case Shading devices - Concrete

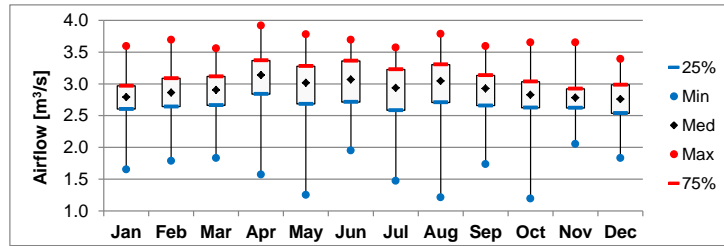


Appendix A. 18 - Monthly mean of the net airflow for each floor – Case Shading devices - Concrete

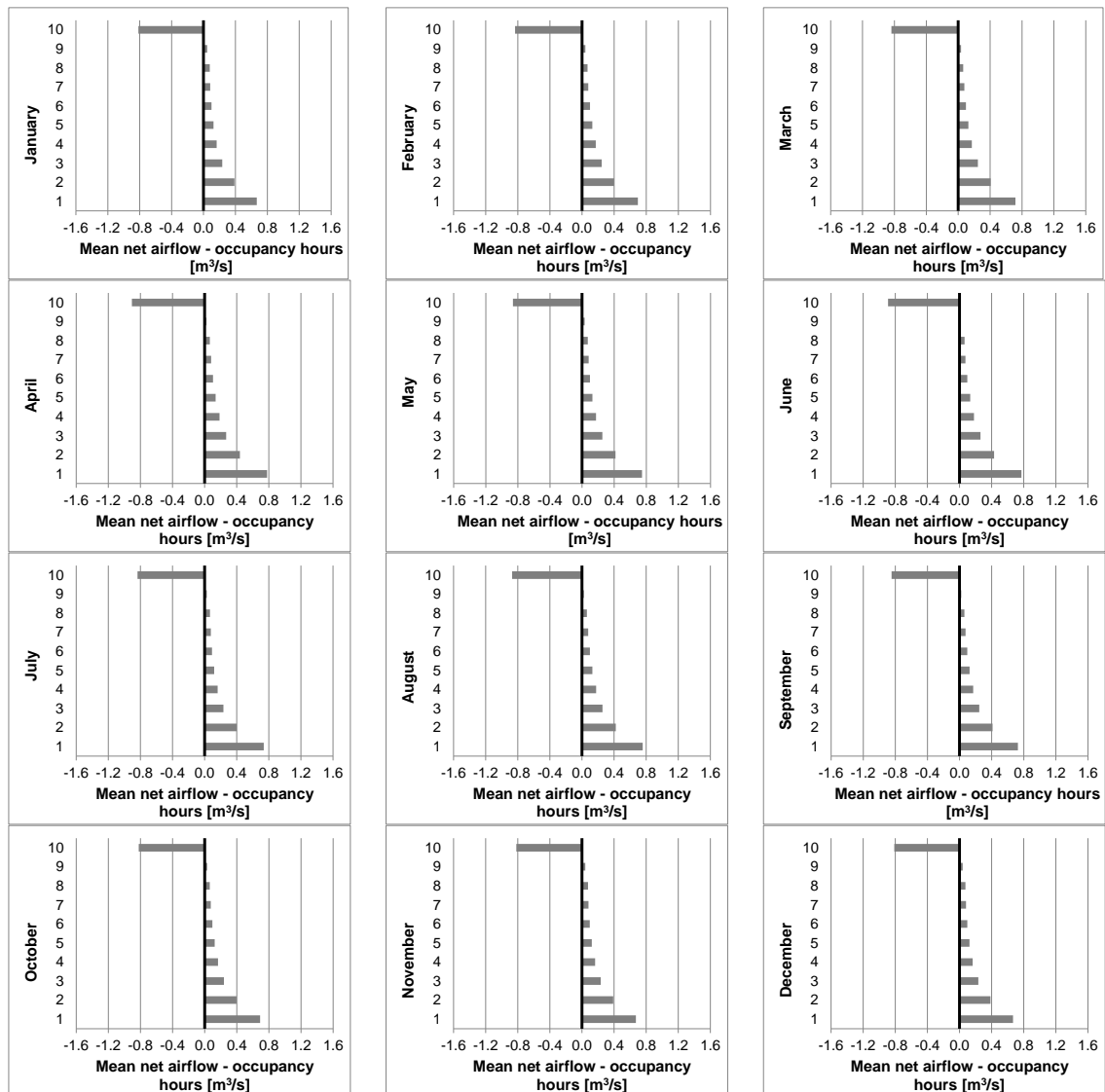
Case B1.2 Shading devices - Aluminium



Appendix A. 19 - Monthly mean of difference of temperature between the cavity and the outside air – Case Shading devices - Metal

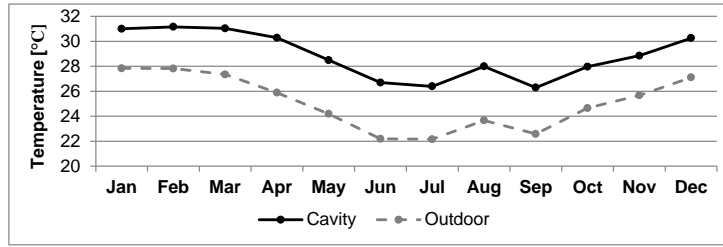


Appendix A. 20 - Monthly mean of airflow on the top of the cavity – Case Shading devices - Metal

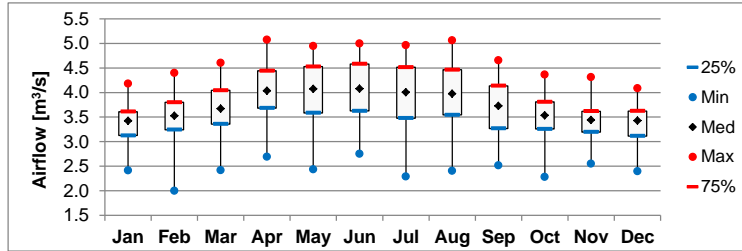


Appendix A. 21 - Monthly mean of the net airflow for each floor – Case Shading devices - Metal

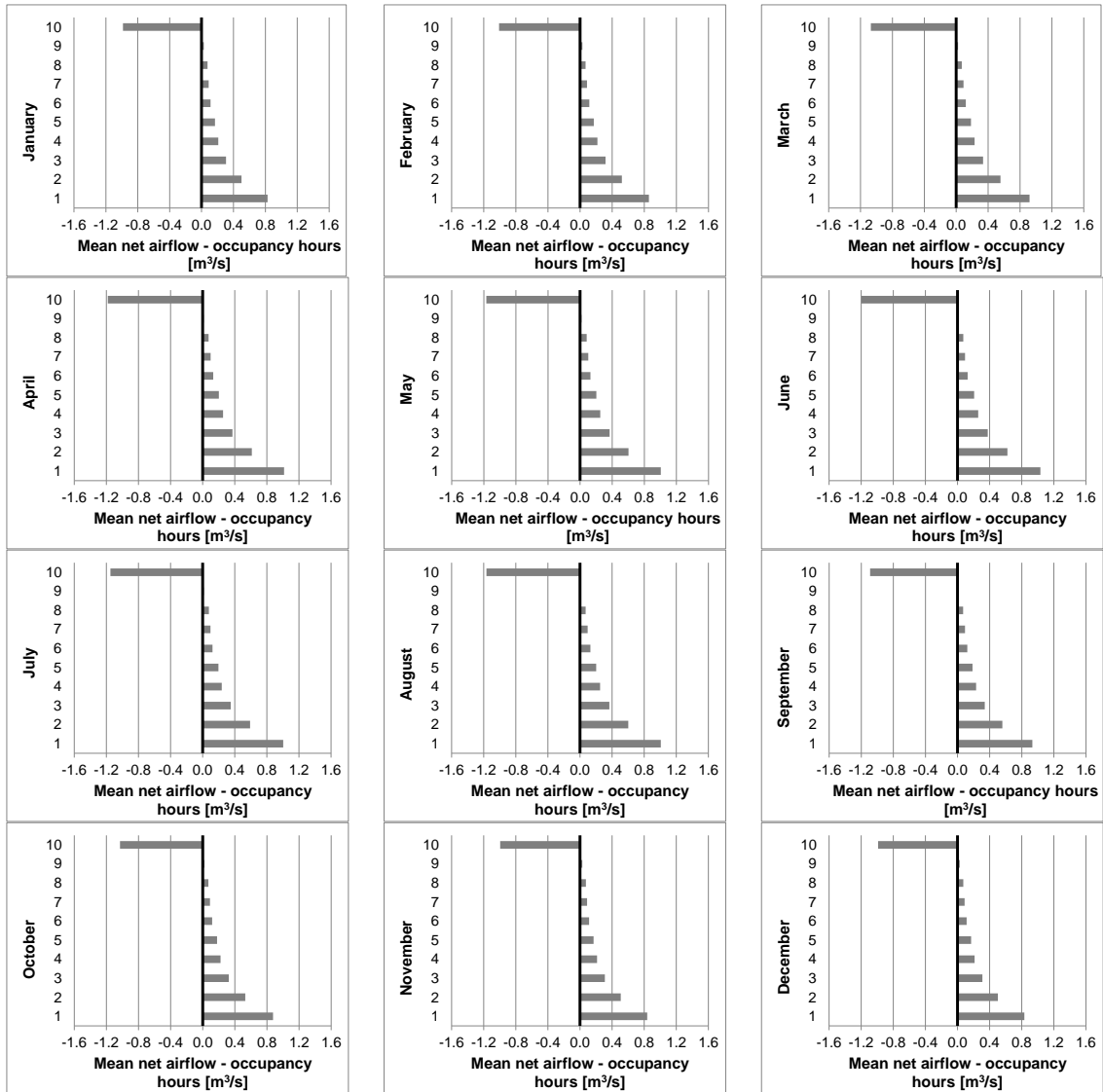
Case B2.2 Inner skin material – Insulation material on the inner surface



Appendix A. 22 - Monthly mean of difference of temperature between the cavity and the outside air – Case Inner skin material – Insulation applied to the inner surface and black painting on the outer surface

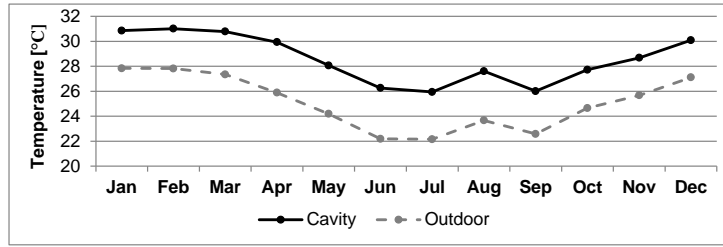


Appendix A. 23 - Monthly mean of airflow on the top of the cavity – Case Inner skin material – Insulation applied to the inner surface and black painting on the outer surface

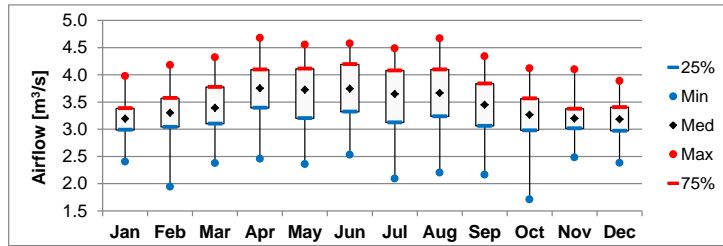


Appendix A. 24 - Monthly mean of the net airflow for each floor – Case Inner skin material – Insulation applied to the inner surface and black painting on the outer surface

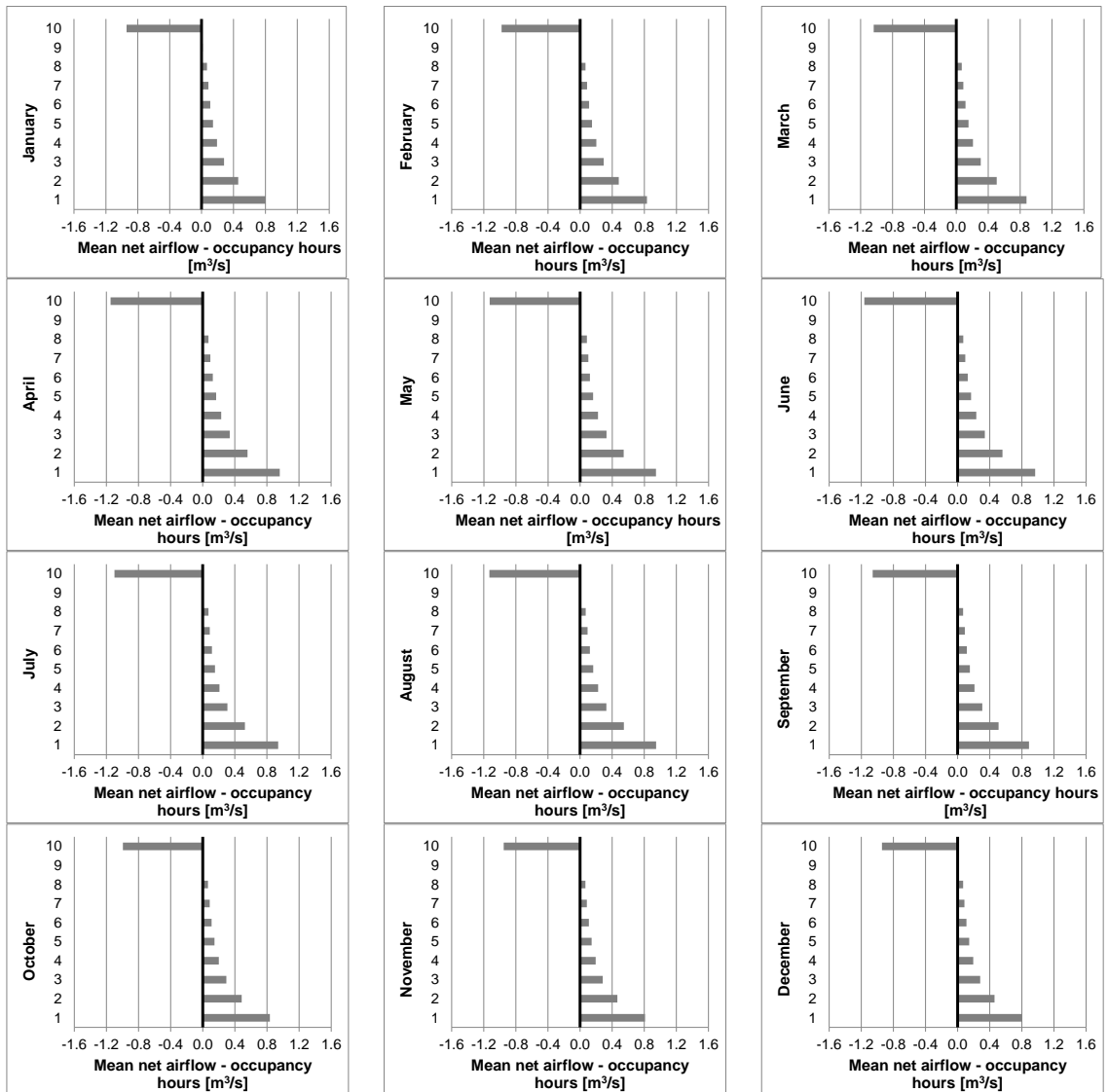
Case C1.2 Cavity extension above roof - 1.75m above roof



Appendix A. 25 - Monthly mean of difference of temperature between the cavity and the outside air – Case Cavity extension above roof - 1.75m above roof

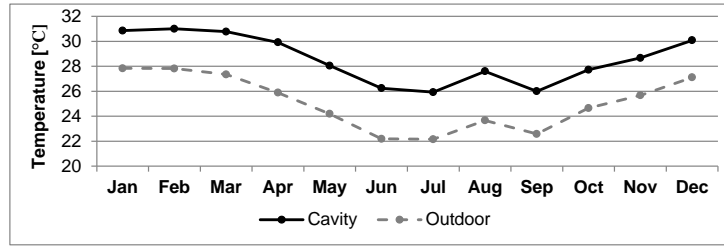


Appendix A. 26 - Monthly mean of airflow on the top of the cavity – Case Cavity extension above roof - 1.75m above roof

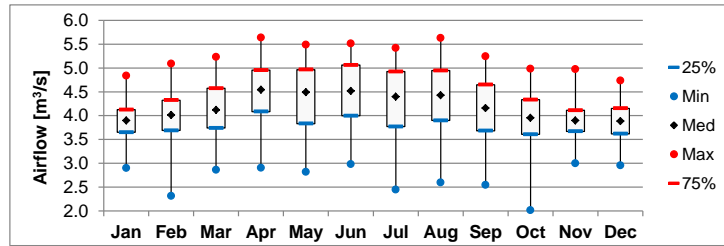


Appendix A. 27 - Monthly mean of the net airflow for each floor – Case Cavity extension above roof - 1.75m above roof

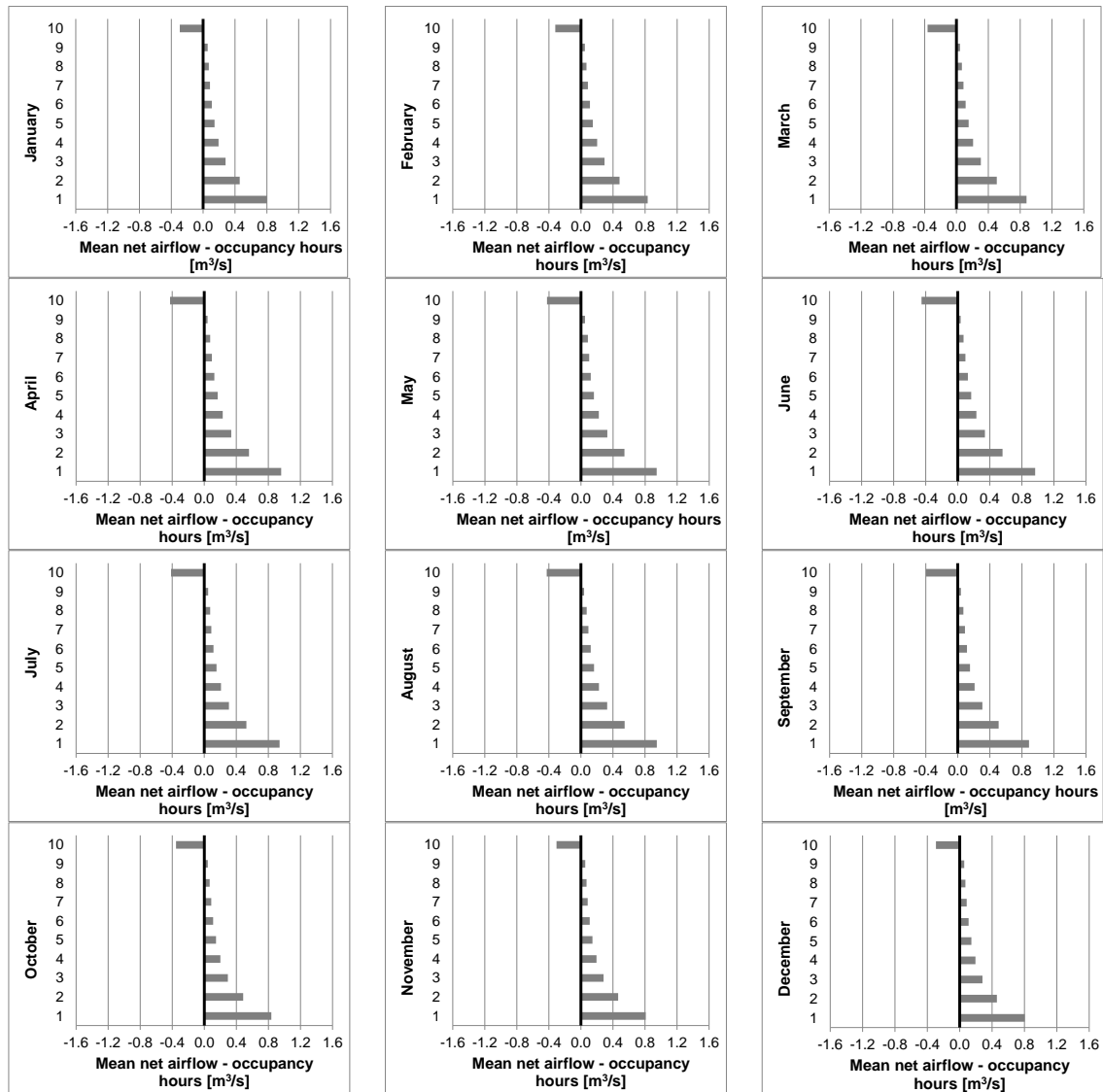
Case C1.3 Cavity extension above roof – 3.50m above roof



Appendix A. 28 - Monthly mean of difference of temperature between the cavity and the outside air – Case Cavity extension above roof – 3.50m above roof

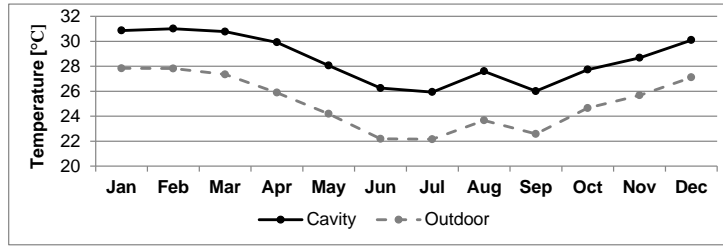


Appendix A. 29 - Monthly mean of airflow on the top of the cavity – Case Cavity extension above roof – 3.50m above roof

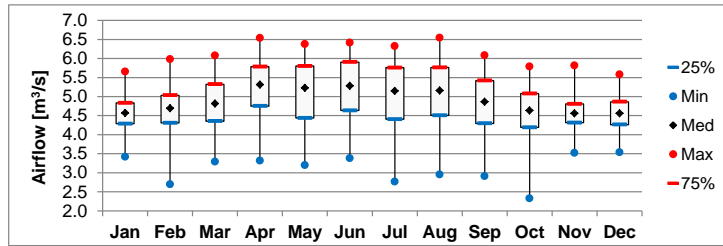


Appendix A. 30 - Monthly mean of the net airflow for each floor – Case Cavity extension above roof – 3.50m above roof

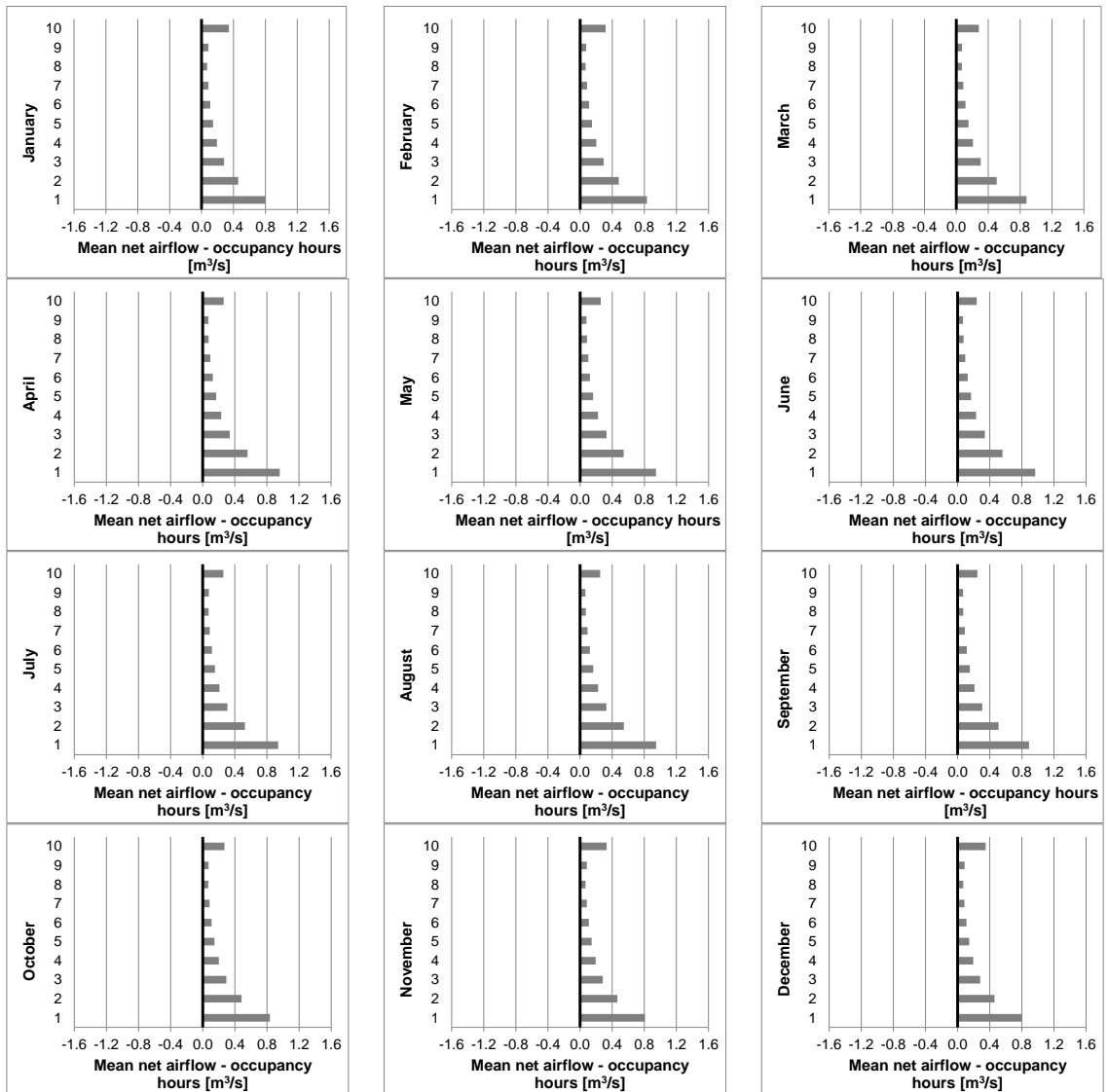
Case C1.4 Cavity extension above roof – 5.25m above roof



Appendix A. 31 - Monthly mean of difference of temperature between the cavity and the outside air – Case Cavity extension above roof – 5.25m above roof

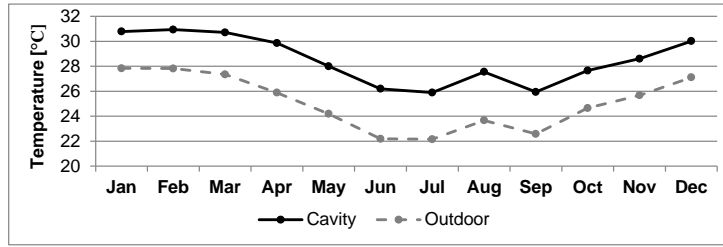


Appendix A. 32 - Monthly mean of airflow on the top of the cavity – Case Cavity extension above roof – 5.25m above roof

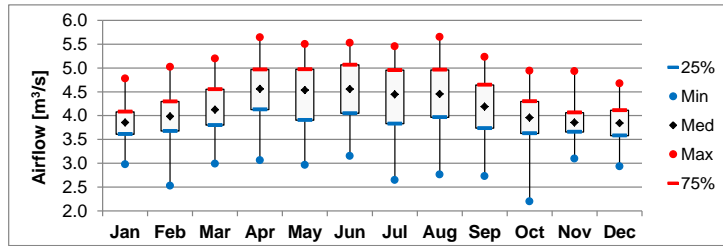


Appendix A. 33 - Monthly mean of the net airflow for each floor – Case Cavity extension above roof – 5.25m above roof

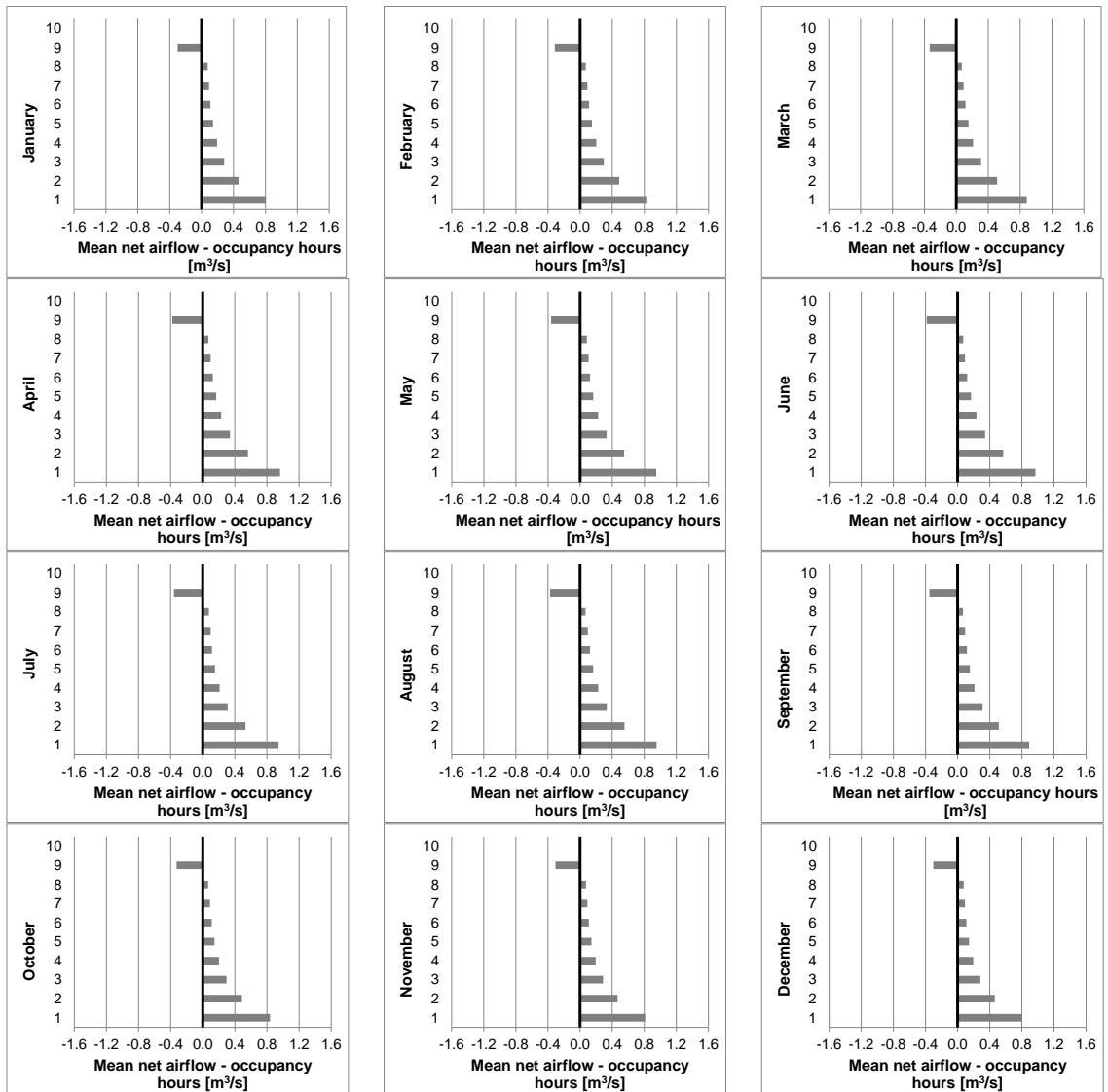
Case C2.2 Upper windows closed – Window of 10th floor closed



Appendix A. 34 - Monthly mean of difference of temperature between the cavity and the outside air – Case Upper windows closed – Window of 10th floor closed

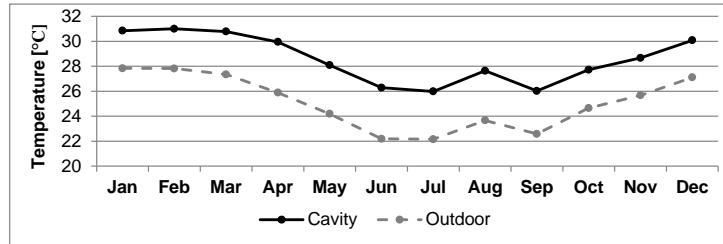


Appendix A. 35 - Monthly mean of airflow on the top of the cavity – Case Upper windows closed – Window of 10th floor closed

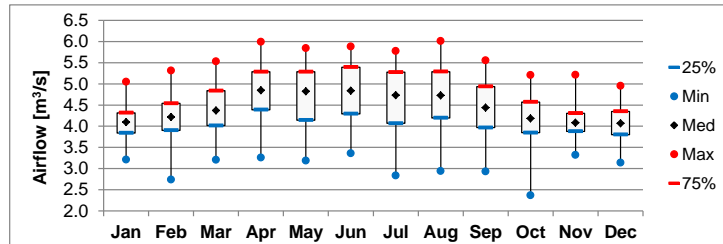


Appendix A. 36 - Monthly mean of the net airflow for each floor – Case Upper windows closed – Window of 10th floor closed

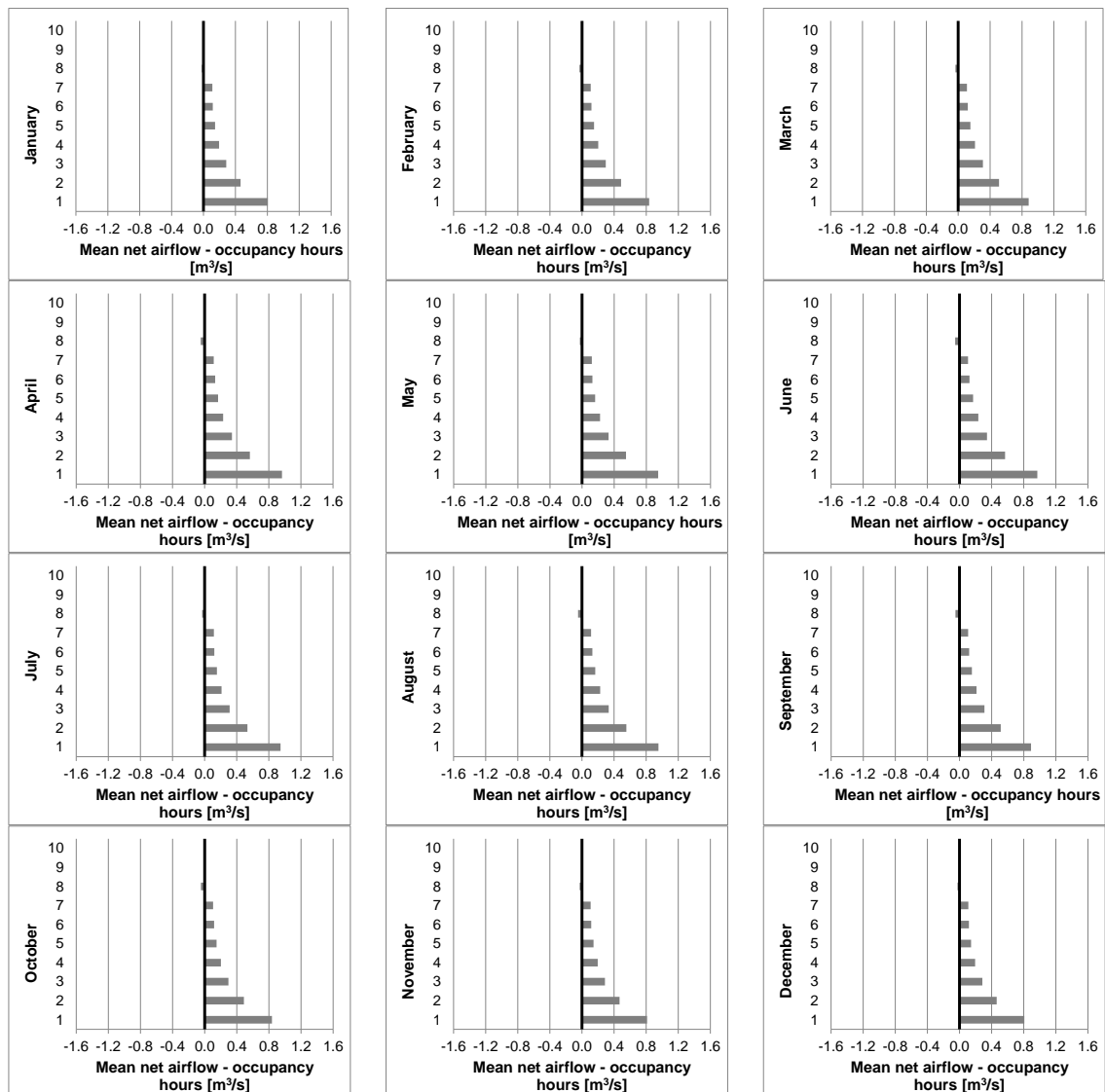
Case C2.3 Upper windows closed – Windows of 9th and 10th floor closed



Appendix A. 37 - Monthly mean of difference of temperature between the cavity and the outside air – Case Upper windows closed – Windows of 9th and 10th floor closed

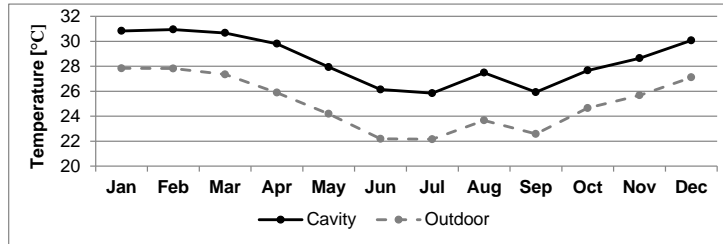


Appendix A. 38 - Monthly mean of airflow on the top of the cavity – Case Upper windows closed – Windows of 9th and 10th floor closed

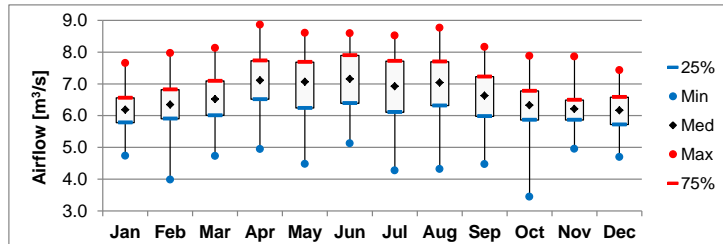


Appendix A. 39 - Monthly mean of the net airflow for each floor – Case Upper windows closed – Window of 9th and 10th floor closed

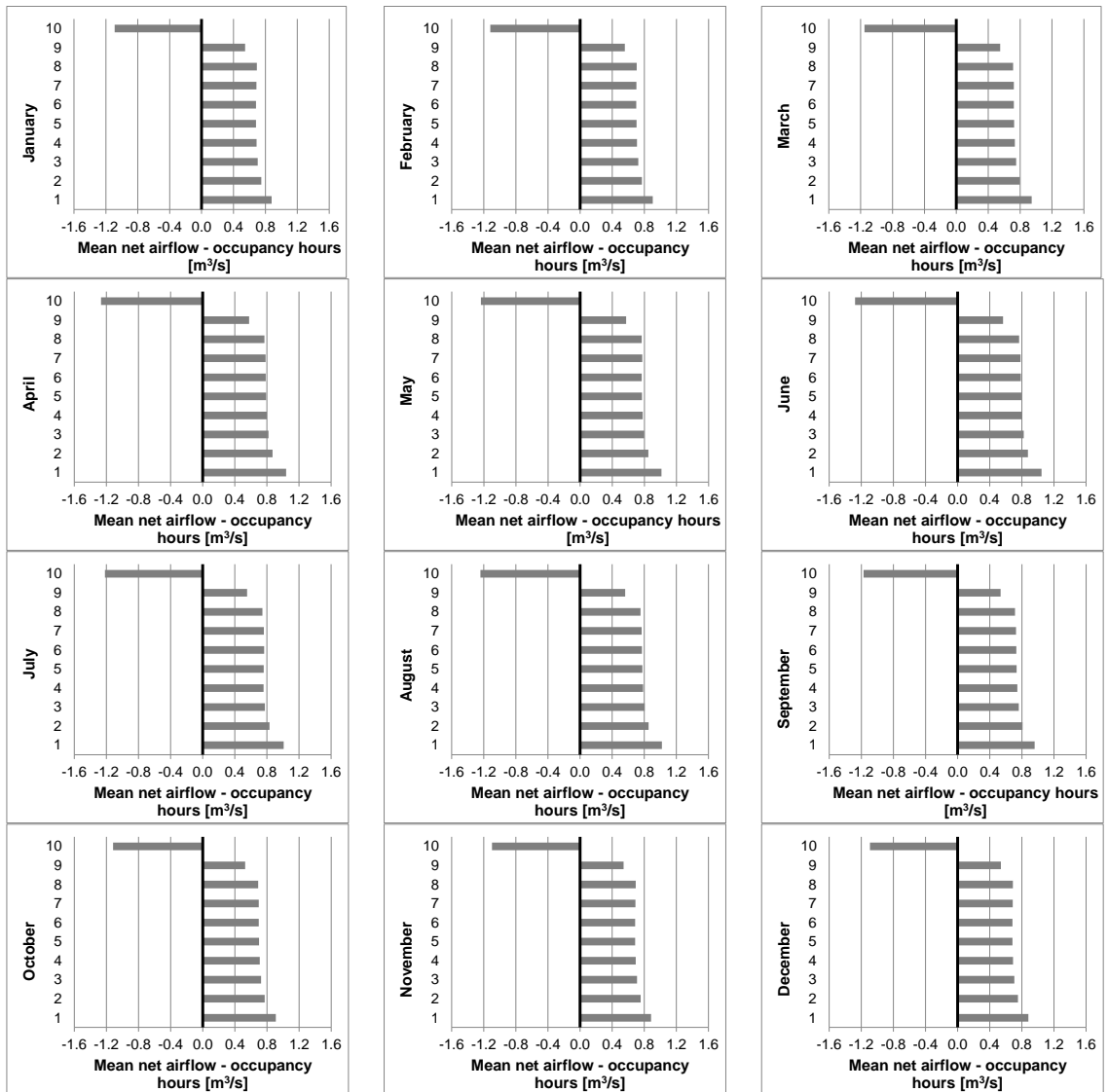
Case D1.2 Tapered cavity – Inclined outer skin



Appendix A. 40 - Monthly mean of difference of temperature between the cavity and the outside air – Case Tapered cavity – Inclined outer skin

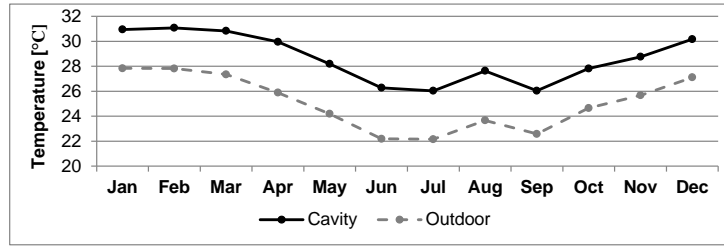


Appendix A. 41 - Monthly mean of airflow on the top of the cavity – Case Tapered cavity – Inclined outer skin

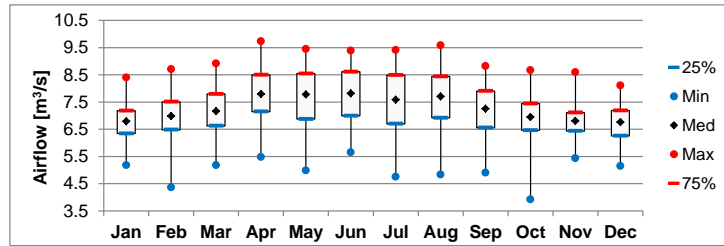


Appendix A. 42 - Monthly mean of the net airflow for each floor – Case Tapered cavity – Inclined outer skin

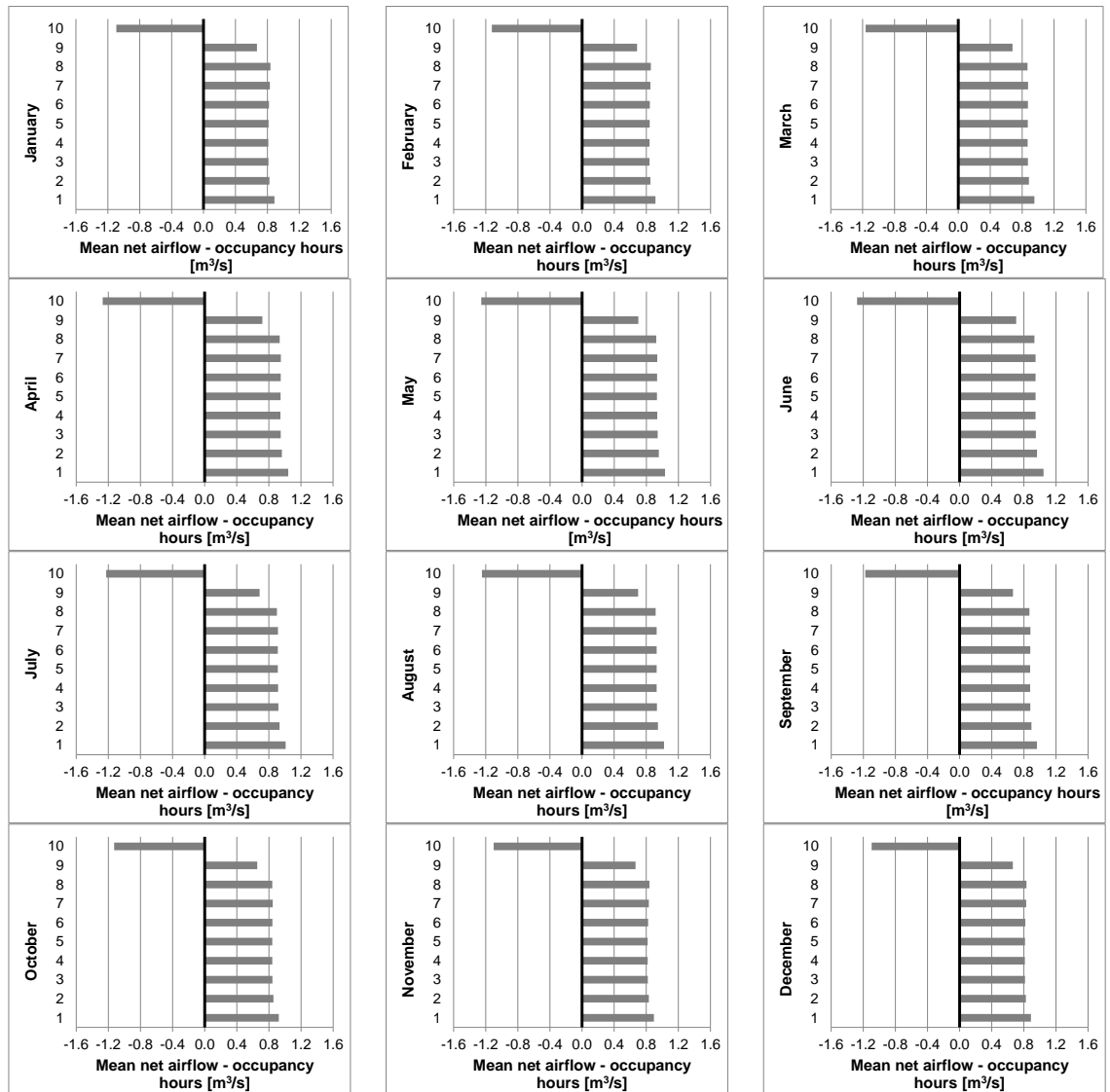
Case D1.3 Tapered cavity – Inclined inner skin



Appendix A. 43 - Monthly mean of difference of temperature between the cavity and the outside air – Case Tapered cavity – Inclined inner skin

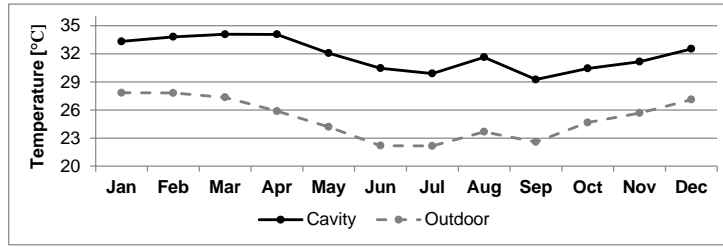


Appendix A. 44 - Monthly mean of airflow on the top of the cavity – Case Tapered cavity – Inclined inner skin

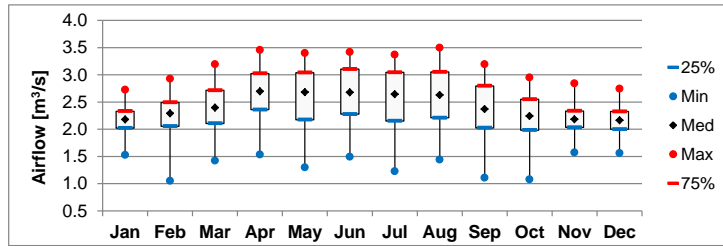


Appendix A. 45 - Monthly mean of the net airflow for each floor – Case Tapered cavity – Inclined inner skin

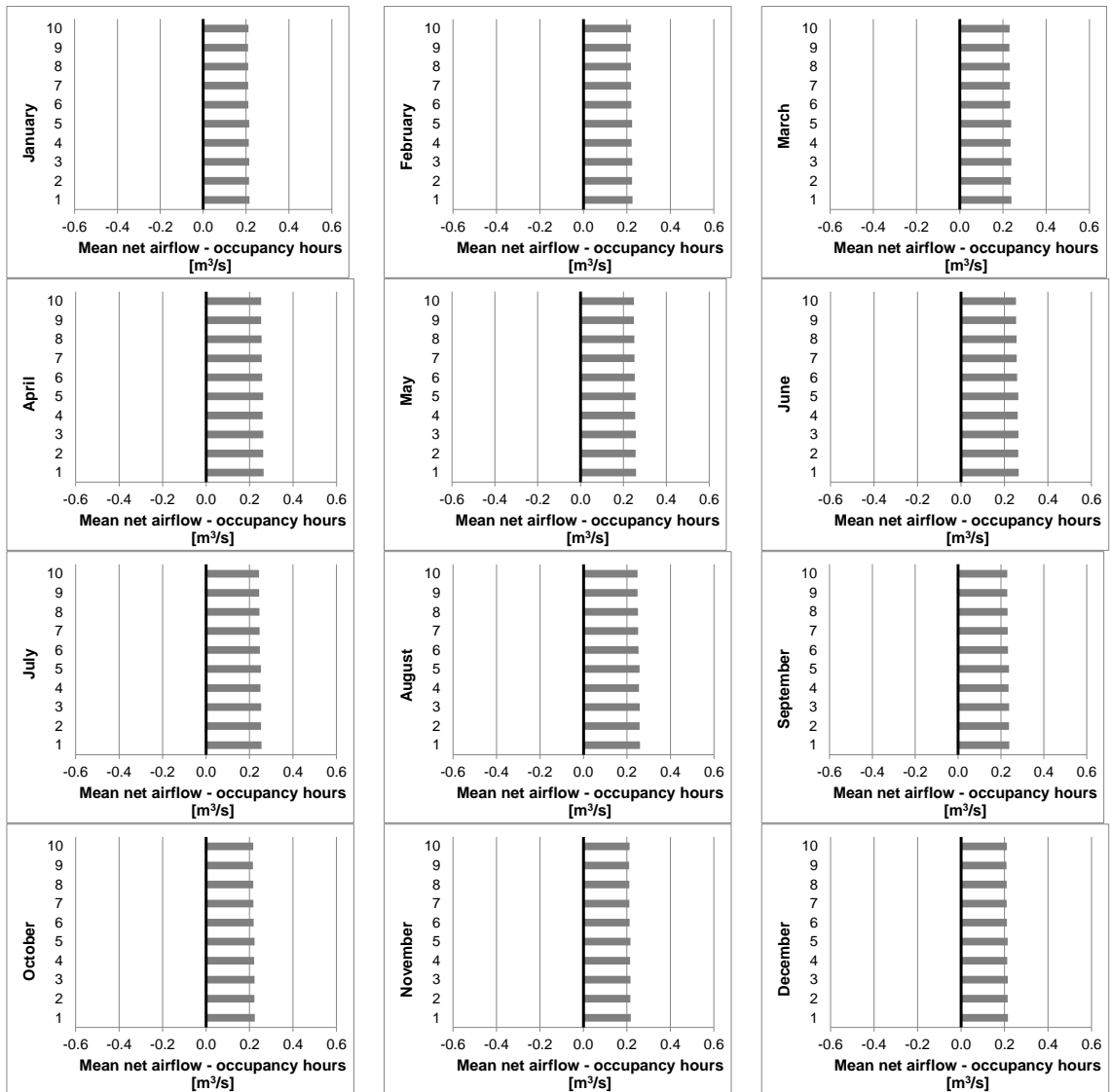
Case D2.2 Windows size – Calculated windows size



Appendix A. 46 - Monthly mean of difference of temperature between the cavity and the outside air – Case Windows size – Calculated windows size



Appendix A. 47 - Monthly mean of airflow on the top of the cavity – Case Windows size – Calculated windows size



Appendix A. 48 - Monthly mean of the net airflow for each floor – Case Windows size – Calculated windows size

APPENDIX B - Calculation of window areas

The following equation (equation 1) is used to calculate the size of the windows according to their position in height (section 5.2.4) such that the neutral pressure line occurs at a point above the highest window and the flows from each floor are balanced.

$$Q = C_D A \sqrt{2g\Delta H_{NPL} (t_i - t_o)/t_i} \quad \text{equation 1}$$

Appendix B. 1 – Windows size calculation - Optimized case

Equation variables	Openings											Outlet Top DSF
	Inlet - Floors levels											
	1	2	3	4	5	6	7	8	9	10		
Area (%)	1.6	1.7	1.8	1.9	2.1	2.3	2.5	2.9	3.4	4.6		100
Opening position in height (m)	0.7	4.2	7.7	11.2	14.7	18.2	21.7	25.2	28.7	32.2		38.5
$\Delta H - NPL$ (m)	36.1	32.6	29.1	25.6	22.1	18.6	15.1	11.6	8.05	4.55		1.75
NPL position (m)	36.75											

Appendix B. 2 – Windows size calculation – 5 floors case

Equation variables	Openings										Outlet Top DSF	
	Inlet - Floors levels											
	1	2	3	4	5							
Area (%)	4.5	5.0	5.8	6.9	9.2							100
Opening position in height (m)	0.7	4.3	7.8	11.3	14.8							21.0
$\Delta H - NPL$ (m)	18.5	15.0	11.5	8.0	4.5							1.75
NPL position (m)	19.25											

Appendix B. 3 – Windows size calculation – 15 floors case

Equation variables	Openings															Outlet Top DSF	
	Inlet - Floors levels																
	1	2	3	4	5	6	7	8	9	10	11	12	13	14	15		
Area (%)	0.85	0.88	0.92	0.95	0.99	1.04	1.09	1.16	1.24	1.33	1.45	1.61	1.84	2.21	2.95		100
Opening position in height (m)	0.8	4.3	7.8	11.3	14.8	18.3	21.8	25.3	28.8	32.3	35.8	39.3	42.8	46.3	49.8		56.0
$\Delta H - NPL$ (m)	53.5	50.0	46.5	43.0	39.5	36.0	32.5	29.0	25.5	22.0	18.5	15.0	11.5	8.0	4.5		1.75
NPL position (m)	54.0																

Appendix B. 4 – Windows size calculation – 20 floors case

Equation variables	Openings																				Outlet Top DSF	
	Inlet - Floors levels																					
	1	2	3	4	5	6	7	8	9	10	11	12	13	14	15	16	17	18	19	20		
Area (%)	0.57	0.58	0.60	0.61	0.63	0.65	0.68	0.70	0.73	0.77	0.80	0.84	0.89	0.95	1.02	1.11	1.23	1.41	1.69	2.26		100
Opening position in height (m)	0.8	4.3	7.8	11.3	14.8	18.3	21.8	25.3	28.8	32.3	35.8	39.3	42.8	46.3	49.8	53.3	56.8	60.3	63.8	67.3		73.5
$\Delta H - NPL$ (m)	71.0	67.5	64.0	60.5	57.0	53.5	50.0	46.5	43.0	39.5	36.0	32.5	29.0	25.5	22.0	18.5	15.0	11.5	8.0	4.5		1.75
NPL (m)	71.75																					

Abstracts of refereed papers in international journals and conferences

BARBOSA, S., IP, K. & SOUTHALL, R. 2015. Thermal comfort in naturally ventilated buildings with double skin façade under tropical climate conditions: The influence of key design parameters. *Energy and Buildings*, 109, 397-406.

Abstract: This paper evaluates the influence of key design parameters on the thermal behaviour of a naturally ventilated building with Double Skin Façade (DSF) under tropical climate conditions. Using a reference model of a conventional office building in the city of Rio de Janeiro and two groups of design parameters, dynamic thermal simulations are systematically applied to optimise design options with the aim to maximize the annual acceptable thermal comfort levels within the occupied spaces. This study not only defines the dimensional parameters to maximise the system airflows, but also investigates the significance of design decisions such as thermal mass and shading devices on the system performance. Options to avoid unintentional reverse flow on the upper floors and maintenance of balanced horizontal airflow rates across the floors are also addressed.

BARBOSA, S. & IP, K. 2014b. Perspectives of double skin façades for naturally ventilated buildings: A review. *Renewable and Sustainable Energy Reviews*, 40, 1019-1029.

Abstract: This paper identifies the parameters affecting the thermal and energy performance of buildings with double skin façades (DSFs). It reviews the state of the art of current body of literature about the application of DSF technologies in order to provide guidelines to optimise such designs in naturally ventilated buildings. Three groups of parameters are identified as having significant impact on the DSF performance: the 'façade' parameters, which comprise the features of the cavity and the external layer of the façade; the 'building' parameters, which are those related to the physical configurations of the building; and the 'site' parameters, which are related to the effects of the outdoor environmental conditions on the building and the DSF behaviours. For each group of parameters, a comprehensive table is compiled summarizing the main findings of the studies that directly and indirectly contribute to the understanding and implementation of such technology. Guidelines established for the design of naturally ventilated buildings indicated potential application of DSF for improving the indoor thermal comfort even in warmer regions. However, further investigations expanding the analysis beyond the cavity are needed in order to evaluate the influence of the DSF on the thermal comfort in the user space.

BARBOSA, S., IP, K. & SOUTHALL, R. 2015. Influence of key site parameters on the thermal performance of double skin façades in naturally ventilated buildings in a tropical climate. *In: CUCINELLA, M., PENTELLA, G., FAGNANI, A. & D'AMBROSIO, L., eds. 31st International PLEA Conference, Bologna. Ass. Building Green Futures, Bologna.*

Abstract: Double skin façades (DSFs) have gained recognition as architectural elements in modern office buildings which, when appropriately applied, can potentially lead to improvements in the indoor thermal comfort and reduction in building energy consumption even in warm or tropical climates. This technology that utilises the renewable resources of solar and wind to reduce the air-conditioning demand in such climates is a potential solution to the current environmental challenges. This study examines the influence of key 'site' parameters, by keeping the 'building' parameters constant, on the thermal behaviour of an optimized building model with DSF. The site parameters represent the variables of two local environmental conditions: the level of local solar incidence, which relates to the influence of hours of the day, solar angle, sky conditions (cloudy and clear) and façade orientation on the building behaviour; and the wind conditions, which account for the effects of speed and direction acting on the DSF. Using the climate data of Rio de Janeiro city as the tropical environmental context, building

energy simulations are performed to the defined DSF models. Airflow levels and periods of thermal acceptance, based on the adaptive comfort criteria in relation to the outdoor environmental variations, are analysed to demonstrate the site conditions under which the technology is likely to operate effectively.

BARBOSA, S. & IP, K. 2014. Double skin façade for naturally ventilated office buildings in Brazil. World Sustainable Building, 2014a Barcelona. Madrid, Spain: Green Building Council Espana, 93-99.

Abstract: The double skin façade (DSF) is a developing design option for buildings that can lead to improvements in the indoor thermal comfort. Most of the studies about the DSF have been conducted using air-conditioned building models, although applied in naturally ventilated buildings. This study investigates if satisfactory thermal acceptance can be achieved in naturally ventilated buildings with DSF in Brazil. It presents the range of natural ventilation performance that can be achieved by the DSF, based on a generic building model, in response to the impact of solar radiation on the façade. Building thermal and computational fluid dynamic simulations were systematically performed to establish air temperature and air movement within the occupied spaces in the model. Periods of thermal acceptance, examined using the adaptive comfort criteria of different regional and seasonal variations in Brazil are presented. The study demonstrated that there is a potential to adopt DSF in some regions of Brazil.

BARBOSA, S. & IP, K. 2014. A feasibility study on the double skin façades application for naturally ventilated buildings under Brazilian climate. *In:* SAYIGH, A., ed. World Renewable Energy Congress WREC 2014, London, UK. Springer International Publishing.

Abstract: Double skin façade (DSF) is a potential low energy passive design alternative for office buildings in warm climates. Although the DSF can enhance natural ventilation in buildings, most of studies about its performance were conducted using air-conditioned building models, treating the cavity as an “isolated” structure” and discounting its effects on the user rooms. To date in Brazil, there is hardly any investigation to assess the DSF potential and applicability that takes into consideration the country’s vast area and diversity in climate. The aim of this study, as part of a comprehensive research on DSF design for naturally ventilated buildings, is to evaluate the viability of the DSF’s operation according to the Brazilian weather conditions, identifying the regions and the periods of year suitable for its application. Thermal computational simulations were performed using a generic naturally ventilated office building model to identify suitable areas in Brazil and the seasonal periods in which the DSF technology can be adopted. The results suggest that the thermal conditions in the model are satisfactory in about one third of the year in zone 8, which covers 60% of the territory including the main coastal cities. Moreover, this acceptability reaches around 70% in some areas of southwest and centre-west regions. The findings of this study are significant to the wider application of DSF in Brazil and the outcomes provide guidance to DSF designers during the conceptual design stage.